6.0 SUPPORTING EXPERIMENTAL STUDIES

To evaluate the plausibility of cancer risk models for asbestos it is useful to examine the current state of knowledge regarding (1) the mechanisms that facilitate the transport of asbestos to the various target tissues of interest (i.e., the lungs and mesothelium) and (2) the mechanisms that contribute to the development of cancer in these target tissues. Accordingly, a review of the relevant literature is provided in this chapter to assure that the quantitative analysis in Chapter 7, and the proposed approach for assessing asbestos-related risks in Chapter 8, are qualitatively consistent with general implications from the broader literature. This review, although extensive, is not exhaustive. A much larger number of studies was reviewed than are actually cited. Studies that are not cited are largely confirmatory or redundant. In selecting studies for review, special effort was expended to assure that opposing views (particularly for controversial issues) were adequately represented.

Although much progress has been made over the last decade toward elucidating the fiber/particle mechanisms that contribute to transport and subsequent cancer induction, at least two critical data gaps remain:

- no one has yet been able to track a specific lesion induced by asbestos in a specific cell through to the development of a specific tumor. There have been experiments that show altered DNA and other types of cellular and tissue damage that are produced in association with exposure to asbestos. Other studies have demonstrated that various tumors of the kinds that result from asbestos exposure exhibit patterns of DNA alteration (or other kinds of cellular damage) that are sometimes (but not always) consistent with the earlier cellular changes associated with asbestos exposure. There are also studies that show that exposure to asbestos can lead ultimately to development of tumors. However, these types of studies have yet to be linked; and

- the specific target cells that serve as precursors to tumors in various target tissues are not known with certainty.

Because of the first of the above limitations, researchers have tended to report on a broad range of tissue and cellular effects induced by asbestos that may lead generally to various kinds of cellular damage or injury. Cytotoxicity, for example, is one of the endpoints typically tracked as a marker for asbestos-induced injury. However, not all of these effects necessarily contribute (either directly or indirectly) to the development of cancer. Therefore, one of the goals of the following discussion is to distinguish among effects that likely contribute to the development of cancer from those that are less likely or unlikely to contribute. Of course, delineating such distinctions are subject to the limitations of the current state of knowledge.

In addition, because the relative effects of fiber size, shape, and mineralogy need to be elucidated to better indicate how asbestos concentrations should be characterized to support risk assessment, studies that address these topics are highlighted. Of particular interest are studies that (1) contrast the effects of different sized fibers, (2) contrast the effects of fibers and non-

fibrous particles of similar mineralogy, and (3) contrast the effects of fibers of comparable morphology (size and shape), but differing mineralogy.

The types of studies that have contributed to the state of knowledge of the effects of asbestos (in addition to the human epidemiology studies that are evaluated in Chapter 7) include:

- whole animal inhalation studies;
- whole animal instillation studies;
- whole animal injection, implantation studies;
- human pathological studies;
- *in vitro* studies in cell cultures; and
- *in vitro* studies in cell-free systems.

Depending on the outcome(s) monitored, the animal studies may alternately be categorized as retention studies, histopathology studies, or dose-response studies.

Each type of study possesses certain advantages and exhibits certain limitations, which have previously been described (Chapter 5) along with descriptions of the nature of each of these study types. In addition to the advantages and limitations that are attributable to the type of study, the quality of the characterization of asbestos (or other particulate matter) determines the utility of the study for addressing issues associated with fiber morphology and mineralogy. Unfortunately, for many published studies, both the characterization of the asbestos (or other particulate matter) and descriptions of the manner in which such materials were handled are insufficient to establish the detailed morphology or mineralogy. Such limitations need to be considered when comparing across study results or evaluating the validity of study conclusions.

The rest of this chapter is divided into separate sections that address the set of factors that have been previously identified (Chapter 3) as those that determine the biological activity of inhaled asbestos (which is the exposure route of primary concern for humans). These are:

- the extent that asbestos structures are respirable and the pattern of deposition of inhaled structures;

- the extent that deposited structures are subsequently cleared or degraded;

- the extent that deposited structures are transported or migrate to the various target tissues; and

- the extent that retained structures induce a biological response in each target tissue.

6.1 FACTORS AFFECTING RESPIRABILITY AND DEPOSITION

Discounting systemic effects resulting from other forms of exposure, factors affecting respirability are common to all of the toxic endpoints associated with asbestos exposure considered in this study (asbestosis, lung cancer, and mesothelioma). Moreover, respirability is common to the factors affecting the toxicity of inhaled, insoluble particles in general. To be

respirable, an inhaled particle must pass the blocking hairs and tortuous passageways of the nose and throat and be deposited in the lungs. Particles deposited in the naso-pharyngeal portion of the respiratory tract are not considered respirable.

Not all of the inhaled particles that reach the lungs will be deposited. Small particles may not impact lung surfaces during inhalation and are subsequently exhaled. Once a particle impacts on a surface, however, it is likely to remain because the surfaces of the lungs are wetted with a surfactant (Raabe 1984).

Adverse health effects potentially result when particles that are deposited in the lungs remain in contact with the tissues in the lung for a sufficient period of time to provoke a biological response. To affect the mesothelium, an offending particle may also need to migrate or be transported from the lung to this surrounding tissue. However, due to the proximity of the mesothelium to peripheral portions of the lung parenchyma (which include locations where particles are typically deposited), it is also possible that diffusable molecules produced in lung tissue in response to deposited particles can have an adverse effect on the mesothelium (see, for example, Adamson 1997). Such effects are considered among the mechanisms of disease induction addressed in the discussion of biological responses (Section 6.3).

The interplay between deposition and removal (clearance) of inhaled particles is an important determinant of biological activity and separating the influence of these two processes in the pathology of asbestos-induced disease is difficult. The term "retention" is used here to represent the fraction of particles remaining in the lungs beyond the time frame over which only the most rapid removal processes (i.e., muco-ciliary clearance) are active. The factors affecting retention are addressed further in Section 6.2.

Published inhalation studies divide the respiratory tract into three units (see, for example, Raabe 1984). The naso-pharyngeal portion of the respiratory tract extends from the nares in the nose through the entrance to the trachea. The tracheo-bronchial portion of the respiratory tract includes the trachea and all of the branching bronchi down to the terminal bronchioles. The respiratory bronchioles and the alveoli, which are collectively referred to as the "deep lung", are the bronchio-alveolar (or pulmonary) portion of the respiratory tract. For a more detailed description of the features of the respiratory tract, see Section 4.4.

The dimensional requirements for respirability have been studied and reviewed in several studies (see, for example, Raabe 1984 or U.S. EPA 1986). A more recent review is also presented by Stober et al. (1993). Much of the data reviewed in these studies is based on earlier studies in which researchers exposed animals or human volunteers to a series of monodisperse spherical particles (although Stober et al. also reviews fiber experiments). In this manner, the impact of the diameter of spherical particles on respirability was elucidated. The respirability of fibrous materials (such as asbestos) tends to be described in terms closely associated with those employed for spherical particles, but with adjustments for density and shape. Importantly, because respirability is a mechanical process: the size, shape, and density of a particle (or fiber) determine its respirability along with the morphometry of the airways through which the particle passes (Stober et al. 1993). Other than affecting the particle’s density or the distribution of fiber shapes, the chemical composition (mineralogy) of a particle (or fiber) does not influence respirability.

The respirability of particles and fibers by humans, and a variety of other mammals of experimental interest, has also been the subject of increasingly sophisticated modeling efforts (Stober et al. 1993). The latest refinements of such models predict particle deposition with a degree of accuracy that is beyond what can be validated with existing, experimental data. The application of several of these models to asbestos (and other fibrous materials) are considered throughout this chapter. However, a detailed overview of the state-of-the-art of such modeling is beyond the scope of this document. Such an overview is presented by Stober et al. (1993).

6.1.1 Respirability of Spherical Particles

Spherical particles larger than 10 μm in diameter are considered non-respirable because virtually all particles in this size range are trapped in naso-pharyngeal passageways and blocked from entering the lungs. As the diameter of the particles fall, an increasing fraction traverses the nose and throat and may be deposited in the lungs. About half of particles 5 μm in diameter are blocked before entering the lungs. Virtually all particles smaller than 1 μm enter the lungs, although other factors determine whether they are in fact deposited or simply exhaled. Figure 6-1 (Raabe 1984) is a representation of the relative deposition in the various compartments of the respiratory tract as a function of particle diameter.

Within the lungs (Figure 6-1), the greatest fraction of respirable particles (over the entire range of diameters down to <0.01 μm) are deposited in the deep lung (the broncho-alveolar portion of the respiratory tract), primarily at alveolar duct bifurcations (see, for example, Brody et al. 1981; Davis et al. 1987; Johnson 1987; Sussman et al. 1991a). These studies also indicate that biological responses appear to be initiated where deposition is heaviest. Generally, the fraction of particles deposited in the deep lung increases regularly with decreasing diameter until a maximum of 60% deposition in the deep lung is reached at about 0.1 μm diameter.

As indicated in Figure 6-1, a transition occurs at particle diameters between 0.5 and 1 μm. For particles in this range and smaller, deposition in the deep lung competes primarily with deposition in the tracheo-bronchial tree and with exhalation; smaller particles have an increasing probability of being exhaled without ever impacting the surface of an air passageway. For particles larger than this transition range, broncho-alveolar deposition is limited chiefly by the fraction of particles that are removed from the air stream prior to reaching the deep lung (either by deposition in the naso-pharyngeal or the tracheo-bronchial portions of the respiratory tract).

The transition between naso-pharyngeal competition with deep-lung deposition and competition from other removal processes is important because, during mouth breathing, a process that bypasses the tortuous pathways of the nose and throat, it has been observed that larger particles (up to several micrometers in diameter) may be deposited in the deep lung (Raabe 1984). Studies of the effects of mouth breathing are also reviewed by Stober et al. (1993). Because most people spend at least small amounts of time mouth breathing, especially during exertion or while snoring, this mechanism for allowing larger particles to settle in the deep lung should not be ignored.

Figure 6-1. Fractions of Respirable Particles Deposited in the Various Compartments of the Human Respiratory Tract as a Function of Aerodynamic Equivalent Diameter[a,b]

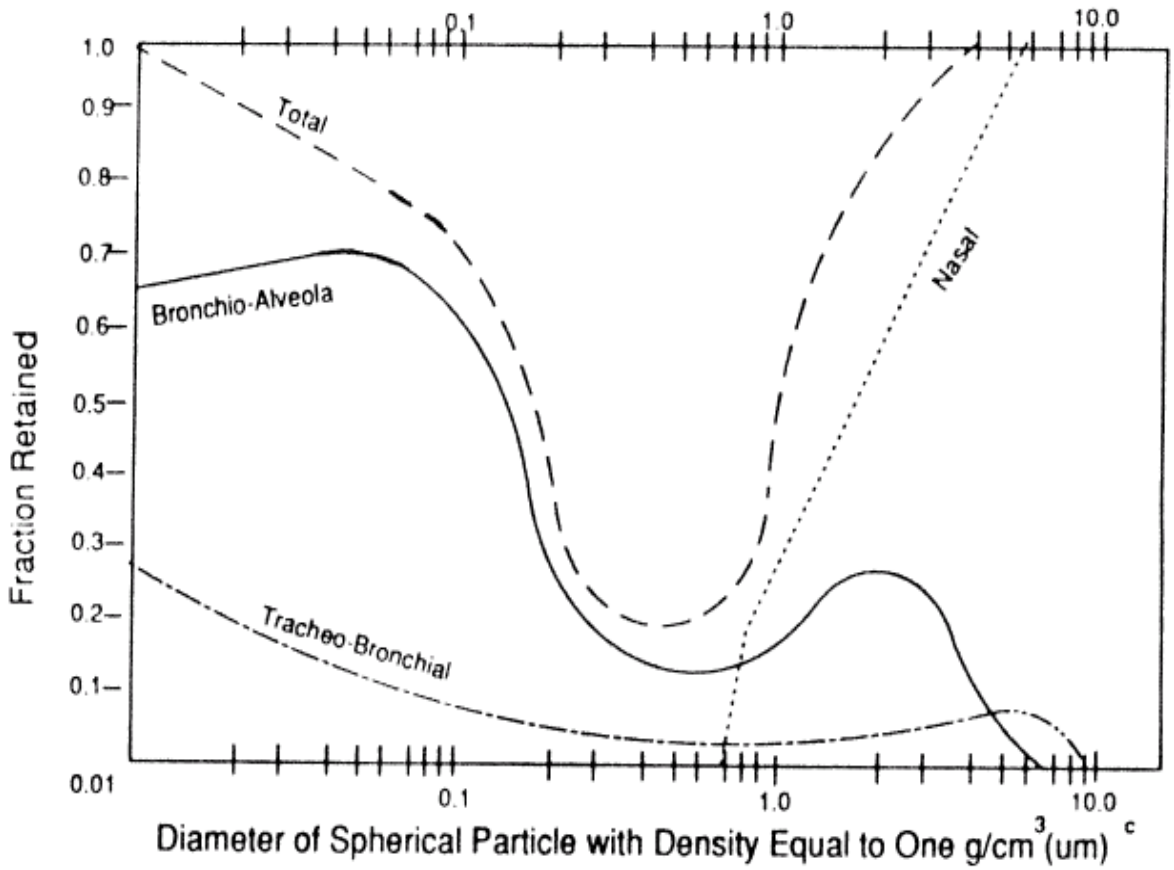

[a]Source: Raabe 1984
[b]Assumes a typical tidal value of 1,450 cm^3 and a rate of 15 breaths a minute
[c]Aerodynamic equivalent diameter

Confidential: Need Permission to Reproduce this Figure

A diameter of 0.5 µm also happens to represent the transition between the regime where inertial flow becomes the major factor controlling deposition in the lungs and the regime where diffusional flow dominates. Below the 0.5 µm transition, the diffusional diameter becomes more important in determining deposition than the aerodynamic equivalent diameter (defined below).

6.1.2 Respirability of Fibrous Structures

Several authors have investigated the effect of the shape of non-spherical particles (including fibers) on respirability and deposition (see, for example, Harris and Timbrell 1977; Strom and Yu 1994; Sussman et al. 1991a,b; Yu et al. 1995a,b). It has been found that the behavior of non-spherical particles can be related to the behavior of spherical particles by introducing a concept known as the aerodynamic equivalent diameter. The aerodynamic equivalent diameter is the

diameter of a hypothetical spherical particle of unit density that would exhibit the same settling velocities and aerodynamic behavior as the real, non-spherical particle of interest. Factors that affect the aerodynamic equivalent diameter are density, true diameter, true length (for elongated particles such as fibers), and the regularity of the particle shape.

Harris and Timbrell (1977) Findings. Because fibrous particles tend to align primarily along the axis of travel under the flow conditions found in the lungs, respirability is predominantly a function of the diameter of a fiber and the effect of length is secondary (Harris and Timbrell 1977). Fibrous structures with aspect ratios (ratio of length to width) >3:1 behave like spherical particles (of similar density) with diameters up to 3 times larger and exhibit only a very weak dependence on length. As previously indicated, however, the aerodynamic equivalent diameter of a fibrous structure must also be adjusted for the effects of density. This is demonstrated in Figure 6-2 where the true diameter of a fiber is graphed on the top horizontal axis against spherical (aerodynamic equivalent) diameters on the bottom horizontal axis. Figure 6-2 is an overlay of Figure 6-1. Note that, to adjust for the density of asbestos, the true diameters listed in the figure have been shifted to the right of where they would appear if the relationship was exactly 1/3 of the aerodynamic equivalent diameter.

Two vertical dashed lines in Figure 6-2 represent effective limits to the range of respirable asbestos. The line on the left side in the figure represents the limiting diameter of the smallest chrysotile fibril (about 0.02 μm true diameter) and thus represents a lower limit to the diameter that is of concern when considering asbestos. The vertical line to the right represents the cutoff where deposition in the deep lung becomes unimportant due to removal of such particles by the naso-pharyngeal passageways. This latter cutoff corresponds to a true fiber diameter of 2.0 μm, which theoretically represents the upper limit to the size of asbestos that is respirable. As indicated in the figure, however, deposition in the deep lung drops precipitously for fibers thicker than about 0.7 μm so that no more than a few percent of asbestos fibers thicker than approximately 1 μm actually reach the deep lung.

Harris and Timbrell (1977) also evaluated the relationship between the overall shape of a particle and the extent of deposition. Over the range of diameters that potentially represent the range of asbestos fibers likely to be encountered, pulmonary deposition decreases with increasing complexity of shape beyond simple cylinders (such as clusters and matrices (see Section 4.2) at the expense of increasing naso-pharyngeal or tracheo-bronchial deposition. This change also becomes increasingly important as the length of the structure increases. For structures <25 μm in length, the difference in deposition between simple fibers and complex clusters or matrices may vary by up to a factor of 2 with the complex structures being more likely to be removed in the naso-pharyngeal portion of the respiratory tract and the fibers more likely to be deposited in the deep lung. At 100 μm lengths, the fraction of complex structures that survive passage through the nose and throat in comparison with simple fibers may vary by a factor of 5. This means that large structures become relatively less respirable as their complexity increases. However, during mouth breathing large clusters and matrices may enter the deep lung.

Figure 6-2. Fractions of Respirable Particles Deposited in the Various Compartments of the Human Respiratory Tract as a Function of the True Diameter of Asbestos Fibers[a,b,d]

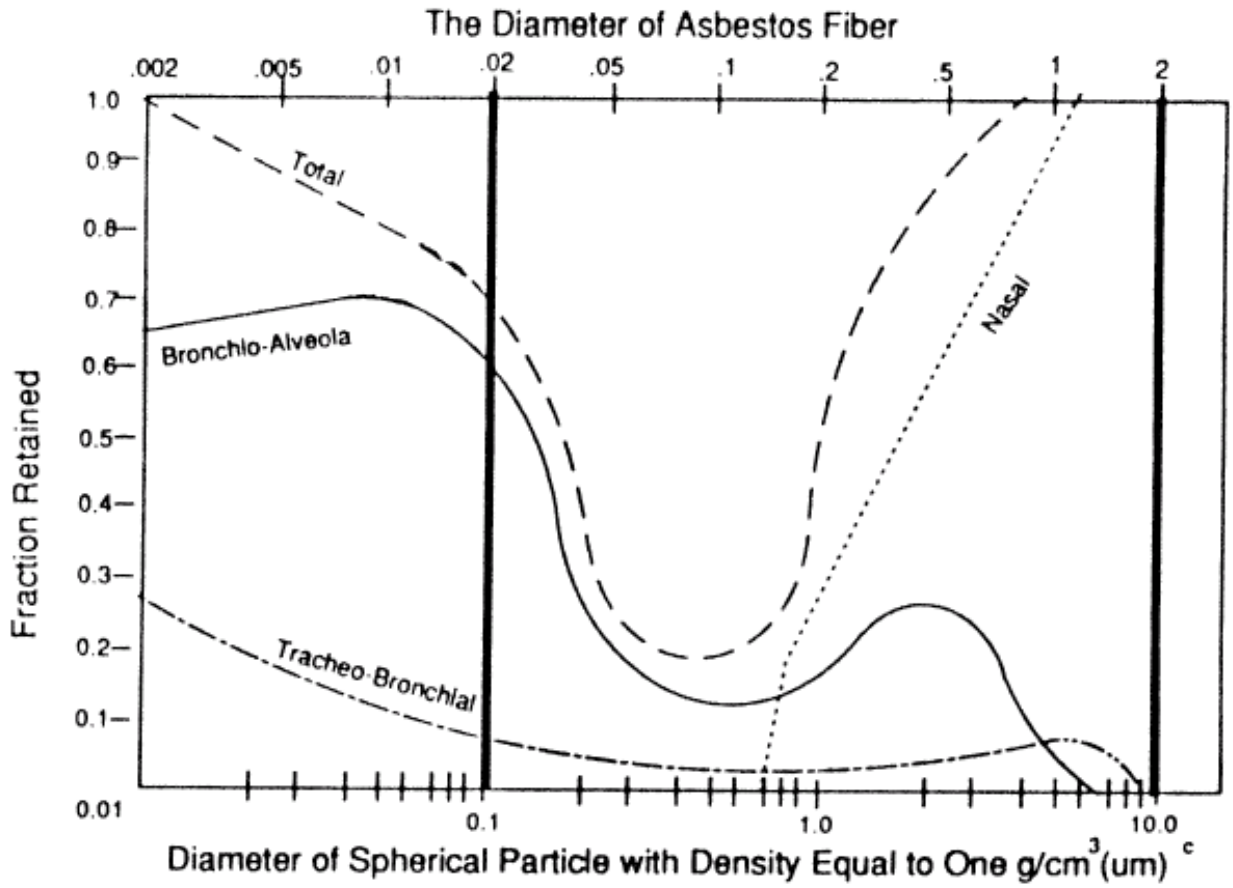

[a]Source of original: Raabe 1984
[b]Assumes a typical tidal value of 1,450 cm^3 and a rate of 15 breaths per minute
[c]The relationship between true diameters and aerodynamic equivalent diameters derived from Harris and Timbrell (1977). Diameters adjusted for shape and density of asbestos fibers.
[d]Aerodynamic equivalent diameter

Confidential: Need Permission to Reproduce this Figure

When all of the factors that Harris and Timbrell (1977) addressed are considered, the efficiency of the deposition of asbestos structures in the deep lung is maximal for short, thin, single fibers (<10 μm in length with a true diameter <0.7 μm). The efficiency decreases slowly with increasing length (up to an effective limit of 200 μm), moderately with increasing complexity of shape, and rapidly with increasing diameter (up to an effective limit of 2.0 μm, true diameter). Thinner fibers, down to the lower limit of the range for asbestos fibers (0.02 μm, true diameter), are deposited with roughly the same efficiency. Approximately 20–25% of the fibers between 0.7 and 0.02 μm in diameter (and <10 μm in length) are deposited in the deep lung.

Sussman et al. (1991a,b) Findings. Based on a series of experiments on human tracheal bronchial casts, Sussman et al. (1991a,b) also developed models of fiber deposition in the human lung. Such experiments are in fact illustrative of several research groups who have developed deposition models based on results from experiments on airway casts (for a review, see Stober et al. 1993).

The results reported by Sussman et al. (1991a,b) appear to be generally consistent with the results reported by Harris and Timbrell (1977) and Yu and coworkers (described below), although the manner in which their results are reported make them somewhat less directly comparable. Briefly, Sussman et al. (1991a,b) report that deposition increases along most generations of the bronchial tree with increasing fiber length and increasing airflow rate for any fixed aerodynamic diameter. This increased deposition efficiency is demonstrated for airway generations at least through the ninth bifurcation and is implied to continue through to airway generations that would be representative of the respiratory (pulmonary) portion of the lung (i.e., airway bifurcations greater than approximately 16 to 22). For definitions and a description of airway generations, see Section 4.4.

Findings of Yu and Coworkers. In a series of studies, Yu and coworkers combined an improved model of human lung physiology (Asgharian and Yu 1988) with a series of more rigorous equations to describe fiber mobility (Chen 1992) and used these to evaluate the deposition of various types of fibrous materials in the lung. The trends indicated in their studies show general agreement with those reported by Harris and Timbrell (1977), but with several notable refinements.

In a study of refractory ceramic fibers (Yu et al. 1995a), a maximum deposition efficiency of 15% is reported for fibers that are approximately 6 μm long and approximately 1 μm in diameter. This is close to the fiber size at which maximal deposition is reported by Harris and Timbrell (1977). As with Harris and Timbrell (1977), Yu et al. (1995a) also report that deposition efficiency decreases precipitously as diameter increases beyond 1 μm and decreases more slowly as diameter decreases below 1 μm. For thinner structures, deposition efficiency increases with both decreasing width and length. As fibers get longer, optimum deposition occurs with decreasing thickness. Thus, for example, a maximum deposition rate of 10% occurs for fibers that are 20 μm long at a thickness of 0.8 μm.

In a study of silicon-carbide whiskers (Strom and Yu 1994), the deposition model is extended to fiber widths as narrow as 0.01 μm. Results from this study indicate that fibers between 0.01 and 0.1 μm in thickness are deposited with a minimum efficiency of 5% up to lengths of approximately 40 μm before efficiency drops below 5%. For thin fibers (thinner than 0.5 μm), shorter fibers tend to be deposited in the deep lung much more efficiently than longer fibers. More than 25% of thin fibers shorter than 1 μm are deposited in the deep lung following inhalation. Strom and Yu (1994) report that the efficiency of deposition in the deep lung of long structures increases substantially during mouth breathing.

Comparing the results reported for refractory ceramic fibers (density=2.7 g/cm^3) and silicon-carbide whiskers (density=3.2 g/cm^3), it also appears that the efficiency of deep-lung deposition increases for thinner and for longer structures as the density of the structures increases. Given the observed density effect, chrysotile fibers that are longer than approximately 6 μm and thinner

than 1 μm would be deposited in the deep lung less efficiently than (denser) amphibole fibers of the same size. However, shorter and thicker chrysotile structures would be deposited somewhat more efficiently than similarly sized amphiboles. This suggests that a greater fraction of the mass of chrysotile that gets deposited in the deep lung will be composed of very short fibers and somewhat longer bundles than the mass fraction of short fibers or longer bundles in the air breathed. Also, to the extent that chrysotile fibers are curved, these would be deposited somewhat less efficiently than straighter (amphibole) fibers of comparable size.

Based on the deposition efficiencies predicted by Yu and coworkers, fibrous structures that reach the deep lung in humans are effectively limited to those thinner than approximately 1 μm. Given that fibrous structures have traditionally been defined as particles exhibiting aspect (length to width) ratios >3:1 (Walton 1982), it is clear that only particles shorter than 3 μm could potentially be respirable and still be excluded from the definition of a fibrous structure based on aspect ratio. Therefore, the thickness constraint for all longer structures is best described as a maximum width (rather than an aspect ratio) when defining the range of structures that potentially contribute to biological activity.

Rats versus Humans. Yu and coworkers also modified their models to evaluate the rates that fibrous materials are deposited in rat lungs and compared these with results for humans. Such comparisons have implications for the manner in which results from animal inhalation studies are extrapolated to humans.

Results from Yu et al. (1994) suggest that pulmonary deposition of all fibrous structures with lengths between about 1 and 100 μm and thinner than approximately 1 μm occurs at much higher rates in rats than in humans. Fibers as long as 90 μm are deposited in rat lungs at efficiencies exceeding 20% while fewer than 5% of structures this long are deposited in the pulmonary region of human lungs. In fact, it is only structures between 1 and about 20 μm within a very narrow range of thicknesses (centered around 1 μm) that are deposited more efficiently in the deep lungs of humans than in rats.

Yu et al. (1995a) also indicate that, even when deposition efficiencies are comparable in rats and humans, due to differences in the total lung mass and breathing dynamics across species, the resulting lung burdens (i.e., the mass or number of structures per mass of lung tissue) are 5–10 times higher in the rat than in humans for any given exposure. Lung burden per lung surface area are also higher in the rat than in humans.

To illustrate, assume rats and humans are similarly exposed to a concentration of 0.1 f/cm^3 (100 f/L) of some fibrous material with a length at which both species retain approximately 10% of the fibers inhaled. Table 6-1 then indicates the calculations required to determine the relative rates at which the lung (volume and surface area) burdens in each species would develop.

Table 6-1. Estimation of Lung Volume and Lung Surface Area Loading Rates for Rats and Humans

Species	Body Weight (kg)	Lung Volume (L)	Lung Surface Area (m^2)	Rest Breaths per Minute (bpm)	Tidal Lung Volume (L)
Human	70	5	140	15	1.5
Rat	0.15	0.01	0.4	70	0.0019

Species	Breathing Rate (L/min)	No. Fibers Inhaled per Minute (f/min)	No. Fibers Deposited per Minute (f/min)	Lung Volume Loading Rate (f/L-min)	Lung Surface Area Loading Rate (f/m^2-min)
Human	21.7	2170	217	43.4	1.6
Rat	0.13	13.3	1.3	130	3.3

From Table 6-1, it is clear that rats exposed to comparable airborne concentrations as humans will increase their loading of fibers per volume (or mass) of lung at a rate that is approximately 3 times that of humans (for fibers in sizes that are deposited with 10% efficiency in both species). Similarly, the fiber load per surface area of lung will increase in rats at a rate that is approximately twice that of humans. Moreover, even higher relative mass or surface area loading rates are expected for the rat than shown in the table, due to the greater efficiency with which most fiber sizes are deposited in rat lungs. Data used to compute the loading rates in the table (which are also presented) are derived from Gehr et al. (1993) and supplemented with information from Stober et al. (1993). A more detailed description of this information is provided in Section 4.4.

6.1.3 The Effects of Electrostatic Charge on Particle Respirability

Electrostatic charge has been shown to affect the retention of particles within the lungs (see, for example, Vincent 1985). Since processes that generate airborne particles generally involve some form of abrasion, airborne dust particles frequently exhibit varying degrees of electrostatic charge. Although this potentially leads to variation in the efficiency of particle retention in the lungs as a function of the source of the dust, a detailed relationship between surface charge and retention was not described in this paper. A more detailed and quantitative treatment was developed by Chen and Yu (1993) and the implications of the Chen and Yu model are described below (following discussion of the results of Davis et al. 1988a). Davis et al. (1988a) report that animals exposed to dusts containing fibrous chrysotile, whose surface charge is reduced with a beta minus source, retain significantly less chrysotile than animals dosed with dusts containing particles whose surface charge has not been reduced. However, the magnitude of the difference in the mass of fibers retained is less than a factor of 2, implying that the absolute variation due to this effect may be small. Further research in this area is needed.

Chen and Yu (1993) report that, based on modeling of lung deposition, overall deposition increases with increasing charge density on the particles inhaled. However, due to the pre-

iltering by the naso-pharyngeal and tracheo-bronchial portions of the respiratory tract, the effects of electrostatic charge on deep lung deposition appear to be only slight to modest.

Given the results of the above studies, the overall effects of electrostatic charge on particle deposition in the deep lung appear to be relatively minor. Therefore, such effects do not need to be considered explicitly when evaluating the health consequences of asbestos.

6.1.4 General Conclusions Concerning Particle Respirability

Based on the information provided in the last several sections, it is apparent that in humans:

- deposition of asbestos fibers in the pulmonary portion of the lung occurs primarily at alveolar duct bifurcations;
- electrostatic effects on pulmonary deposition are likely minor;
- fibers that are deposited in the pulmonary portion of the lung are largely thinner than approximately 0.7 μm and virtually all are thinner than 1 μm (except during mouth breathing, when thicker and more complex structures may be respired);
- the length of a fiber has limited impact on respirability up to a length of approximately 20 μm, but the efficiency of deposition of longer fibers decrease slowly with increasing length for longer fibers;
- as the length of the fibers that are inhaled increases, the thinner fibers are deposited with greater efficiency. Thus, the longer the fibers inhaled, the thinner the fibers retained;
- due to differences in density, shorter and thicker chrysotile structures will be deposited more efficiently in the pulmonary portion of the lung than corresponding amphibole structures and longer and thinner amphibole structures will be deposited more efficiently than corresponding chrysotile structures;
- curly chrysotile structures are less likely to reach the pulmonary portion of the lung than straight amphibole (or chrysotile) structures;
- except for a very narrow range of fiber sizes (centered around 6 μm in length and 1 μm in diameter), virtually all size fibers are deposited with greater efficiency in rat lungs than human lungs;
- due to body morphology and the dynamics of breathing, rats exposed to similar air concentrations will accumulate fiber burdens both per mass (volume) of lung tissue and per lung surface area at a rate that is several times the rate such burdens accumulate in humans; and
- the dynamics of fiber lung deposition can now be accurately predicted in great detail using currently available models.

6.2 FACTORS AFFECTING DEGRADATION, TRANSLOCATION, AND CLEARANCE

Degradation and clearance mechanisms compete with deposition to determine the fraction of asbestos that is retained in the lungs. Other (translocation) mechanisms mediate the movement of asbestos from sites of initial deposition to various target tissues within the lung and mesothelium. These factors affect all of the toxic endpoints of interest. Studies indicating the dependence of the various contributing mechanisms on fiber size and mineralogy are highlighted, as well as studies indicating differences between mechanisms in humans and laboratory animals.

The three units of the respiratory tract defined in the last section (naso-pharyngeal, tracheo-bronchial, and bronchio-alveolar units) differ primarily by the types of clearance (and translocation) mechanisms operating in each unit (Raabe 1984). These are summarized in Table 6-2 along with rough estimates of the time frames over which each mechanism may operate (to the extent that such estimates are available in the literature).

Briefly, the structures of the nose and throat are bathed in a continual flow of mucous, which is ultimately swallowed or expectorated. The mucous traps deposited particles and carries them out of the respiratory tract. The air channels of the tracheo-bronchial section of the respiratory tract are lined with cilia and mucous secreting cells. As in the nose and throat, the mucous traps particles deposited in these air pathways and the ciliary escalator transports the mucous up to the throat where it may be swallowed or expectorated. Neither the alveolar ducts nor the alveoli of the pulmonary compartment of the lung are ciliated (inferred from St. George et al. 1993). Therefore, particles deposited in this section of the respiratory tract can only be cleared by the following mechanisms:

- if the deposited particles are soluble, they may dissolve and be transported away from the lungs in blood or lymph; or

- if they are sufficiently compact, they may be taken up by alveolar macrophages and transported outward to the muco-ciliary escalator of the tracheo-bronchial portion of the respiratory tract.

Due to a combination of chemical and physical stresses in the environment of the lung, deposited asbestos structures may degrade by splitting. Longitudinal splitting, primarily of bundles, produces thinner structures and transverse splitting produces shorter structures. In both cases, the number of structures produced may be larger than the number of structures initially deposited.

By changing the size and number of structures that were initially deposited in the lungs, splitting may affect the rates and efficiency with which the various other degradation and clearance mechanisms operate.

Table 6-2. Relative Rates, Half-lives for Particles Cleared by the Varous Operating Mechanisms of a Healthy Lung

Tissue/Lung Regime	Species	Fiber Type	Particle Half-life[a] (days)	Kinetic Order	Mineralogical Effects	Size Effects	Reference
Mechanisms							
(Component Mechanisms)							
Nasal-pharyngeal							
Expectoration and Swallowing	Human		Minimal				
Muco-ciliary Transport	Human	Particles	0.0028	Zero	No Effect	No Effect	Raabe 1984
Tracheo-bronchial							
Muco-ciliary Transport	Human	Particles	0.021-0.21	Zero	No Effect	No Effect	Raabe 1984
Pulmonary (Bronchio-alveolar)							
AM Phagocytosis, Transport to MC Escalator	Rat	Particles	49	Ps - First	No Effect	Inhibited by length; conc.	Stober et al. 1990 in Stober et al. (1993)
	Rat	Short Chr	14			Fibers <4 um	Yu et al. 1990
Dissolution in Extracellular Fluid	In-vitro	Chr	180	Zero	Affects rate	Diameter determines lifetime	Hume and Rimstidt 1992
	In-vitro	Crc	11,000				Zoitus et al. 1997
Transport to the Interstitium	Rat	Particles	2.3	–	–	–	Stober et al. 1990 in Stober et al. (1993)
(Component Mechanisms)							
(Phagocytosis and expulsion by epithelial cells)							
(AM phagocytosis, transport through epithelium)							

Table 6-2. Relative Rates, Half-lives for Particles Cleared by the Varous Operating Mechanisms of a Healthy Lung *(continued)*

Tissue/Lung Regime	Species	Fiber Type	Particle Half-life[a] (days)	Kinetic Order	Mineralogical Effects	Size Effects	Reference
Mechanisms							
(Diffusive transport through the epithelium)							
(Forced mechanical transport through the epithelium)							
Sequestration							
(Phagocytosis and internalization by epithelial cells)							
(AM phagocytosis, immobilization due to overload)							
Pulmonary (Interstitial)							
IM Phatogyctosis, Transport to Lymphatics	Rat	Particles	2,300		Unspecified negative effect	Inhibited by length; conc.	Stober et al. (1990) in Stober et al. (1993)
	Dog	Ams	2,200				Oberdorster et al. (1988)
Diffusive Fluid Transport to Lymph			2,200				Churg 1994
Dissolution in Extracellular Fluid			(Same as Above)				
Transport to Endothelium, Pleura							
(IM phagocytosis, transport through interstitium)							
(Diffusive transport through the interstitium)							
(Forced mechanical transport through the interstitium)							
Sequestration							
(Encapsulation in granulomatous tissue)							
(Internalization by interstiial/endothelial cells)							

Table 6-2. Relative Rates, Half-lives for Particles Cleared by the Varous Operating Mechanisms of a Healthy Lung *(continued)*

Tissue/Lung Regime	Species	Fiber Type	Particle Half-life[a] (days)	Kinetic Order	Mineralogical Effects	Size Effects	Reference
Mechanisms							
The Pleura							
PM Phatogyctosis, Transport to Lymphatic Stomata							
Dissolution in extracellular fluid							
Sequestration							
(Encapsulation by granulomatous tissue)							
(Phagocytosis by mesothelial cells)							

[a]For zero order mechanisms, half-lives reported are half of the time required for complete clearance for the process that is constant with time. For first order mechanisms, the true half-lives (i.e., the time required for half of the initial population to disappear) is reported.

Particles and fibers that are deposited in the pulmonary portion of the lung may also be transported by a variety of mechanisms into and through the epithelium lining, the alveolar ducts, and alveoli to the underlying interstitium and endothelium that are located within the interalveolar septa (see Section 4.4). In those portions of the lung parenchyma that lie proximal to the pleura, such mechanisms may also facilitate transport to the mesothelium. Putative mechanisms by which such transport may occur include:

- if particles are sufficiently compact to be phagocytized by alveolar macrophages, they may be transported within macrophage "hosts" through the epithelium to the interstitium;

- if particles are sufficiently compact to be phagocytized by the epithelial cells lining the air passageways of the deep lung, they may be transported into cell interiors or transported through to the basement membrane, the interstitium, the endothelium, and (eventually) the pleura;

- particularly when associated biological effects that cause changes in the morphology of epithelial cells, particles may diffuse between the cells of the epithelium to underlying tissues; and/or

- particles may be transported through respiratory epithelium mechanically due to physical stresses associated with respiration within the lung.

Although the transport of fibers and particles from airway lumena to the interstitium is apparent in many studies (see below), the precise mechanisms by which such transport actually occurs has yet to be delineated with certainty.

Particles deposited in the interstitium can also be cleared and the processes by which these particles are ultimately cleared are similar to, but may be substantially slower than, the mechanisms by which particles deposited in airway spaces can be cleared. Such mechanisms include:

- if the deposited particles are soluble, they may dissolve and be transported away from the lungs in blood or lymph; or

- if the particles of the interstitium are sufficiently compact to be phagocytized by interstitial macrophages, they may be taken up and transported to the lymphatic system for removal.

The mechanisms by which particles that reach the pleura and mesothelium may be cleared are also similar to those operating in the interstitium:

- if the deposited particles are soluble, they may dissolve and be transported away from the lungs in blood or lymph; or

- if the particles that reach the pleura are sufficiently compact to be phagocytized by pleural macrophages, they may be taken up and transported to the lymphatic system for removal.

Particles cleared from the pleura by macrophages appear subsequently to be deposited at sites of lymphatic drainage along the pleura (i.e., at lymphatic ducts) from where they are ultimately cleared in lymph (Kane and MacDonald 1993).

The various degradation, clearance, and transport mechanisms that affect the retention of asbestos in the lung and other target tissues (identified above) exhibit disparate kinetics that may be further altered by the size, shape, mineralogy, and concentration of the particles affected. Therefore, the kinetics of these mechanisms are considered below. The mechanisms evaluated include:

- dissolution;
- muco-ciliary transport;
- macrophage phagocytosis and transport; and
- diffusional transport.

Evidence for the existence of these mechanisms and inferences concerning their kinetics derive primarily from retention studies, which may include both studies of retained structures in animals following either short-term or chronic exposure, or human pathology studies in which the lung burdens of deceased individuals are correlated with their exposure history. Other information also comes from *in vitro* studies. Various, increasingly sophisticated models have also been developed to predict the individual and combined effects of these mechanisms.

6.2.1 Animal Retention Studies

Retention studies track the time-dependence of the lung burden of asbestos or other particulate matter (i.e., the concentration of particles in the lung) during or following exposure. Thus, such studies are designed to indicate the degree to which inhaled structures are retained. Depending on the time frame evaluated, however, effects due to deposition and those due to clearance may not easily be distinguished in such studies. Moreover, due to the near impossibility of isolating the various compartments of the lung when preparing for quantitative analysis of tissue burden (e.g., the pure respiratory components vs. the larger airways or the tissues directly associated with airway lumena vs. the underlying interstitium or endothelium), it is nearly impossible to separate the effects of the various clearance mechanisms, which typically operate over vastly different time scales (Table 6-2). This is why modeling has proven so important to distinguishing effects attributable to individual mechanisms.

Results from retention studies must be evaluated carefully. In addition to the limitations highlighted above, the lung burden estimates from such studies may be affected by the manner in which asbestos is isolated from lung tissue for measurement and the manner in which the concentration of asbestos is quantified (Chapter 5). For example, lung burden estimates may vary substantially depending on what portions of lung parenchyma are sampled or whether whole lungs are homogenized. Results may also vary depending on whether lung tissue is ashed or dissolved in bleach during sample preparation. More importantly, because several clearance

mechanisms are affected by the size and even the mineralogy of the structures being cleared, studies (particularly older studies) that track lung burden by mass or by total fiber number may not adequately capture such distinctions.

6.2.1.1 Studies involving short-term exposures

The latest retention studies tend to focus on the fate of long fibers (typically those longer than 20 μm) in support of the generally emerging recognition that these are the fibers that cannot be readily cleared from the pulmonary compartment of the lung and that, not coincidentally, contribute most to disease (further addressed in Section 6.4).

Hesterberg et al. (1998a), for example, tracked the time-dependent retention in rats of two fiber categories: (1) WHO fibers[1] and (2) WHO fibers longer than 20 μm for a range of man-made vitreous fibers (MMVF's), a refractory ceramic fiber (RCF1a), and amosite following a 5-day (6 hr/day), nose-only exposure. Rats were sacrificed at intervals up to a year following exposure. The amosite was size-selected to contain a high proportion of fibers longer than 20 μm. Aerosol concentrations were also adjusted to maintain target concentrations of 150 f/cm^3 for long fibers for each sample tested. Airborne mass concentrations varied between 17 mg/m^3 for amosite to as much as 60 mg/m^3 for the other fiber types. Lungs (without trachea or main bronchi) were weighed and stored frozen. For analysis, each lung was dried to constant weight, minced, and a portion was ashed. The ashed portion was further washed with filtered, household bleach, then filtered and applied to an SEM stub. Fiber numbers and dimensions (in both aerosols and tissue) were determined by SEM with a minimum of 200 fibers counted. In addition, analysis continued until a minimum of 30 fibers longer than 20 μm were counted.

In their study, Hesterberg et al. (1998a) tracked the ratios of retained fiber concentrations with time to the concentration retained 1-day following cessation of exposure. The observed time-dependent decay in these ratios were then fit to one-pool (single first order decay) or two-pool (weighted sum of two first order decays) models. With zero time assumed to be the time immediately following cessation of exposure. The authors recognize that at least some clearance likely takes place during the 5 days of exposure so they expected the assumption that retained concentrations at the end of exposure on day 5 to be equal to deposited concentrations would cause their analysis to slightly underestimate clearance rates. They also recognized that waiting 24 hours after cessation of exposure to measure retention allows some short-term clearance of upper airways, so that they expected their analysis would better focus on slower clearance from deeper in the lung.

Results reported by Hesterberg et al. (1998a) indicate that the dimensions and concentrations of fibers in aerosols from the five synthetic fibrous materials were all similar, but that the amosite aerosol contained a substantially greater number of fibers (including the longest fibers) and that the fibers, on average, were somewhat shorter and substantially thinner than the other aerosols. Of the fibers initially deposited in the lung (based on measurements made 1 day following cessation of exposure), comparable fiber numbers of long (>20 μm) fibers were retained across

[1]WHO fibers are those longer than 5 μm, thinner than 3 μm with an aspect (length to width) ratio greater than 3 (WHO 1985).

all six fiber types. Deposited concentrations of fibers 5–20 μm in length were more variable, but values within one standard deviation still overlapped. About 6 times as many short amosite fibers (<5 μm) were initially deposited than for any of the other fiber types. The authors also indicate that the dimensions of retained fibers were generally shorter and thinner than the original aerosol and were much more similar across retained fiber types than the original aerosols.

Clearance of long fibers (>20 μm) for all six fiber types could best be described using a two-pool model. The first pool cleared relatively rapidly (within the first 90 days) and represented a minimum of 65% of the lung burden observed 1 day following exposure. The second pool cleared much more slowly. For amosite fibers in the second pool, during the approximately 275 days of clearance, retention was only reduced to 80% of the 90-day value. In contrast, all five of the synthetic fibers were reduced to less than 30% of their 90-day value during this period. For amosite, the first pool decayed with a half-life of 20 days (90%CL: 13–27) and all of the other fibers with half-lives of 5–7 days (with varying confidence bounds). For the slower pool, amosite fibers exhibited a half-life of 1,160 days (90% CL: 420–∞) with the other fibers showing half-lives varying between 24 and 179 days. The combined, weighted half-life for amosite was 418 days (90%CL: 0–1060). The authors also note that data reanalyzed from an earlier study (Hesterberg et al. 1996) indicate a corresponding weighted half-life for crocidolite of 817 days (246–∞) and indicate that this was best fit using a single exponential (a one-pool model).

Hesterberg et al. also indicate that in this and previous studies approximately 20–60% of long fibers typically clear from the lung within 2 weeks post-exposure. They further suggest that this rapid clearance may be attributable to muco-ciliary clearance from the upper respiratory tract. They further report from the present study that short amosite fibers cleared much more rapidly than long fibers. Fibers <5 μm in length were reduced by 90% in the first 90 days (in comparison to 65% for long fibers). However, from 90 to 365 days, little or no clearance was observed for amosite fibers of any length.

For four of the synthetic fibers, long fibers cleared at the same rate as short fibers (all more rapidly than amosite) and the authors report that the data suggest transverse breakage for these fibers. Moreover, they attribute the more rapid clearance of long fibers among the MMVF's to dissolution, since these fibers exhibit *in vitro* dissolution rates that are rapid relative to the time scale of macrophage clearance. One synthetic fiber MMVF34, which is a stonewool, disappeared much more rapidly than any other fiber and the long fibers disappeared more rapidly than the short fibers. MMVF34 shows the greatest *in vitro* dissolution rate at neutral pH for any of the fibers tested in ths study and dissolves particularly rapidly at pH 4.5 (the pH found in the phagosomes of macrophages). The authors postulate that clearance of all of the synthetic fibers are enhanced over amosite by dissolution and breakage.

In summary, Hesterberg et al. (1998a) observed that:

- multiple clearance mechanisms (operating over multiple time scales) contribute to clearance;

- for sufficiently soluble fibers, long fibers clear more rapidly than short fibers;

- for insoluble fibers, a subset of long fibers clears rapidly within the first few months following exposure and the remaining long fibers clear only extremely slowly, if at all;

- short fibers of all types are cleared at approximately the same rate (much more rapidly than long, insoluble fibers);

- a small, residual concentration of short fibers may not always clear and may remain in the lungs (sequestered in alveolar macrophages) for extended periods; and

- in this study, there is some suggestion that short amosite fibers clear somewhat more slowly than short fibers of the other, non-asbestos mineral types studied.

Regarding the last observation, whether this is attributable to differences in fiber thicknesses among the various mineral types, due to partial contributions (even among short structures) to dissolution, or due to a unique, toxic effect of amosite is unclear. However, the likeliest of these candidate hypotheses is that the effect is due to partial dissolution.

This general pattern of observations are consistent with the findings of most, recent retention studies following short-term exposure.

In an earlier study of similar design, Bernstein et al. (1996) evaluated the deposition and clearance of a series of 9 glass and rock wools. These authors similarly found that clearance could be modeled using a double exponential for all length fibers (in similar length categories of <5, 5–20, and >20 μm) and that for soluble fibers, long fibers clear more rapidly than short fibers (with the intermediate length fibers in between).

For the Bernstein et al. (1996) study, if one assumes that the pool of longer-lived fibers is representative of macrophage clearance, this suggests that the efficiency of clearance by macrophages decreases with increasing fiber length and that the longest structures are not phagocytized at all, so that they remain exposed to the extracellular medium where dissolution occurs. Lending further support to this interpretation, the authors also report that the clearance rate for long fibers correlate with measured *in vitro* dissolution rates at neutral pH while the clearance rates for short fibers neither correlate with *in vitro* dissolution rates at neutral pH or at pH 4.5. Although the latter pH corresponds to the pH found in the phagosomes of macrophages, there is likely too little fluid available in such organelles to support efficient dissolution. The authors also indicate that a sufficient number of fibers were counted during the study to suggest that breakage is not playing a role in clearance (except at very early times) and that the clearance rate for short fibers appears to be the same or slower than that observed for nuisance dusts.

In another, earlier study of similar design Eastes and Hadley (1995) evaluated four types of MMMF's and crocidolite. All of the samples (including crocidolite) had been size-selected to assure a large fraction of fibers longer than 5 μm. Unfortunately, due to differences in reporting, it is not possible to compare the initial loading of crocidolite fibers to those reported for amosite in the Hesterberg et al. (1998a) study. However, results from this study further support the physical interpretation of clearance suggested in the studies discussed above. In fact, the authors

report that the time-dependent size distribution of retained fibers observed in this study agree well with a computer simulation of fiber clearance. The simulation assumes that long fibers dissolve at the rate measured for such fibers *in vitro* and that short fibers of every type are removed at the same rate as short fiber crocidolite (which is practically insoluble). This is strong evidence that short fibers are cleared by macrophage phagocytosis and that long fibers cannot be cleared by macrophages, but may dissolve in extracellular fluid provided that they are sufficiently soluble.

Regarding crocidolite, the data from the Eastes and Hadley (1995) study suggest that short crocidolite fibers appear to clear at a rate that is somewhat slower than observed for any of the short MMVF fibers. Importantly, however, the interpretation of short fiber clearance in this paper is somewhat confounded because, unlike the studies discussed above, short fibers in this paper are defined as all fibers <20 μm, so there may be some confounding with MMVF fibers that are dissolving. As previously indicated, the Hesterberg et al. (1998a) work also suggests that short asbestos (amosite) fibers may clear more slowly than short fibers of differing mineralogy and Hesterberg et al. only includes fibers <5 μm in their definition. Nevertheless, it is still possible that some effects due to dissolution may still be affecting the clearance of these shorter fibers.

Surprisingly, a visual inspection of the data presented in Eastes and Hadley (1995) table suggests a lack of any long-term clearance for long fiber crocidolite (>20 μm). Yet, the authors model long fiber crocidolite clearance using a single exponential (suggesting no rapidly clearing compartment). The long-term half-life reported for crocidolite in this study is approximately 220 days (with estimated CIs of 165–566 days). This overlaps with the long-term clearance half-life reported by Hesterberg et al. (1996) for crocidolite of approximately 820 days (246–∞).

Equally surprising, Hesterberg et al. (1998a) also modeled crocidolite clearance as a single exponential, which might suggest better penetration to the deep lung by crocidolite, less clearance by muco-ciliary transport or alveolar macrophage transport, or better penetration to the interstitium than other fibers. More likely, however, it may simply indicate that the two-pool model does not represent a statistically significant improvement in model fit over the one-pool model. However, relative size distributions would need to be evaluated carefully before drawing any such conclusions. Eastes and Hadley (1995) also report clearance of short fiber crocidolite is modeled as a double exponential with short and long half-lives of 25 and 112 days, respectively. Since this fiber category contains fibers up to 20 μm in length (in this study only), this does suggest at least some contribution from muco-ciliary and alveolar macrophage mediated clearance for crocidolite.

In two studies, Coin et al. (1992, 1994) evaluated the fate of chrysotile fibers in rats exposed for 3 hours to 10 mg/m^3 (reportedly containing >5,000 fibers longer than 5 μm/cm^3). For lung analysis, the left lung was separated into peripheral and central regions under a dissecting microscope. Slices of peripheral and central portions were separately weighed and minced. Tissue was digested in sodium hypochlorite and then filtered. A quality control test indicated that the digestion process caused a slight (~10%) decrease in fiber number and slight decreases in fiber diameter and fiber length. Fiber-size distributions were evaluated by SEM. A stratified counting procedure was employed to assure equal precision for each length category of interest. Measurements for each category were then converted to mass equivalents.

Results from the Coin et al. (1992, 1994) studies indicates no difference between deposition in central or peripheral regions of the lung. They also confirm that chrysotile splits longitudinally in the lungs with a half-life that is competitive with the clearance rates measured in this study. Clearance was found to be very length-dependent, so that rates decrease from a half-life of about 10 days for fibers about 4 μm in length, through 30 days for fibers 8 μm, to 112 days (which is no different from zero) for fibers longer than 16 μm (all after adjusting for longitudinal splitting). Importantly, the brief follow-up period (30 days) is too short to provide an adequate evaluation of the longer term clearance pools observed in other studies and certainly too short to evaluate any effects potentially associated with chrysotile dissolution. Also, that the decay curves for clearance were limited to four points, makes evaluation of the slopes for these curves highly uncertain.

Coin et al. (1992, 1994) also report that the mass of chrysotile deposited during these short exposures (i.e., no more than 20 μg) is very small compared to levels at which overload has been reported to occur (approximately 1 mg, see, for example, Yu and Yoon 1991) and that the volume of the 16 μm fibers, which have an average diameter of 0.2 μm and therefore a mean volume of 0.5 μm^3, is small relative to the volume at which macrophage clearance of non-fibrous particles is reported to be hindered (Morrow 1988). Thus, the authors conclude that fiber length presents an additional constraint on macrophage clearance, independent of any other overload. They also indicate that inhibition of clearance due to fiber length is independent of fibrosis.

Coin et al. (1992, 1994) also discuss the effect of fibrosis on clearance. They indicate that, although increased concentrations of short fibers are observed in focal areas of fibrosis, it is more likely that such fibers accumulate because clearance is hindered by fibrosis in these areas than the hypothesis that the short fibers are causing fibrosis. This is because, as they point out, there are too many studies demonstrating the lack of ability of short fibers to induce fibrosis.

Evidence in the Coin et al. (1992, 1994) studies suggests that no translocation from central to peripheral regions of the lung were detected. An upper bound rate that is about 20% of clearance is reported. However, the short follow-up time in this study would have precluded slower processes from being detected. Despite the lack of evidence of translocation, the authors report that duct bifurcations in peripheral regions of the lung where fibers are deposited are no more than 1–2 mm from the visceral pleura. In fact, in the 1994 study, the authors show that 50% of the primary duct bifurcations in the peripheral portion of the rat lung occur within 1 mm of the visceral pleura and some occur as close as 220 μm. Deposited fibers may also affect the pleura by inducing generation of diffusable, inflammatory agents.

A short-term inhalation study by Warheit et al. (1997) evaluated retention of chrysotile and aramid fibers. In this study, rats (and hamsters) were exposed, nose only, for 6 hours/day, 5 days/week for 2 weeks by inhalation to UICC chrysotile and p-aramid fibers (each at two doses of 460 or 780 fibers/ml, although the size range of these fibers is not stated nor is the manner in which they were analyzed). Fixed lungs were digested in chlorox during preparation for asbestos analysis. Animals were followed for up to a year post-exposure.

As in studies described above, results from the Warheit et al. (1997) study indicate rapid clearance of short chrysotile fibers, but slow to non-existent clearance of fibers longer than 20 μm. In contrast, aramid fibers apparently degrade and are subsequently cleared fairly rapidly

in vivo. Based on the data provided in figures, although the reported concentrations of chrysotile and aramid fibers to which animals were exposed were equivalent, at both the lower and higher concentrations, it appears that rats initially retain 3 to 5 times as many aramid fibers as chrysotile fibers (at least for the size range counted, which was not reported). For both fiber types, clearance appears rapid for an initial period of approximately 90 days post-exposure. During this time, the mean length of chrysotile fibers also appears to increase steadily, which suggests rapid, preferential clearance of short structures. After the initial period, it appears that (as the authors suggest), a residual concentration of longer fibers are cleared only very slowly, if at all.

Oberdorster et al. (1988) instilled a 3 ml suspension of irradiated amosite into the bronchio-alveolar space of the right diaphragmatic lobe of the lungs of dogs to evaluate clearance and transport. The amosite used was modified by sedimentation from UICC amosite to contain only fibers shorter than 20 μm. One dog also had unmodified UICC amosite instilled directly into a lymph node in the thigh. The dogs had been cannulated to allow collection of lymph from the right lymph duct-RLD and the thoracic duct-TD (both in the neck).

Results from Oberdorster et al. (1988) indicate that within 4 hours following instillation in the lung, low activity was noted in postnodal lung lymph, but not in either the RLD or TD. Within 24 hours, however, activity and fibers (determined by SEM) were observed in both the RLD and the TD. The median length of fibers observed in the lymph were significantly longer than the instilled material, although there appeared to be a cutoff length of 16 μm in fibers observed at nodes and 9 μm in fibers observed directly in lymph. Fibers recovered from lymph were also significantly thinner and appeared to exhibit an absolute cutoff at a maximum width of 0.5 μm. Fibers recovered from the TD and RLD in the dog that had unmodified UICC amosite instilled directly into leg lymph were all short (with a maximum length of 6 μm). Since collection times were all short, the authors indicate that it is unknown whether longer fibers would have been observed at later times. The authors also note the almost total absence of fibers shorter than 1 μm in lymph, which they assume are cleared rapidly and efficiently by alveolar macrophages.

Oberdorster et al. (1988) also report that a rough calculation, based on the fraction of the material originally instilled that was recovered in the first 24 hours, it would take approximately 6 years to clear all of the instilled asbestos (assuming no other clearance mechanisms were active).

Everitt et al. (1997) performed a short-term inhalation study that is interesting, particularly, because it focused on pleural (as opposed to lung) fiber burden. The authors exposed rats and hamsters to one type of refractory ceramic fiber (RCF-1) by nose-only inhalation for periods of 0, 4, and 12 weeks and animals were held for observation for up to an additional 12 weeks post-exposure. Exposures were conducted for 4 hours/day, 5 days/week, at 45.6±10 mg/m^3. Groups of 6 animals were held for 0,4, 12, and 24 weeks to determine pleural fiber burden. An agarose casting method was reportedly used to recover fibers from the pleura. Analysis was by electron microscopy. Fibers were observed in the pleura at each time point examined (including samples from rats sacrificed immediately following the last day of a 5-day exposure). Fibers were all reported to be short and thin (geometric mean length: 1.6 μm with GSD: 1.8, geometric mean diameter: 0.1 μm with GSD: 1.5). Concentrations averaged approximately 40,000 fibers (per whole pleura, units not reported). The authors indicate that such fibers would not typically be

visible by optical microscopy. They also indicate that use of casts may be a more efficient method of recovering fibers from the pleura.

Everitt et al. (1997) indicate that observation of rapid translocation of short, thin fibers to the pleura has also been observed in studies of chrysotile so these results are not unique. Although it is stated that the mechanisms facilitating translocation are currently unknown, the authors indicate that their finding of site-specific mesothelial proliferation supports observations by Boutin et al. (1996) that asbestos fibers accumulate in the parietal pleura of humans at sites associated with lymphatic drainage. Kane and MacDonald (1993) have suggested that fibers are transported to these locations by pleural macrophages. However, the mechanisms by which fibers are transported from the lung to the pleura are still unconfirmed.

Older Retention Studies. Although the older retention studies generally support the results of newer studies (such as those cited above), older studies are sometimes limited by such things as the tracking of lung burden in terms of fiber mass or use of analytical techniques such as infrared spectroscopy for detection of asbestos, which are neither capable of distinguishing individual fibers nor provide any information on their sizes. Tracking of lung burdens in terms of mass may not reflect the fate of long, thin fibers, which (by increasing concurrence) appear to be the legitimate focus of studies evaluating biological hazards attributable to asbestos.

In two studies (Roggli and Brody 1984 and Roggli et al. 1987), Roggli and coworkers tracked the behavior of chrysotile (not UICC) and UICC crocidolite in rats following 1 hour exposure by inhalation to 3.5–4.5 mg/m^3 dusts. The authors indicate that this results in deposition of approximately 21 μg of dust. Portions of the lower lung lobes of selected rats were collected and digested for asbestos analysis using a scheme that was shown to be representative. To evaluate size distributions, more than 400 fibers from each sample were characterized by SEM. Fiber dimensions were then used to estimate total fiber mass.

Based on their study, Roggli and coworkers indicate that similar fractions of inhaled chrysotile and crocidolite dust are deposited in the lung during inhalation (23 and 19%, respectively). The authors therefore concluded that respirability and deposition do not depend on fiber type. Importantly, however, the manner in which this study was conducted does not facilitate distinguishing deposition in the deep lung from deposition in the upper respiratory tract.

Roggli and coworkers further indicate that clearance rates for the two fiber types appear comparable. Of the chrysotile initially deposited, they report that 81% of this material is cleared after 4 weeks. Similarly, 75% of the crocidolite is cleared. Importantly, because this is based on total mass (estimated by summing volume contributions from observed fibers), it may not reflect the specific behavior of long, thin structures. Therefore, it is difficult to compare such results with those of more recent studies. However, the authors do report that short structures are cleared more readily than long structures and that chrysotile is observed to split longitudinally *in vivo* (based on observation that the total number of chrysotile structures initially increases and the mean length increases). The authors further conclude that clearance rates appear to be independent of fiber type.

In another short-term study, Kauffer et al. (1987) report that the average length of retained chrysotile structures increases in rat lungs following 5-hours inhalation of chrysotile dust. Based

on their results, the authors report that fibers shorter than approximately 8 μm are preferentially cleared. Kauffer and coworkers also confirm that chrysotile fibers split longitudinally in the lung. In fact, several other studies (Kimizuka et al. 1987;Le Bouffant 1980) also provide supporting observations that chrysotile fibers (or bundles) split longitudinally in the lung.

In two studies (Morgan et al. 1978, 1980), Morgan and coworkers report on the fate of fibers following short-term inhalation of radio-labeled fibers by rats. In the first study (Morgan et al. 1978), rats inhaled UICC anthophyllite at 35 mg/m^3 for a total of 8.4 hours spread over 3 days. The authors report that the rats retained approximately 190 μg of dust at the end of exposure, mostly in the alveolar region; the authors assumed that conducting airway clearance is sufficiently rapid to clear this portion of the lung within a few days. Beginning about 7 days following exposure, the rats were then sacrificed serially for a period up to 205 days following exposure. Because anthophyllite fibers are relatively thick, fibers were analyzed by optical microscopy. Fibers were determined both in free cells (mostly macrophages) recovered in bronchopulmonary lavage and in lung tissue. Tissue samples and cells were digested in KOH and peroxide in preparation for fiber analysis.

Based on this first study, Morgan et al. (1978) report that anthophyllite lung content declined steadily by a process that could be described as a simple first order decay with a half-life of approximately 76 days. Free macrophages recovered by lavage, initially contained about 8 pg and this too declined steadily with a half-life of about 49 days. The authors further indicate that, if the number of macrophages remains constant with time (i.e., they are replaced at the same rate they are cleared), then the decay of the load in the macrophages should match what is observed in the rest of the lung. They suggest that the discrepancy may be due either to an influx of an increasing number of macrophages in response to injury with time and/or to transfer of some fibers through the alveolar wall. They also cite unpublished work indicating that uptake of fibers by alveolar macrophages is essentially complete within hours after cessation of exposure.

The authors also report that, initially, the lengths of fibers recovered in lung lavage was greater than in the original aerosol, but that the prevalence of the longest fibers decreased after the first 7 days. In lung tissue, however, the fraction of longer fibers (among total fibers) steadily increased with time. This suggests rapid clearance of naked fibers by muco-ciliary transport (which is a length independent process) with later times dominated by slower clearance in the deep lung by alveolar macrophages, which is a length-dependent process.

Morgan and coworkers also radiometrically determined the fraction of fibers in rat feces (prior to sacrifice). They assumed that after 14 days, this would represent the fraction of asbestos cleared primarily from the alveolar region of the lung. Initially 1.4% of lung anthophyllite content was excreted daily, but this fell to 0.5% after 120 days. The authors indicate that this suggests that the elimination from asbestos in lung tissue cannot be described by a single exponential because multiple processes are involved and that, over longer periods of time, the slower processes become increasingly important.

In the second study, Morgan et al. (1980) track the fate of several size-selected radiolabeled glasses in rats, again following short-term inhalation. From an analysis of the size dependence of deposited fibers in this study, the authors suggest that alveolar deposition in the rat is limited to structures with aerodynamic equivalent diameters less than about 6 μm and that deposition in

this region of the lung falls precipitously for fibers with thicknesses between about 2 and 3 μm (aerodynamic equivalent diameter). For fibers that are the density of asbestos, this represents an upper bound limit to alveolar deposition for the absolute thickness of a fiber of approximately 1.5 μm with fibers deposition of fibers thicker than approximately 0.7 μm being drastically reduced. This is in concordance with conclusions concerning deposition provided in Section 6.1.4. Alveolar deposition efficiency is also shown to decrease with increasing fiber length, at least for fibers longer than approximately 8 μm, also in concordance with findings presented in Section 6.1.4.

Intratracheal Instillation. The fate of fibers following intratracheal instillation into the lungs has also proven informative in some studies. For example, Wright and Kushner (1975) intratracheally instilled paired samples each of several types of glass fibers, fluoramphibole, and crocidolite into guinea pigs. For each mineral tested, a sample with predominantly short structures (25 mg total dose for crocidolite, reportedly 99% <5 μm) and another with predominantly long structures (4 mg total dose for crocidolite, reportedly 80% >10 μm) were evaluated. Unfortunately, the authors do not report how fibrous structures were characterized. Results in the cited paper report observations only after 2 years following the last injection.

Wright and Kuschner (1975) report that long structures uniformly caused fibrosis (primarily involving the respiratory bronchioles and alveoli and abutting the terminal bronchioles) while the short structures were uniformly phagocytized and generally removed to thoracic lymph nodes. Among other things, clearance to lymph suggests that fibers reached the interstitium (Section 6.2.5). It is interesting that, even after 2 years of recovery, the authors observe elevated levels of macrophages in the alveoli of animals dosed with short structures. Based on the relative size distributions of the samples analyzed, the authors report that structures up to 10 μm in length appear to be efficiently scavenged by macrophages. Based on the observation of larger numbers of short structures than expected in comparison with their fractions in the original samples, the authors further conclude that glass structures underwent biodegradation so that longer structures broke down into shorter structures that could be phagocytized.

Wright and Kuschner (1975) also report that long fibers are occasionally visible within the fibrotic interstitium of dosed animals. The long-fiber dosed animals also show macrophages in hilar lymph nodes containing fibers that are too small to resolve and all of them are short. In short-fiber dosed animals, some fibers are seen to remain in the lung within aggregates of macrophages, both in alveoli and the interstitium. Short-fiber dosed animals also show many more macrophages within the hilar lymph nodes than long-fiber dosed animals.

In two reports of the same study (Bellman et al. 1986, 1987), Bellman and coworkers followed the fate of UICC chrysotile, UICC crocidolite, several fibrous glasses, and other manmade mineral fibers following a single intratracheal instillation of 0.3 ml of fibrous material in rats. Groups of rats were then sacrificed at 1, 6, 12, 18, and 24 months following instillation. Lungs were low temperature ashed and the resulting, filtered suspension analyzed by transmission electron microscopy. Some of the fiber types were also acid treated with 0.1 M oxalic acid for 24 hours prior to instillation.

Bellman and coworkers (1987) report that short fibers (<5 μm) from all of the fiber types were shown to be cleared from the lungs with half-lives of approximately 100 days, with the asbestos

varieties tending to exhibit slightly longer half-lives than the other fibers. Short crocidolite fibers exhibited a half-life of 160 days. The half-life for clearance of short chrysotile was reported to be 196 days (the longest of all). However, this was attributed to positive contributions from breakage of longer fibers.

Bellman and coworkers (1987) report that the behavior of the different long fibers (>5 μm) for the different fiber types was radically different. The authors report no observed net decline in long crocidolite fibers over the 2 years of follow-up. The also report no observable changes in width of these fibers with time. In contrast, long chrysotile fibers increased in number with time throughout the 18-month follow-up period and this was attributed to longitudinal splitting. The width of these fibers reportedly decreased with time.

Bellman et al. (1987) also report that a more detailed examination of the time dependence of the width of chrysotile fibers indicates a rapid increase in the number of thin fibrils (<0.05 μm in width) and thin bundles (<0.1 μm in width) within 100 days (at the expense of thicker bundles). The authors suggest that this would result in rapid decrease in the number of chrysotile structures visible by optical microscopy and, possibly, increased clearance of the thinnest fibrils by dissolution, but this study shows no increased rate of clearance for thinner chrysotile structures compared to thicker structures (when viewed by electron microscopy). In contrast, long chrysotile fibers that were acid-leached prior to instillation reportedly disappeared with a half-life of 2 days.

Generally, the rate of clearance of the long fractions of the other fibers reported in the Bellman et al. (1986, 1987) papers varies as a function of solubility and overall thickness. Importantly, all half-lives are reported to have high standard errors in this study, due to the small number of animals included for examination.

In summation, virtually all short-term retention studies indicate that:

- fibers retained in the lung tend to be shorter and thinner than the aerosols from which they derive and the size distributions of retained structures tend to be more similar overall than the size distributions observed in the original aerosols;

- chrysotile asbestos undergoes rapid, longitudinal splitting in the lung while amphiboles do not;

- by mass, chrysotile and amphibole asbestos are deposited in the lung with comparable efficiencies, although it is not clear whether chrysotile dusts tend to contain sufficient numbers of curly fibers to limit deposition in the deep lung;

- multiple clearance processes operate over different time frames and some of these processes are strongly length-dependent. Fibers shorter than approximately 10 μm appear to be cleared rapidly relative to longer fibers and those longer than approximately 20 μm are not cleared efficiently at all (if the fibers are insoluble). The Bellman et al. (1986, 1987) studies appear to contrast with other studies in this regard in that they suggest fibers longer than 5 μm do not readily clear;

- the quickest clearance process (presumably muco-ciliary clearance) is not dependent on length; and

- the effects of fiber diameter on clearance have not been well delineated overall, although fibers that reach the deep lung appear to be largely limited to those thinner than approximately 0.7 μm.

These findings are in addition to those mentioned previously from the newer studies:

- multiple clearance mechanisms (operating over multiple time scales) contribute to clearance;

- for sufficiently soluble fibers, long fibers clear more rapidly than short fibers;

- for insoluble fibers, a subset of long fibers clears rapidly while the remaining long fibers clear only extremely slowly, if at all;

- short fibers of all types are cleared at approximately the same rate (much more rapidly than long, insoluble fibers);

- a small fraction of short fibers may be retained for long periods under certain circumstances (sequestered in alveolar macrophages) despite overall rapid clearance of these structures; and

- there is some suggestion that short asbestos fibers clear somewhat more slowly than short fibers of the other, non-asbestos mineral types studied.

Regarding specifically the clearance of long fibers, it appears that a component of all such fibers clears rapidly within the first 2 weeks and this likely represents muco-ciliary clearance. A second component (representing as much as 60% of the fibers) clears within 90 days and this likely represents clearance by alveolar macrophages. The remaining long fibers are cleared only very slowly, if at all, and this likely represents fibers that are sequestered in granulomas or that escape into the interstitium.

6.2.1.2 Studies involving chronic or sub-chronic exposures

Although the results of older retention studies following longer term (sub-chronic or chronic) exposure were difficult to reconcile with the results following shorter-term exposures, newer studies suggest greater consistency and a clearer picture of the fate of fibers in the lung. Moreover, although there are further suggestions of mineralogy (fiber type) dependent effects with some clearance mechanisms, it is important that size effects be considered simultaneously, if the dynamics of these processes are to be understood.

In some of the latest studies, for example, Hesterberg et al. (1993, 1995, and 1998b) exposed rats (nose only) by inhalation to a series of man-made vitreous fibers (including a variety of fibrous glasses, rock wools, and refractory ceramic fibers) and two kinds of asbestos: chrysotile (intermediate length NIEHS fiber) and crocidolite (size selected). Animals were dosed for 6

hours/day, 5 days/week for up to 2 years at target concentrations of 10–60 mg/m^3. The target concentration for chrysotile and crocidolite was 10 mg/m^3. Animals were periodically sacrificed during the exposure regimen to determine the character of the retained fibers. Vitreous fiber aerosols were characterized by PCM, SEM or, for chrysotile, by TEM. The right accessory lung lobe of sacrificed animals was tied off, frozen, and stored for lung burden analysis.

For analysis, lung lobes were dried to constant weight, ashed, the residue suspended in distilled water, and then filtered on Millipore filters (for examination by optical microscopy) or Nuclepore filters (for analysis by SEM or TEM for chrysotile). Approximately 100 fibers were reportedly characterized to establish fiber size distributions. However, this is problematic for this study because chrysotile asbestos concentrations in the aerosols to which the animals were exposed contained approximately 100 times as many fibers as the other aerosols. Thus, although no fibers longer than 20 μm were observed during characterization of the chrysotile, the concentration of such long fibers could still have been larger in this aerosol than the other aerosols and it would not necessarily have been observed. This is also true of lung burden analyses especially because indirect preparation tends to magnify the number of short chrysotile structures observed in a sample.

A comparison of the retention patterns of chrysotile and RCF-1 from the Hesterberg et al. (1998b) study is particularly instructive. First, it should be noted that, in contrast to the values reported by the authors of this study, chrysotile and RCF-1 in fact appear to exhibit comparable *in vitro* dissolution rates (12.7 vs. 8 ng/cm^2-hr, respectively) when rates are measured using comparable techniques (see discussion in Section 6.2.4). The dissolution rates quoted in the Hesterberg et al. study are not derived in comparable studies.

Although a full set of time-dependent analyses are apparently not available for chrysotile, it is reported that approximately 14% of those chrysotile WHO fibers observed to be retained after 104 days of exposure continue to be retained after 23 days of recovery. Under the same conditions, it is reported that 43% of RCF-1 fibers are retained, which suggests more rapid clearance for chrysotile. Even adjusted for the fraction of RCF-1 structures that are longer than 20 μm (and that are presumably cleared even more slowly), approximately 37% of the RCF-1 WHO fibers (<20 μm) are apparently retained over this period, which is still more than twice the rate reported for chrysotile. Still, more detailed characterization of the size distributions of these two fiber types would need to be evaluated before it could be concluded with confidence that chrysotile is cleared more rapidly than RCF-1 or that dissolution plays a role. In fact, dissolution would tend to cause more rapid clearance only of the longest fibers (i.e., the ones that cannot be cleared by macrophages [see Section 6.2.1.1]), which would further reduce the apparent retention rate of the shorter RCF fibers, making it even more comparable to the chrysotile number.

Based on these studies, Hesterberg et al. (1998b) report that fibers deposited and retained in the lung tend to be shorter and thinner on average than the sizes found in the original aerosol. It is also apparent from their data that long RCF-1 fibers clear more rapidly than short RCF-1 fibers (although a small fraction of long structures are retained at all time points following a recovery period after cessation of exposure), which is consistent with observations in other studies for fibers that dissolve at moderate rates. In the short-term study performed by the same laboratory, Hesterberg et al. (1998a), long fiber (>20 μm) RCF-1a appears to clear at approximately the

same rate as the shorter structures (<5 μm), although the scatter in the data (and an unexplained initial rise in long-fiber RCF) prevent a more careful comparison. Similar results are also apparent in the data presented for MMVF21. It should be noted that the dissolution rates for RCF-1 and MMVF21 bracket the estimated dissolution rate for chrysotile asbestos (when the three are derived from comparable studies [see Section 6.2.4]).

The data presented in Table 3 of Hesterberg et al. (1998b), which are reproduced in Table 6-3, can also be used to evaluate the time-trend of retention during chronic exposure. The values presented in Columns 2, 4, and 6 of Table 6-3 present, respectively, measurements of the lung burden for chrysotile WHO fibers, RCF-1 WHO fibers, and RCF-1 long WHO fibers (>20 μm) in animals sacrificed immediately following cessation of exposure for the time period indicated in Column 1. Unlike results reported in some earlier chronic studies based on mass (see below), there is no evidence from this table (based on fiber number) that chrysotile lung burdens reach a plateau. Rather chrysotile lung burdens (as well as RCF-1 lung burdens) continue to increase with increasing exposure.

The data presented in Table 6-3 can also be used to gauge the relative efficiency with which the chrysotile and RCF fibers are retained. Considering that the number of fibers inhaled (N_{inh}) over the period of exposure would be equal to the product of the aerosol concentration (C_{air} in f/cm^3), the breathing rate of the exposed animal (R_B in cm^3/week), and time (in weeks):

$$N_{inh}=C_{air}*R_B*t \qquad \text{(Eq. 6-1)}$$

and the efficiency of retention is simply equal to the quotient of the number of fibers retained (N_{lung}) and the total number inhaled: N_{lung}/N_{inh}, then the efficiency of retention is estimated by the following simple relationship:

$$\text{Efficiency of retention}=N_{lung}/(C_{air}*R_B*t) \qquad \text{(Eq. 6-2)}$$

By rearranging Equation 6-2, one obtains:

$$\text{Efficiency of retention}*t=(N_{lung}/(C_{air})*(1/R_B) \qquad \text{(Eq. 6-3)}$$

Table 6-3. Fraction of Fibers Retained Following Chronic Exposure[a]

	Chrysotile		RCF-1			
Exposure Period	**WHO Fibers**	**Lung/ Aerosol Ratio**	**WHO Fibers**	**Lung/ Aerosol Ratio**	**Long WHO fibers**	**Lung/ Aerosol Ratio**
Weeks	**f/lung x 10^6**		**f/lung x 10^6**		**f/lung x 10^6**	
0.0357			0.009	4.81E-05	0.002	1.98E-05
13	250	0.024	39	0.209	3	0.030
26	180	0.017	56	0.299	6	0.059
52	1020	0.096	119	0.636	20	0.198
78	853	0.080	173	0.925	21	0.208
104	1600	0.151	143	0.765	25	0.248
Aerosol Concentration						
(f/ml)	10600		187		101	

[a]Source: Hesterberg et al. (1998b)

Because the breathing rate for the rats in the Hesterberg et al. (1998b) study can be considered a constant for all experiments, Equation 6-3 indicates that the slope of a plot of N_{lung}/C_{air} versus time should yield estimates of the relative efficiency of retention for each of the fiber types evaluated. The plot for chrysotile is presented in Figure 6-3. Results from this plot and similar plots for RCF-1 WHO fibers and long WHO fibers (data not shown), result in the following estimates of the relative efficiencies of retention (along with the corresponding R^2 value for the fit of the linear trend line):

chrysotile WHO fibers: 0.0014, R^2=0.856

RCF-1 WHO fibers: 0.0095, R^2=0.694

RCF-1 long, WHO fibers: 0.0026, R^2=0.880

Thus, it appears that chrysotile WHO fibers are retained somewhat less efficiently than either RCF-1 WHO fibers or RCF-1 long WHO fibers. However, whether this is due to less efficient deposition or more efficient clearance cannot be determined from this analysis. It is also not possible to determine whether such differences are due to the effects of differences in size distributions among the various fiber types. Interestingly, based on the data presented by Hesterberg et al., which indicates that long RCF-1 WHO fibers clear more rapidly than regular RCF-1 WHO fibers, the differences in the relative retention of these two length categories of fibers is due primarily to relative efficiency of clearance.

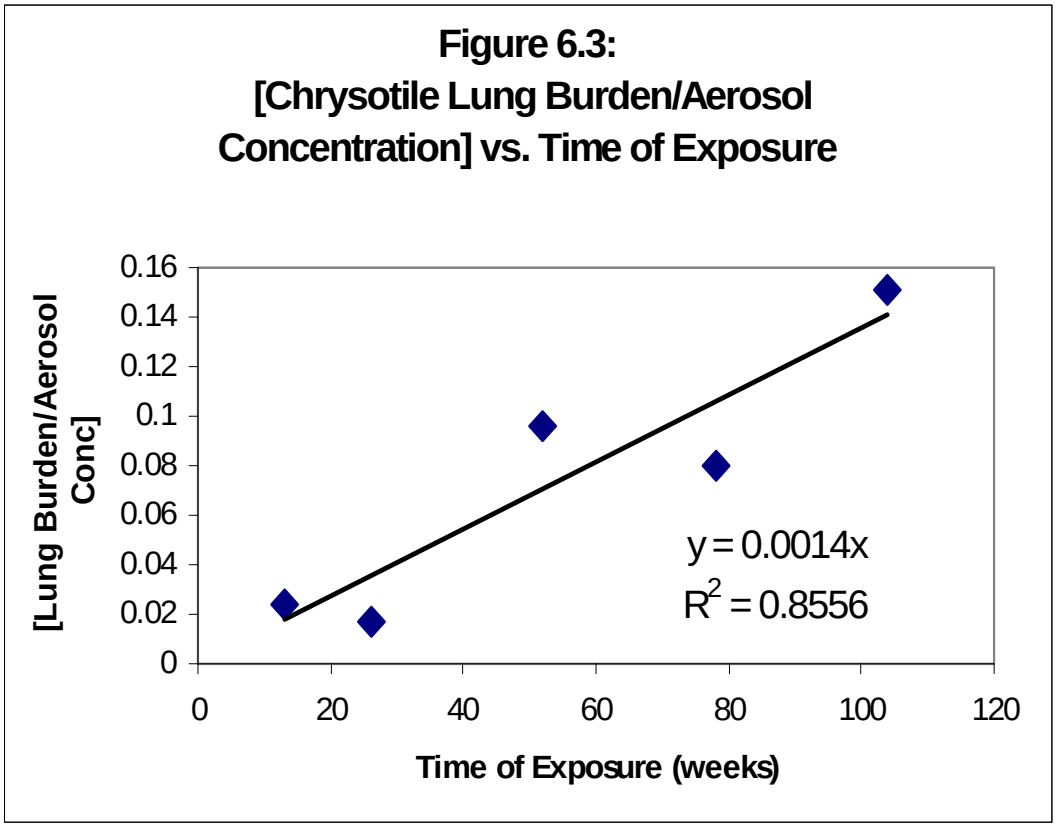

In a similar study involving chronic exposure to Syrian golden hamsters (Hesterberg et al. 1997), fiber retention and biological effects associated with exposure to amosite and a series of MMVFs were evaluated. The amosite was size selected and hamsters were exposed to one of three levels (0.8±0.2, 3.7±0.6, and 7.3±1.0 mg/m^3). Amosite lung burdens were shown to increase regularly with dose and time of exposure. The time dependence for accumulation of some of the MMVF's was more complicated. None of the animals were apparently followed for any recovery periods following cessation of exposure. The authors also indicate that the severity of the effects observed (inflammation, cellular proliferation, fibrosis, and eventually several mesotheliomas), appear to correlate well with the concentration of fibers longer than 20 µm.

Earlier Studies. Earlier studies, in which asbestos concentrations tend to be monitored as total mass tend commonly to show that chrysotile asbestos is neither deposited as efficiently as various amphibole asbestos types nor is it retained as long (i.e., it is cleared much more rapidly from the lungs). In fact, several such studies tend to show that chrysotile asbestos concentrations eventually reach a plateau despite continuing exposure, which suggests that clearance and deposition come into balance and a steady state is reached. In contrast, amphibole asbestos concentrations continue to rise with increasing exposure, even at the lowest exposure levels at which experimental animals have been dosed. Such observations do not appear to be entirely consistent with those reported in newer studies (see above) that track fiber number concentrations (in specific size categories). In these newer studies, chrysotile retention is not observed to level off, but continues to increase in a manner paralleling amosite or other fibers. As indicated below, however, the limitations associated with these older studies suggest that,

although it may not be easy to reconcile them quantitatively with the newer studies, results from these studies are not necessarily inconsistent with those of the newer studies. Moreover, the trends observed in the newer studies are likely more directly relevant to issues associated with the induction of asbestos-related disease. The problems with the older studies are:

- the trends seen in the older studies (based on mass) may mask the more important trends associated with deposition and retention of long, thin fibers. Thus, results from such studies may not be directly relevant to considerations of risk; and

- the observed differences between chrysotile and the amphiboles may be attributed to differences in size distribution (among other possibilities). Thus, lacking detailed information on size distributions, it is difficult to reconcile the results from the older studies with results from the newer studies, which explicitly track specific size ranges of fibers.

Given these limitations, the earlier studies are only mentioned briefly.

Middleton et al. (1979) tracked the fate of asbestos (as mass measured by infrared spectroscopy) in rats following inhalation of several asbestos aerosols (UICC chrysotile A, UICC amosite, and UICC crocidolite) at multiple concentrations (reported at 1, 5, or 10 mg/m^3). To account for possible differences in the nocturnal (vs. daytime) activity level of rats, several groups of rats were also exposed in a "reversed daylight" regimen (in which cages were darkened during the real day and bathed in light during the real night). Acclimatized rats in these groups were thus dosed at times corresponding to their night. Exposure continued for 7 hours/day, 5 days/week, for 6 weeks.

Results from the Middleton et al. (1979) study were fit to a three compartment model (originally proposed by Morgan et al. 1978) and the authors concluded that clearance was independent of fiber type, but that the initial deposition of fibers was very dependent on fiber type. This was indicated by a "K-factor" representing the efficiency of initial deposition. Chrysotile showed K factors that range between 0.17 and 0.36 and vary inversely with the initial exposure concentration. In contrast, amosite exhibits a K factor of 0.69 and crocidolite a K factor of 1.0 and both are independent of exposure level. Although the design of this experiment precluded fitting of the shortest two compartments of the model (with half-lives of 0.33 and 8 days, from Morgan et al. (1978), they did optimize the half-life of the longest compartment. Fibers in this compartment were cleared with a half-life of 170 days.

In a series of studies, Davis and coworkers (1978, 1980, 1988a, and 1988b) report that retention of asbestos (measured in terms of mass) appears to be a function of fiber type and surface charge in addition to fiber size. With regard to fiber type, for example, Davis et al. (1978) report that substantially more amphibole (amosite) asbestos appears to be deposited and retained in the lungs of exposed rats than chrysotile. Chrysotile is also apparently cleared more readily than amosite. However, mineralogical effects should only be judged after adjusting for fiber size.

Rats in the studies by Davis and coworkers were dosed at 6 hours/day, 5 days/week for up to 1 year at dust concentrations of 2, 5, or 10 mg/m^3 (depending on the specific experiment). Right lungs (used for determining lung burden) were ashed and the residue was washed in distilled

water and filtered. The residue was formed into a potassium bromide disc and asbestos (mass) content was determined by infrared spectroscopy.

Jones et al. (1988) report that the lung-tissue concentration of amosite increases continually with exposure (at 7 hours/day, 5 days/week for up to 18 months) and the rate of increase is proportional to the level of exposure. A leveling off of amphibole concentrations in lung tissue was not observed in this study as long as exposure continued, even for the lowest level of exposure (0.1 mg/m^3) studied. The lowest exposure concentration evaluated in this study is only 1% of the concentration at which chrysotile lung burdens were shown to reach equilibrium in other retention studies (see below). Importantly, however, these are only the older studies in which fiber burden is tracked by mass. The newer studies don't show this effect.

The authors also report lack of any apparent change in size distribution with time among the fibers recovered from the animal's lungs, which suggests lack of substantial clearance even of short fibers. However, the longest recovery period following the cessation of exposure evaluated in this study is only 38 days, which may be too short to allow evidence for differential clearance as a function of size to become apparent (at least in a chronic study; the time dependence in chronic studies such as this are more complicated than for short-term studies). Moreover, the apparent inclusion of lymph nodes as part of the lung homogenate may have caused short fibers initially cleared from the lung to be added back in. In this study, lungs were recovered intact including the associated mediastinal and hilar lymph nodes, which were ashed in toto. Ash residue was washed in acid and water, ultrasonicated and filtered for electron microscope analysis. Note that such a procedure would include any fibers cleared to local lymph nodes.

In a widely cited study, Wagner et al. (1974), report that amphibole lung burdens increase continually as long as exposure to amphiboles continues and that amphibole concentrations in lung tissue decrease only slowly following cessation of exposure. In contrast, chrysotile lung burdens reach a plateau despite continued exposure. Importantly, asbestos content was estimated by determining total lung silica content and adjusting for similar analysis on filtered samples of the original aerosols. Thus, in addition to suffering from the limitations associated with tracking fiber burden by mass, there are questions concerning the validity of using total silica to represent asbestos content. Therefore, for these reasons and the additional reason of the lack of controlling for fiber size, the ability to interpret this study and reconcile its conclusions with those of newer studies is severely limited.

Chronic Inhalation of Non-fibrous Particulate Matter. A recent study involving chronic inhalation of non-fibrous materials is helpful at elucidating the relative localization of particles in rats and primates. Nikula et al. (1997) studied lung tissue from a 2-year bioassay, in which Cynomolgus monkeys and F344 rats were exposed to filtered, ambient air or air containing one of three particulate materials: diesel exhaust (2 mg/m^3), coal dust (2 mg/m^3, particles <7 μm in diameter), or a 50/50 mix of diesel exhaust and coal dust (combined concentration: 2 mg/m^3).

Results from Nikula et al. (1997) indicate that responses to all three particulate materials were similar. The particles tended to localize in different compartments of the lung in a species-specific manner:

- 73% of particles remain in the alveolar lumen of rats, but only 43% in monkeys. The remainder can be found in the interstitium;

- in both the alveolar lumen and in the interstitium, virtually all of the particles are observed to be isolated within macrophages; and

- the particles in the interstitium reside in macrophages within the alveolar septa, the interstitium of respiratory bronchioles, the adventitia and lymphatic capillaries surrounding arterioles and veins of pulmonary parenchyma, or in the pleura.

It is not known whether free particles penetrate the epithelial lining of the airway lumena and escape into the interstitium or whether such particles are first engulfed by macrophages and then transported in their macrophage "hosts" into the interstitium.

Importantly, even after 2 years of exposure, the particles in the interstitium do not appear to have elicited a tissue response. Also, the aggregates of particle-laden macrophages observed in alveolar lumena elicited significantly less of a tissue response im monkeys than in rats. Such responses included: alveolar epithelial hyperplasia, inflammation, and focal septal fibrosis.

The authors further indicate that "epithelial hyperplasia concomitant with aggregation of particle-laden macrophages in alveolar lumen is a characteristic response to many poorly soluble particles in the rat lung, both at exposure concentrations that result in lung tumors and at concentrations below those resulting in tumors. Such a response, however, was not characteristic of what was observed in monkeys. Among other things, these differences in responses suggest that rats may not represent a good model for human responses to inhalation of poorly soluble particulate matter. It would also have been interesting had they tested a "benign" dust such as TiO_2.

In summation:

- results of (newer) sub-chronic and chronic retention studies are generally consistent with those of retention studies that track lung burden following short-term exposure (Section 6.2.1.1);

- there is some indication in these sub-chronic and chronic studies that chrysotile asbestos may not be retained as efficiently as amphibole asbestos. It is likely, however, that such distinctions are due more to fiber size than fiber type so that definitive conclusions concerning such effects cannot be reached until better studies that properly account for both size and type are conducted; and

- although earlier studies that track mass instead of fiber number suggest otherwise, chrysotile and amphibole asbestos concentrations (when measured by fiber number) continue to increase with time as long as exposure continues. Due to a lack in the ability to distinguish among size-dependent effects when lung burdens are tracked by mass, the results of the earlier studies are not necessarily inconsistent with the results of the later studies.

6.2.2 Animal Histopathological Studies

Studies in which the lungs of dosed animals are examined to determine the fate and effects of inhaled asbestos are helpful for understanding the movement and distribution of retained particles within the lung and surrounding tissue. Both the newest retention studies and the older retention studies tend to include at least some of this type of information. They also tend to indicate a consistent picture of the fate and effects of asbestos. While such studies tend to confirm that translocation in fact occurs, they are less helpful for elucidating the specific mechanisms by which translocation occurs.

Newer Studies. Ilgren and Chatfield (1998) studied the biopersistence of three types of chrysotile ("short chrysotile" from Coalinga in California, "long" Jeffrey fiber from the Jeffrey mine in Asbestos, Quebec, and UICC-B (Canadian) Chrysotile, a blend from several mines in Quebec). Both the Coalinga-fiber and the Jeffrey-fiber were subjected to further milling prior to use. In this study, rats were exposed via inhalation for 7 hours/day, 5 days/week for up to 2 years. Concentrations were: 7.78±1.46 mg/m^3 for Coalinga-fiber, 11.36±2.18 mg/m^3 for Jeffrey-fiber, and 10.99±2.11 mg/m^3 for the UICC-B fiber. An additional group of rats was also dosed for a single 24-hour period with Jeffrey-fiber at a concentration of 5,000 f/ml >5 μm. Estimates of lung content of chrysotile were based on measurements of total silica content. The character of the three chrysotile types evaluated in this study was previously reported (Campbell et al. 1980; Pinkerton et al. 1983). The animal studies were conducted previously with the overall approach reported by McConnell et al. (1983a,b) and Pinkerton et al. (1984). Based on the characterization presented in these papers, Coalinga-fiber is short, but not as extremely short as suggested by the authors:

Ratio of fibers longer than:	**5 μm:**	**10 μm:**	**20 μm**
Coalinga-fiber:	200:	78:	0.98
Jeffrey-fiber:	591:	220:	78

Such calculations also suggest that the single, "high" dose in this experiment was equivalent only to a concentration that is approximately 10 times the other concentrations studied, so that it is equivalent only to a 10-day exposure and small relative to the longer term (up to 2 years) exposures considered in this study.

Results reported by Ilgren and Chatfield (1998) indicate that the lung burden for short fiber chrysotile initially increases with exposure, reaches a steady state, and then decreases steadily following cessation of exposure. Approximately 95% of this material is cleared within 2 years. Thus, short fibers appear to exhibit the trend suggested by the older chronic retention studies that tracked burden by mass and is consistent with the newer studies indicating rapid clearance of short structures (Section 6.2.1.2).

In the studies reported by Ilgren and Chatfield (1998), most short fibers are found initially within alveolar macrophages and, while concentrations in Type I epithelium, interstitial cells, and interstitial matrix increase with time, little appears to be taken up by Type II epithelium. Small

amounts of short fiber chrysotile are also observed to be taken up by endothelial cells. There is also little sign of inflammation or fibrosis following exposure to the Calidria-chrysotile.

Jeffrey-chrysotile also initially appears to be taken up primarily by alveolar macrophages, but later becomes most prevalent in the interstitial matrix and, to a lesser extent, in interstitial cells. Substantial numbers of fibers are also taken up by Type I epithelium and small amounts by endothelial cells. Similar, but slightly delayed effects were seen for UICC-B chrysotile (which has a smaller fraction of long fibers and therefore, the authors suggest, takes longer to accumulate). Note that, by 12 months, the majority of long fibers from both these types were found in interstitial matrix while the majority of Calidria-material was still found in alveolar macrophages. This is consistent with observations concerning behavior between short and long fibers reported by Wright and Kushner (1975), Section 6.2.1.1. At this point, the Jeffrey-material also caused substantial thickening of the basement membrane and most fibers in the interstitium were trapped within the collagenous matrix. The authors note that some of the most severe interstitial changes occurred adjacent to areas of bronchiolar metaplasia. Such effects were not seen with Calidria-exposure.

Thickened basement membranes, calcium deposits, metaplastic changes, and structural abnormalities were all observed with long fiber exposure, but not with Calidria-exposure. Interstitial macrophages also showed morphological changes following phagocytosis of fibers. While Calidria-material was about evenly distributed between interstitial matrix and cells, the vast majority of long fiber material was found in the matrix. Movement into the matrix was also observed to increase even after exposure ceased. With time, the number of long fibers in interstitial cells declined modestly, but declined precipitously for Calidria-material.

Jeffrey-fibers accumulated in Type I epithelial cells during exposure and then levels decreased slowly after exposure ceased. UICC-B fibers accumulated more slowly, never reaching the same levels as for Jeffrey and decreased more rapidly. Concentrations of Calidria-fibers in Type I epithelial cells was low at all time points.

Type II epithelial cells accumulated very few fibers of any type (although they took up slightly more Jeffrey-fiber than the others). All three fiber types caused substantial increases in interstitial cells (mostly macrophages) at 3 months and this increase persisted for the Jeffrey-fiber, but decreased to background after 24 months for the other two fiber types. Fibroblast numbers also increased with the long fiber types, but not Calidria-chrysotile.

Type II epithelial cells showed decreases in volume and number that persisted until exposure to long fiber ceased and these cells displayed dramatic structural aberrations despite absence of a fiber load. One possible explanation for the observed changes in Type II cells, especially the reduction in their number, is that they were undergoing terminal differentiation to Type I cells (see Section 4.4). In fact, the apparent absence of fibers observed within Type II cells might be explained by such cells taking up fibers, but being induced to terminally differentiate, once fibers are accumulated. Overall, Type II cells displayed greater cellular response than Type I cells (which might also suggests a role for cytokines). All effects were observed to be fiber length dependent and all were exaggerated following exposure to long fiber material.

Rats exposed to long fiber had numerous accumulations of dust-laden interstitial macrophages and/or small focal accumulations of dust within the interstitium at the end of the lifetime study, but such changes were not observed for Calidria-exposed animals.

The lung burden for rats exposed to the single, "high" Jeffrey-fiber exposure (based on total silica) at 12 months (i.e., 12 months post-exposure) was not different from controls. Therefore, the authors conclude that short-term, "high" exposures are rapidly cleared (even exposures containing substantial quantities of long fibers). Other changes induced by the single, short-term high exposure of Jeffrey-fiber that was followed for 24 months also showed reversion to close to background status. Importantly, these observations are not based on quantitation of fiber burden in lung tissue. Rather they are inferred by observing the effects caused by the presence of fibers. This may suggest, for example, that more than 10 day's worth of exposure would be required at this level of exposure before irreversible lesions develop.

In the study by Hesterberg et al. (1997), which was previously discussed (Section 6.2.1.2), the authors note (among dosed hamsters) that the magnitude of cellular effects appeared to differ among the fibrous glasses as a function of their relative biodurability. For animals dosed with the least biopersistent glass, only transient effects (influx of macrophages, development of microgranulomas) were observed and these did not progress further. For the more persistent glasses, injury progressed through more intense inflammation, interstitial fibrosis, pleural collagen deposition, mesothelial hypertrophy and hyperplasia and eventually, mesothelioma. The authors also suggest that amosite appears to be more potent than chrysotile, even when aerosols contain comparable numbers of fibers longer than 20 μm.

Choe et al. (1997) exposed rats to chrysotile and crocidolite (both NIEHS samples) by inhalation for 6 hours/day, 5 days/week, for 2 weeks. The rats were then sacrificed and their pleural cavities lavaged. Results indicate that significantly more pleural macrophages were recovered in plueral lavage fluid at one and 6 weeks following exposure than sham exposed rats. The centrifuged pellet from pleural lavage fluid from one of four rats also exhibited long (>8 μm), thin (<0.5 μm) crocidolite fibers (1 week following exposure). The concentration of fibers in this pellet suggested approximately 1 f per 4,000 cells in the pleura. Note that chrysotile rats were not examined for fiber content.

Older Studies. In the series of studies by Davis et al. (1978, 1980, 1985, 1986a), the authors generally report similar histopathological observations that emphasizes a marked distinction between effects from long and short fibers. From the 1986 study, for example, Davis et al. report that at the end of 12 months of exposure, rats exposed to long fibers (amosite in this case) exhibited deposits of granulation tissue around terminal and respiratory bronchioles. They further indicate that the granulation tissue consists primarily of macrophages and fibroblasts with occasional foreign body giant cells.

As the animals aged, there was increased evidence of collagen deposits in these lesions and the oldest lesions consist mainly of acellular, fibrous tissue. The alveolar septa in these older animals showed progressive thickening. Initially, this was apparently due primarily to hyperplasia of Type II epithelial cells, but with time was increasingly due, first, to reticulin and, later, to collagenous deposits in the septal walls. Asbestos dust was frequently visible in these deposits. Epithelial cells lining alveoli adjacent to the oldest lesions also tended to become

cuboidal in shape. As the animals aged, these areas of interstitial fibrosis became more extensive.

In contrast, animals exposed to short fibers (also amosite in this case) showed no such lesions (peribronchial fibrosis) at any point in time. At the end of exposure, the lungs of these animals contained large numbers of pulmonary macrophages packed with fibers, but these cells remained free in the avleolar spaces. The authors report that large numbers of laden macrophages sometimes aggregated in alveoli close to respiratory bronchioles, but that there would be no formation of granulation tissue or thickening of alveolar septa at these locations. Thus, with the exception of the presence of dust-laden macrophages, the structure of the lung of these rats was not altered.

In the Davis et al. (1987) study of chrysotile, a slight variation of the above scenario is worth noting. In this study, the development of peribronchial fibrosis was reported for animals dosed both with the long fiber material and with the short fiber material. However, the authors also report that the short fiber chrysotile in this study in fact contains a sizable fraction of longer structures and this finding was corroborated by more formal size characterization (Berman et al., unpublished) later conducted in support of a study to evaluate the effects of size (Berman et al. 1995).

In this study, Davis et al. also reported observations on the morphological changes observed in the mesothelium during these studies. The authors indicate that the older animals in these studies exhibit “areas of vesicular pleural metaplasia consisting of loose, fibrous tissue containing large vesicular spaces lined with flattened cells”. The authors also report that examination in previous studies indicates that these cells are of a mesothelial type.

Davis et al. report that, “...occasionally the walls between vesicular spaces were so thin that they consisted of two closely opposed layers of extended and flattened cells with no basement membrane in between them. Where cells were supported by areas of fibrous tissue, a basement membrane was present. While no method for the direct quantification of this pleural metaplasia has been developed, its occurrence is closely related to the presence of advanced interstitial fibrosis or adenomatosis in the lung tissue and it is particularly common where patches of this type of parenchymal lesion have reached the surface. It is not known whether such lesions are precursors to mesothelioma. Davis et al. also note that neither of the two mesotheliomas observed in this study showed histological patterns consistent with the observed vesicular hyperplasia.

Brody et al. (1981) tracked the distribution of chrysotile following inhalation by rats. Asbestos was initially deposited almost exclusively at alveolar duct bifurcations. In agreement with Pinkerton et al. (1986), the degree of deposition appeared to be an inverse function of the path length and bifurcation number for each alveolar duct. Uptake by macrophages and type 1 epithelial cells were observed following deposition. Asbestos was observed both in lipid vesicles and free in the cytoplasm of type 1 cells. After 8 days, alveolar duct bifurcations became thickened with an influx of macrophages. Asbestos was also observed in basement membrane below the epithelium. Apparently, structures had been transported through type 1 cells to the basement membrane. Once in the basement membrane, asbestos may enter the interstitium. Predominantly short structures were monitored in this study. Long structures were

not readily observed (but this is likely a counting problem; under such circumstances, short structures may serve as surrogates for the presence of other structures).

Intratracheal Instillation. Bignon et al. (1979) studied the rate of translocation of various materials in rats. Chrysotile, crocidolite, and glass fibers were intrapleurally injected into rats and their concentration was monitored as a function of time in lung parenchyma and other tissues removed from the pleura. Within 1 day following injection, asbestos was detectable in lung parenchyma. After 90 days, asbestos was found in all of the tissues analyzed. Based on the rate of translocation to the lung, crocidolite migrates about 10 times more rapidly than chrysotile (on a mass basis). The rate of migration of glass is in between the two asbestos types. Structures initially found in the lung were significantly shorter than the average size of structures injected. After 7 months, however, the average lengths of structures in all tissues monitored were longer than the average length of structures originally injected. Thus, short structures migrate more rapidly than longer structures (possibly by a different mechanism), but long structures eventually translocate as well. Within a target tissue, preferential clearance of short structures also contributes to observed increases in the average length of the structures with time.

Studies of Non-Fibrous Particulate Matter. Studies of the fate and effects of respirable, non-fibrous particulate matter provide evidence for at least one mechanism by which particles (and fibers) may be transported to the interstitium.

Li et al. (1997) evaluated the effect of urban PM 10, carbon black, and ultrafine carbon black on rats following intratracheal instillation (0.2 ml volume instilled containing between 50 and 125 μg of particles). After 6 hours, there was a noted influx of neutrophils (up to 15% of total cells observed in bronchioalveolar lavage–BAL fluid) and increases in epithelial permeability was surmised based on increased total protein (including increases in levels of lactate dehydrogenase, which is a marker for cell membrane damage) in BAL fluid.

Conclusions. Overall, observations among both the newer and the older studies (including the study by Wright and Kuschner 1975, see Section 6.2.1.2) tend to be highly consistent, particularly with regard to the distinction between the effects of short and long fibers. Typically, long fibers initially produce substantial inflammation characterized by an influx of macrophages and other inflammatory cells. Ultimately, exposure to such fibers cause thickening of alveolar septa (particularly near avleolar duct bifurcations) due to a combination of epithelial hyperplasia and deposition of reticulin and, later, collagen resulting in interstitial fibrosis. In contrast, short fibers cause an initial influx of macrophages and, long-term, show persistent accumulations of fiber-laden macrophages both in alveolar lumena and in pulmonary lymph nodes, but otherwise no structural changes are observed in the lung tissue of these animals.

These studies also provide ready evidence of the effects of fiber translocation, but generally offer only limited evidence for elucidating the mechanisms by which such translocation occurs. There is evidence that Type I (and possibly Type II) epithelium phagocytize particles and fibers and it is possible that such fibers may be passed through to the basement membrane and the interstitium. For Type I cells, the distance between the alveolar lumen and the basement membrane averages less than 1 μm in any case (Section 4.4). Certainly fibers are also observed in the interstitium. Particulate studies also indicate that oxidative stress induced by particulate matter and fibers may cause morphological changes in Type II cells with consequent loss of

integrity of the epithelium, which increases it's permeability overall and may also allow diffusional passage of particles and fibers.

6.2.3 Human Pathology Studies

Human pathology studies provide additional information concerning the nature of asbestos deposition, clearance, and retention. These are the studies in which lung burdens are measured in samples of lung tissue and correlated with the exposures received by the individuals from which the lung samples derive.

Among the advantages of human pathology studies is that they provide direct insight into the behavior of asbestos in humans. They are also limited, however, by the lack of ability to obtain time-dependent estimates of lung burden (because samples are derived from deceased individuals), by the manner in which lung tissue is stored (several of the fixatives employed to store tissue samples have been shown to enhance dissolution of asbestos (Law et al. 1990, 1991), by the manner in which samples are prepared for asbestos analysis, by the manner in which asbestos is analyzed, and by the limited ability to re-construct the uncontrolled exposures experienced by study subjects (Section 5.2).

Perhaps most importantly, the ability to construct anything but the coarsest quantitative comparisons across subjects is also typically limited by use of "opportunistic" tissue samples (i.e., use of samples that happened to have been collected and stored during autopsy or necropsy) because such samples are not controlled for location on the respiratory tree (i.e., the linear distance and branch number from the trachea) that is represented by the sample. Because it has previously been shown that deposition is a strong function of such location (see, for example, Yu et al. 1991), comparisons across lung samples not controlled for these variables are problematic. It has also been shown that samples collected from adjacent locations in lung parenchyma can in fact exhibit strikingly different fiber concentrations due specifically to the differences in the location of the respiratory tree represented by the alveoli and respiratory bronchioles in the spatially adjacent samples (Brody et al. 1981; Pinkerton et al. 1986 [Section 5.2]).

Despite the above indicated cautions, when interpreted carefully, human pathology studies can provide useful evidence regarding fiber deposition, clearance, and retention in the human lung.

Newer Studies. Among the most recent studies, Finkelstein and Dufresne (1999) evaluated trends in the relationship between lung burdens for different fiber types and different size ranges as a function of historical exposure, the duration of such exposure, the time since last exposure, and other variables. The analyses were performed among 72 cases from which tissue samples could be obtained (including 36 asbestosis cases, 25 lung cancer with asbestosis cases, and 11 mesothelioma cases).

Due to the excessive scatter in the data, most of the analyses presented depend on "Lowess Scatterplot Smoothers". Moreover, although not stated, it is likely that the tissue samples obtained were "opportunistic" in that they were not matched or controlled for relative position in the respiratory tree.

Finkelstein and Dufresne (1999) employed the multi-compartment model developed by Vincent et al. (1985) to evaluate trends in their data. The features of this model include:

- a compartment representing conducting airways that are cleared within minutes to hours by muco-ciliary transport;

- a compartment representing the subset of fibers reaching the pulmonary portion of the lung that are cleared by alveolar macrophages and transported to the muco-ciliary escalator. This type of clearance is also considered relatively rapid with half-lives of no more than several days to several weeks. Macrophage clearance is also considered size-dependent and long fibers are cleared less efficiently than short fibers;

- when sufficient dust is inhaled (or dust is sufficiently cytotoxic) to impair the motility of macrophages (either by volumetric overload or by toxicity), a sequestration compartment forms that consists of laden, but immobile, macrophages. Although this compartment may ultimately be cleared to lymphatic drainage, such clearance is assumed to be slow and size dependent (with half-lives of 2 or 3 years for short fibers and 8 years for fibers longer than 10 μm); and

- once the macrophage system is overloaded, fibers may cross the alveolar epithelium and reach the interstitium and this compartment must be cleared by transport to lymphatic drainage, which is assumed to be an extremely slow process.

Finkelstein and Dufresne (1999) indicate that chrysotile splits both longitudinally and transversely in the lung and that chrysotile lung burdens decrease significantly with time since last exposure (with short fibers clearing even faster than long fibers), while tremolite burdens do not appear to decrease with time since last exposure. They also suggest that smoking does not appear to affect clearance rates.

Finkelstein and Dufresne (1999) indicate that these type of studies are not useful for examining the behavior in rapidly clearing compartments of the lung, but they may provide insight concerning the more slowly clearing compartments. Based on their modeling, they suggest that tremolite is transferred to the sequestration compartment at rates that are 6–20 times that of chrysotile (which they indicate is comparable to what was found for crocidolite by de Klerk). The authors suggest that retained chrysotile concentrations tend to plateau after accumulation of about 35 years of exposure, while tremolite concentrations continue to increase. They also suggest, however, that chrysotile concentrations may begin to increase again after 40 years (suggesting the overload is eventually reached for chrysotile as well). Reported half-lives from the long-term compartment are:

Chrysotile	
fibers shorter than 5 μm	3.8 years
fibers 5–10 μm in length	5.7 years
fibers longer than 10 μm	7.9 years
Tremolite	
fibers shorter than 5 μm	14.3 years (not different from ∞)
fibers 5–10 μm in length	15.8 years (not different from ∞)
fibers longer than 10 μm	150 years (not different from ∞)

In a case-control study, Albin et al. (1994) examined the lung burdens of deceased workers from the asbestos-cement plant previously studied for mortality (Albin et al. 1990). In this study, details of the procedures used to prepare lung tissue for analysis were not provided. It is also assumed that available tissue samples were "opportunistic" in that they were not matched or controlled for relative position in the respiratory tree.

Results from Albin et al. (1994) are consistent with (but do not necessarily support) the hypothesis that chrysotile is cleared more readily from a long-term sequestration compartment than amphiboles. The authors also report that chrysotile fibers observed in this study are much shorter than the amphibole fibers observed, so that differences in clearance rates might be attributable to size differences. The authors also suggest that clearance is impaired by fibrosis.

Studies of Quebec Miners. Several authors also studied the lung content of various groups of deceased chrysotile miners in Quebec and found, despite overwhelming exposure to chrysotile from the ore (which contains only trace quantities of tremolite, see Case et al. 2000 and Sebastien et al. 1986), a substantial number of fibers (in some cases the majority of fibers) observed in the lungs of deceased miners from this area are tremolite. Thus, for example:

- in a study of lung burdens in 6 mesothelioma victims, Churg et al. (1984) showed that amphiboles structures were 5–15 times as plentiful as chrysotile despite the predominantly chrysotile exposure;

- in a study of lung tissue from 20 asbestosis cases, Pooley (1976) found substantial concentrations of tremolite in the lungs of deceased Quebec chrysotile workers;

- in a much larger study comparing lung burdens of Quebec workers with those from the South Carolina textile mill, which has also been extensively studied for asbestos-related mortality (Section 7.2.3), Sebastien et al. (1989) examined 161 lung tissue samples (89 from the Quebec mines). Results from this study indicate that geometric mean tremolite fiber concentrations were more than 3 times mean chrysotile fiber concentrations (18.4 vs. 5.3 f/μg dry lung tissue) among the deceased Quebec miners evaluated. It was also found that, despite these differences, the overall size distributions of tremolite and chrysotile fibers observed in lung tissue were approximately the same, although this conclusion is suspect. A more detailed discussion of the results of this study is provided in Section 7.2.3; and

! in a more focused study using a subset of the lung samples evaluated by Sebastien et al. (1989), Case et al. (2000) found that the majority of long fibers (longer than 18 μm) in the lungs samples from the deceased Quebec miners that he examined were in fact composed of tremolite. These authors also found substantial concentrations of long tremolite fibers (relative to chrysotile fibers) in deceased workers from South Carolina and even higher concentrations of commercial amphibole fibers (amosite and crocidolite) in the lungs of these workers. Thus, in addition to suggesting the relative persistence of amphibole asbestos compared to chrysotile *in vivo*, this finding also suggests that the accepted notion that the South Carolina cohort studied by Dement et al. and McDonald et al. (see Appendix A) was exposed almost exclusively to chrysotile may not be correct. This study is discussed more fully in Section 7.2.3.

These observations provide evidence that either amphibole (tremolite) asbestos is deposited more efficiently in the compartments of the lung where clearance is slow or chrysotile asbestos is cleared more rapidly and efficiently from even the slowest clearing compartments of the lung (or both). Moreover, this conclusion appears to apply similarly to both short and long fibers.

In another study, McDonald et al. (1993) suggest more specifically that lung burden data from Quebec indicate little evidence of decreasing chrysotile concentration with time since last exposure. Rather they suggest simply that tremolite is initially deposited in the deep lung more efficiently. These authors also indicate that tremolite fibers are mostly optical while chrysotile are mostly “Stanton” or thinner.

McDonald et al. (1993) report good correlation of both tremolite and chrysotile with estimated past exposures, which contrasts with the findings of the evaluation we conducted on the data from Sebastien et al. (Section 7.2.3). In McDonald et al.(1985), reported geometric mean measurements for the various fibers in lung are: tremolite: $1x10^6$–$18.2x10^6$, chrysotile : $1.5x10^6$–$15.7x10^6$, respectively, when exposure varied from <30 mpcf to >300 mpcf. However, note that, if these are PCM measurements, this may not be telling the whole story. The authors also report that 66% of those who died 10 years since first exposure and half of those who died 30 years since first exposure showed high chrysotile concentrations in their lungs. Unfortunately, without access to the raw data from this study, it is not possible to identify the route of the apparent discrepancy between the findings of this study and those reported above for ostensibly similar studies.

Some of the pathology studies that have been published suggest that at least some clearance mechanisms show a dependence on fiber size, which is consistent with what is observed in animal studies (Section 6.2.1). Notably, for example, Timbrell (1982) studied deceased workers and relatives from the Paakkila anthophyllite mine in Finland. He found that structures shorter than 4 μm and less than 0.6 μm in diameter are completely cleared from healthy lungs. The efficiency of clearance decreases slowly with increasing size. Structures longer than 17 μm and thicker than 0.8 μm in diameter are not significantly cleared. The study is based on a comparison of structure size distributions in lungs compared to the structure size of the material in the original dust exposure. Timbrell also noted that asbestosis suppresses the removal process.

When considering the dependence of clearance on size (particularly via mechanisms involving phagocytosis), it is necessary to address differences in human and animal physiology. Due to differences in the morphology, for example, human macrophages have been shown capable of phagocytizing larger particles and longer fibers than macrophages found in mice and rats (Krombach et al. 1997 [for details, see Section 4.4]). Thus, the range of fibrous structures that are efficiently cleared from human lungs is expected to include longer fibers than the range efficiently cleared in mice or rats. Unfortunately, given the limited precision of the available data, the size ranges that are reported to be cleared efficiently in rats and humans, respectively, cannot be easily distinguished.

Several human pathology studies also support observations from animal studies indicating that clearance may be inhibited by the development of fibrosis (Albin et al. 1994;Churg et al. 1990; Morgan and Holmes 1980) or by heavy smoking. However, other studies do not indicate such hindered clearance either with smoking (Finkelstein and Dufresne 1999) or with fibrosis.

Older Studies. Morgan and Holmes (1980) examined tissue samples from 21 patients in England (10 who died of mesothelioma, 3 who died of lung cancer, and 8 who died of other causes). In this study, formalin-fixed tissue samples were digested with hypochlorite. The residue was then rinsed, diluted, and an aliquot filtered. The filter was mounted on a microscope slide and clarified for analysis by phase contrast optical microscopy. Importantly, the authors note that chrysotile fibers were ignored in this study because they would not generally have been detected by this technique. Portions of the filters were also carbon coated and prepared for TEM analysis. Based on the observation that only 19% of the fibers observed in this study were between 2.5 and 5 μm, when the authors expect airborne distributions to contain closer to 90% of the fibers within this size range, the authors conclude that short fibers are preferentially cleared from the lung. They also conclude, based on one subject with asbestosis whose lung tissue exhibited 72% short fibers, that asbestosis hinders clearance. The authors also note that fewer than 1% of ferrugenous bodies (iron-coated asbestos bodies) are <10 μm in length, which indicates (in agreement with previously published work) that such bodies seldom form on short fibers. They also suggest that virtually all fibers longer than 20 μm tend to be coated in the distributions they observe.

Le Bouffant (1980) studied the concentrations, mineralogy, and size distributions of asbestos fibers found in the lungs and pleura of deceased asbestos workers. Based on the analysis, Le Bouffant (1980) found that the average ratio of chrysotile fiber concentrations found in the lung versus the pleura is 1.8 while for amosite the ratio is 34. This indicates that chrysotile migrates from the lung to the pleura more rapidly than amphiboles resulting in a higher fraction of total fibers in the pleura being composed of chrysotile (3% in the lungs versus 30% in the pleura). With regard to size, the researchers found the size distribution of amosite is virtually identical in the lung and pleura while chrysotile fibers found in the pleura are much shorter than chrysotile fibers found in lung tissue. This suggests that the movement of chrysotile is a result of a combination of translocation and degradation to shorter fibers (or that tissue samples have been contaminated with environmentally ubiquitous short, chrysotile structures). The authors indicate that chrysotile fibers apparently degrade to shorter fibers more rapidly than amosite and translocate to the pleura more rapidly than amosite. Thus, a greater fraction of chrysotile fibers (albeit short fibers) reach the pleura than amosite fibers over fixed time intervals. However, the

results of this study also confirm that the longer amosite fibers do eventually translocate, although on a much more extended time scale than the translocation of chrysotile.

Importantly, the results of this study need to be evaluated carefully. Boutin et al. (1996) showed that the majority of asbestos fibers in the pleura (particularly the long fibers) are aggregated in localized "black spots" (which surround the sites of lymphatic drainage). Thus, if the tissue samples analyzed by Le Bouffant (1980) do not contain representative sets of such spots, the conclusions drawn by Le Bouffant (1980) may be subject to question.

In summation, human pathology studies tend generally to support the findings of other studies regarding the size effects of asbestos (i.e., short fibers tend to clear more rapidly than long fibers, which can be retained in pulmonary tissues for extended periods). They also appear to highlight drastically different behavior between chrysotile and the amphibole asbestos types (particularly tremolite) regarding the heavily favored retention of the latter, which has also been indicated in animal studies. Unfortunately, the ability to draw quantitative conclusions from human pathology studies is hampered by the severe limitations of these studies (Section 5.2).

6.2.4 Studies of Dissolution/BioDurability

Although asbestos minerals are relatively insoluble *in vivo* in comparison, for example, to various fibrous glasses or other man-made mineral fibers (see, for example, Hesterberg et al. 1998a or Eastes and Hadley 1996), they do eventually dissolve in the body. Therefore, this pathway may contribute importantly to the overall biological clearance of asbestos. Moreover, it has been suggested by several researchers (see, for example, McDonald 1998a and other references cited below) that differences in biodurability between chrysotile and the amphiboles may at least partially explain the disparate potencies observed for these fiber types toward the induction of mesothelioma and, potentially, lung cancer (see Sections 7.2.4.2 and 7.3.3.2).

> Note that the term "biodurability" is used here to indicate the persistence of a particle or fiber attributable specifically to solubility (in the absence of other clearance or degradation mechanisms). In contrast, the term "biopersistence" is used to indicate the overall persistence of a particle or fiber in the body attributable to the combined effect of all mechanisms by which it might be removed. Thus, for example, while biopersistence can be evaluated *in vivo*, biodurability can best be inferred from *in vitro* dissolution studies so that effects from other clearance mechanisms can be eliminated.

Several studies further indicate that both the *in vivo* biopersistence and the bio-activity (including carcinogenicity) of various fiber types may be linked to their observed, *in vitro* dissolution rates (Bernstein et al. 1996; Eastes and Hadley 1995, 1996; Hesterberg et al. 1998a, 1998b). Such studies, however, typically involve fiber types with dissolution rates that are rapid relative to the rates of clearance by other mechanisms (Sections 6.2.1.1 and 6.2.1.2). In such studies, moreover, the various types of asbestos are typically employed as negative (insoluble) controls. In fact, most of these studies are based on experiments with rats and the 2-year lifetime of a rat is comparable to the anticipated lifetime of chrysotile asbestos in the body and short compared to the anticipated lifetimes for the amphiboles (see below). Therefore, such studies are not particularly sensitive to differences in the relative biodurability of the different asbestos

types. In fact, in the majority of these studies, the dissolution rates reported for asbestos were derived indirectly by analogy with other minerals or are quoted from other studies that derive rates similarly and may therefore be somewhat unreliable. Nevertheless, a review of a subset of these studies is instructive.

Eastes and Hadley (1995 and 1996) report a simple model that reasonably predicts the relative fibrogenicity and tumorigenicity for a range of synthetic fibers based on the dissolution rates of the fibers measured *in vitro*. The authors found that they could explain observations by assuming that the effects of the various fibers are a function of an adjusted dose that accounts for biodurability. Thus,

$$F=f(ax)$$

where "F" is the observed incidence of the endpoint, "f" is the dose-response function proposed for the effect, "x" is the measured dose, and "a" is an adjustment factor that accounts for durability.

In the model, "a" is determined simply as "t_d/t_L" where t_d is the time that a fiber of diameter, "D" remains in the lung and t_L is the lifetime of the exposed animal (e.g., 2 years for rats). This simple model reasonably reconciles the results observed in animal inhalation and injection studies of MMVF's, RCF's, and asbestos for endpoints including lung tumors, degree of fibrosis, and (for intrapleural injection studies) mesothelioma. Based on a chi-square test, the simple model is shown to adequately fit the data to a number of databases reviewed. In contrast, the unadjusted doses do not. Importantly, the dissolution rates used for the various asbestos minerals in this study were estimated by analogy with similar minerals and therefore may be unreliable.

In studies comparing *in vivo* biopersistence with dissolution rates measured *in vitro*, Bernstein et al. (1996) and Hesterberg et al. (1998a), indicate that it is necessary to consider only long fibers (typically longer than 20 μm), because shorter structures are typically cleared by other mechanisms. They also indicate, at least for this type of study in which whole lungs were homogenized and dissolved prior to preparation for asbestos analysis,[2] that clearance is initially rapid. This reflects muco-ciliary clearance from the upper respiratory tract. Therefore, it is clearance of long fibers from a longer term pool that tracts *in vitro* dissolution rates.

These authors also report that long, soluble fibers (longer than 20 μm) are actually cleared more rapidly than short fibers in these studies. They indicate that this is likely due to long fibers being too long to be effectively phagocytized by macrophages so that they are left to dissolve in the extracellular fluid at neutral pH. Shorter fibers are effectively taken up by macrophages so that dissolution is hindered by the more acidic environment of the phagosomes (pH 4.5) and by the limited volume of fluid within which to dissolve.

---

[2]When whole lungs are homogenized to determine lung burden, this includes the largest airways, which initially contain substantial concentrations of material that is rapidly cleared by the muco-ciliary escalator. However, because this material dominates the quantity of material observed, such studies are not useful for tracking the longer term clearance processes that occur in the deep lung.

Law et al. (1991) studied the dissolution of a range of fibers in solutions used as common fixatives for biological samples. The authors report that chrysotile and crocidolite, as well as many other fibers, dissolve at measureable rates in the fixatives studied (Karnovsky's fixative and formalin fixative). They therefore recommend that fiber concentrations and size distributions obtained from tissue samples stored in such fixatives should be evaluated carefully to account for the possible effects of the fixatives.

Although Coin et al. (1994) reported seeing no effective reduction in long fiber (>16 μm) chrysotile (nor other evidence of dissolution) in their study of fiber biopersistence, the limited time frame of this study (30 days) may have been too short to allow detectable changes to accumulate.

The most consistent data for the comparative biodurability of chrysotile and the amphiboles (specifically crocidolite) is found in two *in vitro* studies of the dissolution rates of fibers that were conducted under comparable conditions. In the first of these studies, Hume and Rimstidt (1992) measured the dissolution rate for chrysotile asbestos at neutral pH under conditions analogous to biological systems. The dissolution rate that they report for chrysotile converts to: K_{diss}=12.7 ng/cm^2-hour and this is reportedly independent of pH. In a comparable study Zoitus et al. (1997) report the following dissolution rate for crocidolite: K_{diss}=0.3 ng/cm^2-hour, which is 40 times slower than for chrysotile. Dissolution rates for several MMVF's and RCF-1 are also reported in the latter paper, which are listed from fastest dissolving to slowest in Table 6-4.

Table 6-4. Measured *in vitro* Dissolution Rates for Various Fibers[a]

Fiber Type	K_{diss} (ng/cm^2-hr)
MMVF 10	259
MMVF 11	142
MMVF 22	119
MMVF 21	23
Chrysotile	12.7[b]
RCF 1	8
Crocidolite	0.3

[a]Source: Zoitus et al. (1997)
[b]Source: Hume and Rimstidt (1992)

Note that dissolution rates for other amphiboles, such as amosite are probably no more than a factor of two or three different than that reported above for crocidolite (see, for example, Hesterberg et al. 1998a,b).

To compare the effect of biodurability on the *in vivo* biopersistence of asbestos and other fiber types, both the detailed kinetics of dissolution and the distribution of fiber sizes must be considered.

As reported by Zoitus et al. (1997), at a sufficiently high rate of fluid flow, the rate of mass loss from a fiber is proportional to its surface area, A. Thus:

$$dM/dt=-kA. \qquad \text{(Eq. 6-4)}$$

This means that for a uniform mass fiber dissolving congruently:

$$1-(M/M_o)^{0.5}=2kt/D_o\rho. \qquad \text{(Eq. 6-5)}$$

where:

- M is the mass at time t;
- M_o is the initial mass at time t=0;
- D_o is the initial diameter of the fiber; and
- ρ is the density of the fiber.

Substituting the equation relating the mass and the diameter of a fiber ($M=\rho\pi d^2h/4$) into the above equation, cancelling terms, and rearranging indicates that (during dissolution) the diameter of a fiber decreases linearly with time:

$$D=D_o -2kt/\rho. \qquad \text{(Eq. 6-6)}$$

where:

D is the diameter at time t; and
all other terms have been previously defined.

Furthermore, the rate of reduction in radius is given by: k/ρ. Based on the dissolution rates given above for chrysotile and crocidolite, the radius reduction rates (v_{rad}) for these fiber types are determined to be: 1.26×10^{-8} µm/sec and 2.6×10^{-10} µm/sec, respectively. Thus, the dissolution of each fiber is a zero order process (i.e., the rate is constant with time and independent of concentration). Given these rates, a chrysotile fiber 1 µm in diameter will disappear in approximately a year (3.9×10^7 sec) and a crocidolite fiber of the same diameter in approximately 60 years (1.9×10^9 sec).

The number rate of disappearance of a population of fibers due to dissolution is a function of the rate of radial reduction for the fiber type and the distribution of fiber diameters in the population. The time at which the entire population finally dissolves can be estimated simply by dividing the radius of the largest fiber by the radius reduction rate, v_{rad}, that is appropriate for the fiber type. The number of fibers remaining from the population at time t will be equal to the number of fibers in the original distribution with radii larger than $v_{rad}t$ for the reduction rate that is appropriate for the fiber type.

Note that dissolution will not cause an immediate reduction in fiber concentration. The number of fibers will not begin to decrease until sufficient time has elapsed for the thinnest fibers to completely dissolve. Eastes and Hadley (1994) therefore recommend tracking the time dependence of the mode of the distribution of fiber diameters to best gauge the effects of dissolution *in vivo*.

Importantly, fibers *in vivo* will only dissolve at the rates predicted by the above equations if the fluid in which they are dissolving flows past the fibers sufficiently rapidly to prevent saturation from limiting the rate (Mattson 1994). Especially for slow dissolving materials of limited solubility like asbestos, it is expected that the observed dissolution rate *in vivo* will generally be slower than the rates predicted based on *in vitro* measurements. Even for more rapidly dissolving fibers like most fibrous glasses and manmade mineral fibers, dissolution is hindered in compartments of the body in which the volume of available solute is limited.

In summary, dissolution is a zero-order (i.e., constant with time, independent of concentration) clearance mechanism that is dependent on fiber mineralogy, that the effect it has on fiber populations (concentrations) is a function of the distribution of fiber diameters within the population, and that the theoretical rate of dissolution may not be achieved in all tissues in all compartments of the lung or mesothelium due to limits in the rate of *in vivo* solute flow.

6.2.5 Dynamic Models

Unlike particle deposition in the lungs, which is an entirely mechanical process, clearance, transport, and degradation mechanisms tend to be complex biochemical processes. Due to the incomplete understanding of such processes, state-of-the-art modeling of degradation and clearance is not as advanced as that for deposition. Even the most sophisticated of degradation and clearance models remain semi-empirical. Although, current models in this area show general agreement with the sparse, available data, there are clearly areas of weakness that require additional research. Nevertheless, the models provide a good indication of the kinds of processes that are important in the body and their overall constraints. It is also noted that models for degradation and clearance in humans tend to be better developed than those for animals, primarily due to confounding uncertainties associated with animal ventilation rates. An overview of the state of the art, which was current as of the date of publication, can be found in Stober et al. (1993).

According to Stober et al. (1993), the general conclusions that can be drawn from the current models are that:

- clearance from ciliated airways is rapid, independent of particle/fiber type, apparently independent of particle size, and can be described as the sum of two, weighted exponentials (i.e., an assumed combination of two first-order decay processes), although the process may in fact be zero order (i.e., the reduction in concentration with time is constant and independent of concentration) with rates that differ primarily by the distance that a particle must traverse to return to the trachea.

Based on studies of particle clearance reported by Raabe (1984), muco-ciliary transport in the nose and throat generally exhibits a half-life for clearance of 4 minutes. Clearance of the tracheo-bronchial section of the respiratory tract is a function of the distance from the trachea and generally varies from a half-life of 30 minutes for the largest bronchi to approximately 5 hours for the smallest and most remote bronchi. In healthy humans, material deposited in this region is generally cleared within 24 hours. In contrast, the clearance mechanisms operating in the deep lung, beyond the muco-ciliary escalator, operate over time frames of many days to years (see Table 6-2);

! clearance of insoluble particles from the pulmonary portion of the lung occurs primarily by macrophage transport and such transport has several components. One component represents the population of "free" macrophages located within the alveoli that engulf particles and transports them to the muco-ciliary escalator. Macrophages are also renewed at some rate of recruitment that may be dependent on particle concentrations. In fact, numerous studies have demonstrated that macrophage recruitment is induced by the deposition of asbestos and other particles in the lung (Section 6.3.5). Particles also migrate into the interstitium where another population of macrophages clears these particles to lymph. This second component (interstitial clearance) is much slower than the first (see Table 6-2);

! each macrophage can carry a maximum load and the mobility of each macrophage decreases with increasing load. At sufficient loading, macrophages become immobile and aggregates of overloaded macrophages in the alveoli may then sequester particles for some period of time as this clearance mechanism is shut down. In the interstitium, masses of immobile macrophages may trigger development of granulomas that sequester particles for extended periods of time by effectively preventing clearance of the particles within such tissue, at least until or unless the granulomas resolve. Thus, these models incorporate overload mechanisms and the incorporation of such overload mechanisms are required to explain observed trends in experimental results; and

! in various published studies, overload (immobilization of laden macrophages) has been modeled as dependent on the total volume or mass of phagocytized material (for compact particles) and (additionally) on the length of phagocytized material (for fibers). It is also possible that the motility of macrophages and the consequent overall rate of this clearance process is additionally a function of fiber diameter and/or particle toxicity (the latter for special cases).

Interestingly, while it is reported that large, spherical particles are not readily cleared by this mechanism, the range of sizes over which clearance becomes hindered corresponds reasonably well to the limits of overall respirability. In contrast, fibers that are clearly too long to be cleared by macrophages, if they are sufficiently thin, are quite respirable. Thus fibrous materials present a unique challenge to the respiratory tract based solely on the dimensions of these materials.

Stober et al. (1993) also notes that many models incorporate the assumption that most clearance processes are first order (i.e., that the rate of reduction of mass or fiber number is proportional to the remaining mass or fiber number, respectively, and independent of other factors). Thus, the combined effects of multiple clearance processes can be expressed as a weighted sum of exponentials and this approach has been fairly successful at mimicking actual processes. This means, however, that the half-lives "$t_{1/2}$'s" attributed to the various first order decays are empirical and do not necessarily correspond to any specific physiological or biochemical features of the processes being modeled. Depending on the specific process, clearance rates may be zero order or may be a more complicated function of multiple variables than can be described by a first order decay. Nevertheless, models incorporating these simplifying assumptions have shown good success at adequately describing observed effects.

Note that half-lives for first order decay processes represent the time required for half of the initial mass to decay (or be transported or whatever) and can be estimated as: $t_{1/2}=(\ln 2)/k$ with k being the first order rate coefficient or proportionality constant between rate and mass. This is why so many of the retention studies cited above provide estimates of a series of decay constants or half-lives that are assumed to correspond approximately to the major clearance processes contributing to the observed, overall reduction in concentration.

Due to the complexity of the processes involved, only a small number of dynamic models for fiber retention have been developed. Interpretation of the results of these models requires that the meaning of the term "retention" first be reconciled across studies.

Dement and Harris (1979) report that, based on a mathematical model, the fraction of structures retained in the deep lung is unlikely to vary by more than a factor of 2 for different asbestos mineral types. In this study, however, the term retention appears to refer primarily to a very short time period that primarily includes consideration of deposition, but not clearance processes.

Using a definition for retention that reflects long-term residence in the lung, Yu et al. (1990) developed a model of chrysotile retention that explicitly incorporates longitudinal splitting, dissolution, and size-dependent clearance. Time-dependent lung burden estimates derived using the model were shown to compare reasonably well with published data (Abraham et al. 1988, as cited by Yu et al. 1990) both in terms of fiber concentrations and fiber size-distributions.

In a later modification of their retention model for chrysotile, Yu et al. (1991) also considered the effect of airway asymmetry on fiber retention. In this version of the model, Yu and coworkers incorporated information concerning the geometry of the bronchio-alveolar tree (including mean distance and the mean number of airway bifurcations between the trachea and the alveoli in each section of the lung) and studied the effects of such considerations. The modified model predicts a non-uniform distribution of the asbestos that is retained in the lung and the predictions reasonably reproduce the distributions observed by various researchers and measured formally by Pinkerton et al. (as cited by Yu et al. 1991).

Yu and Asgharian (1990) also modeled the long-term retention of amosite in rat lungs. In contrast to the models employed for chrysotile, the model presented for amosite incorporates a term for the clearance rate that is not a constant but, rather, is a function of the lung concentration of asbestos, which was adapted from an earlier model for diesel soot. This

modification was incorporated to adequately mimic the suppression of clearance with increasing lung burden that has been observed by several research groups (e.g., Davis et al. 1978; Wagner et al. 1974) for amphiboles. Conditions under which elevated asbestos (or dust) concentrations are observed to reduce clearance are referred to as "overload" conditions. Model predictions were shown to reasonably reproduce the time-dependence of amosite lung burdens (in terms of mass) in several studies.

Importantly, the overload conditions addressed in the Yu and Asgharian (1990) model were primarily observed among older retention studies where lung burden was tracked as total asbestos mass (Section 6.2.1). Such studies tend to suggest a difference in the behavior of chrysotile and the amphiboles. As indicated in Section 6.2.1, however, later retention studies, which track lung burden as a function of fiber number (in specific size categories) tend to show this effect is a function of fiber length more than fiber type and newer models may need to incorporate such factors that indicate reduced macrophage motility as a function of fiber length.

Moreover, it is important to consider the major, confounding effects, if the goal is to develop a model that not only reproduces the time-dependence of clearance, but also captures relevant physical phenomena. Thus, for example, Yu et al. (1994) were able to reproduce the time-dependence of the retention in rats of inhaled RCF-1 (as a function of fiber size) using a model in which macrophage motility was limited only by total lung burden and not dependent on fiber size. However, these authors also failed to consider that long RCF-1 fibers in fact dissolve at rates competitive with the clearance of short fibers (see Section 6.2.1), which is probably why they did not find a dependence on length; the two effects cancelled out.

6.2.6 General Conclusions Regarding Deposition, Translocation, and Clearance

The current literature on deposition, translocation, and clearance paint a consistent picture of the fate of fibrous structures in the lung. The ultimate fate of biodurable fibers depends overwhelmingly on their size. Although there may be additional effects due to mineralogy (addressed further in Section 6.3) and for rare, special cases this may be important, generally such effects appear to be minor.

The primary effect attributable to mineralogy that is important to consider in relation to clearance is that associated with biodurability. Fibers that dissolve in the lung at rates that are competitive with the other clearance mechanisms described below may be cleared sufficiently rapidly to preclude adverse effects, even when such fibers are too long to be cleared efficiently by macrophages (see Section 6.2.1).

A schematic representation of the complex set of mechanisms that contribute to the translocation and clearance of fibrous structures that have been deposited in the deep lung is presented in Figure 6-4. This description was developed based on the complete spectrum of observations reported in each of the previous sections of this chapter including, primarily, the descriptions of the most sophisticated of the models reviewed by Stober et al. (1993).

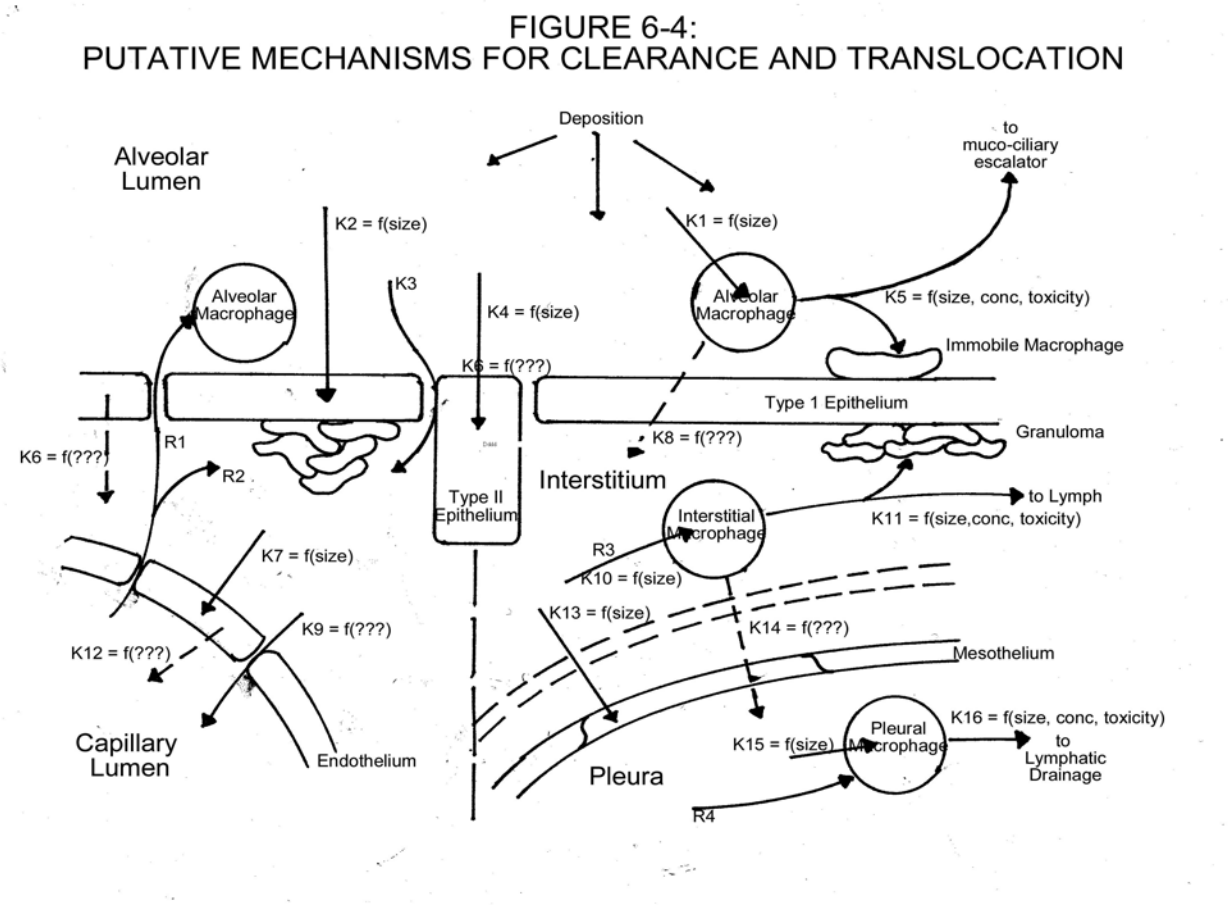

Figure 6-4. Key for Putative Mechanisms for Clearance and Translocation of Fibers in the Lung

K_1 = rate constant for phagocytosis of fibers by alveolar macrophages. This mechanism is an inverse function of fiber length and, likely, diameter. This mechanism is likely pseudo first order (assuming sufficient numbers of macrophages, the rate will be proportional to the number of fibers);

K_2 = rate constant for phagocytosis of fibers by Type I epithelial cells. This mechanism is an inverse function of fiber length and, likely, diameter. This mechanism is likely pseudo first order;

K_3 = rate constant for diffusion of fibers from the alveolar air space (lumen) through the epithelial lining to the underlying interstitium. This mechanism is diffusion limited and likely independent fiber size or type. This mechanism likely parallels the behavior of diffusion in through a finite, column of fixed diameter.

K_4 = rate constant for phagocytosis of fibers by Type II epithelial cells. This mechanism is an inverse function of fiber length and, likely, diameter. This mechanism is likely pseudo first order;

Figure 6-4 Key for Putative Mechanisms for Clearance and Translocation of Fibers in the Lung *(continued)*

K_5 = rate constant for transport by macrophage to the muco-ciliary escalator. This mechanism is likely an inverse function of fiber length and the volume (or mass) of the fibers phagocytized. Macrophages that become immobilized tend to aggregate in alveolar lumena. For macrophages with fixed loads, this mechanism may be first order or zero order.

K_6 = rate constant for putative discharge to interstitium of phagocytized fibers by Type I epithelial cells. There has been no direct verification of this mechanism;

K_7 = rate constant for phagocytosis of fibers by endothelium. This mechanism is an inverse function of fiber length and, likely, diameter. This mechanism is likely pseudo first order;

K_8 = rate constant for putative mechanism in which fibers internalized by macrophages are transported through the epithelial lining of the alveolar space to the underlying interstitium. There has been no direct verification of this mechanism;

K_9 = rate constant for diffusion of fibers from the interstitium through the endothelial lining to the enclosed, capillary lumen. This mechanism is diffusion limited and

likely independent fiber size or type. There has been no independent verification of this mechanism;

K_{10} = rate constant for phagocytosis of fibers by interstitial macrophages. This mechanism is an inverse function of fiber length and, likely, diameter. This mechanism is likely pseudo first order (assuming sufficient numbers of macrophages, the rate will be proportional to the number of fibers);

K_{11} = rate constant for transport by macrophage from the interstitium to the lymphatic system. This mechanism is likely an inverse function of fiber length and the volume (or mass) of the fibers phagocytized. Macrophages that become immobilized tend to induce formation of interstitial granuloma. For macrophages with fixed loads, this mechanism may be first order or zero order.

K_{12} = rate constant for putative discharge to capillary lumena of phagocytized fibers by endothelial cells. There has been no direct verification of this mechanism;

K_{13} = rate constant for phagocytosis of fibers by mesothelial cells of fibers transported to the mesothelium. This mechanism is an inverse function of fiber length and, likely, diameter. This mechanism is likely pseudo first order;

Figure 6-4 Key for Putative Mechanisms for Clearance and Translocation of Fibers in the Lung *(continued)*

K_{14} = rate constant for putative mechanism in which fibers internalized by macrophages are transported from the interstitium through intervening tissue and the mesothelium to the pleural space. There has been no direct verification of this mechanism;

K_{15} = rate constant for phagocytosis of fibers by pleural macrophages. This mechanism is an inverse function of fiber length and, likely, diameter. This mechanism is likely pseudo first order (assuming sufficient numbers of macrophages, the rate will be proportional to the number of fibers);

K_{16} = rate constant for transport by macrophage to sites of lymphatic drainage (lymphatic ducts) along the pleura. This mechanism is likely an inverse function of fiber length and the volume (or mass) of the fibers phagocytized. For macrophages with fixed loads, this mechanism may be first order or zero order.

Not shown: apparently fibers that are too large to pass through lymphatic ducts attract accumulation of macrophages at sites of lymphatic drainage (Kane and MacDonald (1993).

R_1 = rate constant for the renewal of the alveolar macrophage population. While the there is likely a steady state rate for background renewal, given that the average life of an alveolar macrophage is reported to be on the order of 7 days, this rate is also stimulated in response to insult by foreign substances in the lung;

R_2 = rate constant for the renewal of the interstitial macrophage population. While the there is likely a steady state rate for background renewal, this rate is also expected to be stimulated in response to insult by foreign substances in the interstitial space;

R_3 = rate constant for the renewal of the pleural macrophage population. While the there is likely a steady state rate for background renewal, this rate is also expected to be stimulated in response to insult by foreign substances in the pleura;

As shown in Figure 6-4, briefly, the first reaction to the introduction of fibers (or other particulate matter) into the alveolar lumen is scavenging by alveolar macrophages. It has been reported that the initial uptake by macrophages is a rapid process that is essentially complete within hours after initial deposition. Rates for several of the mechanisms depicted in Figure 6-4 have been estimated in the literature and are summarized in Table 6-2.

The rate of removal (to the muco-ciliary escalator) by alveolar macrophages is then determined by a variety of effects. Macrophage motility is a size dependent-process so that only fibers that are sufficiently compact (<~20 μm) can be removed from the lung. The rate of removal by this process may also be suppressed both for fibers of intermediate lengths (10–20 μm, which are short enough to be phagocytized, but long enough to suppress macrophage motility) and by the overall mass/volume of particles deposited (and, proportionally, taken up by each macrophage). Note that the dimensions provided are the ones that are apparently appropriate for humans. For rats, the corresponding dimensions may be somewhat smaller.

Likely competing with scavenging by macrophages are (1) phagocytosis by the epithelial cells lining the alveolus and (2) diffusive transport to the intersititium. Both Type I and Type II epithelial cells appear to phagocytize fibers. Although relatively few fibers are observed to be taken up by Type II cells, as previously discussed (Section 6.2.2), one possible explanation for the limited observation of fibers in Type II cells is that uptake of fibers induces terminal differentiation to Type I cells. It is expected that phagyctosis by epithelial cells is a size-dependent process.

Especially when the presence of fibers (or other particulate matter) induces morphological changes in Type II cells that increase the overall permeability of the epithelial lining (Section 6.3.7), fibers can apparently diffuse into the interstitium. This process, potentially supplemented with expulsion of phagocytized fibers by epithelial cells and/or transport of fiber laden macrophages through the epithelial lining, represents the set of putative mechanisms by which fibers may reach the interstitium. It is expected that these processes are somewhat slower than uptake by alveolar macrophages (see Table 6-2).

Therefore, if this latter mechanism is operating at peak efficiency, relatively few fibers may reach the interstitium. Note that diffusive transport is likely independent of fiber length, but may be dependent on fiber width with thinner fibers more rapidly diffusing to the interstitium.

Fibers reaching the interstitium are likely cleared primarily by interstitial macrophages, which phagocytize the fibers and transport them to the lymphatic system. Both the efficiency of phagocytosis and motility of macrophage transport in the interstitium likely depend on fiber size and the total volume/mass of fibers in the same way described above for transport by alveolar macrophages. However, all such mechanisms are substantially slower in the interstitium than in the alveolar lumen (see Table 6-2).

Macrophages that have been immobilized (due to fiber size or volume/mass) in the interstitium tend to aggregate and induce formation of granulomas, which may sequester the fibers in these cells. Although there is less evidence for this, fibers free in the interstitial matrix might also trigger such a process. Such fibers would typically be too large to have been effectively phagocytized by any of the cells of the interstitium.

Fibers may also reach the endothelium and be taken up by endothelial cells lining the capillaries of the deep lung. Because fibers have also been observed in capillary lumena, mechanisms similar to those described for transport through the alveolar epithelium to the interstitium may be operating to transport fibers into capillary lumena. While it is expected that such mechanisms will also show size dependence similar to that previously described, little is known about the details or the rates of such processes.

Also by mechanisms similar to some or all of the putative mechanisms described for translocation of fibers from the alveolar lumen to the interstitium, fibers may reach the pleura. Whether fibers can also reach the pleura via transport in blood or lymph has not been definitively determined. Fibers reaching the pleura may be phagocytized by mesothelial cells or may pass through such cells to the pleural cavity. Fibers reaching the pleural cavity are apparently phagocytized by pleural macrophages (probably showing a similar size or volume/mass effect as described above for similar mechanisms) and are apparently transported to (and deposited at) sites of lymphatic drainage along the pleura. If such fibers are then too large to pass through the lymphatic ducts, they may trigger accumulation of additional macrophages and other inflammatory cells.

Overall, the effects of size appear to be:

- few fibers thicker than approximately 0.7 μm and virtually none thicker than approximately 1.5 μm appear to reach the deep lung. Of these, the longer the fiber, the thinner the fiber. Importantly, the distribution of sizes of structures deposited in the deep lung tend to be much more similar across studies than the distributions in the aerosols originally inhaled. Thus, deposition is a very effective filtering process; and

- short fibers (or compact particles) that are shorter than somewhere between 10 and 20 μm tend to be taken up almost entirely by macrophages and are either cleared via the muco-ciliary escalator, isolated in immobilized macrophages that remain within alveolar lumena, or transported to lymphatics (presumably after first reaching the interstitum). These processes appear to be efficient for the shortest of the fibers in this range (and all shorter fibers) so that no further effects are manifest. In contrast, longer fibers, which are not efficiently cleared or isolated by macrophages either in the alveolar lumen or the interstitium appear to trigger a range of additional responses, some of which appear to lead to disease.

Therefore, based on deposition, translocation, and clearance, it is fibers thinner than approximately 0.7 μm and longer than a minimum of approximately 10 μm (with relative contributions increasing with increasing length up to at least 20 μm) that likely contribute to disease. Modifications to this range of structure sizes due to effects attributable to direct biological responses are addressed further in Section 6.3.

Regarding putative differences in behavior between chrysotile asbestos and amphibole asbestos, such effects are adequately addressed by the unifying discussion provided above. To make sense of such differences, the effects of fiber size must first be explicitly considered. Thus, chrysotile fibers may not be as efficiently deposited in the deep lung to the extent that they are curlier or

occur in thicker bundles than amphibole fibers. The overall load of chrysotile deposited in the deep lung may also be cleared more rapidly than amphiboles to the extent that (1) short, thin fibrils ultimately represent a greater fraction of the total load of chrysotile than the amphiboles and (2) a subset of long chrysotile fibers, not sequestered in an environment with limited fluid flow, may be cleared more rapidly than similarly long amphibole fibers due to contributions from dissolution.

Importantly, the concentrations of asbestos to which humans are exposed are much lower than the concentrations to which animals were exposed in the various literature studies cited. Moreover, as indicated in Section 6.1.2, for virtually any exposure of interest, the resulting (volumetric or surface area) lung burden will be substantially higher in rats than in humans. Therefore, overload conditions or other processes that might impede or alter the clearance mechanisms described above, will never occur in humans without first having affected the results of the animal studies reported. Thus, conclusions concerning size-dependence and related effects (except to the extent that they need to be adjusted for cross-species differences) should remain valid when extrapolated between animals and humans.

6.3 FACTORS GOVERNING CELLULAR AND TISSUE RESPONSE

For inhaled structures that survive degradation and clearance, a series of complex reactions between the structures retained in the lung and surrounding tissue may induce a biological response. Asbestosis (fibrosis), pulmonary carcinomas, or mesotheliomas may result. Mesotheliomas are likely associated with structures that are translocated from the lung to the mesenchyme, although diffusable growth promoters and other chemical signals produced by asbestos exposed cells in lung tissue immediately proximal to the mesothelium may also play a role (see Adamson 1997, as described in Section 6.3.4.1).

That the specific biochemical triggers for asbestos-related diseases have not been definitively delineated as of yet is not surprising. Despite great progress in elucidating candidate mechanisms, the number of candidate mechanisms is large and confounded by “cross-talk” between mechanisms. Moreover, similar toxic endpoints may result from entirely independent mechanisms that exhibit disparate dose-response characteristics but, nevertheless, may be triggered by the same or similar toxins. In such cases, however, the relative contributions from each mechanism to a particular endpoint may vary substantially. Unfortunately, the ability to compare results across studies of different mechanisms is currently limited due to the inability to reconcile the quantitative effects of dose and response across dissimilar studies.

Table 6-5 illustrates the range and complexity of the biological responses triggered by asbestos in lung tissue. The table was developed based on the information gleaned from the studies described in this section. Importantly, not all of the mechanisms listed contribute equally to the toxic endpoints that are attributable to asbestos, but their relative importance has yet to be entirely delineated. The toxic endpoints of potential interest to which each of the listed mechanisms potentially contribute are indicated in bold italics.

Table 6-5. Putative Mechanisms by Which Asbestos May Interact with Lung Tissue to Induce Disease Following Inhalation

Asbestos (*in vivo*)

Generates reactive oxygen species (ROS)

! may affect neighboring cells and tissues

Interacts with macrophages

Interacts with lung epithelium

Asbestos interacts with macrophages

Induces generation and release of reactive oxygen species/reactive nitrogen species (ROS/RNS)

! may affect neighboring cells and tissues

! may induce inflammatory response ***(which may promote cancer)***

! may induce fibrogenesis ***(which may promote cancer)***

! induces signaling cascades in macrophages and neighboring tissues

– mediates apoptosis ***(which may regulate cancer)***

– mediates proliferation ***(which may promote cancer)***

! causes genotoxic effects in neighboring tissues

– ***may cause cancer initiation***

– may induce arrest of cell cycle

– induces signaling cascades

• mediates apoptosis ***(which may regulate cancer)***

• mediates proliferation ***(which may promote cancer)***

! depletes reserves of antioxidants in macrophages and neighboring tissues

– may induce cytotoxicity ***(which may promote cancer, by inducing proliferation)***

– may increase susceptibility to insult by other toxic agents ***(which may promote cancer)***

Induces release of various cytokines

! affects neighboring cells and tissues

! mediates inflammatory response ***(which may promote cancer)***

! mediates fibrogenesis ***(which may promote cancer)***

! induces signaling cascades in macrophages and neighboring tissues

Table 6-5. Putative Mechanisms by Which Asbestos May Interact with Lung Tissue to Induce Disease Following Inhalation *(continued)*

– mediates apoptosis ***(which may regulate cancer)***

– mediates proliferation ***(which may promote cancer)***

! mediates proliferation in neighboring tissues ***(which may promote cancer)***

Induces signaling cascades and mediates apoptosis in macrophages ***(which may regulate cancer)***

At high enough concentrations, promotes cytotoxic cell death ***(which may promote cancer by inducing proliferation)***

Asbestos interacts with Lung Epithelium

Induces release of reactive oxygen species/reactive nitrogen species (ROS/RNS)

! may affect neighboring cells and tissues

! may induce inflammatory response ***(which may promote cancer)***

! may induce fibrogenesis ***(which may promote cancer)***

! induces signaling cascades in epithelium and neighboring tissues

– mediates apoptosis ***(which may regulate cancer)***

– mediates proliferation ***(which may promote cancer)***

! causes genotoxic effects in epithelium and neighboring tissues

– ***may cause cancer initiation***

– may induce arrest of cell cycle

– induces signaling cascades

• mediates apoptosis ***(which may regulate cancer)***

• mediates proliferation ***(which may promote cancer)***

! depletes reserves of antioxidants in epithelium and neighboring tissues

– may induce cytotoxicity ***(which may promote cancer by inducing proliferation)***

– may increase susceptibility to insult by other toxic agents ***(which may promote cancer)***

Induces release of various cytokines

! affects neighboring cells and tissues

! mediates inflammatory response ***(which may promote cancer)***

! mediates fibrogenesis ***(which may promote cancer)***

! induces signaling cascades in epithelium and neighboring tissues

– mediates apoptosis ***(which may regulate cancer)***

Table 6-5. Putative Mechanisms by Which Asbestos May Interact with Lung Tissue to Induce Disease Following Inhalation *(continued)*

– mediates proliferation ***(which may promote cancer)***

! mediates proliferation in epithelium and neighboring tissues ***(which may promote cancer)***

Causes genotoxic effects

! ***may cause cancer initiation***

! may induce arrest of cell cycle

! induces signaling cascades

– mediates apoptosis ***(which may regulate cancer)***

– mediates proliferation ***(which may promote cancer)***

Induces signaling cascades

! mediates apoptosis ***(which may regulate cancer)***

! mediates proliferation ***(which may promote cancer)***

Increases epithelial permeability

! encourages fibrosis ***(which may promote cancer)***

! facilitates translocation

At high enough concentrations, promotes cytotoxic cell death ***(which may promote cancer by inducing proliferation)***

As indicated previously (Section 6.0), although much has been learned about specific components of the underlying mechanisms by which asbestos causes the above-listed diseases, substantial knowledge gaps remain. Moreover, because of these gaps, multiple candidate effects have been explored as potential contributors to carcinogenicity (or fibrogenicity) and one of the goals of this document is to distinguish among those effects that are likely to contribute to the induction of cancer from those that are less likely or unlikely to contribute (given the current state of knowledge). Accordingly, an overview of recent studies is presented below following a brief description of the current model of the general mechanism for cancer. Note that, due to the availability of several recent reviews (including, for example, Economou et al. 1994; Floyd 1990; Kamp et al. 1992; Kane and MacDonald 1993; Mossman and Churg 1998; Mossman et al. 1996; Oberdorster 1994; Robledo and Mossman 1999), only the most recent primary articles are included in the following review.

Also, as indicated below, many of the biological responses provoked by retained asbestos are in fact dependent on fiber size and type. Therefore, studies that distinguish among effects induced by different size fibers (or fibers and non-fibrous particles) of the same mineralogy and studies that distinguish among effects induced by comparably sized fibers (or non-fibrous particles), but differing mineralogy are highlighted. However, due to the limits with which fibrous materials have tended to be characterized in many of these studies, the database from which to distinguish among the effects of size and mineralogy are limited and conclusions from differing studies must be compared with caution.

A large body of evidence supports the conclusion that it is primarily (if not exclusively) long fibers (those longer than a minimum of 5–10 μm) that contribute to disease (see Sections 6.2.1, 6.2.2, and 6.4). Much evidence also indicates that the potency of long fibers increases with length at least up to a length of approximately 20 μm. Therefore, because short and long fibers are both respirable (for fibers that are sufficiently thin, less than approximately 0.7 μm in diameter), differences in the ultimate response to short and long fibers must be attributable to differences in tissue and cellular responses to the retained fibers in each size range.

At least at a histopathological level, clear differences have been observed in the responses evoked by short and long structures (see Sections 6.2.1 and 6.2.2). It is a goal of this section to determine whether the biochemical triggers that mediate the disparate responses to short and long fibers can also be identified. Unfortunately, while a large body of knowledge has been amassed, definitive conclusions are not yet possible. This is because the specific mechanisms by which asbestos acts have still not been definitively determined, although many candidate mechanisms have been elucidated (see above). However, important inferences can still be gleaned from the available studies.

Evidence for the relationship between fiber diameter and disease is somewhat less clear. Although there appears to be a fairly sharp cutoff in the diameter of fibers that are respirable (see Section 6.1.4), several studies suggest that the most potent fibers are substantially thinner than the sharp cutoff in respirability (see Section 6.4). If these latter observations are valid then, as with length, differences in the ultimate response to thick and thin fibers must be attributable to differences in the tissue and cellular responses elicited by retained fibers of each width. As indicated with length, however, definitive conclusions regarding biochemical triggers and the effect of size on such triggers are not yet possible because the specific triggers that lead to

specific asbestos-related diseases have not been definitively identified. Still, useful inferences can be developed.

6.3.1 The Current Cancer Model

The following description of the current model for cancer is derived from the ideas presented in Moolgavkar et al. 1988, Mossman 1993, and Economou et al. 1994.

In the current model of cancer, normal cells must accumulate specific, multiple mutations before a tumorigenic cell is created that can lead to the development of cancer. Each successive mutation produces an initiated cell (a cell that is transformed from normal cells because it incorporates one or more of the requisite mutations, but that has not yet acquired all of the changes needed to produce cancer). Each initiated cell may then proliferate to generate a population of similarly initiated cells, which increases the probability that other events will lead to further mutation in at least one of these cells. Individual mutations may occur spontaneously or may be induced by exposure to mutagens.

Generally, the minimum, heritable changes required before a normal cell is transformed into a metastatic tumor cell include, but may not be limited to (see, for example, Hei et al. 1997 or Kravchenko et al. 1998):

- escape from terminal differentiation or programmed cell death (especially in response to DNA damage);
- escape from anchorage/neighbor dependent growth inhibition;
- development of self-promoting growth and proliferation; and
- active expression of cytokines needed to promote angiogenesis and allow tissue invasion.

It is not clear whether the mutations associated with these changes need to occur in a particular order, although the first of the above-listed changes would facilitate accumulation of all later changes. It is also unclear which of the above changes contribute to the time dependence of tumor development and this may vary among tumor types. It is likely that only a subset of the required mutations determine the ultimate time development of the associated cancer. For example, once a cell begins self-promoting growth, later mutations (even relatively rare ones) may become incorporated rather quickly. Also, some mutations may be rare or may require intervention by a toxic agent, while other mutations may occur spontaneously and may thus occur frequently, once a sufficient number of initiated precursor cells are generated. This is one of the reasons that models with as few as one or two stages have proven successful at predicting the time course of many types of cancer (see, for example, Moolgavkar et al. 1988).

To produce cancer, the mutations that occur must also be "heritable" meaning that they must be preserved and passed on to daughter cells during mitosis. Thus, it is not only necessary to cause alteration in the DNA of a cell (genetic damage), but the mechanisms by which the cell subsequently repairs such changes or prevents cell division (e.g., arrest of the cell cycle, programmed cell death, terminal differentiation) in the presence of such changes must also be defeated. Generally, if a cell proceeds through DNA synthesis (in preparation for mitosis) before accumulated alterations to DNA are repaired, the sites of such alterations can lead to errors in replication during synthesis, which in turn result in permanent, heritable mutations in one or both of the daughter cells that are created from mitosis.

Toxic agents that (directly or indirectly) cause DNA alterations may contribute to the development of cancer by inducing one or more of the set of requisite mutations required for cancer to develop. In traditional parlance, such agents are termed "initiators". In addition, any toxic agent that enhances proliferation also facilitates the development of cancer both by increasing the probability of creating spontaneous mutations (due to errors that infrequently, but unavoidably, occur whenever DNA is synthesized in support of mitosis) and by increasing the numbers of any initiated cells that may be present, which may then serve as additional targets for initiators or may incorporate additional spontaneous mutations. Agents that facilitate the development of cancer by inducing proliferation are traditionally termed "promoters."

Multiple mechanisms have been identified by which both initiators and promoters may act. Initiators, for example, may react directly with DNA to cause genetic damage, or may induce generation of other reactive species (such as reactive oxygen species or reactive nitrogen species) that, in turn, react with DNA to cause genetic damage. In addition, fibrous materials may uniquely damage chromosomes by interfering with mitosis causing aneuploidy (incorporation of an incorrect number of chromosome copies in cells) and/or various clastogenic changes (alterations in the organization and structure of specific chromosomes).

Promoters may also induce proliferation via a variety of mechanisms. Cytotoxic agents, for example, may induce proliferation in a tissue by damaging or killing cells and thereby induce stem cells to proliferate to replace the damaged cells. Promoters may also induce release of various growth factors that, in turn, induce proliferation in targeted tissues. This may occur, for example, as part of the inflammatory response to tissue insult.

Promoters that are biopersistent (such as long asbestos fibers) or promoters that are continually reintroduced (through chronic, external exposure) may also chronically up regulate (or down regulate) certain cell signaling cascades that may contribute to cancer development in a variety of ways including: (1) activation of genes that mediate proliferation or production of various growth factors (including any of various oncogenes) or (2) suppression of genes that inhibit proliferation or growth (including any of various tumor-suppressor genes).

There is growing evidence that all varieties of asbestos fibers (and certain other fibrous materials) can act both as cancer initiators and promoters. However, the biological responses to these materials appear to vary in different tissues so that it may be important to separately evaluate the behavior of asbestos in specific tissues. Biological responses to varying fiber types also appear to vary, particularly in relation to a fiber's biopersistence (Sections 6.2.1 and 6.2.4). Accordingly, an overview of the generic evidence that specific types of asbestos may act as an

initiator and, separately, as a promoter is reviewed below, followed by consideration of the more limited data suggesting tissue-specific variation in biological responses.

6.3.2 Evidence for Transformation

Several recent studies provide evidence that specific types of asbestos can induce transformation of cells in specific tissues (both lung epithelium and mesothelium) to create tumor cells. This provides further, confirmatory support for the whole animal studies in which cancer is induced by exposure to asbestos (see Sections 6.4).

An immortalized, but non-tumorigenic, cell line of human bronchial epithelial cells (BEP2D cells) was transformed by a single exposure to 4 ug/cm^2 UICC chrysotile B (Rhodesian). Surviving cells (the treatment caused 18% cell death) went through several transformations including: altered growth kinetics, resistence to serum induced terminal differentiation, and loss of anchorage dependent growth, before becoming tumorigenic (Hei et al. 1997). Tumorigenicity developed in the various exposed cell lines over a period of several to 11 weeks following exposure. When injected into nude mice, secondary tumors developed with a latency of 8–10 weeks.

The authors indicate that there were no mutations in these cells at either codon 12 or 13 or the ras gene (mutations that have sometimes been observed in asbestos-induced lung cancers. Also, because this cell line already contains alterations in genes for p53 (a protein that plays a role in cell-cycle control, among other things, see Table 6-6) and Rb (Table 6-6), the authors speculate that such changes are not rate controlling for transformation to cancer.

It should also be noted that cultures of Type II cells have been particularly difficult to maintain due to the tendency of these cells to undergo terminal differentiation (to Type I cells) once they are removed from their natural environment in the epithelial lining of lung alveoli (see Leikoff and Driscoll 1993, as described in Section 4.4).

Kravchenko et al. (1998) indicates that, unlike cultures of lung epithelial cells, *in vitro* cultures of rat mesothelial cells tend to transform spontaneously to tumorigenic cells. The major changes that occur with time include: altered response to epithelial growth factor (from growth-proliferation inhibition by this factor to growth-proliferation stimulation), morphological changes (from polygonal epithelial-like cells to elongated fibroblast-like cells and, eventually, polynucleated cells exhibiting broad polymorphism), and multi-layered growth and an ability to grow as colonies and masses in semi-solid agar. Eventually, these cells become immortal and induce cancer when harvested and injected into other rats. The authors indicate that asbestos-induced transformations in such cultures proceed through identical stages, but that they occur much more rapidly. For example, incorporation of the stimulating response to EGF occurs spontaneously at passages 9 or 10, but at passages 6 or 7 when induced by asbestos. Asbestos was applied at 5 μg/cm^2, which was noted to be sub-lethal (95% cell survival was noted at this rate of application).

Table 6-6a. Sources of Various Cytokines and Other Chemical Transmitters

Chemical Species	Abbrev.	Sources	Reference	Effects	Reference
Signal Transmitters					
Activator Protein-1	AP-1			A transcription factor	Mossman and Churg 1998 (Citing: Angel and Karin 1991)
				Binds the DNA promoter region of genes governing inflammation, proliferatin, and apoptosis	
	BAX	Induced by high concentrations of p53	Lechner et al. 1997	Induces apoptosis	Lechner et al. 1997
	Bcl-2			Inhibits apoptosis	Lechner et al. 1997
Fifth Component of Compliment	C5			Mediates asbestos-induced fibrosis	McGavran et al. 1989
Cyclin Dependent Kinases	CDK's			Mediates cell cycle	Lechner et al. 1997
Cyclin Dependent Kinase Inhibitors	CDI's			Inhibits advance of cell cycle	Lechner et al. 1997
	CINC				
Epithelial Growth Factor	EGF			Inhibits proliferation of mesothelial cells	Kravchenko et al. 1998
				Stimulates proliferation of mesothelioma tumor cells	Goodglick et al. 1997
Epithelial Growth Factor Receptor	EGFR			Mediates MAPK signaling	Mossman et al. 1997

Table 6-6a. Sources of Various Cytokines and Other Chemical Transmitters *(continued)*

Chemical Species	Abbrev.	Sources	Reference	Effects	Reference
EGFR regulated kinase	ERK			Mediates apoptosis	Mossman et al. 1997
Granulocyte-macrophage colony Stimulating Factor	GM-CSF				
	GRP78				
Human neutrophil elastase	HNE	Released from asbestos activated PMN	Kamp et al. 1993	By itself, increases pulmonary epithelial cell detachment in culture	Kamp et al. 1993
				With asbestos, increases pulmonary epithelial cell lysis	Kamp et al. 1993
	HSP72/73				
Intercellular adhesion molecule-1	ICAM-1	Released by lung epithelial and endothelial cells following exposure to silica but not TiO2	Nario and Hubbard 1997	Facilitates migration of leukocytes out of blood to sites of injury	Nario and Hubbard 1997
		Enhanced expression by RPM cells exposed to chrys or crc	Choe et al. 1997		
Interleukin-1	IL-1				
Interleukin-6	IL-6	Induced by ROS in Type II epithelial cells	Luster and Simeonova 1998	Is a pleiotropic cytokine	Luster and Simeonova 1998
Interleukin-8	IL-8			Is a neutrophil chemoattractant	Luster and Simeonova 1998

Table 6-6a. Sources of Various Cytokines and Other Chemical Transmitters *(continued)*

Chemical Species	Abbrev.	Sources	Reference	Effects	Reference
Inducible Nitric Oxid Synthase	iNOS	Expressed by activated macrophages, but not in primates	Jesch et al. 1997		
Keritonizing Growth Factor	KGF	Derived from fibroblasts	Adamson 1997	Induces transient proliferation of mesothelial cells	Adamson 1997
Mitogen Activated Protein Kinase	MAPK			Mediates transcription of AP-1	Mossman et al. 1997
				Mediates ERK signaling	Mossman et al. 1997
Macrophage Inflammatory Protein-1alpha	MIP-1 alpha				
Macrophage Inflammatory Protein-2	MIP-2			A chemoattractant for PMN's, but may not be involved with inflammatory response	Osier et al. 1997
Matrix Metallo-proteinases	MMP's	Relative expression affected by cigaret smoke and fiber exposure	Morimoto et al. 1997		
	Neu				
Nuclear Factor-KB	NF-KB			A transcription factor that regulates genes involved with the inflammatory response, cell adhesion, and growth control.	Barchowsky et al. 1998
Nitric Oxide Synthase	NOS				

Table 6-6a. Sources of Various Cytokines and Other Chemical Transmitters *(continued)*

Chemical Species	Abbrev.	Sources	Reference	Effects	Reference
Ornithine Decarboxylase	odc			Promoted by AP-1	Mossman and Churg 1998
				Encodes a key enzyme for the biosynthesis of polyamines	Mossman and Churg 1998
Platelet-Derived Growth Factor	PDGF	Activated macrophages	Bauman et al. 1990	Induces proliferation of lung fibroblasts	Bauman et al. 1990
		Elevated expression in mesothelioma cells	Lechner et al. 1997	Induce proliferation of mesothelial cells	Brody et al. 1997
		Asbestos and iron treated AM and Interstitial macrophages release PDGF	Osornio-Vargas et al. 1993	Is a chemotactic attractant for rat lung fibroblasts	Osornio-Vargas et al. 1993
	p53	Induced by DNA damage	Lechner et al. 1997	At low conc, arrests cell cycle at G1/S	Unfried et al. 1997
				At higher conc, induces BAX protein, which induces apoptosis	
Poly(ADP-ribosyl)polymerase		Inhibited by 3-aminobenzamide	Broaddus et al. 1997		
	Rb				
Tissue inhibitors of MMP's	TIMP's	Relative expression affected by cigaret smoke and fiber exposure			

Table 6-6a. Sources of Various Cytokines and Other Chemical Transmitters *(continued)*

Chemical Species	Abbrev.	Sources	Reference	Effects	Reference
Tumor Necrosis Factor Alpha	TNF-alpha	Some particles induce activated macrophages to release this (shown both in vitro and in vivo)	Driscoll et al. 1997	Induces JNK arm of MAPK cascade	Mossman et al. 1997
		Regulated by oxidant-sensitive transcription of NF-KB	Driscoll et al. 1997	Is involved in the recruitment of inflammatory cells	Driscoll et al. 1997
		Macrophages in BAL from asbestosis and idiopathic interstitial fibrosis patients release TNFalpha	Zhang et al. 1993	Stimulates macrphages, epithelial cells,endothelial cells, fibroblasts to secrete chemokines and adhesion molecules	Driscoll et al. 1997
				Can induce apoptosis among neutrophils	Leigh et al. 1997
				Can induce ROS production in leukocytes	Kaiglova et al. 1999
				Intradermal inj stimulates local accumulation of fibroblasts and collagen	Zhang et al. 1993
				In vitro, stimulates fibroblast DNA synthesis and proliferation	Zhang et al. 1993
Transforming Growth Factor Alpha	TGF-alpha	Expressed in BA epithelium exposed to asbestos	Brody et al. 1997	Is a mitogen for epithelial cells	Brody et al. 1997

Table 6-6a. Sources of Various Cytokines and Other Chemical Transmitters *(continued)*

Chemical Species	Abbrev.	Sources	Reference	Effects	Reference
Transforming Growth Factor Beta	TGF-beta	Expressed in BA epithelium exposed to asbestos	Brody et al. 1997	Inhibits fibroblast proliferation but stimulates formation of extracellular matrix	Brody et al. 1997
		Macrophage stimulated Type II epi cells produce both TGF-beta1 and TGF-beta2	Brody et al. 1997	Can induce apoptosis in different types of cells	Leigh et al. 1997
		All three isoforms expressed in the fibrotic lesions (by hyperplatic type II cells) of asbestosis and pleural fibrosis patients from Quebec	Jagiirdir et al. 1997	Does not appear to induce chemotaxis of rat lung fibroblasts	Osornio-Vargas et al. 1993
		Mesothelial tumor cells expressed only TGF-beta1 and 2	Jagiirdir et al. 1997	Induces chemotaxis of rat mononuclear leukocytes	Osornio-Vargas et al. 1993
		Also type II cells of silicosis patients express all three forms	Jagiirdir et al. 1997		
		Asbestos and iron treated AM and Interstitial macrophages release TGF-beta	Osornio-Vargas et al. 1993		
Urokinase-type Plasminogen Activator	uPA			Associated with increased pericellular protyolytic activity in endothelial tissue	Barchowsky et al. 1998

Table 6-6a. Sources of Various Cytokines and Other Chemical Transmitters *(continued)*

Chemical Species	Abbrev.	Sources	Reference	Effects	Reference
Vascular Cell Adhesion Molecule	VCAM-1	Enhanced expression by RPM cells exposed to chrys or crc	Choe et al. 1997		
	WT1			Forms a heterodimer w p53 and alters behavior	Unfried et al. 1997
Enzymes					
Mn-dependent SuperOxide Dismutase	Mn-SOD				
Gene Products					
	c-fos			Linked to apoptosis	Timblin et al. 1998a
				Transcription factor that activates the TGF-beta1 promotor	Jagirdar et al. 1997
				Proteins of c-fos dimerize with c-jun to create activator protein-1 (AP-1)	Mossman and Churg 1998
	c-jun			Linked to proliferation	Timblin et al. 1998a
				Transcription factor that activates the TGF-beta1 promotor	Jagirdar et al. 1997
				Transcription factor that activates the TGF-beta1 promotor	Mossman and Churg 1998
	mdm2			A protococoncogene that inhibits p53	Lechner et al. 1997
	c-myc				

Table 6-6b. Effects of Various Cytokines and Other Chemical Transmitters

Chemical Species	Abbrev.	Effects	Reference
Signal Transmitters			
Activator Protein-1	AP-1	A transcription factor	Mossman and Churg 1998 (Citing: Angel and Karin 1991)
		Binds the DNA promoter region of genes governing inflammation, proliferatin, and apoptosis	
	BAX	Induces apoptosis	Lechner et al. 1997
	Bcl-2	Inhibits apoptosis	Lechner et al. 1997
Fifth Component of Compliment	C5	Mediates asbestos-induced fibrosis	McGavran et al. 1989
Cyclin Dependent Kinases	CDK's	Mediates cell cycle	Lechner et al. 1997
Cyclin Dependent Kinase Inhibitors	CDI's	Inhibits advance of cell cycle	Lechner et al. 1997
Cytokine-induced Neutrophil Chemoattractant	CINC		
Epithelial Growth Factor	EGF	Inhibits proliferation of mesothelial cells	Kravchenko et al. 1998
		Stimulates proliferation of mesothelioma tumor cells	Goodglick et al. 1997
Epithelial Growth Factor Receptor	EGFR	Mediates MAPK signaling	Mossman et al. 1997
EGFR regulated kinase	ERK	Mediates apoptosis	Mossman et al. 1997
Granulocyte-macrophage colony Stimulating Factor	GM-CSF		
	GRP78		
Human neutrophil elastase	HNE	By itself, increases pulmonary epithelial cell detachment in culture	Kamp et al. 1993

Table 6-6b. Effects of Various Cytokines and Other Chemical Transmitters *(continued)*

Chemical Species	Abbrev.	Effects	Reference
		With asbestos, increases pulmonary epithelial cell lysis	Kamp et al. 1993
	HSP72/73		
Intercellular adhesion molecule-1	ICAM-1	Facilitates migration of leukocytes out of blood to sites of injury	Nario and Hubbard 1997
Interleukin-1	IL-1		
Interleukin-6	IL-6	Is a pleiotropic cytokine	Luster and Simeonova 1998
Interleukin-8	IL-8	Is a neutrophil chemoattractant	Luster and Simeonova 1998
Inducible Nitric Oxid Synthase	iNOS		
Keritonizing Growth Factor	KGF	Induces transient proliferation of mesothelial cells	Adamson 1997
Mitogen Activated Protein Kinase	MAPK	Mediates transcription of AP-1	Mossman et al. 1997
		Mediates ERK signaling	Mossman et al. 1997
Macrophage Inflammatory Protein-1alpha	MIP-1 alpha		
Macrophage Inflammatory Protein-2	MIP-2	A chemoattractant for PMN's, but may not be involved with inflammatory response	Osier et al. 1997
Matrix Metalloproteinases	MMP's		
	Neu		
Nuclear Factor-KB	NF-KB	A transcription factor that regulates genes involved with the inflammatory response, cell adhesion, and growth control.	Barchowsky et al. 1998
Nitric Oxide Synthase	NOS		
Ornithine Decarboxylase	odc	Promoted by AP-1	Mossman and Churg 1998

Table 6-6b. Effects of Various Cytokines and Other Chemical Transmitters *(continued)*

Chemical Species	Abbrev.	Effects	Reference
		Encodes a key enzyme for the biosynthesis of polyamines	Mossman and Churg 1998
Platelet-Derived Growth Factor	PDGF	Induces proliferation of lung fibroblasts	Bauman et al. 1990
		Induces proliferation of mesothelial cells	Brody et al. 1997
		Is a chemotactic attractant for rat lung fibroblasts	Osornio-Vargas et al. 1993
	p53	At low concentration, arrests cell cycle at G1/S	Unfried et al. 1997
		At higher concentration, induces BAX protein, which induces apoptosis	
Poly(ADP-ribosyl)polymerase			
Tissue inhibitors of MMP's	TIMP's		
Tumor Necrosis Factor Alpha	TNF-alpha	Induces JNK arm of MAPK cascade	Mossman et al. 1997
		Is involved in the recruitment of inflammatory cells	Driscoll et al. 1997
		Stimulates macrphages, epithelial cells,endothelial cells, fibroblasts to secrete chemokines and adhesion molecules	Driscoll et al. 1997
		Can induce apoptosis among neutrophils	Leigh et al. 1997
		Can induce ROS production in leukocytes	Kaiglova et al. 1999
		Intradermal inj stimulates focal accumulation of fibroblasts and collagen	Zhang et al. 1993
		In vitro, stimulates fibroblast DNA synthesis and proliferation	Zhang et al. 1993
Transforming Growth Factor Alpha	TGF-alpha	Is a mitogen for epithelial cells	Brody et al. 1997
Transforming Growth Factor Beta	TGF-Beta	Inhibits fibroblast proliferation but stimulates formation of extracellular matrix	Brody et al. 1997

Table 6-6b. Effects of Various Cytokines and Other Chemical Transmitters *(continued)*

Chemical Species	Abbrev.	Effects	Reference
		Can induce apoptosis in different types of cells	Leigh et al. 1997
		Does not appear to induce chemotaxis of rat lung fibroblasts	Osornio-Vargas et al. 1993
		Induces chemotaxis of rat mononuclear leukocytes	Osornio-Vargas et al. 1993
Urokinase-type Plasminogen Activator	uPA	Associated with increased pericellular protyolytic activity in endothelial tissue	Barchowsky et al. 1998
Vascular Cell Adhesion Molecule	VCAM-1		
	WT1	Forms a heterodimer w p53 and alters behavior	Unfried et al. 1997
Enzymes			
Mn-dependent SuperOxide Dismutase	Mn-SOD		
Gene Products			
	c-fos	Linked to apoptosis	Timblin et al. 1998a
		Transcription factor that activates the TGF-beta1 promotor	Jagirdar et al. 1997
		Proteins of c-fos dimerize with c-jun to create activator protein-1 (AP-1)	Mossman and Churg 1998
	c-jun	Linked to proliferation	Timblin et al. 1998a
		Transcription factor that activates the TGF-beta1 promotor	Jagirdar et al. 1997
		Transcription factor that activates the TGF-beta1 promotor	Mossman and Churg 1998
	mdm2	A protococoncogene that inhibits p53	Lechner et al. 1997

Table 6-6b. Effects of Various Cytokines and Other Chemical Transmitters *(continued)*

Chemical Species	Abbrev.	Effects	Reference
	c-myc		
	H-RAS		
	K-RAS		

In a study in which p53 deficient mice were intrapleurally injected with UICC crocidolite (200 μg/week), Marsella et al. (1997) showed that p53 deficient mice exhibited substantially increased susceptibility to development of mesothelioma. In this study, 12.5% of homozygous mice (p53 deficient) developed mesothelioma and the rest died of lymphomas or hemangiosarcomas that develop spontaneously in these mice; 76% of heterozygous mice died of mesothelioma, and only 32% of wild-type mice (p53 competent) died of mesothelioma. The authors suggest that p53 deficient mice are susceptible to excess proliferation induced by crocidolite due to loss of control at the G1/S check point that is normally mediated by p53.

In further confirmation of this hypothesis, Marsella et al. (1997) report in the same study that 7.5 $\mu g/cm^2$ of crocidolite applied to wild murine mesothelial cells in culture induced substantial apoptosis while p53-deficient cells were resistant to apoptosis. The authors also note that most of the p53-deficient cells are tetraploid (suggesting a loss of a spindle check point) while the wild type cells are all diploid.

Note that, although these studies suggest that asbestos alone can induce complete transformation of both lung epithelial cells and mesothelial cells, such studies must be evaluated with caution. In the case of the Hei et al. (1997) study, for example, the effects of the (asbestos-independent) mutations required to initially establish the immortal line of lung epithelial cells are not entirely known. Therefore, the response to asbestos of epithelial cells *in vivo* may be substantially different.

In the case of the Kravchenko et al. (1998) study, it is clear that mesothelial cells *in vitro* do not behave in the same manner as those *in vivo*; *in vitro*, they spontaneously transform to tumorigenic cells. This suggests that one or more growth inhibitory signals exist *in vivo* (which are absent *in vitro*) that are critical to maintaining the health of the mesothelium

6.3.3 Evidence that Asbestos Acts As a Cancer Initiator

As indicated in a review by Jaurand (1997), historically, the status of asbestos as a mutagen was questioned, due primarily to the failure to produce detectable gene mutations in short-term assays. However, more recent studies provide clear evidence that asbestos (and other fibrous materials) can produce mutations. Moreover, fibrous materials may induce mutations by multiple mechanisms including, for example:

- direct interference with mitosis;
- production and release of reactive oxygen species (ROS); or
- production and release of reactive nitrogen species (RNS).

Of these, the most consistent, positive evidence that asbestos can act as a cancer initiator (i.e., a genotoxin or mutagen) has been from assays designed to detect the kinds of genetic damage that result from interference with mitosis (Jaurand 1997). Although generation of ROS and RNS plays a clear role in mediating asbestos-induced disease, the direct link to a role of asbestos as an initiator is somewhat more tenuous (see Sections 6.3.3.2 and 6.3.3.3).

6.3.3.1 Interference with mitosis

Apparently, the physical presence of asbestos fibers can interfere with proper spindle formation and the function of other structural units required for mitosis (Jaurand 1997). This typically leads to aneuploidy (an incorrect number of copies of the chromosomes contained within a cell), development of micronuclei (fragments of chromosomes enclosed in a membrane that are isolated from the main nucleus of the cell), and has also been shown to lead to clastogenic effects (changes in the organization and structure of the

chromosomes). Assays for these kinds of genetic alterations have consistently shown asbestos capable of inducing these effects.

Jaurand (1997) also indicates that:

- fibers must be phagocytized by the target cells before they can interfere with mitosis;
- once phagocytized, all asbestos types are observed to interfere with mitotic activity; and
- samples enriched in long, thin fibers enhance these effects. In contrast, short fibers do not appear to contribute to these effects.

Jaurand (1997) notes, however, that results related to fiber size have not been entirely consistent, primarily because not all studies have rigorously controlled for or even adequately characterized the sizes of the fibrous structures in test materials. Jaurand (1997) also notes that this mechanism is not dependent on the formation of reactive oxygen species or any other reactive free radicals.

Among studies that suggest that surface chemistry (or presumably fiber type) may not be an important factor in determining the degree to which asbestos (or other fibrous materials) interfere with mitosis, Keane et al. (1999), exposed cultured V79 cells (hamster lung fibroblasts) to untreated and HCl-treated chrysotile asbestos. The acid treatment substantially reduces the magnesium content on the surface of the chrysotile. The authors also noted a “small” effect on fiber size due to treatment (treated fibers showed a 20% excess of short fibers). Cells were exposed to doses ranging between 0.4 and 12.7 $\mu g/cm^2$ (each dose left in place for 24 hours and then rinsed off). Cells were harvested after an additional 24 hours and evaluated for cytotoxicity and the presence of micronuclei.

Results from the Keane et al. (1999) study indicate that untreated fibers were shown to be slightly more cytotoxic than treated fibers, but both treated and untreated fibers were observed to increase the abundance of micronuclei in a similar, dose-dependent fashion. The induction of micronuclei appeared to saturate at approximately 35/1,000 cells observed at an applied asbestos concentration of 40 $\mu g/cm^2$. In contrast, substantial cytotoxicity was only observed at the highest doses employed. The authors thus concluded that surface chemistry (at least in terms of magnesium content) does not appear to have a major affect on induction of micronuclei and that the observed genetic damage and cytotoxicity appear to occur through entirely independent mechanisms.

In other studies, cultured cells were assayed for a variety of genotoxic effects following exposure to a range of fibrous materials.

For example, Dopp and Shiffmann (1998) dosed human amniotic fluid (HAF) cells or Syrian Hamster Embryo (SHE) cells with UICC amosite, Rhodesian chrysotile, crocidolite, or ceramic fibers at concentrations of 0.5, 1.0, 5.0, and 10.0 $\mu g/cm^2$ and assayed the cultures for formation of micronuclei and a variety of clastogenic effects.

Based on their study, Dopp and Shiffmann (1998) report that all asbestos types induced formation of micronuclei in SHE cells in a dose-dependent fashion at rates that were significantly elevated over control animals. The effect appeared to saturate at doses between 1 and 5 $\mu g/cm^2$ and rates appeared to peak at between 48 and 66 hours post-exposure. Ceramic fibers, which were noted to be longer but thicker than the asbestos fibers tested, also showed significantly increased induction of micronuclei, but at rates less pronounced than for asbestos. However, it is difficult to judge whether this is due to differences in fiber type because the data in the paper are not adequate to distinguish effects of fiber size and number from effects of fiber type. Similar results were obtained with HAF cells, but overall rates were about one third those observed in SHE cells.

The authors also note observing various disturbance of chromatin structure during interphase. They report observing formation of chromatin bridges and chromosome displacements in meta and anaphases and impaired chromatin separation in mitosis. They also report that cytokinesis was frequently blocked.

In addition to the effects that they observed that are attributable to fiber interference with mitosis, Dopp and Shiffmann report observing a variety of clastogenic effects. In all cases where the authors labeled specific regions of specific chromosomes, fiber-exposed cells showed significantly greater frequencies of DNA breaks over controls or gypsum-exposed animals. Different regions of various chromosomes also showed significantly different frequencies of breakage with patterns that were specific to the different fiber types. The authors hypothesize that the observed clastogenic effects may be due to production of reactive oxygen species, to formation of some type of clastogenic factor, or to the direct interactions between fibers and chromosomes during mitosis that are the apparent cause of the disturbances discussed in the previous paragraphs. However, It was not possible to distinguish among hypothetical causes of the observed clastogenic effects in this study.

Kodama et al. (1993) exposed cultures of human bronchiolar epithelial (HBE) cells to asbestos (chrysotile at 0 to 4 $\mu g/cm^2$ and crocidolite at 0 to 300 $\mu g/cm^2$). They then examined cells at 24, 48, 72, and 96 hours following exposure for cytotoxic effects and cytogenetic effects. Results indicate that both fiber types induced concentration-dependent inhibition of cell proliferation and colony-forming ability, but chrysotile was 100 to 300 times more toxic. The authors report this translates to a 40-fold increase in toxicity on a fiber for fiber basis (although the range of sizes included in this count is not indicated).

Kodama et al. (1993) also report that, at 72 hours, chrysotile (4 $\mu g/cm^2$) caused a 2.7-fold increase in binuclei and a 1.6-fold increase in micronuclei. Over the same time interval, at 300 $\mu g/cm^2$, crocidolite caused a 1.9-fold increase in binuclei, but did not cause micronuclei. They also report that chrysotile failed to produce significant numerical chromosome changes in HBE cells and increased structural aberrations only at the 24-hour time point. The frequency of neither aneuploidy nor polyploidy was increased at any time point following exposure to asbestos in this study. The authors indicate that this contrasts with observations of relatively high incidences of asbestos-induced chromosome changes observed in some rodent cell cultures and clastogenic effects observed in human mesothelial cell lines. They further speculate that phagocytic cells with high mitogenetic activity are likely most susceptible to the effects of asbestos, which primarily interferes with mitosis. However, they suggest that epithelial cells that are exposed to fibers may undergo terminal differentiation (from Type II to Type I cells) and thus cease mitosis. This would effectively prevent adverse genetic effects from asbestos exposure. Such pathways are not available to mesothelial cells.

Hart et al. (1994) studied the effects of a range of fiber types (with varying size distributions) on Chinese hamster ovary (CHO) cells. The authors indicate that such cells are very different from cells in pulmonary tissues in that they are immortalized, aneuploid, undifferentiated, and preneoplasic. They also note that the responses observed in these cells differs from responses observed in cells from pulmonary tissues. Nevertheless, the implications concerning fiber size are instructive. Fibers evaluated included long, medium, short, and UICC crocidolite and chrysotile along with a range of MMVF's, RCF's, and fibrous glasses. Exposure concentrations ranged between 10 and 225 $\mu g/cm^2$.

Results from the Hart et al. (1994) study indicate that all of the fibers caused qualitatively similar toxic effects: concentration-dependent reduction in cell numbers and an increase in the incidence of abnormal nuclei with little or no loss in viability. Fiber-induced cell death in CHO cells appears to be minor, even at relatively high exposure concentrations. Based on mean dimensions (which is problematic), the diameter dependence on the observed toxic effects, particularly on the formation of aberrant nuclei, was slight or absent. However, the effect with length was striking. For lengths up to at least 20 μm, potency toward both cytotoxicity and the induction of aberrant nuclei increased dramatically with increasing length. The authors also note that the lack of an observed fiber composition associated effect on the

toxicity of CHO cells does not correlate with findings from recent rodent inhalation studies using the same test fibers. The authors therefore speculate that CHO cells may not represent an appropriate *in vitro* model for fiber effects. However, it may also be that effects *in vitro* occur over time scales that are rapid relative to those that occur *in vivo* so that biodurability is not important *in vitro*.

In a study by Takeuchi et al. (1999) cultured human mesothelioma cells (MSTO211H) and, separately, cultured human promyelocytic leukemia cells (HL60), which are not phagocytic, were dosed with crocidolite between 0.6 and 6.6 $\mu g/cm^2$ (no size range indicated). Studies with latex beads confirmed that the mesothelioma cells are actively phagocytic, but that the leukemia cells are not. The authors indicate that dosed mesothelioma cells showed significantly increased numbers of polynucleated cells, tetraploid cells, and cells with variable DNA content at the G0/G1 transition in the cell cycle and that the extent of effects was dose-dependent. Leukemia cells showed no such effects.

The authors further indicate that, when the mesothelioma cells were sorted by fiber content, those with the highest fiber content showed the greatest effects. The authors also indicate that cells are stimulated neither to release superoxide nor NO at the concentrations of crocidolite studied. However, they hypothesize that intracellular ROS may have been generated because they report finding increased levels of 8-OH-dGua (and oxidized form of one of the DNA bases) following crocidolite exposure. Nevertheless, the authors conclude that the mechanisms by which crocidolite induce cytotoxicity and, potentially, carcinogenicity is related to phagocytosis. Importantly, the effects described in the Takeuchi et al. study are entirely consistent with effects attributable to interference with mitosis, despite any speculation by the authors.

6.3.3.2 Generation of reactive oxygen species (ROS)

ROS have been implicated as mediators in a variety of toxic effects (including cancer initiation) associated with a broad range of toxins (see, for example, Floyd 1990). Moreover, substantial evidence indicates that asbestos can induce generation of ROS by several mechanisms and that asbestos-induced ROS play a role in several of the toxic effects attributable to asbestos (see below). However, whether ROS play an important role in asbestos-associated cancer initiation is less clear and needs to be evaluated carefully. Therefore, evidence that asbestos induces the production of ROS and that ROS contribute to the adverse health affects attributable to asbestos are reviewed below with particular attention to effects that may contribute to the initiation of cancer. Contributions by ROS to other asbestos-related toxic effects are also evaluated in later sections of this chapter.

Note, that generation of certain reactive nitrogen species (specifically the peroxinitrite ion) is closely associated with ROS generation so that evidence for the generation of certain reactive nitrogen species (Section 6.3.3.3) constitutes additional evidence for the generation of ROS.

Asbestos-induced Generation of ROS. Asbestos has been shown capable of generating a variety of reactive oxygen species (ROS) including hydrogen peroxide (H_2O_2), superoxide ($O2^-$), and hydroxyl radical (OH•) via several mechanisms (see, for example, Fubini 1997; Jaurand 1997; Kamp et al. 1992) including:

- catalytic production of superoxide from oxygen in aqueous solution;
- catalytic production hydrogen peroxide from oxygen in aqueous solution;
- catalytic production of hydroxyl radical by the Fenton reaction (degradation of hydrogen peroxide catalyzed by iron on the surface of fibers or mobilized from the surface of fibers);

- catalytic production of several ROS by redox cycling of iron on the surface of fibers or mobilized from the surface of fibers (Haber-Weiss type reactions);

- catalytic production of ROS by release of heme and heme protein from various cellular components;

- by inducing release of various ROS species from phagocytes during “frustrated” phagocytosis; and

- by binding to cell receptors or other features of surface membranes that trigger signaling cascades mediating the production and release of various ROS (and RNS).

For a general review of the chemistry involved in these processes, see Floyd (1990).

Fenton, Haber-Weiss, and Related Reactions. Most of the evidence for Fenton and Haber-Weiss reactions (and related free radical generating reactions) that take place on the surface of asbestos fibers comes from experiments in cell-free systems (see below). Therefore, their relevance to the conditions found *in vivo* may be limited. Moreover, the size of the fibers (especially in terms of their cumulative surface area) and the history of their surfaces (in terms of metal contaminants or coatings that might be present) may substantially alter the effects of such experiments (Fubini 1997). Unfortunately, however, few of the available studies report characterization of fiber sizes or surface conditions in sufficient detail to judge the importance of these effects.

***For fibers*.** Zalma et al. (1987) evaluated a range of fibers (UICC crocidolite, UICC amosite, UICC Canadian and Zimbobwean chrysotile, industrial chrysotile, and magnetite) for their ability to produce free radicals by the direct reduction of oxygen in aqueous solution. In some cases, hydrogen peroxide was also added to the solution. Results indicate that all of the fibers tested were able to generate hydroxyl radicals (even in the absence of hydrogen peroxide), but that the efficiency of production was a strong function of the activation (by grinding) or pacification (by coating with benzene or other agents) of the fiber surface. Chrysotile was reported to be the most efficient at generating radicals and the authors assumed that this is due to iron contamination on the surface (since iron is not a component of the “ideal” chrysotile fiber). However, such conclusions are difficult to evaluate in the absence of simultaneous consideration of fiber size.

Governa et al. (1998) evaluated the ability of wollastonite fibers to generate ROS in both a cell free system and a suspension of polymorphonucleocytes (PMN’s). The fibers were observed to produce ROS in both systems and that ground wollastonite produced substantially more ROS than unground. The efficiency of ROS generation in PMN suspension is also reported to be greater for wollastonite than for either chrysotile or crocidolite (tested in previous studies). However, no size information is given. Based on additional work with various inhibitors added to the system, the authors also indicate that only a fraction of the ROS generated was composed of hydroxyl radicals.

Brown et al. (1998) subjected several different fiber types (amosite, silicon carbide whiskers, RCF-1, and various fibrous glasses) to two standard chemical assays for free-radical production (in cell-free systems). The authors indicate that, of the fiber types tested, only amosite showed free radical activity significantly above controls in both assays and only RCF-1 additionally showed significantly elevated free radical activity in one assay. However, there is not enough information provided in this study to determine whether the observed differences are due to differences in fiber sizes, sample preparation (i.e., surface condition), or fiber type. In apparent contrast, for example, Gold et al. (1997) report that amosite and crocidolite produce few free radicals in cell free systems, unless they are ground.

Weitzman and Graceffa (1984) indicate that chrysotile, crocidolite, and amosite are all capable of catalyzing the generation of hydroxyl radicals and superoxide from hydrogen peroxide *in vitro* and that, based on experiments with various iron chelators, these reactions are iron dependent. The authors further indicate that hydrogen peroxide is produced in large quantities as a normal bi-product of tissue metabolism, but that it is effectively scavenged by various enzymes. The authors speculate that, by physically damaging cell membranes, asbestos may allow release of the precursor hydrogen peroxide before it can be scavenged.

For particles. Silica, residual fly ash, and ambient air dusts also can create ROS *in vitro* and the efficiency of production correlates with ionizable concentrations of various transition metals complexed on the dust (Martin et al. 1997). *In vivo*, such metal containing particles also cause release of ROS from macrophages (Martin et al. 1997). Additionally, binding of silica to plasma membranes of airway lung cells and phagosomes provokes generation of ROS.

Castronova et al. (1997) further indicate that it is the concentration of contaminating iron on the surface of freshly fractured quartz that enhances free radical production in aqueous solution (in cell free systems). These authors also showed that high iron-containing (430 ppm) quartz dust inhaled by rats (at 20 mg/m^3 for 5 hours/day for 10 days) induced 5 times more leukocyte recruitment, 2 times more lavageable red blood cells, 30–90% increase in macrophage production of ROS, 71% increase in nitric oxide production by macrophages, and 38% increase in lipid peroxidation of lung tissue than observed in rats exposed to low iron-containing (56 ppm) quartz.

Although iron is required for the reactions considered here, studies indicate that the iron content of the fiber itself is not a good indicator of reactivity (Gold et al. 1997). Studies also indicate that the iron that participates in these reactions need not originate with the fiber (Fubini 1997; Jaurand 1997) and biological systems contain abundant sources of iron. Therefore, both iron-containing fibers and iron-free fibers have been shown to participate in these reactions *in vivo*.

Release of heme and heme protein. At least one research group (Rahman et al. 1997) indicates that heme and heme protein cause extensive DNA damage in the presence of asbestos *in vitro* and, based on previous studies, that this may involve heme catalyzed production of ROS following asbestos-induced release of heme from cytochrome P-450, from prostaglandin H synthetase (or perhaps from other heme containing proteins). Importantly, the authors indicate that such observations relate to a nuclear pool of heme, which suggests that ROS generation via this mechanism may occur in the immediate vicinity of DNA. The work by this group suggests at least one additional pathway by which asbestos may induce the production of ROS and by which ROS-mediated damage to DNA might occur.

Frustrated phagocytosis. Numerous studies indicate that long asbestos fibers (longer than somewhere between 10 and 20 μm) cannot be efficiently phagoycitized by macrophages (see, for example, Sections 4.4 and 6.2) and that macrophages that are damaged by such "frustrated" phagocytosis release ROS (see, for example, Kamp et al. 1992; Mossman and Marsh 1991). Due to the differences in the size of macrophages across species (see discussion of Krombach et al. [1997] in Section 4.4). The minimum length beyond which phagocytosis may become frustrated may differ in different animals. However, it is clearly longer fibers that contribute to this mechanism for generating ROS. Shorter fibers (<10 μm) are unlikely to cause frustrated phagocytosis in any of the mammalian species of potential interest.

Lim et al. (1997) showed that alveolar macorphages in culture (after stimulation with lippopolysaccharide) generated free radicals (ROS) when subsequently exposed to chrysotile, crocidolite, or amosite (all UICC). They found chrysotile to be the most potent inducer of free radical activity (which is not surprising given that UICC chrysotile contains the highest fraction of long fibers of the UICC samples tested (Berman, unpublished). Based on tests with various inhibitors, the authors indicated that

the free radicals generated by the alveolar macrophages occurred through a pathway mediated by protein tyrosine kinase, phospholipase C, and protein kinase C and that the effects are dose-related.

Kostyuk and Potapovich (1998) cultured peritoneal macrophages and showed that treatment with chrysotile asbestos (1 μg, no size data given) resulted in production of frustrated phagocytosis and cell injury (the latter as evidenced by release of lipid dehydrogenase, LDH, a marker for membrane damage). By working with various chelators and flavonoids (natural plant products, some of which quench superoxide and some of which chelate iron), the authors indicate that cell injury was likely induced by superoxide and that the superoxide was likely produced by an iron-dependent mechanism. Note that this contrasts with the above studies that suggests production of radicals by frustrated phagocytosis in culture is an iron-independent mechanism.

At least for one kind of phagocyte: polymorphonucleocytes (PMN's), a study by Ishizaki et al. (1997) suggests that crocidolite and erionite may induce production of ROS from PMN's by each of two mechanisms. The first requires phagocytosis and may represent the traditional, "frustrated" phagocytosis pathway indicated above. The second pathway is triggered by an interaction between the fiber and the cell surface and is mediated by NADPH. The authors also cite evidence that chrysotile may similarly act through both of these pathways.

Afaq et al. (1998) cultured alveolar macrophages and peripheral red blood cells (RBC's) that were harvested from rats 30-days following a single 5 mg intratracheal instillation of UICC crocidolite, UICC chrysotile, or ultrafine titanium dioxide. The authors indicate that populations of alveolar macrophages were significantly increased (over sham-exposed rats) for all three particle types and that acid phosphatase and lipid dehydrogenase (LDH), which are markers of cell membrane damage, were observed in cell-free lung lavage from animals exposed to all three particle types. Both alveolar macrophages taken from asbestos-exposed animals (both types) showed significantly elevated lipid peroxidation and hydrogen peroxide production over titanium dioxide exposed animals. However, the latter also showed elevated peroxidation and peroxide production that were significantly elevated over sham-exposed animals. Similar results were observed among RBC's from asbestos-exposed animals, but not from titanium dioxide-exposed animals. Note, it is possible that ROS production induced by TiO_2 occurs by a different mechanism (or set of mechanisms) than that for asbestos (see, for example, Palekar et al. 1979, Section 6.3.4.4).

***In vivo* Evidence for Asbestos-generated ROS.** Several studies involving whole animals also indicate that asbestos exposure induces the generation of ROS. Importantly, in such studies, evidence for generation of ROS is generally determined based on observation of the putative effects of ROS, rather than ROS directly.

Ghio et al. (1998) intratracheally instilled 500 μg of crocidolite (NIEHS) into rats. This was observed to induce a neutrophilic inflammatory response within 24 hours (in contrast to saline-exposed rats). The authors collected chloroform extracts from exposed lungs and subjected them to electron spin residence (ESR) spectrometry. Results indicate the presence of a carbon-centered radical adduct that has a structure consistent with products of lipid-peroxidation. The radical signal was only observed in asbestos-exposed animals and persisted even after one-month following exposure. The authors also report that depletion of neutrophils did not affect the signal and that dextrin-induced inflammation did not produce the signal.

Yamaguchi et al. (1999) studied effects in rat lung tissue at 1, 3, 5, 7, and 9 days following a single intratracheal instillation of 2mg of either glass fiber or UICC crocidolite. The authors indicate significantly increased levels of 8-OH-Guanine (an oxidized form of the DNA base Guanine) one day after crocidolite instillation and increasing repair activity for this oxidized form of guanine with time that became significant at days 7 and 9 following instillation. Glass fibers (noted to be non-fibrogenic and

non-tumorigenic) did not produce either increases in 8-OH-Gua or its repair activity. The effects associated with crocidolite were all noted to be dose related.

Several of these studies also suggest distinctions in ROS generation (either the absolute generation of ROS or generation of specific ROS species by specific tissues) due to differences in fiber (or particle) size or type.

Nehls et al. (1997) intratracheally instilled rats either with quartz (2.5 mg) or corundum (2.5 mg). The latter mineral is reportedly non-tumorigenic. Results indicate that lung epithelial cells in quartz exposed rats exhibited increased 8-oxo-Guanine levels (a DNA adduct generated by reaction with ROS, see above) that persisted for up to 90 days post-exposure. Elevated levels of the DNA adduct appeared in all cell types in all areas of the lung. The authors suggest that the observed persistence of the elevated levels of 8-oxo-Guanine suggests that it was produced at a rate in excess of the lung's capacity for repair. The authors also report enhanced and persistent inflammation, cell proliferation, and an increase in neutrophil population in bronchio-alveolar lavage (BAL) fluid and an increase in tumor necrosis factor alpha (TNF-α) in BAL fluid in the quartz exposed animals. TNF-α is a cytokine linked to a variety of effects including the recruitment of inflammatory cells (see Table 6-6). In contrast, exposure to corundum produced none of the effects observed with quartz.

Timblin et al. (1998b) report that ROS induced responses by rat lung epithelial cells vary depending on whether exposure is to crocidolite, hydrogen peroxide, or cadmium chloride ($CdCl_2$). In response to ROS generation induced by the first two agents increased levels of cJun protein (a protooncogene, Table 6-6) is observed. Further, crocidolite, but not hydrogen peroxide, causes elevation in the levels of manganese-containing superoxide (MnSOD) dismutase (an enzyme that catalyzes dismutation of superoxide, Table 6-6). Neither of these agents affect levels of either of two common stress proteins (Table 6-6): GRP78 or HSP72/73, nor do they affect cellular glutathione levels. In contrast, cadmium chloride does not alter MnSOD levels, but increases levels of GRP78 and HSP72/73 in addition to cJun protein. Therefore, ROS-related mechanisms may be complex and may be toxicant-specific. Thus, it may not be correct to assume that all fibers and particles act through common ROS-related pathways.

In contrast to the results of the above study (which showed no affect on glutathione levels), Golladay et al. (1997) showed that human lung epithelial cells (cultured A549 cells) exposed to crocidolite (NIEHS sample) showed substantial reduction in intracellular levels of glutathione (without increases in the oxidized forms of glutathione). Rather, an associated increase in extracellular, reduced glutathione was observed, suggesting that crocidolite induces release of glutathione from the interior of these cells to the environment. The authors also indicate that, given that the half-life for reduced glutathione outside of cells is on the order of an hour, while extracellular reduced glutathione levels remained elevated for more than 24 hours following exposure, cells must have been releasing reduced glutathione continuously. Because no concomitant release of LDH or labeled adenine was observed (despite loading of cells with labeled adenine prior to the experiment), the authors conclude that release of glutathione is not associated with membrane disruption or apoptosis (which is induced to some degree by exposure to crocidolite). Also, all of the effects described above were similarly associated with exposure to de-ironized crocidolite. Thus, the iron content of the fibers does not play a role in this process.

Note that the apparent difference in the reported effect of crocidolite exposure on intracellular glutathione levels in the above two studies might be due (individually or in combination) to differences in the cell-types studied, differences in the size distribution of the crocidolite employed, differences in study design, or other factors. Insufficient information is available to distinguish among these possibilities.

Kaiglova et al. (1999) intrapleurally injected rats with 10 mg of long amosite and collected bronchio-alveolar lavage (BAL) fluid 24 hours following exposure and at later time intervals. They indicate that total protein and alkaline phophatase (AP) were both elevated in BAL 24 hours after exposure and that

AP remained elevated for at least 3 months following exposure. They also noted increased levels of lipid peroxides in BAL at 24 hours, but not 3 months following exposure. The authors indicate that antioxidants were significantly decreased following exposure: glutathione was significantly decreased in lung tissue at both 24 hours and 3 months following exposure, but was normal in BAL fluid at all time points; α-tokopherol and retinol were significantly decreased at 3 months in lung tissue; and ascorbic acid was significantly decreased in both lung tissue and BAL at 24 hours and remained low at 3 months. The authors indicate that decreases in antioxidants implies a role for ROS (or RNS) in lung tissue injury. It is also possible that the varied responses of specific antioxidants may suggest a role for toxin- and injury-specific ROS/RNS.

Conclusions Concerning Generation of ROS. Except for frustrated phagocytosis (which is unique to long fibers), ROS generation by the mechanisms discussed above are considered a common response to respiration of particles in general (see, for example, Martin et al. 1997 who suggest that ROS "...may be a global signaling mechanism mediating response to particulate insult mostly by activation of kinases and transcription factors common to many response genes." They further indicate that if the load of ROS generated is too great, or the airway in which it is generated has been previously impaired, "...these same mechanisms can result in deleterious respiratory lesions and outright pathology"). However, not all non-fibrous particles are similarly capable of inducing production of ROS. As indicated above, for example, while crystalline silica is a potent inducer of ROS production, carundum is not (Nehls et al. 1997). Moreover, the spectrum of ROS (set of species) that are induced by particular toxicants are generally specific to the offending toxicant (Timblin et al. 1998b). Therefore, the generic grouping of ROS mediated pathways by particles and, especially, by particles and fibers, does not appear justified. These mechanisms are more complex and individualized than such generic grouping suggests.

ROS can be generated by multiple pathways that are variously dependent on particle size, whether a particle is a fiber, fiber size, and particle or fiber type (i.e., chemical composition). The primary mechanism(s) through which ROS are generated in response to one type of particle or fiber may be very different than that through which ROS generation is induced by another and the resulting suite of ROS (set of species) may also differ. Importantly, the relationship between dose and response for each mechanism may also differ (see, for example, Palekar et al. 1979, Section 6.3.4.4).

Given the above, comparing among the ability of fibrous materials and non-fibrous analogs to induce generation of ROS requires that such analogs be properly matched before valid conclusions can be drawn. Thus, for example, the appropriate non-fibrous analog for crocidolite is the massive habit of reibeckite and the appropriate analog for chrysotile is the massive habit of antigorite or lizardite. Due to differences in both chemistry and crystal structure, crystalline silica is not an appropriate non-fibrous analog for any of the asbestos types. Moreover, because ROS can be generated by different mechanisms, critical comparison across analogs requires more than the simple confirmation that ROS are generated or even whether the relative efficiency with which ROS are generated is comparable. It is also necessary to contrast the specific complexion of ROS (set of species) generated and the specific tissue/cellular environments (i.e., locations within a cell) in which they are generated in response to each analog.

It is also clear that ROS are generated by both iron-dependent and iron-independent pathways. Even for the iron-dependent pathways, however, the source of iron need not derive from the fibers or particles themselves. Therefore, since iron is abundant *in vivo* (and the environment), both iron-containing and iron-free fibers (or particles) can potentially participate in both the iron-independent and the iron-dependent pathways.

Effects Mediated by ROS. ROS have been implicated as mediators in a variety of toxic effects (including cancer initiation) associated with a broad range of toxins (see, for example, Floyd 1990; Martin et al. 1997). Cellular and tissue effects that have been associated with the effects of ROS include:

- enhancement of overall uptake of particles by epithelium;
- stimulation of inflammatory responses;
- stimulation of various signaling cascades and production of cytokines;
- inducement of apoptosis;
- cytotoxicity;
- mediation of cell proliferation;
- formation of oxidized macromolecule (including DNA) adducts; and
- induction of DNA strand breaks.

However, only the last two of the above list of ROS effects are potentially relevant to the initiation of cancer (the topic of this section). The other effects in the above list likely contribute to the induction of other asbestos-related diseases and may even promote (but not initiate) asbestos-related cancer. Thus, they are addressed further in later sections of this chapter (see below).

Although, ROS generation is associated with exposure to various particles and fibers (including all forms of asbestos), generation of ROS does not necessarily imply carcinogenesis. For example, Zhu et al. (1998) indicate that ROS generation is induced in response to exposure to asbestos, crystalline silica, and coal mine dust. However, based on an extensive record of human exposure, the latter (coal mine dust) is not carcinogenic in humans. Therefore, evidence related to the last two of ROS-associated effects listed above, are examined in more detail below.

Several studies indicate that, once generated by exposure to asbestos, ROS can interact with DNA *in vitro* and *in vivo* to produce oxygenated adducts, primarily 8-oxo-Guanine. Of the studies reviewed above, for example, Yamaguchi et al. (1999) observed that crocidolite, but not (non-tumorigenic) glass produced dose-dependent increases in 8-oxo-Guanine in rat lung tissue following intratracheal instillation. Also, Leanderson et al. (1988), Park and Aust (1998), Keane et al. (1999) indicate that asbestos induces formation of oxidized DNA adducts in *in vitro* assays. Brown et al. (1998) indicate that asbestos induces ROS-mediated DNA strand breaks.

However, not all DNA strand breaks attributable to asbestos occur through pathways involving ROS. Ollikainen et al. (1999) exposed cultures of human mesothelial cells (MeT-5A, transfected with SV-40, but nontumorigenic) to hydrogen peroxide (100 μM) or crocidolite (2–4 $\mu g/cm^2$), either alone or in combination with TNF-α and performed assays for DNA strand breaks. The authors note that the concentrations of asbestos evaluated are well below those that have been associated with cytotoxic effects. Crocidolite alone was shown to produce DNA strand breaks at the concentrations tested. The authors also note that, at lower concentrations, only reversible effects were observed (presumably indicating DNA repair). Co-exposure to crocidolite and TNF-α increased the observed incidence of DNA damage, but the effect was less than additive. The authors indicate that additional studies with antioxidants indicate that the DNA damage induced by crocidolite in this study occurs through a mechanism that does not involve ROS. In fact, a potentially much more substantial mechanism by which asbestos may induce DNA breaks and various clastogenic alterations involves its ability to interfere with mitosis (Section 6.3.3.1).

There is also evidence that different tissues may respond to asbestos-induced ROS generation differently. For example, Zhu et al. (1998) indicate that MnSOD is found in the mitochondria of Type II epithelial cells of rats exposed to crocidolite. The authors further indicate that, because fibroblasts, alveolar macrophages, or endothelial cells do not display this protein when stimulated by exposure, this suggests a difference in the susceptibility of epithelial cells to certain types of asbestos-induced injury.

Importantly, although these studies provide evidence that indicates asbestos is capable of producing oxidized DNA adducts (or strand breaks) through ROS mediated processes, they do not address the question of whether such adducts can lead to heritable mutations in DNA *in vivo* nor do they indicate

whether such adducts lead to tumor production. Therefore, such studies should only be construed to suggest a potential that asbestos can act as a cancer initiator through ROS-mediated pathways.

As previously indicated, not all mechanisms involving the generation or effects of ROS are similarly fiber-size or fiber-type dependent and those that are do not necessarily depend on these variables in the same way. At this time, it is not possible to distinguish among the relative importance of the different mechanisms, so that it is difficult to judge the relative importance of the different effects. However, the overall general implication (with the few exceptions noted) is that ROS generation more likely contributes to other asbestos-related diseases and to cancer promotion than to cancer initiation.

One final note concerning the effects of ROS that specifically involves the behavior of the hydroxyl radical is also warranted. The hydroxyl radical is an extremely reactive species. Whether *in vitro* or *in vivo*, this species will react with virtually 100% efficiency with every organic molecule it encounters. Therefore the effects attributable to the hydroxyl radical are limited to those involving reactions in the immediate vicinity of the location at which it is generated. Thus, unless asbestos-induced generation of this radical occurs within the nucleus and in the immediate vicinity of susceptible strands of DNA, it is unlikely that these radicals are the direct cause of DNA damage.

Rather, hydroxyl radicals tend to react with cell membranes and other cellular components to produce further intermediate radicals (primarily lipid peroxides), which are much more stable than the hydroxyl radical and may migrate substantial distances before having an effect. It is likely that these intermediate radicals are ultimately responsible for any ROS-mediated DNA damage that may be attributed to asbestos.

6.3.3.3 Generation of reactive nitrogen species (RNS)

Nitric oxide (NO) is produced ubiquitously in biological systems and serves many functions (Zhu et al. 1998). It is highly reactive and, therefore, generally short-lived *in vivo*. However, nitric oxide has been shown to react with superoxide (O_2^-) to form the peroxynitrite ion ($ONOO^-$) at near diffusion-limited rates (see, for example, Zhu et al. 1998). This the peroxynitrite ion (an RNS) may represent the primary species responsible for the effects attributed to ROS (at least when the primary ROS formed is superoxide).

Asbestos-induced Generation of RNS. Alveolar macrophages, lung endothelial and epithelial cells, and alveolar epithelium (in both rats and humans), when stimulated by inflammatory agents, generate both superoxide and over-produce nitric oxide. These then combine to produce the perxoynitrite ion (Martin et al. 1997; Zhu et al. 1998). These cells up-regulate production of NO when stimulated by various cytokines, lipopolysaccharide, and interferon γ. Because the peroxynitrite ion is a strong oxidant and nitrating agent and is extremely reactive, evidence for its production is generally indicated in most studies by the presence of nitrotyrosine, the stable product of tyrosine nitration, (Zhu et al. 1998). Evidence for production of NO is frequently indicated by observation of nitrite. Numerous studies also provide evidence of nitric oxide and peroxynitrite ion production specifically in response to exposure to asbestos in various tissues.

Both chrysotile and crocidolite up-regulate the production of nitric oxide by alveolar macrophages in the presence of interferon-γ and the interaction between asbestos and interferon is synergistic. Non-fibrogenic carbonyl iron did not induce nitric oxide formation (Zhu et al. 1998). These authors also cite a study in which intratracheal instillation of silica and coal mine dust caused more inflammation and nitric oxide formation than TiO_2 or carbonyl iron (on an equal particle basis). This suggests both the geometry and chemical composition of particles determine their ability to up-regulate nitric oxide.

Inhalation of chrysotile or crocdolite induces secretion of both TNF-α and nitric oxide by pleural macrophages (Tanaka et al. 1998). Tanaka et al. (1998) studied the effects of RNS in rats exposed by inhalation to 6 to 8 mg/m^3 crocidolite or chrysotile (both NIEHS samples) for 6 hours/day, 5 days/week for 2 weeks. Rats were sacrificed at 1 and 6 weeks following exposure. The authors indicate that asbestos induces formation of stable products of nitric oxide in cells obtained by lung lavage 1 week after asbestos exposure. Nitrotyrosine (a marker for $ONOO^-$ formation) was also observed. Also, a greater number of alveolar macrophages and pleural macrophages were shown to express iNOS protein (the inducible form of nitric oxide synthase, Table 6-6) than sham exposed animals. Exposed rats showed significantly elevated immuno-staining for nitrotyrosine in the region of thickened duct bifurcations as well as within bronchiolar epithelium, alveolar macrophages, and mesothelial cells of both the visceral and parietal pleura. Nitrotyrosine staining was persistent, being observed at both 1 and 6 weeks following exposure.

Quinlin et al. (1998) studied the production of nitric oxide in rats exposed to crocidolite or chrysotile asbestos (both NIESH reference samples). Rats were exposed by inhalation at 6 hours/day, 5 days/week and lavaged at 3, 9, and 20 days. Lavaged macrophages showed significantly increased nitrite/nitrate (indicating production of nitric oxide) and this was suppressed with inhibitors to iNOS. Thus, nitric oxide is produced via an iNOS pathway. The authors also note that nitric oxide production correlated temporally with neutrophil influx in the lavage fluid. They also indicate that asbestos exposed animals showed a 3- to 4-fold increase in iNOS positive macrophages in their lungs.

Quinlin et al. (1998) also exposed cultured murine alveolar macrophages (RAW 264.7 cells) to crocidolite, riebeckite, and crstobalite silica *in vitro*. These cells showed increased iNOS mRNA following exposure to asbestos and even greater increases if the cells were also stimulated with lipopolysaccharide (LPS). Both crocidolite and riebeckite (but not cristobalite silica) stimulated increased iNOS promoter activity when applied in combination with LPS. Thus, in this case, their appears to be a mechanism that is sensitive to particle composition, but not size.

Park and Aust (1998) treated cultures of human lung epithelial (A549) cells with crocidolite and observed induction of iNOS and reduction of intracellular glutathione (GSH) levels. Based on studies with inhibitors, the authors further indicate that iron mobilized from crocidolite was required both for formation of nitric oxide and to generate 2'-deoxy-7-hydro-8-oxoguanosine, but not for the observed decrease in intracellular glutathione. The authors note that approximately 5 times as much chrysotile (containing approximately 3% iron) as crocidolite was required to produce the same level of nitric oxide formation. Importantly, these experiments were conducted *in vitro* in serum-free medium, so that no extra-biological source of iron was present.

Choe et al. (1998) dosed cultured rat pleural mesothelial cells with either chrysotile or crocidolite (both NIEHS samples) at concentrations between 1.05 and 8.4 $\mu g/cm^2$ with or without co-stimulation with 50 ng/ml of interleukin-1β (IL-1β). The authors report that mRNA for iNOS in asbestos and IL-1β dosed cells increased progressively from 2 to 12 hours following exposure. Both types of asbestos also stimulated production of nitric oxide (measured as nitrite) in IL-1β stimulated cells in a dose- and time-dependent fashion. Both types of asbestos also induced expression of iNOS protein and formation of nitrotyrosine (based on nitrate detection) in IL stimulated cells. In contrast, carbonyl iron particles did not induce any of the effects observed for asbestos in IL stimulated cells. Thus, formation of RNS appears to be either fiber size dependent (not induced by particles) or mineralogy-dependent (or both).

As with the production of ROS, RNS production is apparently a function of multiple, complex mechanisms. Also, as with production of ROS, the dose-response characteristics of the various mechanisms differ. Several of the mechanisms show a strong dependence on fiber size and some dependence on fiber type. However, there are other mechanisms that are dependent primarily on fiber (or particle) type, but may not be dependent on size (or at least not dependent on fiber size). At this point in

time, it is not possible to gauge the relative importance of the various mechanisms by which RNS may be generated, except that it is likely that the importance of the various mechanisms likely differ in different cells and tissues and likely differ as a function of the specific toxin whose presence is inducing RNS production.

There are also indications that production of RNS may be (animal) species specific. For example, Jesch et al. (1997) report that alveolar macrophages harvested from rats expressed iNOS when stimulated with either LPS (lippopolysaccharide) or interferon-γ. In contrast, iNOS expression could not be induced in hamster, monkey or human macrophages.

Effects Mediated by RNS. Based on Zhu et al. (1998), over-production of nitric oxide can:

- inactivate critical enzymes;
- cause DNA strand breaks that result in activation of poly-ADP-ribosyl transferase (PARS);
- inhibit both DNA and protein synthesis; and
- form peroxynitrite by reaction with superoxide.

In turn, peroxynitrite ion may:

- initiate iron-dependent lipid peroxidation;
- oxidize thiols;
- damage the mitochondrial electron transport chain; and
- nitrate phenolics (including tyrosine).

Also, some of the damage to alveolar epithelium and pulmonary surfactant system previously attributed to reactive oxygen species may actually be caused through ROS generation of peroxynitrite. For example, Chao et al. (1996) report that crocidolite treatment of human lung epithelial cells (A549 cells) results in formation of 8-hydroxy-2'-deoxyguanosine (8-OHdG) in DNA and synthesis of mRNA for iNOS. An iNOS inhibitor reduces intracellular nitrite and eliminates production of 8-OHdG. Addition of independent NO donor, recovers production of 8-OhdG. Thus, production of the oxygenated DNA adduct in this case appears to be generated by reaction with RNS.

As with ROS, it is primarily the potential for RNS to contribute to DNA damage (e.g., strand breaks or generation of oxygenated adducts) that represent the primary pathways by which RNS might participate in cancer initiation (as opposed to cancer promotion or other asbestos-related diseases). It appears that RNS-mediated DNA damage is closely associated with ROS generation and mediation of DNA damage (see Section 6.3.3.2). Thus, there is little to add here.

6.3.3.4 Conclusions concerning asbestos as a cancer initiator

The strongest, most consistent evidence that asbestos can act as a cancer initiator relates to the tendency of asbestos to interfere with mitosis. Although there is evidence that asbestos may induce production of DNA adducts and DNA strand breaks (through ROS and RNS mediated pathways), whether such adducts or breaks ultimately lead to permanent, heritable changes to DNA remain to be demonstrated. The relative importance of the ROS/RNS mediated pathways compared to the pathway involving interference with mitosis also remains to be determined. As indicated in later sections, however, ROS/RNS mediated pathways may play substantial roles in cancer promotion and induction of other asbestos-related diseases.

Regarding the primary mechanism by which asbestos may initiate cancer (interference with mitosis), the pathway is length dependent (short fibers do not appear to contribute to the effect). Further, although

there may also be a dependence on fiber type (chemical composition), it is apparent that all types of asbestos can act through this pathway. The dependence of this pathway on fiber diameter is less clear. Thus, other than to suggest that fibers must be respirable (and therefore thinner than approximately 0.7 μm, Section 6.1) to have an opportunity to act, whether further diameter constraints are associated specifically with the mechanism of cancer initiation is not known.

For pathways involving generation of ROS or RNS, some mechanisms (such as those associated with frustrated phagocytosis) are length dependent, others are not. Although there appears to be some dependence on fiber type for several mechanisms and a general dependence of several of these mechanisms on surface chemistry, the relative importance of fiber type to the overall contributions from these pathways remains to be determined.

Importantly, although crystalline silica may also act to produce some of the same effects as asbestos (including potentially induction or promotion of cancer), there is substantial evidence that this material does not act through the same pathways and that the characteristics of its respective dose-response relationships may differ. Thus, for example, while asbestos likely initiates cancer through a mechanism that favors long (and potentially thin) fibers, silica more likely acts through a mechanism that is dependent on total surface area, with freshly and finely ground material likely being the most potent. In contrast, grinding asbestos fibers tends to lesson carcinogenicity overall. Due to differences in chemistry and crystallinity (reinforced by studies indicating a lack of correspondence in behavior) crystalline silica does not appear to be an appropriate analog for any of the asbestos types. Rather, for example, the appropriate non-fibrous analog for crocidolite is riebeckite and the appropriate non-fibrous analog for chrysotile is antigorite or lizardite.

There is also evidence that the relative importance of asbestos as a cancer initiator may differ in differing tissues. For example, asbestos can only interfere with mitosis in cells that actively phagocytize fibers and not all cell types actively phagocytize particles (although both mesothelial cells and pulmonary epithelial cells appear to actively phagocytize fibers, Section 6.3.3.1). However, there is also evidence that pulmonary epithelial cells (Type II) may undergo terminal differentiation to Type I cells and thus escape potential cancer initiation by asbestos (Section 6.3.3.1). Such a pathway is not available to mesothelial cells. To the extent that pathways involving generation of ROS or RNS contribute to cancer initiation, as indicated throughout this section, the rates of generation and the spectrum of the species generated varies as a function of cell type.

6.3.4 Evidence that Asbestos Acts As a Cancer Promoter

Primarily, asbestos may promote cancer by facilitating tissue proliferation. However, additional mechanisms associated with the observed interaction between asbestos exposure and smoking (Section 6.3.4.6) also need to be considered.

Substantial evidence exists indicating that asbestos induces proliferation in target tissues associated with lung cancer and mesothelioma and this is summarized below followed by an overview of studies that suggest the various mechanisms by which asbestos may facilitate such proliferation. Evidence suggesting the various mechanisms related to the interaction between smoking and asbestos exposure are also briefly reviewed.

There are numerous mechanisms by which asbestos may facilitate proliferation including:

- direct cell signaling to induce proliferation. This may occur by:
  - direct interactions between fibers and receptors on the cell surface;
  - interactions between phagocytized fibers and intracellular components of

signaling cascades; and
– or interactions between cells and intermediate species (e.g., ROS or RNS) whose generation and release has been induced by asbestos; or

! response to induced cell death in target tissues, which then stimulates stem cells to proliferate to replace killed cells. Cell death may be induced either through:
– inducing apoptosis (programmed cell death); or
– direct cytotoxic effects, which leads to necrosis.

These pathways are summarized in Table 6-5, which provides a perspective on the complexity of the interactions between asbestos and the cells and tissues of the body.

Regarding asbestos-induced cell death, asbestos-induced apoptosis (and all of the other effects described above) typically occurs at exposure concentrations that are much lower than required to induce frank cytotoxic effects (Sections 6.3.4.3 and 6.3.4.4). Therefore, it is primarily the former that is of potential interest in terms of implications for asbestos-induced diseases in humans. Due to the high exposure concentrations typically required, the importance of contributions from frank cytotoxicity to human disease is unclear (Section 6.3.4.4).

6.3.4.1 Asbestos-induced proliferation

Numerous *in vivo* studies indicate that all types of asbestos induce proliferation in target tissues relevant to lung cancer and mesothelioma. Such proliferation is also suggested by the animal histopathological observations previously described (Section 6.2.2). Moreover, many of these studies suggest that the underlying mechanisms may be fiber size- and fiber-type specific. Responses may also be species-specific.

Importantly, there are some studies (primarily *in vitro* studies) that suggest asbestos acts to inhibit (rather than induce) proliferation. Although it is likely that the contrasting observations found in such studies are due to differences in conditions, timing, dose, or the type of asbestos employed, the underlying reason for the contrasting observations is not always apparent.

The evidence for proliferation is summarized by tissue below.

In lung epithelium. Brody et al. (1997) showed that rats and mice exposed for a brief (5 hour) period to chrysotile asbestos at 1,000 fibers/cm^3 (no size indicated) exhibited focal scarring at bronchio-alveolar duct junctions that are identical to those seen in asbestos-exposed humans. After 3-consecutive exposures, the lesions persisted for 6 months. In regions where fibers are deposited, macrophages are observed to accumulate, epithelium is injured, and proliferation is observed to occur. In this study, the authors also showed by immunohybridization staining that the four genes required to express three peptide growth factors (TGF-α, TGF-β, and the A and B chains of PDGF) and the proteins themselves are expressed in bronchio-alveolar tissue within 24 hours of exposure. PDGF is expressed almost immediately and expression remains elevated for 2-weeks post-exposure, but only in regions where fibers are deposited.

The authors report that PDGF is a potent growth factor for mesenchymal cells, TGF-α is a potent mitogen for epithelial cells, and TGF-β inhibits fibroblast proliferation, but stimulates synthesis of extra-cellular matrix (Table 6-6). The authors also report additional experiments with knockout mice indicate that TNF-α is required to induce the early stages of proliferation. The authors also indicate that Type II cells produce TGF-β1 and TGF-β2 (two of three isoforms of this protein) and that they are stimulated to do so when co-cultured with macrophages.

Adamson (1997) intratracheally instilled size-separated (by sedimentation) long and short crocidolite fibers into rats (0.1 mg in a single dose) and noted that the long fibers damaged the bronchiolar epithelium and that fibers were incorporated into the resulting connective tissue; granulomas formed with giant cells containing fibers). The long fibers also appeared to escape into the interstitium. Labeled thymidine uptake (which indicates DNA synthesis and suggests proliferation) following long fiber exposure was seen in lung epithelial cells, fibroblasts, and pleural mesothelial cells. Such labeling peaked at 2% in mesothelial cells and 3% in epithelial cells within one week following exposure. Proliferation appeared to end shortly beyond one week. Short fibers were observed to have been efficiently phagocytized by alveolar macrophages and a small increase in macrophage population appeared to have been induced. Otherwise, none of the other effects attributable to long fibers (described above) were observed with short fibers. Note that such observations are entirely consistent with those reported for the range of studies described in Section 6.2.2.

McGavran et al. (1989) exposed both normal (C5+) mice and compliment deficient (C5-) mice to asbestos (at 4 mg/m^3) by inhalation and observed proliferation of bronchio-alveolar epithelium and interstitial cells at alveolar duct bifurcations (based on incorporation of tritiated thymidine) between 19 and 72 hours after a single, 5-hour exposure. Sham exposed rats showed fewer than 1% of epithelial and interstitial cells at alveolar duct bifurcations incorporate labeled thymidine. In contrast, thymidine uptake in asbestos exposed animals is significantly elevated for the first few days, begins to decrease at 8 days, and returns to normal by one month following exposure. Both C5+ and C5- mice show similar increases in volume density of epithelial and interstitial cells at 48 hours post-exposure. However, one month following exposure C5+ mice developed fibrotic lesions while C5- mice were no different than controls. The authors conclude that the depressed macrophage response in C5- mice does not appear to change the early mitogenic (and proliferative) response to asbestos, but apparently attenuates later fibrogenesis.

Chang et al. (1989) describes the morphometric changes observed in rats following 1 hour inhalation exposure to chrysotile (at 13 mg/m^3). Within 48 hours following exposure: the volume of the epithelium increased by 78% and the interstitium by 28% at alveolar duct bifurcations relative to sham-exposed animals. Alveolar macrophages increased 10-fold and interstital macrophages 3-fold. Numbers of Type I and Type II epithelial cells increased by 82% and 29%, respectively. At 1 month following exposure, the numbers of Type I and Type II pneumocytes were still elevated, but not significantly. However, the volume of the interstitium had increased by 67% accompanied by persistently high numbers of interstitial macrophages, accumulation of myofibroblasts, smooth muscle cells, and an increased volume of interstitial matrix.

In lung endothelium. In addition to the general evidence for proliferation of epithelial cells provided by Adamson (1997), McGavran et al. (1989), and Chang et al. (1989), as cited above, a more detailed description of the nature of asbestos-induced proliferation of endothelial cells is also available.

Proliferation of endothelial cells and smooth muscle cells of arterioles and venules near alveolar duct bifurcations is induced in rats inhaling chrysotile (no size information given) for 5 hours at 4 mg/m^3 (McGavran et al. 1990). This is based on the observed uptake of labeled thymidine (which indicates DNA synthesis and suggests proliferation) that is significantly increased over controls between 19 and 72 hours following exposure. Twenty-eight percent of vessels near bifurcations exhibited labeled cells 31 hours after exposure. One month following exposure, the thickness of the smooth muscle layers around these blood vessels is significantly increased (doubled). In contrast, labeling of these same endothelial and smooth muscle cells in sham exposed rats is zero. The authors indicate that endothelial cells and smooth muscles associated with pulmonary blood vessels are normally quiescent with turnover rates on the order of years.

In mesothelium. In the second part of the study addressing epithelial proliferation, Adamson (1997) reports that rats instilled with 0.5 mg of unmodified, UICC crocidolite were sacrificed at 1 week and 6 weeks following exposure and subjected to bronchiolar lavage and pleural cavity lavage. Lavaged alveolar macrophages were observed to contain fibers, but pleural macrophages did not. At 1 week, collected pleural macrophages were shown to induce proliferation of fresh mesothelial cells in culture and pleural lavage fluid showed an even greater effect. No effects were observed at 6 weeks. Further work with anti-bodies to various cytokines indicated that early, transient proliferation of mesothelial cells was dependent on kertinocyte growth factor (KGF), but not on PDGF, FGF, or TNF-α (Table 6-6). This suggests that early, transient proliferation is induced by diffusing cytokines rather than direct fiber exposure. Adamson further reports that KGF is a fibroblast-derived cytokine that acts on epithelial cells so that it's up-regulation likely results from epithelial injury with penetration of asbestos to the interstitium (where fibroblasts are found, Section 4.4). A similar transient proliferative response in mesothelial cells was also observed following exposure to chrysotile and in response to crystalline silica exposure. Thus, it appears that the mesenchymal proliferative response may be mineralogy specific for particles and is size-specific for fibers.

Everitt et al. (1997) exposed rats and hamsters by inhalation to RCF-1 (45 mg/m^3–650 f/cm^3) for 12 weeks and then let them recover for up to an additional 12 weeks prior to sacrifice. The authors indicate that both rats and hamsters showed qualitatively similar levels of inflammation at time examined (4 weeks and 12 weeks). They also indicate the mesothelial cell proliferation was observed in both animal types, but was more pronounced in hamsters at all time points examined. The greatest proliferation in both species was in the parietal pleura lining the diaphragm. The authors also report that fibers (primarily short and thin) were also observed in the pleural cavities of both species at all time points.

Several *in vitro* studies provide evidence that asbestos either induces or inhibits proliferation in lung tissues of interest and that at least some of the mechanisms involved are fiber size and mineralogy dependent. As previously indicated, the specific reasons for the apparent contrast between results observed *in vivo* (where asbestos consistently promotes proliferation) and the inhibition sometimes observed in *in vitro* studies is not always apparent. However, it must be due to the special conditions that must be created to conduct *in vitro* studies, which may not support certain mechanisms that are important *in vivo*.

Timblin et al. (1998a) completed a study in which rat pleural mesothelioma (RPM) cells in culture were dosed with crocidolite or various cation-substituted erionites. The expression of several gene and gene products were then tracked. Cultures in this study were exposed to 1, 5, or 10 μg/cm^2 of the various fibrous materials. Analysis of the fibrous materials indicated that crocidolite contained many more fibers per gram of material (probably because they are thinner) and that the preparation contains somewhat longer fibers than the erionites evaluated. In crocidolite, for example, 88% of the fibers are longer than 5 μm, 68% longer than 10 μm, and 37.5% longer than 20 μm. All of the cation substituted erionites showed approximately the same size distribution: 50% longer than 5 μm, 10–20% longer than 10 μm, and 1–5% longer than 20 μm.

Results indicate that the various cation substituted erionites behave differently and that the Na substituted erionite shows the largest overall potency, at least for some endpoints, but not others. Fe, Na, and Ca substituted erionite all appear to induce c-fos expression in a dose-dependent fashion (increasing regularly among the 1, 5, and 10 μg applications). K-erionite may also show the same pattern, but the changes were not indicated as significant over controls (apparently due to greater variability). Only Na-erionite showed significantly increased expression of c-jun (at 1 and 5 μg applications, but not significantly at 10 μg, apparently due to greater variability. However, the mean result for 10 μg shows a consistent trend with the lower concentration application results).

Na-erionite induces c-fos at the same or greater rates as crocidolite asbestos for the same mass application (but not the same fiber number). Crocidolite also appears to show a dose-response trend for c-jun expression, but only the result for the highest application (10 μg) is significantly different from controls. In contrast, Na-erionite appears to show greater induction of c-jun expression at lower dose than crocidolite, but the increase with increasing dose is much lower for Na-erionite. Crocidolite also appears to induce substantial apoptosis (even at the low dose of 5 μg) and that the induction is dose-dependent. In contrast, non-fibrous riebeckite does not appear to induce apoptosis. Comparison between crocidolite dosed cultures and Na-erionite dosed cultures indicate that crocidolite induces substantial apoptosis at all time periods following application, but that Na-erionite induces little apoptosis even at higher mass dose and longer time periods than crocidolite. The authors also indicate that crocidolite and Na-erionite appear to stimulate DNA-synthesis, which appears to be a compensating mechanism to fiber cell toxicity. The authors indicate that chemistry is important in fiber toxicity as Na-erionite was a strong inducer of c-jun, even at relatively low concentrations, but several of the other cation substituted erionites (including Fe-erionite) were not. They further suggest that, given the difference in the fiber lengths of the crocidolite samples and Na-erionite samples, that fiber length may be a less important consideration than fiber surface chemistry. However, despite the author's assertion, considering that non-fibrous riebeckite does not induce any of the effects observed for crocidolite, there appears to be a clear size effect. It may simply require that a defined, minimum length is necessary to induce the effect.

The authors also indicate that balance between proliferation and apoptosis is required to maintain homeostasis in healthy tissue. They further indicate that other studies suggest that c-Jun expression is linked to proliferation and induction of cancer, while c-fos expression is linked to apoptosis. Thus, suppression of c-fos may be linked to carcinogenesis by allowing establishment or maintenance of a transformed cellular phenotype. This is in fact an early step in carcinogensis. Many environmental agents stimulate both apoptosis and proliferation and, depending on the degree, may cause imbalances that lead to disease. Relative stimulation of c-fos and c-jun may reflect some of these pathways. Since crocidolite induces both c-fos and c-jun in this study, the implication is that it mediates both apoptosis and proliferation.

Wylie et al. (1997) dosed hamster tracheal epithelial (HTE) cells and rat pleural mesothelial (RPM) cells with various asbestos and talc samples and evaluated proliferation based on a colony-forming efficiency (CFE) assay. The samples were NIEHS crocidolite and chrysotile and three different talcs. Samples were characterized in the paper by mineralogical composition, surface area, and size distributions.

The authors indicate that both asbestos samples increased colony formation of HTE cells (suggesting induction of proliferation), but talc samples did not. RPM cells, in contrast, showed only dose-dependent decreases in colony forming efficiency for all samples, which the authors indicate is a sign of cytotoxicity. The authors report that all samples show corresponding effects when concentrations are expressed as fibers longer than 5 μm or by total surface area. They also suggest that the "unique" proliferative response by HTE cells could not be explained by either fiber dimension or surface area and suggests a mineralogical effect.

Barchowsky et al. (1997) dosed cultured (low passage) endothelial cells to NIEHS chrysotile, crocidolite, or RCF-1. After 1 to 3 hours exposure to 5 $\mu g/cm^2$ (non-lethal concentrations), asbestos (but not RCF-1) causes changes in cell morphology (cells elongate), increases in cell motility, and increases in gene expression. Further work by the authors indicate that these effects are mediated by interaction between asbestos and the receptor for urokinase-type plasminogen activator (uPAR). The authors also suggest that attachment of asbestos to cell membranes, internalization of asbestos fibers by the cells, and the morphological changes induced by asbestos are each mediated by different proteins.

Examples of *in vitro* studies that indicate asbestos (and other fibrous materials) may inhibit proliferation in culture include the following.

In contrast to the above, Levresse et al. (1997) found that chrysotile and crocidolite act to inhibit proliferation in cultured rat pleural mesothelioma (RPM) cells. In this study, RPM cells (diploid, no more than 25 passages) were dosed with either UICC crocidolite or NIEHS Zimbabwean Chrysotile at concentrations varying between 0.5 and 20 $\mu g/cm^2$. The authors also note that the chrysotile sample contains approximately 4 times the number of fibers as the crocidolite samples. Cells were then examined at 4, 24, and 48 hours following treatment. In untreated cultures, the number of cells in replicative phase decrease with time, which indicates that such cells are headed for confluence (completion of a monolayer on the culture medium). At 48 hours, for example, 10% of untreated control cells were observed to be in replicative stage. Chrysotile (but not crocidolite) decreased the fraction of cells in replicative phase in a time- and dose-dependent manner. At 48 hours, for example, cells treated with 10 $\mu g/cm^2$ chrysotile showed only 1.5% in replicative phase. Further tests confirmed that this was due to blockage of cells at the G1/S boundary of the cell cycle. Both chrysotile and crocidolite appears to induce a time-dependent increase in the number of cells at G2/M in the cell cycle, although this effect was not observed to be dose-dependent for chrysotile. Even on a fiber-number basis, chrysotile appears to be elicit a greater response (arrest a greater percentage of cells) than crocidolite.

The authors also indicate that chrysotile caused nuclear-localized, time-dependent increases in p53 concentrations. Crocidolite produced much lower levels that were not detectable in the nucleus. Chrysotile was also observed to produce blockage at the G0/G1 transition of the cell cycle, but crocidolite did not. They also note that p53 is known to mediate arrest at this stage in the cycle so observing that chrysotile induces arrest at this transition in the cell cycle may be consistent with the observed increased expression of p53. The authors also note that chrysotile triggers apoptosis in this study and that crocidolite shows a smaller, but detectable effect. Spontaneous apoptosis in untreated cultures ran between 0.5 and 1% at 24–48 hours whereas chrysotile induced 4% apoptosis, peaking at 72 hours following exposure to 10 $\mu g/cm^2$. The authors indicate that the lower level of effects observed with crocidolite could be due to the substantially smaller number of long fibers in UICC crocidolite compared to NIEHS chrysotile.

The previously reviewed (Section 6.3.3.1) study by Hart et al. (1994) also suggests that long, medium, short, and UICC crocidolite and chrysotile along with a range of MMVF's show a dose-dependent inhibition on proliferation of cultured CHO cells and that potency toward the effect is a direct function of fiber length.

Several of the above-described studies, in addition to providing evidence that asbestos induces proliferation in various lung tissues, also suggests certain mechanisms. Asbestos may induce proliferation, for example, by inducing production of specific cytokine growth factors (Adamson 1997; Brody et al. 1997), or by inducing certain signaling cascades (Barchowsky et al. 1997, Timblin et al. 1998b). It is also possible that the two effects may be related (i.e., that stimulation of a particular signaling cascade may result in production of certain growth-stimulating cytokines). Other mechanisms may also be important (Table 6-5).

6.3.4.2 Asbestos induced cell signaling

Asbestos has been shown to induce a variety of cell signaling cascades in a variety of target cell and tissue types. Such signaling may then trigger effects in the stimulated cells that may include:

- proliferation;
- morphological changes;
- generation and release of various cytokines, enzymes, or extracellular matrix; or
- programmed cell death.

Note, due to the large number of chemical species that need to be considered in this discussion, Table 6-6 provides a summary of the sources of such species (Table 6-6A) and the effects attributable to such species (Table 6-6B).

In specific cases, asbestos may initiate cell signaling by interacting directly with receptors on the cell surface, by causing generation and release of intermediate species (e.g., ROS or RNS) that trigger cell signaling, or (for phagocytized fibers) by interacting with intracellular components of a particular signaling cascade. The specific responses to cell signaling induced by asbestos are frequently cell- or tissue-type specific. Moreover, depending on the specific mechanism, cell signaling by asbestos may be dependent on fiber size and/or type.

Barchowsky et al. (1998) showed in a set of studies that long chrysotile and long crocidolite, but not RCF-1 fibers (at concentrations between 1 and 10 $\mu g/cm^2$), which is reportedly below levels that typically induce cytotoxic effects) induced up-regulation of urokinase-type plasminogen activator (uPA) and its receptor (uPAR) in both lung endothelial cells (vascular cells) and lung epithelial cells. They also showed that the increased pericellular protolytic activity (requiring cleavage of plasminogen to plasmin) that is induced by asbestos in these cells is mediated by uPA.

In prior studies, chrysotile has been shown to cause endothelial cells to elongate and increase expression of adhesion molecules for phagocytes. They also show enhanced proteolytic activity and matrix interactions. Chrysotile has also been shown to stimulate fibrinolytic activity in lung epithelial cells and extravasating macrophages. All such stimulation appears to result from up-regulation of uPA. Thus, this mechanism may explain the observed asbestos-induced changes in lung endothelial and epithelial cells including vascular remodeling, development of vascularized granular tissue, increased matrix turnover, and leukocyte extravasation (which in turn may be caused by cell activation and elaboration of proteases and adhesion molecules). The authors suggest that asbestos-induced up-regulation of uPA and uPAR expression may represent a global mechanism for pulmonary toxicity and fibrosis induced by crystalline fibers. Importantly, chrysotile was shown to induce uPA and uPAR expression in the absence of serum, so the effect is apparently due to direct binding of fibers to cell-surface receptors.

Mossman et al. (1997) observed that concentrations of 1.25–5 $\mu g/cm^2$ of crodidolite (sample from TIMA) caused expression of c-jun and AP-1 in both cultured hamster tracheal epithelial (THE) cells and cultured rat pleural mesothelial (RPM) cells. Crocidolite was also observed to trigger the EGFR-regulated kinase (ERK) and mitogen activated protein kinase (MAPK) pathways in RPM cells. The authors indicate that these pathways are also stimulated by hydrogen peroxide and that NF-κβ induction stimulated by crocidolite is also stimulated by crystalline silica (although silica stimulation of the MAPK pathway was not investigated). They also note that the non-fibrous analog to crocidolite, riebeckite does not elicit these activities.

The authors indicate that induction of the NF-κβ cascade was inhibited by excess glutathione, which is stimulated by N-acetylcysteine (NAC), suggesting that this pathway is induced by asbestos-caused oxidative stress (perhaps through ROS or RNS intermediates). Application of NAC also diminished crocidolite induced c-fos and c-jun RNA levels and inhibited activation of the ERK-MAPK cascade. Further work suggests that asbestos triggers the MAPK pathway by interaction with the Epithelial Growth Factor Receptor (EGFR), either directly or by phosphorylation of this receptor by ROS. At the concentrations examined, crocidolite induces substantial apoptosis (apparently through activation of the ERK-MAPK cascade). In contrast, the authors note that TNF-α induces the JNK arm of the ERK-MAPK cascade, which leads to proliferation. Asbestos does not elevate JNK over the time-period of the study. The authors note that it has been shown in some studies that inhibition of ERK in some cells, also inhibits asbestos-induced apoptosis. Importantly, given that these processes are induced by crocidolite, but not by its non-fibrous analog, riebeckite, induction of the ERK-MAPK cascade appears to be a fiber-size dependent process.

In a related study to that conducted by Mossman et al. (1997), Zanella et al. (1999) report that the (TIMA) crocidolite (at concentrations of 2.5–10 μg/cm^2, but not its non-fibrous analog, riebeckite, eliminated binding of EGF to its receptor EGFR. Because EGF does not bind to crocidolite in the absence of membrane, this is not simply a case of crocidolite tying up ligand. Crocidolite also induces a greater than 2-fold increase in steady-state message and protein levels of EGFR.

The authors also note that the tyrphostin, AG-1478 (which specifically inhibits the tyrosine kinase activity of EGFR), significantly mitigated asbestos-induced increases in mRNA levels of c-fos, but not c-jun, and that the asbestos action was not blocked by a non-specific tyrphostin, AG-10. Moreover, pretreatment of RPM cells with AG1478 significantly reduced asbestos-induced apoptosis. Therefore, the authors concluded that asbestos-induced binding to EGFR initiates signaling pathways responsible for increased expression of the protooncogene c-fos and the development of apoptosis. This apparently occurs through the EGFR-extracellular signaling regulated kinase (ERK). It is hypothesized that asbestos may induce dimerization and activation (phosphorylation) of EGFR, which also prevents binding of EGF. Asbestos apparently serves the same role as EGF in that it promotes aggregation of EGFR, which in turn promotes binding to the extracellular domain of tyrosine kinase receptors and the activation of their intracellular kinases. The authors also indicate that other work suggests that crocidolite fiber exposure leads to aggregation and accumulation of EGFR at sites of fiber contact and that asbestos also stimulates biosynthesis of the EGFR and activates ERK in an EGFR-dependent manner.

The authors speculate that asbestos binding may not be ligand-site specific, but may be charge related or may induce EGFR phosphorylation by local production of ROS, which has previously been demonstrated to cause EGFR activation. As previously indicated, that this effect is driven by crocidolite exposure, but not by exposure to riebeckite indicates that this mechanism is fiber-size specific.

Johnson and Jaramillo (1997) showed that UICC crocidolite, but not JM-100 glass, applied to a culture of immortalized human Type II epithelial (A549) cells at non-cytotoxic concentrations (for 20 hours) results in increased expression of p53, Cip1, and GADD153 in a dose- and time-dependent fashion. Expression was observed to be maximum at 18 hours. The crocidolite treatment was also shown to cause an increase in the number of cells arrested in Stage G2 of the cell cycle (with a persistent decrease in the number of cells in G1). This was considered surprising because both p53 and Cip1 are known to mediate arrest in Stage G1. The authors suggest that these findings indicate a strong dependence on both fiber type and fiber size (JM-100 glass contains substantially more long fibers than crocidolite). However, it is not possible to separate the effects of fiber type versus fiber size in this study.

Luster and Simeonova (1998) indicate that at high concentrations, ROS may induce frank cytotoxicity. At low or moderate levels, ROS are more likely to induce cell signaling cascades that may, in turn, contribute to asbestos-related disease. The authors dosed cultures of immortalized human Type II epithelial (A549) cells, originally derived from a lung carcinoma, and normal human bronchioepithelial (NHBE) cells with long (Certain-Teed supplied) crocidolite (reported mean length: 19 μm) at concentrations ranging between 0 and 24 μg/ml. Results indicate that secretion of both Interluken-8 (IL-8) and IL-6 was stimulated by crocidolite exposure in a dose-dependent manner. In contrast, increases in LDH levels (which indicate cell damage) was only detected at the highest exposure concentrations tested. Further work indicates that stimulation of IL-6 and IL-8 secretion occurs through ROS that are generated in an iron-dependent process (that may also include NF-κβ induction). Note that the trend of cell signal induction at low and moderate levels of asbestos exposure with evidence for cytotoxicity observed only at the highest exposure concentrations is common to many of these kinds of studies.

Choe et al. (1999) conducted a combined *in vivo*/*in vitro* study of the effects of low level exposure to chrysotile or crocidolite at inducing leukocyte attachment to rat pleural mesothelial cells. The authors note that similar populations of rat pleural leukocytes (74% macrophages, 2% neutrophils, 10% mast cells, and 10% eosinophils) were observed in both asbestos-exposed and unexposed rats.

In the second part of the study, cultured RPM cells were exposed to either crocidolite or chrysotile (both NIEHS samples) at concentrations ranging between 1.25 and 10 $\mu g/cm^2$, which was noted to be below levels at which substantial cytotoxicity is observed. Attachment of rat pleural leukocytes to RPM cells was then observed to increase with increasing dose of asbestos to the RPM cells. In contrast, carbonyl iron (a non-fibrous particle) also induced enhanced attachment, but at much lower levels and the effect was not dose-dependent. Further analysis indicated that asbestos-induced adhesion is mediated by up-regulation of IL-1β (but not dependent on TNF-α or nitric oxide production, although it is noted that TNF-α independently increases attachment). Asbestos also induces increased expression of vascular cell adhesion molecule (VCAM-1). The authors also note that rat pleural leukocytes harvested from asbestos-exposed rats also showed increased adhesion to *in vitro* RPM cells over leukocytes harvested from sham exposed rats. Thus, asbestos appears to trigger alterations in these cells as well.

In a recent paper, Driscoll et al. (1997) reviewed the role of tumor necrosis factor alpha (TNF-α) in mediating the inflammatory response to lung insult by particulate matter. The authors indicate that quartz, coal dust, crocidolite, and chrysotile are all potent inducers of TNF-α production. Titanium dioxide (TiO_2), corundum (aluminum oxide: Al_2O_3), and latex beads are not. Pulmonary macrophages have been shown to secrete TNF-α *in vivo* in response to exposure to some of the dusts listed above (including asbestos). This is also observed among macrophages from asbestosis patients.

The authors indicate that rats immunized against TNF-α show reduced recruitment of neutrophils, which demonstrates that TNF-α is involved in the recruitment of inflammatory cells. TNF-α stimulates macrophages, epithelial cells, endothelial cells, and fibroblasts to release chemokines that include adhesion molecules (Eselectin, ICAM, VCAM). Inflammatory cells then interact with such molecules and migrate along gradients from vascular structures in the lung to the lung interstitium and even the lung air spaces. It has also been shown that release of TNF-α by macrophages is apparently dependent on oxygen stress (i.e., exposure to ROS/RNS) that is induced in pathways that require iron. Production of TNF-α and other compounds that mediate the inflammatory response are regulated by the oxidant-sensitive transcription factor NF-κβ. This factor exists as a heterodimer in the cytoplasm in an inactive form because it is bound to the inhibitory 1-kappaBalpha (1-κBα), which masks a nuclear translocation signal. Appropriate stimulation of a cell induces phosphorylation of 1-κBα, which then marks it for proteolytic degradation. Then, NF-κβ translocates to the nucleus and induces transcription. The process is stimulated by oxidants and inhibited by antioxidants.

In another review, Finkelstein et al. (1997) indicated that Type II epithelial cells and Clara cells (non-ciliated bronchiolar epithelial cells) respond to and produce specific cytokines during the inflammatory process. Early responses to particle challenge include increases in mRNA and protein for IL-1β, IL-6, and TNF-α. These are also accompanied by changes in specific epithelial genes including those for surfactant protein C and Clara cell secretory protein. The authors further indicate that these responses are due to direct interaction with particles rather than a result of macrophage-derived mediators and they suggest a more significant role for epithelial secretions in the overall pulmonary response than previously suspected. Results also suggest that Type II pneumocyte-derived growth factors may play a significant role in the pathogenesis of pulmonary fibrosis.

Also in this paper, Finkelstein et al. (1997) report that intratracheal instillation of lipopolysaccharide (a potent inflammatory agent) caused increases in both lavage fluid and plasma levels of TNF-α and IL-6. Intrapleural injection induced primarily increases in plasma levels. The authors indicate that this suggests that the observed cytokines are produced primarily at the site of injury. The authors further indicate that

IL-6 is elevated in lavage fluids following exposure to Ni_2S_3, a suspected human carcinogen, but not following exposure to TiO_2 or NiO. *In vitro* studies indicate that release of IL-1β and TNF-α by Type II cells occurred only following exposure to crocidolite or ultrafine TiO_2, but not pigment grade TiO_2. The authors also indicate that protein C and Clara cell secretory protein were both expressed in their respective source cells following exposure only to the fibrogenic of the above particles. They also report that crystalline silica has been shown to promote cytokine release and hypertrophy in Type II cells.

Jagirdar et al. (1997) used immunohistochemistry in a study to show that all three isoforms of TGF-β (1,2, and 3) are expressed in the fibrotic lesions of asbestosis and pleural fibrosis patients from the Quebec mines, primarily by Type II pneumocytes. The cases examined averaged 38 years of exposure to the Quebec chrysotile. The authors also indicate that the hyperplastic epithelium of silicosis patients also show elevated expression of all three isoforms. They further indicate from previous studies that mesothelioma tumor cells frequently express TGF-β2 while the cells in the stroma of such tumors frequently express TGF-β1. It is also noted in this study that jun and fos are both transcription factors that activate the TGF-β1 promoter.

Zhang et al. (1993) indicate that macrophages obtained in BAL fluid from idiopathic pulmonary fibrosis (IPF) patients and asbestosis patients show significantly increased secretion of TNF-α and asbestosis patients also showed significantly increased secretion of IL-1β. Macrophages and monocytes obtained from both kinds of patients also show elevated expression of mRNA for these cytokines. In an *in vitro* part of this study, Zhang and coworkers, showed that chrysotile, crocidolite, amosite, and crystalline silica all stimulated IL-1β and TNF-α release and up-regulated their respective mRNA in both macrophages and monocytes. The authors also report that these two cytokines have been shown to up-regulate collagen Types I and III and fibronectin gene expression in human diploid lung fibroblasts after short-term, serum free exposure *in vitro*.

Holian et al. (1997) exposed cultures of normal human alveolar macrophages (AM) (obtained by lavage) to varying concentrations (up to 25 μg/ml) of short chrysotile, UICC crocidolite, ground silica, wollastonite, and titanium dioxide to determine whether these materials cause a phenotypic shift in macrophage populations by inducing selective apoptosis. The authors indicate that normal lungs contain: 40–50% RFD1+7+ suppressor AM, and 5–10% RFD1+ immune activator. In this study, the fibrogenic subset of the particles tested (not wollastonite or titanium dioxide) increased the ratio of activator/suppressor AM by a factor of 4 within a few hours and the effect was seen to increase with time. The authors also note that fibrogenic particles decrease the abundance of RFD7+ AM (phagocytic), but the consequences of this phenotypic shift are unclear.

The authors indicate that AM taken from fibrotic patients release a variety of proinflammatory mediators capable of stimulating fibroblast proliferation and collagen synthesis. Even in the absence of evidence of fibrosis, workers who have been heavily exposed to asbestos yield similarly activated AM. In contrast, they also note that, *in vitro* studies in which AM are stimulated with fibrogenic particles, while such AM are activated to release inflammatory cytokines, such releases are orders of magnitude less than that seen from AM derived from fibrotic patients. The authors indicate that the apoptosis-driven phenotypic shift in AM that is indicated by this study may explain the apparent discrepancy.

In a previously described study, Timblin et al. (1998a), see Section 6.3.4.1, showed that crocidolite asbestos and several cation substituted erionites all stimulate c-jun and c-fos in rat pleural mesothelial cells, but to varying degrees depending on fiber chemistry. The effect also appears to be size dependent as crocidolite, but not its non-fibrous analog riebeckite induces the effect.

In general, the kinds of signaling cascades that are potentially stimulated by exposure to asbestos are important due to their potential to contribute to the promotion of cancer. Such pathways, for example, may mediate proliferation or may suppress apoptosis. Alternately, they may mediate an inflammatory

response that in turn may lead to proliferation or to production and release of other, mutagenic agents (e.g., ROS or RNS). Pathways that facilitate development of fibrosis may also contribute to cancer promotion, given the apparent link between fibrosis and the development of lung cancer, which may relate (among other possibilities) to inhibition of fiber clearance (Section 6.3.4.5).

The ERK-MAPK signaling pathway evaluated in multiple studies by Mossman and coworkers (Mossman et al. 1997; Timblin et al. 1998a,b; Zanella et al. 1999) in rat pleural mesothelial (RPM) cells is a case in point (see above). These studies suggest that crocidolite stimulates the ERK-MAPK cascade through interaction with the EGF receptor. This ultimately leads to transcription of mRNA for c-fos. Crocidolite has also been shown to induce c-jun (apparently through a separate mechanism) and the balance between c-jun and c-fos has been implicated in guiding a cell toward either proliferation or apoptosis. Although the direct connection between c-jun/c-fos and apoptosis has not been established, it is observed that crocidolite induces substantial apoptosis in RPM cells at the same concentrations at which it induces substantial expression of c-fos and c-jun. The link is also implied because inhibition of the ERK pathway has been shown in some studies to inhibit asbestos-induced apoptosis. Na-erionite has also been shown to induce c-fos at levels comparable or higher than crocidolite for comparable exposures (at least on a mass basis) and induce c-jun at higher levels. However, it is not known whether Na-erionite and crocidolite act via the same pathways. Potentially due to the increased, relative expression of c-jun induced by Na-erioinite, increased apoptosis is not observed in association with exposure to Na-erionite. However, the link between increased c-jun expression and inhibition of apoptosis has not been demonstrated explicitly.

Both crocidolite and Na-erionite were also shown by Mossman and coworkers to induce uptake of bromodeoxyuridine (BrdU) by RPM cells in these same experiments. Uptake of BrdU is an indicator of DNA synthesis. Since it has also been shown that crocidolite is capable of damaging DNA via ROS and other pathways (Sections 6.3.3) and both crocidolite and erionite are known to induce mesotheliomas in any case, the balance between proliferation and apoptosis in this cell population that is struck by exposure to these toxins may very well determine whether development of cancers are promoted or prevented. Of course, both proliferation and apoptosis may also be mediated by other pathways independent of the ones described here.

The problem is that the range of responses that are induced by asbestos in the lung are varied and complex (see Table 6-5) so that it has not yet been possible to definitively identify the biochemical triggers that lead to lung cancer or mesothelioma. It is even likely, for example, that different mechanisms (or combinations of mechanisms) predominate under different exposure conditions or in association with differing fiber types or particle sizes. Still, examination of the dependence of candidate mechanisms on fiber type and particle size can be instructive, especially to the degree that such indications are consistent with observations in whole animal studies (see, for example, Section 6.2.2). For the signaling cascade described above by Mossman and coworkers, for example, the effects attributable to crocidolite are clearly dependent on fiber size because the non-fibrous analog to crocidolite, riebeckite does not induce any of the effects. It also appears that the chemistry of the fibers is important, given the observed differences in responses among the various, substituted erionites.

6.3.4.3 Asbestos-induced apoptosis

Apoptosis (programmed cell death) is generally triggered when a cell accumulates certain types of genetic damage, when cell signaling cascades are triggered by external stimuli that may occur, for example, as part of the need to maintain tissue homeostasis or to cause a phenotypic shift in response to toxic challenge (see, for example, Holian et al. 1997, Section 6.3.4.2), or when a cell has completed a pre-programmed number of divisions. Asbestos can induce apoptosis in a variety of cells by several mechanisms including primarily:

- by causing sufficient genetic damage to trigger apoptosis; or
- by triggering a signal cascade that leads to apoptosis.

As previously indicated, asbestos may trigger signaling cascades by interacting directly with receptors on the cell surface, or by inducing production of intermediate species (such as ROS or RNS) that may in turn induce cell signaling.

Some of the mechanisms by which asbestos may act to induce apoptosis may be fiber size- or type-dependent. Also, responses may vary in different target tissues.

Fibers. As indicated in Section 6.4.3.2, crocidolite (but not the non-fibrous analog riebeckite) induces apoptosis in hamster tracheal epithelial cells and rat pleural mesothelial cells when applied at non-cytotoxic concentrations (Mossman et al. 1997). Results from the study also indicate that apoptosis is triggered in this case by inducing an ERK-MAPK signaling cascade as a consequence of interaction with EGF receptors on the cell surface. The interaction may be direct or may be caused by asbestos-induced ROS. In a related study (also previously summarized, Section 6.3.4.1), Timblin et al. (1998a) indicate that the asbestos-induced apoptosis reported in the Mossman et al. (1997) work is fiber-type specific and the pathway involved appears to stimulate expression of c-fos.

In a study previously reported in greater detail (Section 6.3.4.1), Levresse et al. (1997) indicate that chrysotile induces apoptosis in cultured rat pleural mesothelioma cells with the effect peaking at 4% at 72 hours following exposure to 10 $\mu g/cm^2$. Although the authors observed a much smaller effect with crocidolite, they indicate that the difference is likely due to the much smaller number of long fibers in the particular crocidolite sample evaluated.

Broaddus et al. (1997) indicates that crocidolite (not UICC), but not wollastonite, glass beads, or non-fibrous riebeckite cause substantial apoptosis in rabbit pleural mesothelioma cells in culture in a dose-dependent fashion. The extent of apoptosis induced was inhibited by treatment with catalase and by 3-minobenzamide (an inhibitor of poly(ADP-ribosyl) polymerase. The former indicates a role for ROS mediation and the latter indicates that this enzyme, which mediates DNA repair, also mediates asbestos-induced apoptosis (perhaps triggered by asbestos-induced DNA damage). Asbestos induced apoptosis was also inhibited by treatment with desfeoxamine, but effects were restored by adding iron to the medium. The authors note that in other studies, crocidolite has been shown to induce DNA strand breaks within 2 hours after exposure and induces unscheduled DNA synthesis within 24 hours following exposure. Asbestos also induces production of poly(ADP-ribosyl) polymerase.

Non-fibrous particles. Leigh et al. (1997) intratracheally instilled rats with silica (a non-fibrous particle) at doses varying between 2 and 22 mg. They then collected cells by bronchio-alveolar lavage (BAL) 10 days after instillation. The authors observed large numbers of apoptotic cells in BAL fluid and that the number of such cells was dose-dependent. The dead cells were primarily neutrophils (so that this might represent some type of mechanism to restore homeostasis). Engulfment of apoptotic cells by macrophages was also observed. The authors report that, 56 days after instillation, apoptotic cells were observed in granulomatous tissue within the lungs of rats exposed to silica. This suggests that apoptosis may also occur in response to chronic inflammation. The authors conclude that silica induces apoptosis among granulomatous cells and alveolar cells and that such apoptosis and the subsequent engulfment of apoptotic cells by macrophages may play a role in the evolution of silica-related disease. The authors also note that granuloma formation is a hyperplasia-related event.

At least some of the mechanisms suggested above for asbestos-induced apoptosis are dependent on fiber size (the non-fibrous analog of crocidolite does not induce the effect) and dependent on the chemistry of the fibers involved (various, cation-substituted analogs of erionite exhibit disparate ability to induce the

effect). Although non-fibrous particles (such as crystalline silica) may also induce apoptosis, as previously suggested, this may be through separate mechanisms from those responsible for asbestos-related effects, even if the same endpoint results.

6.3.4.4 Asbestos-induced cytotoxicity

While there is ample evidence from various *in vitro* studies that asbestos is cytotoxic, such effects are observed almost exclusively at the highest concentrations evaluated in an experiment (for example, Luster and Simeonova [1998], Section 6.3.4.2 and Choe et al. [1999], Section 6.3.4.2). Many experiments are conducted at concentrations below those for which cytotoxicity is important because the other toxic effects attributable to asbestos occur at substantially lower exposure levels and researchers prefer to study such effects in the absence of potentially confounding cytotoxicity. For *in vitro* studies, for example, non-cyotoxic effects are typically studied at concentrations less than approximately 10 $\mu g/cm^2$ (or 20 μg/ml) while substantial cytotoxicity is not typically observed until exposure concentrations are several times higher.

Because most of the other effects attributable to asbestos occur at concentrations that are substantially lower, this begs the question as to whether frank cytotoxicity is an effect that is relevant to human exposures. There is also substantial evidence that the mechanisms associated with asbestos-induced cytotoxicity are separate from the mechanisms that mediate most of the other asbestos-related effects of interest.

Kamp et al. (1993) dosed cultured pulmonary epithelial (PE) cells with UICC amosite asbestos. In some studies, polymorphonuclear leukocytes (PMN) were also added to the culture. Typical doses in this experiment were on the order of 250 $\mu g/cm^2$, which is quite high for these types of studies. For example, compare this level with the levels reported for studies of ROS/RNS generation (Section 6.3.3), cell signaling (Section 6.3.4.2), proliferation (Section 6.3.4.1) or apoptosis (Section 6.3.4.3).

Kamp and coworkers indicate that the effect of amosite exposure on cultured PE cells (at the concentrations studied) was to induce substantial cell lysis (cytotoxicity) and little cell detachment (from the culture medium), which would indicate increased cell motility. Addition of PMN to the culture resulted in both increased cell lysis and cell detachment for comparable exposures to amosite. The observed cell detachment was mitigated in a dose-dependent fashion by adding protease inhibitors. Further work indicated that asbestos induces release of human neutrophil elastase (HNE), which may mediate the combined effects with PMN. PE cell exposure to HNE alone causes increases in cell detachment in a dose-dependent fashion. However, when combined with asbestos exposure, cell lysis increases at the expense of cell detachment. The authors suggest that HNE becomes bound to asbestos, which also becomes bound to PE cells and this facilitates augmented cytotoxicity by proteases that are secreted by PMN's.

Blake et al. (1998) studied the effect of fiber size on the cytotoxicity of alveolar macrophages *in vitro*. Cultured cells were dosed with concentrations varying between 0 and 500 μg/ml of each of 5 different length preparations of JM 100 glass fiber. Cytotoxicity was monitored by assays for extracellular LDH and by chemiluminescence following zymosan addition. The latter assy is intended to show macrophage stimulation. Results indicate that all samples showed dose-dependent increases in toxicity (i.e., increasing LDH and decreasing chemiluminescence). Comparing across samples, relatively long fibers (mean=17 μm) showed the greatest toxicity. The authors further indicate that microscopic examination suggests that frustrated phagocytosis plays a role in cytotoxicity.

Goodglick and Kane (1990) studied the effect of three different length preparations of crocidolite (long, short, and UICC) on elicited macrophages (stimulated initially with thioglycolate) *in vitro* and *in vivo*.

The long and short samples were reportedly prepared from the UICC sample by repeated centrifugation. Goodglick and Kane (1990) report that all three types of crocidolite stimulated release of ROS from macrophages. At sufficiently high concentrations, all three also caused substantial cytotoxicity, although apparently due to the longer time required to settle in culture, the full effects from short fibers take longer to develop. They suggest that, on a total fiber number or surface area basis, long and short crocidolite appear to exhibit approximately equal potency toward the cytotoxicity of macrophages. Further work with various inhibitors indicates that cytotoxicity is mediated by production of ROS and that ROS are produced via an iron-dependent pathway. They also indicate that, among the effects of crocidolite exposure is that macrophage mitochondrial membranes are depolarized.

Goodglick and Kane (1990) also evaluated the effects of long and short crocidolite *in vivo*. This was done by evaluating the effects of intraperitoneal injection of the various samples (long, short, or mixed crocidolite or titanium dioxide particles) in C57B1/6 mice. Results indicate that a single injection of long crocidolite (480 μg) induced an intense inflammatory response, leakage of albumin, and fibers observed scattered across the diaphragm. In contrast, a single injection of short crocidolite (600 μg) induced only a relatively mild inflammatory response and only limited clusters of fibers observed on the surface of the diaphragm.

To test whether short fibers would show a greater response, if they were not cleared more readily than long fibers, Goodglick and Kane (1990) also subjected mice to 5 consecutive, daily injections of 120 μg of short crocidolite and noted more substantial aggregations of fiber clusters along the diaphragm as well as a more pronounced inflammatory response. Cell injury was also assessed by Trypan blue staining (which indicates cell death). All mice singly or multiply injected with mixed or long crocidolite showed marked Trypan blue staining. Single injections of short structures showed only limited Trypan blue staining. However, following 5 daily injections of short fibers, multiple Trypan blue stained cells were observed on the diaphragm in the vicinity of the locations were clusters of fibers were also observed. The authors also indicate (in contrast) that neither single injections of 160 or 800 μg nor 5 consecutive (160 μg) injections of titanium dioxide produced any Trypan blue staining.

The authors conclude from this study that both short and long crocidolite fibers appear to be cytotoxic to macrophages while titanium dioxide particles are not (suggesting that not only fiber length, but fiber type is important to cytotoxicity). They further suggest that, while short fibers tend to be cleared rapidly *in vivo*, when such clearance mechanisms are overwhelmed (such as by repeated insult through repeated, daily injections in this study), then the toxic effects of short structures becomes apparent. As indicated in other studies, however, there may be multiple mechanisms working to produce similar responses, that such mechanisms may exhibit varying dose-response characteristics, and that cytotoxicity may not generally be directly related to mechanisms that contribute to carcinogenesis. Moreover, there almost certainly are at least some longer fibers in the short fiber preparation and extended analysis to determine their relative concentration with adequate precision would be helpful to see if the relative magnitude of the observed effects correlate.

Palekar et al. (1979) studied the ability of four different samples of commingtonite-grunerite, each also subjected to varying degrees of grinding, to induce hemolysis of mammalian erythrocytes and cytotoxicity to Chinese hamster ovary (CHO) cells. The samples studied include: UICC amosite (4.13 m^2/g surface area/mass), which is denoted as “asbestiform grunerite; “semi-asbestiform” commingtonite (3.88 m^2/g); acicular commingtonite (ground to three particle sizes: 3.76, 2.45, and 0.82 m^2/g), and acicular grunerite (2.82 m^2/g).

Results from this study indicate that amosite induced the greatest hemolysis of erythrocytes by far (approximately 50%) while acicular, unground grunerite caused no hemolysis. However, grinding the acicular grunerite to increasingly smaller particle sizes and greater surface area ultimately results in some hemolysis. Both semi-asbestiform and acicular, unground commingtonite show hemolytic activity

between amosite and unground, acicular grunerite and grinding acicular commingtonite also increased its hemolytic activity.

Similar results were also observed for cytotoxicity. Amosite was by far the most cytotoxic and the effect was dose-dependent. A dose of 0.05 mg/ml caused approximately 75% cell death for CHO cells. At 0.2 mg/ml, only 1% of cells survived. Acicular grunerite was nontoxic even at 0.5 mg/ml. With grinding, acicular grunerite cytotoxicity increased, albeit only slowly. The most heavily ground sample killed fewer than 25% of cells at 0.2 mg/ml and killed only 65% at 0.5 mg/ml. The cytotoxicity of semi-asbestiform commingtonite was substantially less than amosite, but greater even than ground, acicular grunerite. For this material, 0.2 mg/ml killed approximately 65% of cells and 0.5 mg/ml killed approximately 90%. Interestingly, approximately the same dose-response curve for cytotoxicity was observed for the 3.88 and 1.61 specific surface area samples of this material. The 1.21 samples was somewhat less cytotoxic. Acicular commingtonite was somewhat less cytotoxic (for corresponding doses) than semiasbestiform commingtonite at the highest specific surface area (3.76) and its toxicity decreased with decreasing surface area.

The authors also indicate that neither surface charges on crystal particles nor Magnesium ion content appear to correlate with biological activity. The authors conclude that the degree of "asbestiform" character of a mineral has a dominant effect on biological activity. Moreover, although non-fibrous particles may also be biologically active (and their activity increases with increasing specific surface area), the effects of particles and fibers lie along entirely separate dose-response curves. The biological activity of fibrous materials does not appear to depend directly on specific surface area.

Importantly, the results of the Palekar et al. (1979) study are also consistent with the possibility that fibrous structures within a specific range of sizes and shapes contribute strongly to biological activity while largely non-fibrous particles act through a separate mechanism that depends primarily on total surface area, but that particle-for-particle elicits a substantially lower overall response than the mechanism by which fibers act. Such a scenario is supported by several studies. Jaurand (1997), for example, indicate that ROS are implicated in the cytotoxicity of long, but not short fibers on tracheal epithelial cells. Although the evidence for distinct mechanisms for fibers and particles discussed here is specific to cytotoxic and hemolytic effects, evidence in other studies suggest similar scenarios for other toxic endpoints (potentially including endpoints that contribute to carcinogenicity).

Comparisons of the rate and extent of effects observed in epidemiology studies, whole animal dose-response studies, and *in vitro* studies suggests that cytotoxicity may not be important to human exposures. Unfortunately, however, there is currently insufficient information to compare doses and exposures across these studies in a more quantitative fashion. Therefore, the importance of cytotoxicity to human asbestos exposure cannot be definitively determined at this time.

6.3.4.5 Association between fibrosis and carcinogenicity

The hypothesis that lung tumor induction is associated with the fibrosis has been examined by several authors. There appears to be a debate as to whether fibrosis is a necessary precursor for development of lung cancer (associated with exposure to fibers), whether the presence of fibrosis is an additional factor contributing to increased risk for lung cancer, or whether the two diseases are largely unrelated. This is an important consideration because the characteristics of the exposure-response relationship between asbestos and lung cancer or asbestosis (fibrosis) apparently differ (Sections 6.3.6 and 6.4).

Based on animal studies, Davis and Cowie (1990) found that rats that developed pulmonary tumors during inhalation experiments exhibited a significantly greater clinical degree of fibrosis than rats that did not develop tumors. Furthermore, Davis and Cowie (1990) reported suggestive evidence that the

pulmonary tumors that did develop in the dosed rats tended to develop within portions of the rat's lungs that were already scarred by fibrosis.

As part of a review, Mossman and Churg (1998) indicate that fibrosis of any cause (including diffuse idiopathic fibrosis) appears to be associated with an increased risk of lung cancer and that this is observed in both human and animal studies. They also indicate that only those strains of mice and hamsters that develop fibrotic lesions following exposure to crystalline silica show an increased risk of developing cancer. They also report that, in parallel to what is reported for asbestos by Davis and Cowie (1990), lung tumors that develop following exposure to crystalline silica tend to occur primarily (if not exclusively) in those portions of the lung where fibrotic lesions predominate.

In contrast, Case and Dufresne (1997) from their study of lung burdens among Quebec miners and millers indicate that there is high overlap in the range of concentrations that lead to both lung cancer and asbestosis and those that lead to lung cancer alone, which the authors suggest show a lack of relationship between the two diseases (one is not predictive of the other). The authors indicate that, based on regression of the 111 cases they examined, the only indicator that reasonably tracks lung cancer is severity of smoking and they indicate that this is true despite the level of fiber content in the lung.

Although a definitive determination concerning the relationship between fibrosis (asbestosis) and lung cancer cannot be developed at this time, it does appear that there is some association between the two diseases. Most likely, fibrosis is an additional risk factor for lung cancer and thus represents an additional set of mechanisms that may contribute to the overall risk of developing lung cancer in association with exposure to asbestos. However, based on the evidence as a whole, including the evidence that the character of the dose-response relationship for lung cancer and asbestosis differ, it is not clear that development of fibrosis is an absolute precursor that is required before asbestos-related lung tumors can develop. Interestingly, based on the studies reviewed by Mossman and Churg (1998), the relationship between fibrosis and lung cancer induced by silica may be substantially stronger than that between fibrosis and lung cancer induced by asbestos.

6.3.4.6 Interaction between asbestos and smoking

Numerous studies have indicated a synergistic relationship between smoking and asbestos exposure toward the induction of lung cancer (see, for example, Hammond et al. 1979; Kamp et al. 1992, 1998; Mossman et al. 1996). Smoking is also suspected to facilitate development of asbestos-induced fibrosis (Kamp et al. 1992). However, a more recent study (Liddell and Armstrong 2002) suggests a more complicated relationship that is closer to additive than multiplicative (for a more detailed discussion of this study, see Section 7.2.3). Therefore, discussion of a more complex interaction (which may not be specifically synergistic) is addressed below.

Putative mechanisms that may contribute to an interaction between asbestos exposure and smoking include:

- facilitated transport of carcinogenic components of smoke that may be adsorbed on the surface of asbestos fibers, which may then serve as vehicles to transport these materials through cell membranes to cell interiors and even to locations adjacent to or within the nucleus (see, for example, Fubini 1997; Mossman et al. 1996);

- asbestos-catalyzed production of more highly mutagenic metabolites of the various components of smoke, including benzo(a)pyrene (see, for example, Mossman et al. 1996);

- smoke-product induced inhibition of clearance of asbestos fibers and/or asbestos induced inhibition of clearance of smoke products (see, for example, Mossman et al. 1996); and

- smoke-product induced facilitation of uptake of asbestos by lung epithelium (see, for example, Mossman et al. 1996).

Although much progress has been made at elucidating the nature of these mechanisms and other candidate mechanisms, at this point in time it is possible to indicate definitively neither what mechanisms are important to any observed interaction between smoking and asbestos exposure nor to indicate the relative magnitude of the contributions from such mechanisms. Moreover, a detailed review of such mechanisms is beyond the scope of this document.

6.3.4.7 Conclusions concerning asbestos as a promoter

There is strong evidence that asbestos acts as a promoter for cancer. While this may primarily involve mechanisms the contribute to the induction of proliferation, mechanisms associated with the an interaction between smoking and exposure to asbestos (for the induction of lung cancer; smoking does not appear to affect mesothelioma) are also important. There also appears to be an association between the development of fibrosis and an increased risk for lung cancer.

Evidence indicates that multiple mechanisms may be involved with asbestos-induced cancer promotion and that such mechanisms may be complex and interacting. The different mechanisms also appear to exhibit dose-response relationships with differing characteristics. While there are indications that the most important among these mechanisms may be strong functions of fiber size (with long fibers contributing most to the induction of disease), mechanisms that depend primarily on surface area or total fiber (particle) number (for any size range) may also contribute to overall cancer promotion. Importantly, these latter mechanisms also appear to be strongly associated with the composition of fibers (particles) and may therefore contribute more substantially to the disease induction of agents that have been shown to be particularly toxic (such as crystalline silica), as opposed to particles, fibers, or asbestos in general.

At this point in time, the available data may not be sufficient to distinguish among the relative contributions from the various mechanisms to the overall promotion of cancer, at least in terms of the mechanistic data itself. Importantly, however, the mechanistic data should not be considered to be inconsistent with the results from whole animal studies, where there are clearer indications that fiber size plays a major role in carcinogenicity and fiber (particle) type is also important (see Sections 6.2 and 6.4). Such studies indicate, for asbestos (and other biodurable fibers) that:

- short fibers (less than somewhere between 5 and 10 μm) do not appear to contribute to disease;

- potency likely increases regularly for fibers between 10 μm and a minimum of 20 μm (and, perhaps, continues to increase up to lengths of at least 40 μm); and

- fiber type may be important primarily in determining biodurability.

They further indicate that particularly (or uniquely) toxic particles (such as crystalline silica) may act through a different set of mechanisms that are not dependent on fiber length, but that induce toxic endpoints paralleling those observed for asbestos.

Importantly, the mechanisms by which asbestos may act as a promoter appear to occur in cell lines that may contribute both to the induction of lung cancer and mesothelioma.

6.3.5 Evidence that Asbestos Induces an Inflammatory Response

There is ample evidence that asbestos induces an inflammatory response in pulmonary tissues and the pleura (see, for example, Sections 6.2.2 and 6.3). Moreover, there appears to be multiple biochemical triggers that mediate this response and various mechanisms may be fiber size- and/or fiber type-specific (Table 6-5). Because the role that inflammation plays in the induction of cancer has been addressed elsewhere (Sections 6.3.3 and 6.3.4), it is beyond the scope of this document to provide a detailed review of the mechanisms that lead specifically to inflammation.

6.3.6 Evidence that Asbestos Induces Fibrosis

There is ample evidence that asbestos induces fibrosis in pulmonary tissues (see, for example, Sections 6.2.2 and 6.3). Moreover, there appears to be multiple biochemical triggers that mediate this response and various mechanisms may be fiber size- and/or fiber type-specific (Table 6-5). Because the role that fibrosis plays in the induction of cancer has been addressed elsewhere (Sections 6.3.3 and 6.3.4), it is beyond the scope of this document to provide a detailed review of the mechanisms that lead specifically to fibrosis. Such mechanisms have also been the subject of recent reviews (see, for example, Mossman and Churg 1998; Robledo and Mossman 1999).

6.3.7 Evidence that Asbestos Mediates Changes in Epithelial Permeability

As previously indicated (Section 4.4), maintaining the overall integrity of the epithelial surface of the lung is among the various functions of Type II epithelial cells (Leikauf and Driscoll 1993). It has been shown that asbestos induces changes in the morphology of Type II epithelial cells (see, for example, Ilgren and Chatfield 1998), which has the effect (among others) of increasing the overall permeability of lung epithelial tissue to various macromolecules and, potentially to asbestos fibers themselves. The former plays a role in asbestos-induced fibrosis (by allowing cytokines that stimulate fibroblast proliferation or stimulate fibroblasts to generate extracellular matrix to pass through the epithelium and reach the underlying fibroblasts, Section 6.3.6). The latter may be important to facilitating transport of asbestos from the alveolar lumen to the interstitium (see, for example, Lippmann 1994).

Changes in epithelial permeability may be triggered by cytokines released from other cells or by the action of asbestos fibers on epithelial cells directly. Moreover, some of the mechanisms that mediate this response may be sensitive to fiber size and/or fiber type. For example, Gross et al. (1994) showed that monolayers of human bronchial epithelial cells cultured over a porous medium and exposed to cryogenically ground chrysotile (average length: 1 μm, average aspect ratio:14 at 15 μg/culture plate) became permeable to fibrin breakdown products (FBP's). The cultures were grown over human serum with labeled fibrinogen. This was based on observed increased concentrations of FBP's (double in 24 hours) in the ablumenal chambers of exposed cells compared to cells in control cultures. Because the epithelium showed greater permeability to all concentrations, the increased concentrations were not due to increased breakdown. The observed FDP flux was not vectoral, not saturable, and required neither proteolytic processing nor active transport. Thus, asbestos increases the paracellular flux of intact FDP across airway epithelium.

6.3.8 Conclusions Regarding the Biochemical Mechanisms of Asbestos-Related Diseases

That the specific biochemical triggers for asbestos-related diseases (particularly, the asbestos-related cancers) have not been definitively delineated as of yet is not surprising. The detailed interactions between fibers (and particles) and the cells and tissues of the lung are complex and there are complex, multiple, interacting mechanisms by which such interactions may contribute to disease. Despite great progress in elucidating candidate mechanisms, the number of candidate mechanisms is large and

distinguishing among their relative contributions has been difficult. This is because, among other things, the ability to compare results across studies of different mechanisms is currently limited due to the inability to reconcile the quantitative effects of dose and response across dissimilar studies.

Nevertheless, a number of important implications can be gleaned from the available literature. First, it appears that asbestos can function both as a cancer initiator and a promoter. It also appears that both the initiation and promotion of cancer may occur through more than one mechanism.

Regarding cancer initiation, asbestos likely acts primarily through a mechanism involving interference with mitosis. By this mechanism, asbestos fibers are phagocytized by target cells, migrate to perinuclear locations, and interact with the spindle apparatus and other cell assemblages required to complete mitosis. This tends to result in aneuploidy and may cause various clastogenic effects. This mechanism is driven by long fibers; short fibers do not appear to contribute to the effect. It also appears that all asbestos fiber types (and potentially other durable fibers with sufficient dimensions) cause genetic damage via this mechanisms. If there are effects due to fiber type, they appear only to play a secondary role.

Although there is also evidence that asbestos may induce production of DNA adducts and DNA strand breaks (through ROS and RNS mediated pathways), whether such adducts or breaks ultimately lead to permanent, heritable changes to DNA remain to be demonstrated. The relative importance of ROS/RNS mediated pathways for initiating cancer, compared to the pathway involving interference with mitosis, also remains to be determined.

There is also some evidence that the relative importance of asbestos as a cancer initiator may differ in different tissues. Lung epithelial cells, for example, appear to be relatively resistant to the mechanisms by which asbestos may initiate cancer. Mesothelial cells are not. Among several possibilities, this may be due to the ability of proliferation-competent lung epithelial cells (Type II cells) to undergo terminal differentiation when challenged with certain toxins and this is a pathway not available to mesothelial cells.

The mechanisms by which asbestos may promote cancer primarily involve mechanisms that contribute to the induction of proliferation, although mechanisms associated with an interaction between smoking and exposure to asbestos to induce lung cancer are also important. There also appears to be an association between the development of fibrosis (including asbestosis) and an increased risk of lung cancer.

Evidence indicates that multiple mechanisms may be involved with asbestos-induced cancer promotion and that such mechanisms may be complex and interacting. The different mechanisms also appear to exhibit dose-response relationships with differing characteristics. While there are indications that the most important of these may be strong functions of fiber size (with long fibers contributing the most to carcinogenicity), mechanisms that depend primarily on surface area or total fiber number (for any size range) may also contribute to overall cancer promotion. These latter mechanisms also appear to be strongly associated with the composition of fibers and may therefore contribute more substantially to the disease induction of agents that have been shown to be particularly toxic, as opposed to particles, fibers, or asbestos in general.

Although crystalline silica may act to produce some of the same effects as asbestos (including carcinogenicity), there is substantial evidence that this family of materials do not act through the same pathways and that the characteristics of their respective dose-response relationships may differ. Thus, for example, while asbestos likely induces cancer through mechanisms that favor long (and potentially thin) fibers, silica more likely acts through a mechanism that is dependent on total surface area, with freshly and finely ground material likely being the most potent. In contrast, grinding asbestos fibers tends to lesson its carcinogenicity overall. Due to differences in chemistry and crystallinity (reinforced by studies indicating a lack of correspondence in behavior), crystalline silica does not appear to be an appropriate

analog for any of the asbestos fiber types. Rather, for example, the appropriate non-fibrous analog for crocidolite is riebeckite and the appropriate non-fibrous analog for chrysotile is antigorite or lizardite.

6.4 ANIMAL DOSE RESPONSE STUDIES

Ideally, human epidemiology studies (reviewed in Chapter 7) provide the best data from which to judge the effects of asbestos in humans and from which to derive exposure-response factors for humans. However, animal dose-response studies have proven useful for elucidating certain features of the relationship between asbestos dose and response that cannot be adequately explored in the human studies, primarily due to limitations in the manner that exposures were characterized in the human studies (see Chapter 5).

Unlike human epidemiology studies, exposures in animal studies are controlled and better quantified. Frequently, the characteristics (in terms of fiber size, shape, and type) of such exposures have also been better quantified and this has allowed exploration of the effects that such characteristics (fiber size, shape, type) have on disease response. Accordingly, an overview of animal dose-response studies is provided in this section. Both injection-implantation studies and inhalation studies are reviewed. Particular attention is also focused on a "supplemental" animal inhalation study that we conducted with the specific aim of identifying the characteristics of asbestos that best relate to risk. The strengths and limitations of these kinds of studies are described in Chapter 5.

6.4.1 Injection-Implantation Studies

Because the fibrous materials in injection and implantation studies are placed immediately against the target tissue, the effects of processes associated with inhalation, retention, and translocation are avoided. The only active mechanisms that need to be considered in these studies are those that occur directly in the target tissue (including degradation, clearance, and biological responses of the types described in the previous sections of this chapter). Fibrous materials placed against the tissue surface are subject to dissolution, phagocytosis by macrophages, and phagocytosis by the cells of the target tissue. These mechanisms are described in greater detail in Section 6.2. A range of biologic responses have also been observed (described in Section 6.3).

Numerous researchers have performed these types of studies.

The Work of Stanton and Coworkers. In a series of studies, Stanton and coworkers (1972, 1977, 1981) implanted fibrous materials and induced mesotheliomas in rats. In the studies, a pledgette composed of coarse glass is loaded with hardened gelatin containing sample material and is surgically implanted immediately against the left pleura of the rats. Control studies demonstrate that the coarse glass of the pledgette does not induce significant tumors in the absence of other tumorigenic agents in the gelatin.

Although the mass dose of material implanted was the same for all experiments (40 mg), the observed incidence of mesothelioma varied among samples. By characterizing the dimensions of fibrous structures in the samples using a microscope, the researchers were able to explore the relationship between fiber size and the incidence of mesothelioma. By studying a wide range of fibrous materials, Stanton and his coworkers concluded that the induction of mesothelioma is determined primarily by the physical dimensions of fibers and that mineral composition is secondary. Further, potency appears to increase with the length and decrease with the diameter of fibrous structures. The researchers also concluded that the incidence of malignant tumors correlates with the degree of fibrosis induced by the presence of the fibrous materials. This does not necessarily imply, however, that fibrosis is a necessary step in the induction of asbestos-induced tumors (see Section 6.3.4.5).

Conclusions from the Stanton et al. (1972, 1977, 1981) studies indicating that mineralogy is not a factor in biological response conflicts with evidence provided in Chapter 7 and implications gleaned from mechanism studies presented in Section 6.3. However, the studies by Stanton and coworkers have been shown to suffer from certain methodological limitations (Berman et al. 1995) so that results from these studies should be considered more qualitative than quantitative.

Due to limitations in the ability to produce samples composed of uniform fibers, quantitative relationships between size and potency were explored by Stanton and coworkers using a regression analysis. Structures longer than 8 μm with diameters less than 0.25 μm or longer structures with diameters less than 1.5 μm were found to represent the range of sizes that best correlate with carcinogenicity. It was further stated that such correlations did not eliminate the possibility that other size ranges also contribute to potency, only that the two size ranges identified appear to correlate best. Samples that varied significantly from the reported correlations were attributed to errors in the characterization of structure size distributions in those samples. However, other methodological limitations might also have contributed to the observed deviations or such “outliers” may also suggest evidence for a mineralogical effect that is similar to what is reported in other studies (see Section 6.3 and Berman et al. 1995).

The precision of estimates for the ranges of sizes that contribute to biological activity that are derived from the Stanton and coworkers (1972, 1977, 1981) studies is limited so that such estimates should also be considered qualitative. Size distributions were determined by characterizing 200 to 1,000 structures using TEM and there is no indication that statistically balanced counting rules were employed (Section 4.3). Under such conditions, counts of structures longer than 8 μm are likely small and subject to large uncertainties for most of the samples characterized. Confidence intervals are not provided for any of the exposure values presented in these studies.

Potentially larger errors in the studies by Stanton and coworkers could have been introduced by the method employed to relate fiber counts to sample mass. As indicated in Chapter 5, estimating contributions to mass by sizing total particles and assuming that this is proportional to total sample mass is subject to error from the limit to the precision of characterizing structure dimensions (particularly diameter) and by not accounting for nonasbestos (and possibly nonfibrous) material in the samples. Thus, for example, there is no discussion of the precision with which the cut point of 8 μm was determined in these studies.

Re-analysis and Extension of the Stanton Studies. Several researchers have re-evaluated data from the implantation studies to test additional hypotheses. Using the Stanton and coworkers (1972, 1977, 1981) data, Bertrand and Pezerat (1980) examined the relationship between mesothelioma incidence and several characteristics not evaluated by Stanton and coworkers including: average fiber length, average fiber diameter, average fiber aspect ratio, total fiber surface area and total fiber volume. Results from the regression analysis indicate that potency varies directly with average length and inversely with average diameter, but that neither parameter is a good indicator alone. Combining the effects of length and diameter, average aspect ratio is highly correlated with potency. Biological activity does not correlate highly with structure count, surface area or volume except when fiber sizes are restricted to the long, thin structures that Stanton and coworkers defined. Results of this study are not inconsistent with those originally presented by Stanton and coworkers except that they emphasize a set of characteristics that relate parametrically to biological activity rather than expressing exposure as a single restricted size range of structures.

Bertrand and Pezerat (1980) were able to find good correlations between response and specific "average" characteristics of the samples that are not proportional to the quantity of the material present in the sample ("intensive" characteristics). Such intensive characteristics as average aspect ratio, average length, or average diameter are properties that are independent of the mass of material in a sample. Since response

must be a function of the quantity of sample present, intensive characteristics should have to be multiplied by characteristics that are proportional to the mass of a sample (e.g., fiber number, sample mass, or sample volume) in order to relate them to response. Properties that vary with the mass of a sample are termed "extensive" properties.

The correlations between intensive properties and response reported by Bertrand and Pezerat (1980) likely succeed within the Stanton and coworkers (1972, 1977, 1981) database because a constant sample mass (40 mg) was employed for all of the implantation experiments. However, to apply dose-response relationships that are dependent only on intensive characteristics beyond the data presented by Stanton and coworkers (where mass dose will not be constant), it is necessary to pair intensive characteristics with extensive characteristics (such as mass or number of fibers per sample). Therefore, it is unclear how the conclusions from this paper may be generalized to other data sets.

In a similar study, Bonneau et al. (1986) also examined parametric relationships between structure characteristics and mesothelioma induction. The paper examined specifically correlations between carcinogenicity and dose in terms of two specific relationships: dose expressed as fibers longer than 8 μm that are thinner than 0.25 μm ("Stanton" fibers) and dose expressed as mean aspect ratio. The researchers conclude that mean aspect ratio provides an excellent indication of carcinogenicity for individual fiber types, but that each fiber type must be treated separately. Poorer correlations are found for the relationship between the concentration of "Stanton" fibers and mesothelioma, even when fiber types are considered independently. Although these results appear to be consistent with findings reported from mechanistic studies (Sections 6.2 and 6.3) in that they posit a role for fiber mineralogy, the relationships evaluated by Bonneau et al. (1986) also suffer from the limitation of expressing dose only in terms of intensive quantities, as discussed above. Direct comparison with other studies is therefore difficult.

Following up on the reported problems of the studies by Stanton and coworkers in characterizing crocidolite, Wylie et al. (1987) reanalyzed seven crocidolite samples originally studied by Stanton et al. She and coworkers then used the new size distributions to reevaluate the "Stanton hypothesis" (that the concentration of “Stanton” fibers in a sample correlates with carcinogenicity). Wylie and coworkers note that substantial deviations from the Stanton hypothesis occur for specific samples. They conclude that a specific structure size range alone is not sufficient to characterize biological activity and that a parametric relationship with other structure characteristics (potentially including mineral type) may be necessary to sufficiently describe biological activity.

Conclusions from the Wylie et al. (1987) paper must be interpreted carefully because the researchers evaluated only the relationship between carcinogenicity and the single specific size range indicated ("Stanton" fibers). Thus, the possibility that improved correlations exist between biological activity and different size ranges or a combination of size ranges cannot be ruled out. Qualitatively, conclusions presented in this paper are not inconsistent with the conclusions reported by Stanton and coworkers regarding the general relationship between response and fiber dimensions.

The Wylie et al. (1987) study appears to suffer from several methodological problems. These relate to the manner in which the sample reanalysis was performed. The drop method for preparing electron microscopy grids (used in this study) is not satisfactory for preparing grids. In fact, as reported in the study itself, grids prepared as duplicates by this method were shown to be non-uniform at the 95% confidence interval using a chi-square test. In addition, only 100 to 300 fibers were counted for each sample. Since there is no indication that statistically balanced counting was performed, the uncertainty associated with counts of “Stanton” fibers may be substantial. Such errors would be further multiplied by uncertainty introduced during the sizing of total particles to determine the number of fibers per unit mass.

In a later study, Wylie et al. (1993) examined the effect of width on fiber potency. In this latter study, results from animal injection and implantation studies were pooled and subjected to regression analyses to

identify correlations between exposure and tumor incidence. The animal studies selected for inclusion in this analysis were performed on a variety of tremolite samples exhibiting a range of morphological and dimensional characteristics.

In their regression analyses, Wylie et al. (1993) evaluated a range of exposure indices that emphasize different morphological or size characteristics to help elucidate the characteristics of asbestos that induce a biological response. Because all of the animal studies included in their analyses involved tremolite, mineralogy was not an issue. Results from this study suggest that fibers longer than 5 µm and thinner than 1 µm best correlate with tumor incidence among the animal injection and implantation studies examined. Further, they suggest that a width limit, rather than a limit on aspect ratio, better reflects the bounds of the asbestos characteristics that determine biological activity. They also suggest that complex structures (bundles and clusters) need to be evaluated as part of the determination of exposure because such structures can breakdown and contribute to the population of thinner fibers.

Although the results of the Wylie et al. study tend to support the general conclusions in this document related to width, if not to length (see Section 6.5 and Appendix A), as the authors themselves indicate, such results should be considered qualitative due to the limitations imposed on their study by the methodology employed. Their study was conducted by:

- combining results from multiple studies without careful consideration of variation introduced by methodological differences across the studies;

- employing asbestos concentrations determined by SEM and without careful consideration of differences in the counting methodologies employed by differing research groups across studies; and

- considering injection and implantation studies, which do not account for mechanisms related to inhalation and deposition that affect the exposure-response relationship in humans.

The limitations imposed by the above constraints are highlighted in Chapters 4 and 5 of this report.

Other Injection Studies. A series of injection studies were conducted by several research groups. In these studies, fibrous materials were suspended in saline and injected into rats immediately adjacent either to the pleura or peritoneum. A large number of fibrous materials have now been studied by this process, as reported by: Bolton et al. (1982, 1984, 1986); Davis et al. (1985, 1986a,d, 1987, 1988a); Muhle et al. (1987); Pott et al. (1974, 1976, 1978, 1982, 1987); and Wagner et al. (1976, 1982, 1985). Newer studies are also discussed in Section 6.2. Results confirm that it is the fibrous nature of the materials that is the primary factor leading to the induction of tumors and that potency appears to depend directly on length and inversely on diameter.

The authors of these studies tend to indicate that, except where fibers are not persistent *in vivo*, due to solubility or other degradation processes, the mineralogy of the fibers appears to play only a secondary role in determining disease incidence. Researchers conducting injection experiments also tended to report a correlation between tumor incidence and the degree of fibrosis induced by the sample. These observations are consistent with the ideas originally articulated by Stanton.

Pott developed Stanton's ideas further by suggesting that carcinogenicity is a continuous function of fiber dimensions, which decreases rapidly for lengths less than 10 µm and also decreases with increasing diameter. The possibility was also raised that the apparent inverse dependence on diameter may be an artifact due to the limited number of thick fibers that can be injected in a sample of fixed mass.

Although the published injection studies indicate that potency decreases with decreasing length, researchers in these earlier studies were reluctant to identify a length below which contributions to carcinogenicity can be considered inconsequential. This may be due in part to the skewed distribution of fiber sizes typical of asbestos dusts. Thus, for example, even if structures less than 5 µm are only 1% as potent as structures longer than 5 µm, they may be as much as 100 times as plentiful in some asbestos dusts, so that the total contribution to potency would be equal for both size fractions.

Reasonable dose-response curves have been generated using various sample masses of a single material in some of these studies. This has been demonstrated for UICC crocidolite and UICC chrysotile "A" (Bolton 1984). Results indicate that the relationship between tumor incidence and the log of the dose may be linear and there is no effective threshold. A consistent difference between the two dusts is apparent; the points lie along separate curves and chrysotile appears to be more potent per unit sample mass.

In general, the analytical techniques used for quantifying size distributions in these studies are not fully documented. To the extent that they are, it appears that similar approaches were adopted to those described for the implantation studies above. Consequently, similar limitations apply to the interpretation of results. Briefly, large uncertainties are likely associated with counts of long fibers and estimates of the number of fibers per unit sample mass. Counts in several of the studies also suffer from limitations in the ability of SEM or PCM to detect thin fibers (Section 4.3); whenever SEM or PCM was employed, the thinner fibers were likely under-represented in reported fiber size distributions.

Because samples are placed against mesenchyme in the published implantation and injection studies, results of these studies most directly represent processes associated with the induction of mesothelioma. Assuming, however, that clearance and degradation processes are similar in the deep lung, once a fiber reaches a target tissue, results from the implantation and injection studies may also provide a model of biological response in lung tissue and the factors that lead to the induction of pulmonary tumors. Such a model must be considered qualitative at best, however, because it has been shown that the mechanisms of tissue response to the presence of asbestos in lung parenchyma and in the mesenchyme differ in detail (Section 6.3). The time periods over which the various clearance mechanisms operate in the deep lung and the mesenchyme also differ (Section 6.2), although, it is apparent that the general nature of the clearance and degradation processes in the two tissue types are generally similar.

6.4.2 Animal Inhalation Studies

Animal inhalation studies measure response to exposure in controlled systems that model most of the relevant variables associated with asbestos disease mechanisms in humans (including respirability, retention, degradation, clearance, translocation, and tissue-specific response). Thus, the available inhalation studies are the best database from which to evaluate the integrated effects that lead to the development of asbestos-related disease. Such studies can be used both to identify the characteristics of asbestos that determine biological activity and to qualitatively elucidate the nature of the corresponding relationship between exposure via inhalation and the induction of disease.

In this section, the existing animal inhalation studies are reviewed. In the following section, a project undertaken to overcome the limitations of the existing animal inhalation studies is described (the supplemental inhalation study). Because this latter project was specifically designed to support the risk protocol presented in this document, the nature and results of this project are described in detail.

The existing animal inhalation database consists of approximately 30 studies of which approximately 20 contain dose-response information based on lifetime monitoring of exposed animals, including the work by: Bellman et al. (1986, 1995); Bolton et al. (1982); Davis et al. (1978, 1980, 1985, 1986a,d, 1988a,b);

Goldstein et al. (1983); Le Bouffant et al. (1987); Lee et al. (1981); McConnell et al. (1982); Muhle et al. (1987); Platek et al. (1985); Smith et al. (1987); and Wagner et al. (1974, 1982, 1985, 1987). The studies are similar in overall design, although differences in experimental details potentially affect the comparability of results from separate studies.

In the inhalation studies, plugs formed from bulk samples of fibrous asbestos and related materials are placed in a dust generator and aerosolized. The generators (Beckett 1975), usually a modified version of the apparatus originally designed by Timbrell et al. (1968), consist of a rotating brush that sweeps over an advancing plug of bulk material and liberates fibers that are entrained in the controlled air flow passing through the device. The airborne dust is then passed either into a delivery system for nose-only exposure or into an exposure chamber where animals are kept for fixed periods of time (usually 7 hours per day) on a weekly routine (typically 5 days per week). The exposure routine is continued for as long as 2 years in some of the studies. In some, but not all of the studies, fiber-containing air is passed through a cyclone or elutriator prior to the exposure chamber so that exposure consists primarily of particle sizes within the respirable range.

Asbestos concentrations in the animal inhalation experiments are monitored by a combination of techniques. The concentration of total dust in the chamber is generally monitored gravimetrically. Simultaneously, membrane filter samples are collected and fibers counted by PCM. The quotient of these two measurements yields the number of (PCM) fibers per unit mass of dust (Section 4.3). The distribution of fiber sizes within the dusts introduced into the animal exposure chambers may also be determined in these studies by any of a variety of methods. As indicated previously (Section 4.3), however, the utility of such measurements depends on the precise manner in which they are derived.

To derive fiber size distributions, dust samples from these studies have generally been collected on polycarbonate filters for analysis by SEM. However, such distributions suffer both from the limitations of SEM (Section 4.3) and from the manner in which they are tied to the inhalation experiments (see Chapter 5).

Theoretically, the dose of any fiber size fraction can be estimated in a two-step process. The procedure incorporates consideration of a size fraction termed the PCM-equivalent fraction (PCME), which is the fraction of structures measured by SEM (or TEM) that correspond to the size range of structures known to be visible and therefore countable by PCM. First, the concentration of the PCM-equivalent fraction of the fiber size distribution (measured by SEM) is normalized by dividing its value by the PCM-measured concentration per unit dust mass observed in the inhalation experiment. This ratio is then multiplied by the fractional concentration of any specified size range of interest within the distribution (measured by SEM) to determine the exposure level for that size fraction. However, because bivariate (length by diameter) size distributions have not typically been developed in the available studies and because the number of total fibers longer than 5 μm observed by SEM (without adjustment for width) does not correspond to the number of total fibers longer than 5 μm observed by PCM, it is not possible to derive a true PCME fraction from the SEM data. Therefore, the theoretical approach described above for estimating exposure to specific size fractions cannot generally be applied in the existing studies.

Note that SEM analyses are typically conducted on limited dust samples only to provide information on size distributions. SEM is not used routinely to monitor daily asbestos concentrations in these experiments. Therefore a procedure like that described above is required to link the absolute concentrations to which rats are exposed to the measured and relative size distributions that are determined by SEM.

As indicated above, the data within the published animal inhalation studies are further constrained by the limitations of the analytical methods employed to generate the data (Section 4.3). Comparison of data between studies is also hindered by the lack of sufficient documentation to indicate the specific methods

and procedures employed in each study. Frequently, for example, it is unclear whether respirable dusts or total dusts have been monitored. Also, several studies fail to report one or both of two critical pieces of information: fiber-number-to-mass conversion factors and fiber size distributions. In addition, few studies indicate the precise counting rules employed for generating size distributions.

When structure-number-to-mass conversion factors are provided, unless the conversion factor is derived by counting fibers in a specific size range in a known mass of sample, and fiber concentrations in other size ranges are normalized to this count, several types of error may be introduced. For example, if total sample mass is assumed proportional to calculated mass derived from volume characterizations of the particles counted, unless isometric particles are sized along with fibers and both asbestos and nonasbestos particles are included in the count, a bias will be introduced in the conversion factor because total sample mass will have been under-represented to the extent that such particles are ignored in the estimation of fiber mass. Even if such particles are included, significant uncertainty may result from estimating the volumes of irregular particles and the limited precision associated with the count of the largest particles (due to their limited number). The uncertainty in the measurement of a fiber's diameter is squared in contributing to the uncertainty associated with a mass estimate.

Among reported variations in study design, differences in the detailed design and operation of the aerosolization chamber and the frequency and duration of exposure also potentially contribute to variation in results between studies. Also, use of differing animal strains and species across the various studies suggest the possibility that physiological differences may contribute to the observed variation in study results. Such differences are discussed further in Chapter 5.

A small subset of the asbestos dusts evaluated in the animal inhalation studies have been analyzed by TEM. However, even the published fiber size distributions from these TEM studies are subject to variation from differences in procedures used for sample preparation, from differences in counting rules, and from precision limitations due to the limited number of fibers actually characterized (Section 4.3). This latter limitation particularly affects the precision with which longer fibers are counted.

Although fiber-size distributions are primarily based on SEM analyses rather than TEM analyses in the existing animal inhalation studies, results generally echo the results of the injection and implantation studies. Thus, longer fibrous structures are observed to contribute most to asbestos biological activity, at least qualitatively. For example, dusts containing predominantly long amosite or long chrysotile fibers induce far more pulmonary tumors than samples containing predominantly short structures (Davis et al. 1986a,b). However, dusts evaluated in the existing inhalation experiments have not been characterized sufficiently to distinguish the dependence of biological activity on fiber diameter. Neither are the existing studies sufficient to evaluate the importance of mineralogy (or other potentially important asbestos characteristics) in determining risk.

6.4.3 Supplemental Inhalation Study

Given the problems with the existing animal inhalation studies, a project was undertaken to overcome some of the attendant limitations (Berman et al. 1995). To control for effects from variation in study design and execution (including choice of animal strain, animal handling procedures, equipment design, sample handling procedures, dosing regimen, and pathology protocols), the project focused on a set of studies generated from a single laboratory (i.e., the studies published by Davis and coworkers). Ultimately, the results from six studies covering nine different asbestos samples (including four types of asbestos with samples exhibiting multiple size distributions for two asbestos types) and a total of 13 separate experiments (some samples were studied at multiple exposure levels or in duplicate runs) were pooled for analysis. The database of experiments employed in the project is described in Table 6-7.

To overcome the limitations in the Davis et al. studies associated with the characterization of asbestos itself, the dusts studied in the thirteen experiments listed in Table 6-7 were regenerated by the same group who performed the original studies, from the same starting materials, using the same equipment, and reproducing the same conditions under which the original studies were conducted. Samples of the regenerated dusts were then collected and analyzed by TEM using a modified version of the Superfund air method (Chatfield and Berman 1990) to generate bi-variate size distributions that also include detailed characterization of the shapes and complexity of fibrous structures observed.

The total mass concentration of the regenerated dusts and fiber measurements by PCM were also collected to provide the data required to link size distributions in the regenerated dusts to absolute structure concentrations in the original inhalation experiments. The manner in which such calculations are performed has been published (Berman et al. 1995).

The concentration estimates (for asbestos structures exhibiting a range of characteristics of interest) that were derived from the TEM analyses of the regenerated dusts were then combined with the tumor response data from the set of inhalation experiments listed in Table 6-7 and a statistical analysis was completed to determine if a measure of asbestos exposure could be identified that satisfactorily predicts the lung tumor incidence observed. A more limited analysis was also performed to address mesothelioma; the small number of mesotheliomas observed Davis et al. studies constrained the types of analyses that could be completed for this disease. The detailed procedures employed in this analysis and the results from the first part of the study have been published (Berman et al. 1995). These are summarized below along with results from the parts of the study that remain to be published.

Table 6-7. Summary Data for Animal Inhalation Experiments Conducted by Davis and Coworkers[a,b]

Fiber Type	Description	Abbreviations	Mass Concentration (mg/m^3)	PCM f/ml	Number of Animals	Number of Benign Pulmonary Tumors	Number of Malignant Pulmonary Tumors	Total Number of Pulmonary Tumors	Meso-theli-omas	Reference
Chrysotile	UICC-A	UC	2	390	42	6	2	8	1	Davis et al. 1978
Chrysotile	UICC-A	UC	10	1,950	40	7	8	15	0	Davis et al. 1978
Chrysotile	Long	LC	10	5,510	40	8	12	20	3	Davis et al. 1988a
Chrysotile	Short	SC	10	1,170	40	1	6	7	1	Davis et al. 1988a
Chrysotile	UICC-A	UC	9.9	2,560	36	6	8	14	0	Davis et al. 1988b
Chrysotile	UICC-A (Discharged)[c]	DC	9.9	2,670	39	4	6	10	1	Davis et al. 1988b
Chrysotile	WDC Yarn[d]	WC	3.6	679	41	5	13	18	0	Davis et al. 1986b
Amosite	UICC	UA	10	550	43	2	0	2	0	Davis et al. 1978
Amosite	Long	LA	10	2,060	40	3	8	11	3	Davis et al. 1986a
Amosite	Short	SA	10	70	42	0	0	0	1	Davis et al. 1986a
Crocidolite	UICC	UR	4.9	430	43	2	0	2	1	Davis et al. 1978
Crocidolite	UICC	UR	10	860	40	1	0	1	0	Davis et al. 1978
Tremolite	Korean	KT	10	1,600	39	2	16	18	2	Davis et al. 1985
None	Control	C	0		20	0	0	0	0	Davis et al. 1978
None	Control	C	0		36	0	0	0	0	Davis et al. 1985
None	Control	C	0		61	1	1	2	0	Davis et al. 1986a
None	Control	C	0		64	1	1	2	0	Davis et al. 1986b
None	Control	C	0		47	1	1	2	0	Davis et al. 1988a

[a]Source: Berman et al. 1995
[b]Exposure occurred for 7 hours per day, 5 days per week for 1 year.
[c]UICC-A chrysotile in this experiment was treated with mixed polarity air (produced with a source of beta radiation) following generation to reduce the surface charge on individual particles within the dust.
[d]Chrysotile samples used for dust generation in this experiment were obtained from material treated by a commercial wet dispersion source.

In the statistical analysis performed in this study, the individual dose-response profiles from each of the two data sets were fit to a linear dose-response model:

$$P_i=1 - \exp(- Q_o - b_i \sum_j a_j x_{ij}) \qquad \text{(Eq. 6-7)}$$

where:

"P_i" is the probability of inducing pulmonary tumors observed in the "ith" study;

"Q_o" is a parameter that accounts for the background incidence of pulmonary tumors (assumed to be the same in all studies);

"x_{ij}" is the concentration of the "jth" size fraction of fibers in the "ith" study;

"a_j" is the coefficient of potency for the "jth" size fraction of fibers; and

"b_i" is a coefficient that represents the absolute potency of asbestos. In some analyses this coefficient is allowed to assume different values for different types of asbestos (e.g., chrysotile vs. amphibole), or other differences in experimental conditions.

The "a_j"s in this analysis are constrained to be positive because it is assumed that no fiber prevents cancer. The "a_j"s are also constrained to sum to 1.0, which means that they represent relative potency rather than absolute potency. Asbestos size fractions evaluated represent disjoint (mutually exclusive) sets.

The model (Equation 6-7) allows separate potency coefficients to be assigned to individual size fractions in a dose-response relationship that depends on multiple size fractions. Simultaneously, the "b" coefficients allows separate potencies to be assigned to different fiber types or to results from different studies performed under different experimental conditions.

Several investigators (Bertrand and Pezerat 1980; Bonneau et al. 1986; Stanton et al. 1977; Wylie et al. 1987) have used a logit curve to investigate the dose-response relating various measures of asbestos exposure to tumor response. The logit formula specifies that the tumor probabilities satisfy the relation:

$$\log[P/(1-P)]=a + b\cdot\log x \qquad \text{(Eq. 6-8)}$$

where log x is some measure of asbestos exposure, such as log of concentration of fibers in some size range. In some instances, the logit model was expanded by replacing b·log x with a term representing a linear combination of exposure indices, so that multiple exposure indices could be explored simultaneously. The models were fit using standard linear regression based on normal theory.

An equivalent form for the logit model is:

$$P=e^a x^b/(1 + e^a x^b) \qquad \text{(Eq. 6-9)}$$

Written in this form, it is clear that this model does not permit a background response (i.e., P=0, whenever x=0). This is not a serious limitation when there are no tumors in control animals, such as was the case in Stanton et al. (1977). However, the model will not adequately fit data in which tumors are found in control animals. This was one reason for adopting the linear model (Equation 6-7) used in the investigation of the animal data reported in the study described here.

There is no evidence from this study that the linear model is inadequate. For cases in this study in which the fit between exposure and response is shown to be inadequate, the lack of fit is typically observed to be due to an inconsistent (non-monotonic) dose-response curve so that there is no indication that a non-linear model, such as the logit, would provide a better fit.

The linear model (Equation 6-7) used in this study was fit using a maximum likelihood (Cox and Lindley 1974) approach that utilizes the actual underlying binomial probabilities. This is a more efficient estimation method than use of regression methods based on normal theory, which was the fitting method used in the earlier studies (described above). In addition, the regression procedures applied in the earlier studies indicate only whether the exposure measures that were studied are significantly correlated with tumor response. In contrast, statistical goodness of fit tests were applied in this study to determine whether exposures that are described by a particular characteristic (or combination of characteristics) satisfactorily *predict* the observed tumor incidence. To illustrate, it is apparent from Text Figure 2 of Stanton et al. (1981) that the exposure measure they identify as being most highly correlated with tumor incidence (fibers longer than 8 μm and thinner than 0.25 μm) does not provide an acceptable fit to the observed tumor incidence. Similarly, although all of the univariate exposure measures listed in Table 2 of Berman et al. (1995) are highly correlated with tumor incidence, none of them adequately describe (fit) lung tumor incidence.

To test for goodness-of-fit in this study, each relationship was subjected to a chi-square goodness-of-fit test in which the fit of the model was rejected if the corresponding p-value was less than 0.05, indicating that the true model would provide a worse fit only 5% of the time. Among models that were not rejected based on a goodness-of-fit test, several hypotheses concerning the relative merit of the various models were also examined using the method of maximum likelihood (Cox and Lindley 1974).

An example of an adequate fit to the tumor response data is provided in Figure 6-5 (Figure 3 of Berman et al. 1995). Note that Figures 2 and 3 of the original paper were inadvertently switched during publication; the correct Figure 3 is reproduced here. The exposure index plotted in Figure 6-5 is the sum:

$$\text{Exposure}=a_1 x_{i1} + a_2 x_{12} + a_3 x_{i3}=0.0017C_1 + 0.853C_2 + 0.145C_3 \qquad \text{(Eq. 6-10)}$$

Figure 6-5. Fit of Model. Tumor Incidence vs. Structure Concentration by TEM (Length Categories 5–40 μm, >40μm, Width Categories: <0.3 μm and >5 μm)

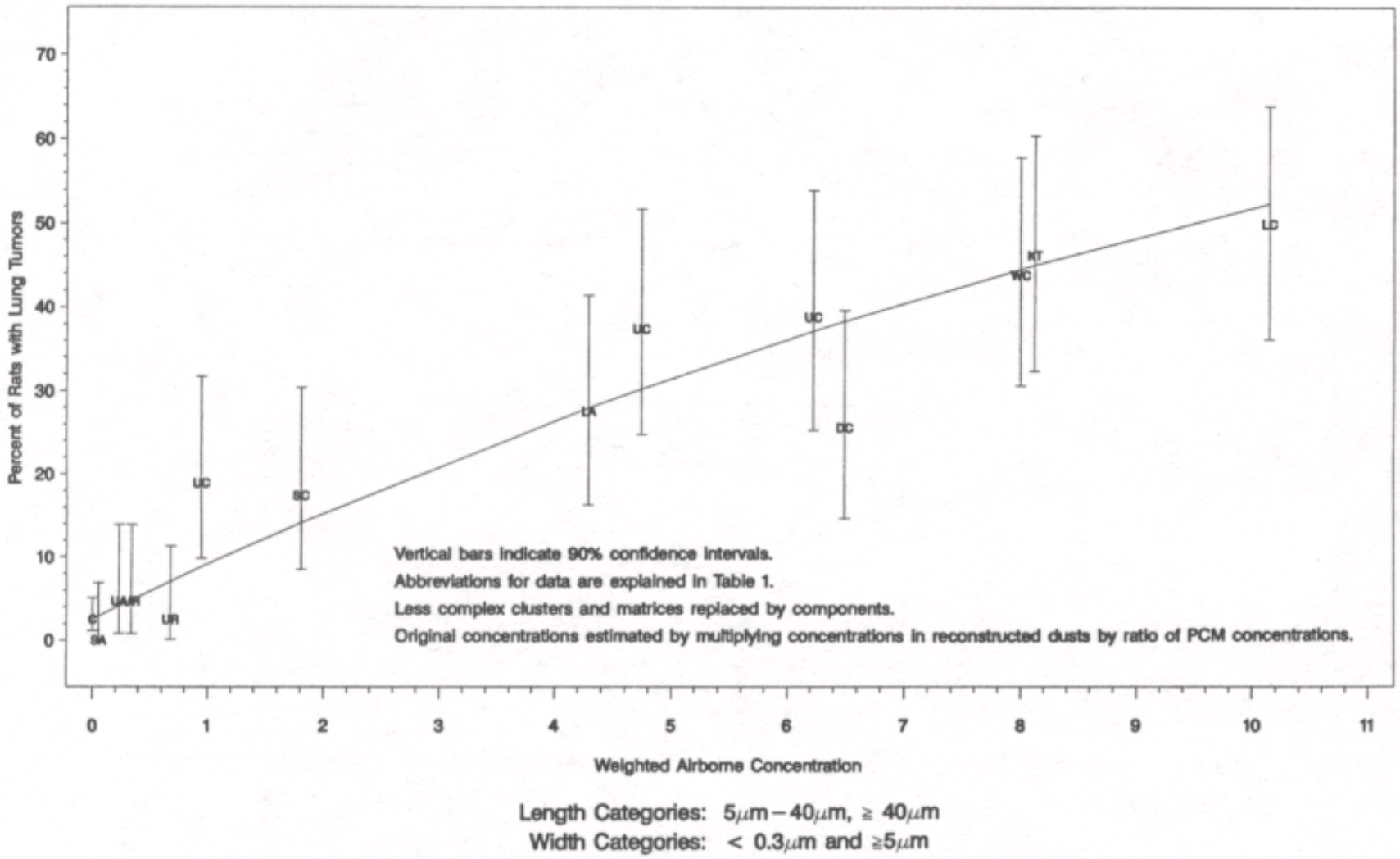

where:

"C_1" (= x_{i1}) is the concentration of structures between 5 and 40 μm in length that are thinner than 0.3 μm;

"C_2" (= x_{i2}) is the concentration of structures longer than 40 μm that are thinner than 0.3 μm; and

"C_3" (= x_{i3}) is the concentration of structures longer than 40 μm that are thicker than 5 μm.

This index of exposure represents one of the optimum indices reported in Berman et al. 1995.

As is clear from the figure, when exposure is expressed in the manner described above, the tumor responses observed in the 13 separate experiments that were evaluated increase monotonically with increasing exposure. It is also apparent that the data points representing each study fall reasonably close to the line representing the optimized model for this exposure index. This was verified by the fact that the corresponding goodness-of-fit test p-value was greater than 0.05. Thus, exposure adequately predicts response.

Results obtained from completing more than 200 statistical analyses to determine whether various measures of asbestos exposure adequately predict lung tumor response (Berman et al. 1995) indicate that:

- neither total dust mass nor fiber concentrations determined by PCM adequately predict lung tumor incidence;
- no univariate measure of exposure (i.e., exposure represented by the concentration of a single size category of structures as measured by TEM) was found to adequately predict lung tumor incidence. Of the univariate measures of exposure examined, the concentration of total structures longer than 20 μm provides the best fit (although still inadequate); and
- lung tumor incidence can be adequately predicted with measures of exposure representing a weighted sum of size categories in which longer structures are assigned greater potency than shorter structures.

The set of analyses completed in support of this work are summarized in Appendix C.

One example of an exposure measure that adequately describes lung tumor incidence is presented in Figure 6-5. Another exposure index shown to provide an adequate fit is:

$$0.0024C_a + 0.9976C_b \qquad \text{(Eq. 6-11)}$$

where:

"C_a" is the concentration of structures between 5 and 40 μm in length that are thinner than 0.4 μm; and

"C_b" is the concentration of structures longer than 40 μm that are thinner than 0.4 μm.

The fit of this index is depicted in Figure 6-6.

In addition to the above, a series of hypotheses tests were also conducted to test such questions as: whether fiber type affects potency or whether the component fibers in complex clusters and matrices should be counted individually. Questions concerning whether mesothelioma incidence can be adequately described by the same measure(s) of exposure that describe lung tumor incidence were also addressed. Taken as a whole, the results presented in Berman et al. (1995) support the following general conclusions:

- structures contributing to lung tumor incidence are thin (<0.5 μm) and long (>5 μm) with structures longer than 20 μm being the most potent;
- the best estimate is that short structures (<5 μm) are non-potent. There is no evidence from this study that these structures contribute anything to risk;
- among long structures, those shorter than 40 μm appear individually to contribute no more than a few percent of the potency of the structures longer than 40 μm;
- lung tumor incidence is best predicted by measurements in which the component fibers and bundles of complex structures are individually counted;
- at least for lung tumor induction in rats, the best estimate is that chrysotile and the amphiboles are equipotent;
- for equivalent size and shape structures, amphiboles are more potent toward the induction of mesothelioma than chrysotile; and
- after adjusting for the relative potencies of fiber type, the size categories that contribute to lung tumor incidence appear also to adequately describe mesothelioma incidence.

Figure 6-6. Fit of Model. Tumor Incidence vs. Structure Concentration by TEM (Length Categories 5–40 µm, >40µm, Width Categories: <0.4 µm)

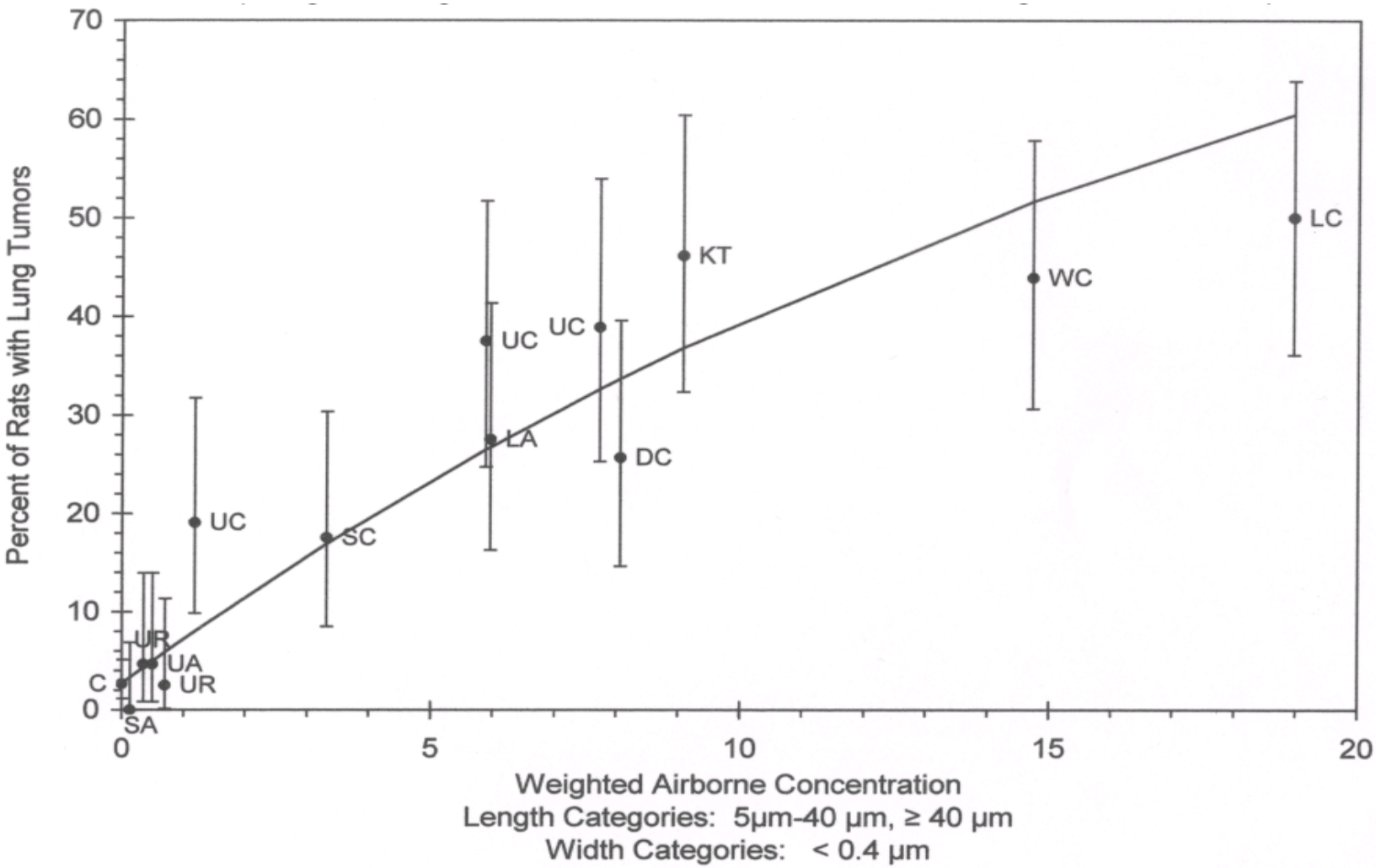

A number of supplemental analyses were also conducted, primarily to identify optimal procedures for performing asbestos analysis and for estimating concentrations. These analyses have not yet been published, but they are included in the summaries in Appendix C. The most important results of the supplemental analyses are that:

- tumor incidence can only be adequately fit by data derived from TEM analysis of samples prepared by a direct transfer procedure. Measurements derived from indirectly prepared samples could not be fit to lung tumor incidence in any coherent fashion; and

- it was not possible to identify an exposure measure in which potency is expressed in terms of a single, continuous function of structure length.

Regarding the last point, although we were not able to identify a continuous function of length that provides an adequate fit to the tumor incidence data, the general results from the above analysis are not inconsistent with the hypothesis that potency is a continuous function of length (i.e., the Pott hypothesis, Pott 1982). The Pott hypothesis suggests that relative potency is low for short fibers, rises rapidly over an intermediate range of length, and approaches a constant for the longest fibers.

6.4.4 Conclusions Concerning Animal Dose-Response Studies

Results from our evaluation of the animal dose-response data for asbestos (including the existing injection/implantation studies, the existing inhalation studies, and our supplemental study) indicate that:

- short structures (less than somewhere between 5 and 10 μm in length) do not appear to contribute to cancer risk;

- beyond a fixed, minimum length, potency increases with increasing length, at least up to a length of 20 μm (and possibly up to a length of as much as 40 μm);

- the majority of structures that contribute to cancer risk are thin with diameters less than 0.5 μm and the most potent structures may be even thinner. In fact, it appears that the structures that are most potent are substantially thinner than the upper limit defined by respirability;

- identifiable components (fibers and bundles) of complex structures (clusters and matrices) that exhibit the requisite size range may contribute to overall cancer risk because such structures likely disaggregate in the lung. Therefore, such structures should be individually enumerated when analyzing to determine the concentration of asbestos;

- for asbestos analyses to adequately represent biological activity, samples need to be prepared by a direct-transfer procedure; and

- based on animal dose-response studies alone, fiber type (i.e., fiber mineralogy) appears to impart only a modest effect on cancer risk (at least among the various asbestos types).

Regarding the last of the above bullets, that only a modest effect of fiber mineralogy was observed in the available animal dose-response studies (when large effects are observed among human studies, Chapter 7), may be due at least in part to the limited lifetime of the rat relative to the biodurability of the asbestos fiber types evaluated in these studies, although it is also possible that different mechanisms drive the effects observed in the animal studies than those that dominate for asbestos-induced cancers in humans and that such mechanisms depend more strongly on mineralogy. Other explanations are also possible. Issues relating to both fiber mineralogy and fiber size are addressed further in Section 6.5 and Chapter 7.

6.5 CONCLUSIONS FROM AN EVALUATION OF SUPPORTING STUDIES

Although gaps in knowledge remain, a review of the literature addressing the health-related effects of asbestos (and related materials) provides a generally consistent picture of the relationship between asbestos exposure and the induction of lung cancer and mesothelioma. Therefore, the general characteristics of asbestos exposure that drive the induction of cancer can be inferred from the existing studies and can be applied to define appropriate procedures for evaluating asbestos-related risk. Furthermore, although it would be helpful to definitively identify the underlying biochemical triggers and associated mechanisms that drive asbestos-induced cancer, this is not an absolute prerequisite for the development of a technically sound protocol for assessing asbestos-related risk.

As previously indicated (Sections 6.3.8), the biochemical mechanisms that potentially contribute to the induction of asbestos-induced cancer are complex and varied. Moreover, different mechanisms appear to exhibit differing dose-response characteristics (i.e., the various mechanisms do not all show the same kind of dependence on fiber size or fiber type). Some mechanisms, for example, suggest that fiber length is important and that only structures that are sufficiently long induce a response. In contrast, other mechanisms suggest that fibers (and even non-fibrous particles) may all contribute to response and that the magnitude of the response is a function of the total surface area of the offending fibers (or particles). Among these mechanisms, additionally, some suggest that fiber type (i.e., mineralogy) is not an important determinant of potency while other mechanisms indicate that fiber type is an important determinant of potency.

The existing studies are not currently adequate to support definitive identification of the specific mechanisms that drive the induction of asbestos-related cancer (versus other mechanisms that may contribute only modestly or not at all). However, whatever mechanisms in fact contribute to the induction of disease, they must be consistent with the gross characteristics of exposure that are observed to predict response in the available whole-animal dose-response studies and human epidemiology studies. Therefore, the implications from these latter studies regarding the dependence of asbestos-induced cancers on fiber size and type are reviewed here in some detail. Further, in Chapter 8, they are used to support development of a protocol for evaluating asbestos-associated risks.

Fiber Length. Fibers less than a minimum length between 5 and 10 μm do not appear to contribute to risk. This is supported both by the results of our re-analysis of the animal inhalation studies conducted by Davis and coworkers (Section 6.4.3 and Berman et al. 1995), in which this hypothesis was tested formally, and by inferences from the broader literature. As long as fiber size is adequately characterized, the animal inhalation studies (Section 6.4.2) and injection/implantation (Section 6.4.1) studies consistently indicate lack of ability of short structures to contribute to the induction of cancer. Furthermore, animal retention studies (Section 6.2.1) and histopathology studies (Section 6.2.2) provide strong mechanistic evidence that explains the lack of potency for short structures; they are readily cleared from the respiratory tract. Even when sequestered in large numbers in macrophages within the lung, there is little indication that such structures induce the kinds of tissue damage and related mechanisms that appear to be closely associated with the induction of cancer.

Although there are mechanism studies that may suggest a role for short fibers in the induction of asbestos-related disease (see, for example, Goodglick and Kane 1990, Section 6.3.4.4), such studies do not track cancer as an endpoint. Therefore, the relationship between the toxic endpoint observed and the induction of cancer needs to be adequately addressed before it can be concluded definitively that short structures can contribute to cancer. Moreover, such a conclusion would be surprising given the substantial evidence that exists to the contrary.

Beyond the minimum length below which structures may be non-potent, potency appears to increase with increasing length, at least up to a length of 20 μm and potentially up to a length of 40 μm. The latter limit is suggested by our re-analysis of the Davis et al. studies (Section 6.4.3) in which it was also found that structures longer than 40 μm may be as much as 500 times as potent as those between 5 and 40 μm in length. The former limit is suggested by broader inferences from the literature that suggest the cutoff in the length of structures that are at least partially cleared by macrophages from the lung may lie close to 20 μm and that the efficiency of clearance likely decreases rapidly for structures between 10 and 20 μm in length (Section 6.2). Such inferences are further reinforced by measurements of the overall dimensions of macrophages in various mammals by Krombach et al. (1997), as reported in Section 4.4.

Importantly, the inferences that potency increases for structures longer than 10 μm (up to some limiting length) from these various studies are strongly reinforcing, even though the upper limits to the points at which potency stops increasing do not precisely correspond. Furthermore, that the longest structures are substantially more potent than shorter structures (and that the shortest structures are likely non-potent) dictates that asbestos analyses performed in support of risk assessment need to provide adequate sensitivity and precision for counts of the longest structures.

Fiber Diameter. Because fibers that contribute to the induction of cancer must be respirable, they must also be thin. The studies reviewed in Section 6.1 indicate that respirable fibers are thinner than 1.5 μm and the vast majority of such structures are thinner than 0.7 μm. In fact, the results of injection, implantation, and inhalation studies reviewed in Sections 6.4.1 and 6.4.2 and the results of our supplemental re-analysis of the Davis et al. studies (Section 6.4.3) indicate that the fibers that contribute most to the induction of asbestos-related cancers are substantially thinner than the limit suggested by respirability alone.

Importantly, the results of all of the studies cited above indicate that it is a cutoff in absolute width that defines the bounds of biological activity rather than a cutoff in aspect ratio (the ratio of length to width) that has been used to define fibrous structures heretofore. That is why the exposure index recommended based on our review of the studies by Davis and coworkers incorporates a maximum width as a cutoff, rather than a minimum aspect ratio.

Fiber Complexity. In our supplemental evaluation of the Davis et al. studies (Section 6.4.3), the tumor incidence data from the animal inhalation studies were best fit (predicted) by exposure indices in which the component fibers and bundles of complex structures (clusters and matrices) were separately enumerated and included in the exposure index used to represent concentration (Section 6.4.3). The appropriateness of such an approach is further supported by the observation that loosely bound structures (including, for example, chrysotile bundles) readily disaggregate *in vivo* (Section 6.2). Therefore, it is recommended in this report that those components of complex structures that individually exhibit the required dimensional criteria be individually enumerated and included as part of the count during analyses to determine the concentration of asbestos in support of risk assessment.

Fiber Type (Mineralogy). The magnitude of any effect of mineralogy upon cancer risk in rodents appears to be modest at best. On the other hand, mineralogy appears to be an important determinant for cancer risk in human epidemiology studies (Chapter 7), with chrysotile appearing less potent than amphibole for inducing mesothelioma and (with lesser certainty) lung cancer. This difference may be due to differences in the life spans of rats and humans compared to the differential biodurability of the different fiber types. It must also be emphasized that, due to confounding, the effects of fiber size and fiber mineralogy need to be addressed simultaneously, if one is interested in drawing useful conclusions concerning fiber mineralogy.

Results from some (but not all) of the animal injection, implantation, and inhalation studies previously reviewed (Sections 6.4.1 and 6.4.2) suggest that mineralogy plays an important role in determining biological activity. However, the nature of the effects of mineralogy are not easily separated from size effects, due to the methodological limitations of the studies cited. Therefore, the evidence from these studies can be considered ambiguous. Formal hypothesis testing during the re-analysis of rat inhalation studies (Section 6.4.3) indicates that, when size effects are addressed, chrysotile and the amphiboles exhibit comparable potency toward the induction of lung cancer. In contrast, amphiboles were estimated to be approximately 3 times more potent than chrysotile toward the induction of mesothelioma, once fiber size effects are addressed.

Several of the human pathology studies cited previously (Section 6.2.3) suggest that mineralogy is an important factor in determining cancer risk, but these studies similarly suffer from methodological difficulties that introduce ambiguity into the inferences drawn. However, it is clear from the human epidemiology data (Chapter 7) that mineralogy plays a substantial role in the determination of risk for human cancer (primarily, mesothelioma).

The underlying cause(s) for the observed difference in potency between chrysotile and the amphiboles may relate to differences in fiber durability (Section 6.2), to size/shape related differences in fibers that are a function of mineralogy and that cause differences in deposition, retention, or translocation (Sections 6.1 and 6.2), and/or to the dependence on mineralogy of the

specific mechanisms underlying the biological responses of specific tissues (Section 6.3). The relative magnitudes of such effects on animal and human pathology also need to be considered, if the observed differences in potency among animal and human studies, respectively, is to be reconciled. Such considerations are addressed further in Chapter 8.

Importantly, whether the observed differences in the role of mineralogy toward animal and human pathology can be reconciled, the effects of mineralogy can be adequately addressed when assessing asbestos-related cancer risk for humans by incorporating dose-response coefficients explicitly derived from the human epidemiology data. Because this is the approach proposed in this document, effects due to mineralogy are properly addressed.

An Appropriate Exposure Index for Risk Assessment. The optimum exposure index defined based on the re-analysis of the animal inhalation studies conducted by Davis and coworkers (Section 6.4.3) is a weighted sum of the concentrations of (1) structures between 5 and 40 μm in length that are thinner than 0.4 μm, and (2) structures longer than 40 μm that are thinner than 0.4 μm (Equation 6-11).

This index was shown to adequately fit (predict) the tumor incidence data across the 13 separate animal inhalation experiments evaluated (P=0.09). Whether the exposure index defined in Equation 6-11is also optimal for capturing the relevant characteristics of fibers that contribute to the induction of human cancer is an open question. Because it captures the major characteristics (concerning length and diameter) identified above that are indicated to be important for human exposures, it represents a promising candidate. Unfortunately, however, the data required to match this index to a set of human-derived exposure-response coefficients does not currently exist (Section 7.4). Therefore, compromises are required to apply the general conclusions of this Chapter to the human data. These are addressed further in Section 7.4.1.

7.0. EPIDEMIOLOGY STUDIES

The existing epidemiology studies provide the most appropriate data from which to determine the relationship between asbestos exposure and response in humans. As previously indicated, however, due to a variety of methodological limitations (Section 5.1), the ability to compare and contrast results across studies needs to be evaluated to determine the confidence with which risk may be predicted by extrapolating from the "reference" epidemiology studies to new environments where risk needs to be assessed. Reliable extrapolation requires both that the uncertainties contributed by such methodological limitations and that several ancillary issues (identified in Chapter 2) be adequately addressed.

A detailed discussion of the methodological limitations inherent to the available epidemiology studies was provided in the Health Effects Assessment Update (U.S. EPA 1986) and additional perspectives are provided in this document (Section 5.1). The manner in which the uncertainties associated with these limitations are addressed in this document are described in Appendix A. As previously indicated (Chapter 2), the ancillary issues that need to be addressed include:

(1) whether the models currently employed to assess asbestos-related risk adequately predict the time and exposure dependence of disease;

(2) whether different mineral types exhibit differential potency (and whether any differences in potency relate to the relative *in vivo* durability of different asbestos mineral types);

(3) whether the set of minerals included in the current definition for asbestos adequately covers the range of minerals that potentially contribute to asbestos-related diseases; and

(4) whether the analytical techniques and methods used to characterize exposures in the available epidemiology studies adequately capture the characteristics of exposure that affect biological activity.

All but the third of the above issues are addressed in this chapter. Currently, the third issue can best be addressed by evaluating inferences from the broader literature (see Chapter 6). The remaining issues are addressed separately for lung cancer and mesothelioma following a brief overview of the approach adopted for evaluating the epidemiology literature.

7.1 APPROACH FOR EVALUATING THE EPIDEMIOLOGY LITERATURE

To develop exposure-response relationships (and corresponding exposure-response coefficients) for use in risk assessment from epidemiological data, two basic types of information are necessary: information on the disease mortality experienced by each member of the study population (cohort) and information on the asbestos exposure experienced by each member of the cohort. So that disease mortality attributable to asbestos can be distinguished from other (background) causes of death, it is also necessary to have knowledge of the rates of mortality

that would be expected in the study population, absent exposure. Normally, such information must be determined based on a “reference” or “control” population.

Ideally, one would like to have complete knowledge of exposure at any period of time for each individual in the cohort and complete access to the data to fit different types of exposure/response models to the data so that the approach for evaluating the relationship between exposure and response can be optimized. In most instances, unfortunately, the data suffer from multiple limitations (see Section 5.1 and Appendix A) and the analysis is further constrained by less than complete access to the data.

Briefly, the major kinds of limitations that potentially contribute to uncertainty in the available epidemiology studies (and the effect such limitations likely produce in estimates of exposure-response coefficients) include:

- limitations in the manner that exposure concentrations were estimated (contributing to variation across studies);
- limitations in the manner that the character of exposure (i.e., the mineralogical types of fibers and the range and distribution of fiber dimensions) was delineated (contributing to systematic variation between industry types and, potentially, between fiber types);
- limitations in the accuracy of mortality determinations or incompleteness in the extent of tracing of cohort members (contributing to variation across studies);
- limitations in the adequacy of the match between cohort subjects and the selected control population (contributing to variation across studies and may have a substantial effect on particular studies); and
- inadequate characterization of confounding factors, such as smoking histories for individual workers (contributing to variation across studies and may have a substantial effect on particular studies).

More detailed discussion of the above limitations is provided in Section 5.1. The manner in which these limitations are being addressed in this evaluation are described briefly below and in more detail in Appendix A.

The existing asbestos epidemiology database consists of approximately 150 studies of which approximately 35 contain exposure data sufficient to derive quantitative exposure/response relationships. A detailed evaluation of 20 of the most recent of these studies, which includes the most recent follow-up for all of the cohorts evaluated in the 35 studies, based on the considerations presented in this overview, is provided in Appendix A.

This new analysis of the epidemiology database differs from the evaluation conducted in the 1986 Health Effects Assessment Update (U.S. EPA 1986) in several ways. It incorporates new studies not available in the 1986 update that contain information on exposure settings not previously evaluated as well as more recently available follow-up for exposure settings

previously evaluated. It also incorporates new features in the manner in which the analysis was conducted. These new features include:

- estimation of "uncertainty" bounds for the exposure-response coefficients (potency factors) derived from each study; and

- for the lung cancer model, introducing a parameter, α, which accounts for the possibility that the background lung cancer mortality rate in the asbestos-exposed cohort differs systematically from the rate in the control population.

The uncertainty bounds were developed to account for uncertainty contributed by the manner that exposure was estimated, by the manner that work histories were assigned, by limitations imposed by the manner in which results were reported in published papers, and by limitations in the accuracy of follow-up, in addition to accounting for the statistical uncertainty associated with the observed incidence of disease mortality. A detailed description of how the uncertainty bounds were constructed is provided in Appendix A.

Exposure-response coefficients were estimated for each cohort both by requiring that $\alpha=1$ (the approach followed in the 1986 Health Effects Assessment Update, U.S. EPA 1986) and by allowing α to vary while fitting the lung cancer model to data. Allowing α to vary addresses potential problems due to differences in background lung cancer rates between the cohort and the control population due, for example, to differences in smoking habits in the two populations. As indicated in Appendix A, this adjustment has a substantial effect on the fit of the U.S. EPA model to the data for several specific cohorts and a corresponding effect on the estimates of the lung cancer exposure-response coefficients for those cohorts.

We were also able to obtain the original, raw data for selected cohorts from a limited number of the more important of the published epidemiology studies. This allowed us to more formally evaluate the appropriateness of the existing U.S. EPA models for lung cancer and mesothelioma (Sections 7.2 and 7.3).

Exposure-response coefficients, and corresponding risk estimates derived therefrom, must be based upon an "exposure index" that expresses the relative potency of asbestos fibers of different dimensions. For example, the exposure index utilized in the 1986 Health Effects Assessment Update (U.S. EPA 1986) assigns equal potency to all fibers longer than 5 μm that exhibit an aspect ratio >3 and a thickness >0.25 μm, regardless of type of asbestos, and assigns zero potency to shorter, squatter, or thinner fibers. In this update, we evaluated a range of such exposure indices, both with respect to agreement with evidence from the literature on the relative potency of asbestos structures of differing types and dimensions (Section 7.4) and with respect to overall agreement across the exposure-response coefficients derived from the available epidemiology studies and adjusted for exposure index. This analysis led to proposed new exposure indices that better reflect the evidence from the literature on the relative potency of different structures and provide improved agreement among exposure-response coefficients estimated from different environments. Such improvement in agreement across studies correspondingly increases the confidence with which the exposure-response factors derived from the existing studies can be applied to new environments.

7.2 LUNG CANCER

The 1986 U.S. EPA lung cancer model (U.S. EPA 1986) assumes that the relative risk, (RR), of mortality from lung cancer at any given age is a linear function of cumulative asbestos exposure in units of fiber-years/ml (f-y/ml) as measured by PCM, disregarding any exposure in the most recent ten years. This exposure variable is denoted by CE_{10}, and its use embodies the assumption that asbestos exposures during the most recent 10 years do not affect current lung cancer mortality risk. The mathematical expression for this model is:

$$RR = 1 + K_L * CE_{10} \qquad \text{(Eq. 7-1)}$$

where the linear slope, K_L, is termed the "lung cancer exposure-response coefficient." This parameter is generally estimated by fitting the model to data from an occupational mortality cohort study consisting of observed and expected numbers of cancer deaths categorized by cumulative exposure, with the expected numbers determined from age- and calendar-year-specific lung cancer mortality rates from an appropriate control population (e.g., U.S. males). This model predicts that the mortality rate in an asbestos-exposed population is the product of the mortality rate in an unexposed, but otherwise comparable, population, and the RR. Consequently the excess mortality due to asbestos is the product of the background mortality rate and the excess RR, $K_L * CE_{10}$. Since smokers have a higher background mortality from lung cancer, the model predicts a higher excess asbestos-related lung cancer mortality in smokers than in non-smokers.

To account for the possibility that an occupational cohort may have a different background mortality rate of lung cancer than the control population (e.g., due to different smoking habits or exposures to other lung carcinogens), in the present analysis Equation 7-1 is expanded to the form,

$$RR = \alpha * (1 + K_L * CE_{10}) \qquad \text{(Eq. 7-2)}$$

where α is the RR in the absence of asbestos exposure relative to the control population. This form of the model contains two parameters, the background RR, α, and the lung cancer exposure-response coefficient, K_L.

7.2.1 The Adequacy of the Current U.S. EPA Model for Lung Cancer

Access to the raw epidemiology data from two key studies allowed us to evaluate the adequacy of the U.S. EPA model (Equation 7-2) for describing the time and exposure dependence for lung cancer in asbestos-exposed cohorts. For this analysis, the raw data for the cohort of crocidolite miners in Wittenoom, Australia was graciously provided by Dr. Nick de Klerk (de Klerk 2001) and the raw data for the cohort of chrysotile textile workers (described by Dement et al. 1994) was graciously provided by Terri Schnoor of NIOSH (Schnoor 2001). The Wittenoom cohort was originally described by Armstrong et al. (1988), but the data provided by de Klerk includes additional follow-up through 1999.

7.2.1.1 Exposure Dependence

To evaluate the adequacy of the linear exposure response relationship assumed by the U.S. EPA lung cancer model, the lung cancer model (Equation 7-2) was fit to the raw data from both the South Carolina and Wittenoom cohorts. In these analyses, each person-year of follow-up was categorized by cumulative exposure defined using a lag of 10 years. The data were then grouped into a set of cumulative exposure categories and the observed and expected numbers of lung cancers were computed for each category. For South Carolina, expected numbers were based on sex-race-age- and calendar-year-specific U.S. rates. Separate analyses were conducted for white males, black males, and white females, as well as for the combined group. For Wittenoom expected rates were based on age- and calendar-year-specific rates for Australian men. The categorized data and the resulting fit of the model to the data from Wittenoom and South Carolina are presented in Tables 7-1 and 7-2, respectively.[1]

For the Wittenoom data (Table 7-1), the fit with $\alpha=1$ is poor ($p<0.0001$), as the model overpredicts the number of cancers in the highest exposure category and underpredicts at lower exposures. By contrast the fit of the model with α variable is adequate ($p=0.1$). This model predicts a relatively high background of lung cancer in this cohort relative to Australian men in general ($\alpha=2.1$) and a correspondingly shallow slope, with the RR increasing only from 2.1 at background to 3.6 in the highest exposure category. A test of the hypothesis that $\alpha=1$ for this cohort is rejected ($p<0.01$) and the model fit to the data (with α variable) predicts $K_L=0.0047$ $(\text{f/ml-yr})^{-1}$.

The fit of the U.S. EPA model to the South Carolina lung cancer data categorized by cumulative exposure is shown in Table 7-2. The model with $\alpha=1$ cannot be rejected both when the model is applied to white males only ($p=0.54$) or with all data combined ($p=0.92$). Since the values α and K_L estimated from white males only are similar to those estimated using the complete cohort (black and white males and white females), the fit to the complete data is emphasized in this analysis. This fit predicts $\alpha=1.2$ and $K_L=0.021$ $(\text{f-y/ml})^{-1}$. A test of the hypothesis that $\alpha=1$ for this cohort cannot be rejected ($p=0.21$), and in this fit $K_L=0.028$ $(\text{f-y/ml})^{-1}$

[1]The fitting of the lung cancer model to the cohort data was carried out by assuming that the observed numbers of cancers in different exposure categories were independent, with each having a Poisson distribution with expectation equal to the expected number based on the control population times the relative risk predicted by Equation 7-2. In the computation of the relative risk for a cumulative exposure category, the person-year-weighted average cumulative exposure (lagged 10 years) for the category was used to represent the exposure in that category. With these assumptions, α and K_L were estimated by the method of maximum likelihood, confidence intervals were constructed using the profile likelihood method, and likelihood ratio tests were used to test hypotheses (Cox and Oakes 1984; Venson and Moolgavkar 1988).

Table 7-1. Fit of EPA Lung Cancer Model to Observed Lung Cancer Mortality Among Wittenoom, Australia Miners (Deklerk 2001) Categorized by Cumulative Exposure Lagged 10 Years

Cumulative Exposure Lagged 10 Years (f-y/ml)		Observed Deaths	Expected Deaths	Predicted Deaths by Model	
Range	**Average**			**(α=1)**	**(α=2.1)**
0	0	5	4.6	4.6	9.8
0–0.4	0.19	27	7.9	8.0	17.0
0.4–1.0	0.69	11	8.2	8.3	17.6
1.0–2.3	1.6	22	11.6	12.1	24.9
2.3–4.5	3.3	28	12.9	14.0	27.9
4.5–8.5	6.2	38	14.3	16.7	31.4
8.5–16	11.8	31	13.2	17.4	29.8
16–28	21.5	21	9.2	14.5	21.6
28–60	41.1	25	11.6	24.5	29.6
60+	142.0	43	11.6	56.5	41.6
Total		251	105.1	176.6	251.0
		Goodness of Fit P-value		<0.0001	0.1

Test of H_0: $\alpha=1$
$p<0.01$

Estimates of K_L $(\text{f-y/ml})^{-1}$

($\alpha=1$)
$K_L=0.027$
90% CI: (0.020, 0.035)

($\alpha=2.1$ [MLE])
$K_L=0.0047$
90% CI: (0.0017, 0.0087)

Table 7-2. Fit of EPA Lung Cancer Model to Observed Lung Cancer Mortality Among South Carolina Textile Workers (Schnoor 2001) Categorized by Cumulative Exposure Lagged 10 Years

Cumulative Exposure Lagged 10 Years (f-y/ml)				Predicted Deaths by Model	
Range	**Average**	**Observed Deaths**	**Expected Deaths**	**(α=1)**	**(α=1.2)**
0	0	0	0.9	0.9	1.1
0–0.5	0.35	4	2.6	2.7	3.2
0.5–1.0	0.75	7	5.5	5.6	6.8
1.0–2.5	1.7	10	9.7	10.1	12.1
2.5–4.5	3.4	13	7.9	8.6	10.2
4.5–8.5	6.2	11	7.7	9.1	10.5
8.5–16	11.8	11	7.2	9.6	10.9
16–28	21.3	8	5.3	8.4	9.2
28–60	41.5	14	6.3	13.8	14.3
60–80	69.2	9	3.0	9.0	9.0
80–110	93.3	10	2.9	10.8	10.5
110+	173	25	4.3	25.6	24.2
Total		122	63.4	114.1	122.0
		Goodness of Fit P-value		0.92	0.96

Test of H_0: $\alpha=1$
p=0.21

Estimates of K_L (f-y/ml)$^{-1}$

($\alpha=1$)
$K_L=0.028$
90% CI: (0.021, 0.037)

($\alpha=1.2$ [MLE])
$K_L=0.021$
90% CI: (0.012, 0.034)

Appendix A contains fits of the model to published exposure-response data from 18 studies (all, with the exception of Wittenoom and South Carolina, obtained from the published literature). In each of these 18 cases the linear model (Equation 7-2) provides an adequate description of the exposure-response. However, α was estimated as >1.0 in 15 of these cases and statistically significantly so in six cases, compared to only one case where α was found to be significantly <1.0. If the true background lung cancer rates in these 15 cohorts with α>1.0 are equal to that in the corresponding control population (i.e., so that a fit with α=1.0 is appropriate), the exposure-response would appear to be supra-linear. At the same time, the data in 11 of the 18 studies (more than half) can be adequately fit with α=1.0 and the studies for which α=1.0 does not provide an adequate fit do not appear to be related by mineral type, by industry, or by the size of the study (Appendix A). Thus, while we completed our analysis using the current lung cancer

model (Equation 7-2), further evaluation of the lung cancer exposure-response relationship appears to be warranted.

7.2.1.2 Time Dependence

The lung cancer model (Equation 7-2) was next evaluated to determine whether it adequately describes the time-dependence of the lung cancer mortality observed in the Wittenoom and South Carolina cohorts. Of particular interest is whether the model accurately predicts lung cancer mortality many years after exposure has ceased. The model predicts that RR increases linearly with cumulative exposure lagged 10 years until 10 years following the end of exposure, after which it remains constant from that time forward. However, it has been suggested (e.g., Walker 1984) that RRs for lung cancer eventually decline after cessation of exposure. Any investigation of this issue should control for exposure level, since exposures can also fall with increasing time due to higher death rates in more heavily exposed subjects. The availability of the raw data from the South Carolina and Wittenoom cohorts provides an opportunity to explore this issue in more depth.

To investigate the assumption inherent in the lung cancer model (Equation 7-2) that the RR remains constant following the secession of exposure, bivariate tables were constructed from both the Wittenoom and South Carolina data in which observed and expected numbers of lung cancers were cross-classified by both cumulative exposure (using the same exposure categories as in Tables 7-1 and 7-2) and time since last exposure categorized using 5-year intervals. The lung cancer model (Equation 7-2) was then fit to these bivariate data. A formal statistical test was conducted of whether the lung cancer RR changed following the end of exposure. This test consisted of appending the multiplicative factor, $\exp(-K_{*}TSLE)$, to the lung cancer model (Equation 7-2), where TSLE is time since last exposure, and conducting a likelihood ratio test of whether the estimated parameter, K, is statistically significantly different from zero. For presentation the bivariate tables were collapsed into univariate tables (Tables 7-3 and 7-4) categorized only by time since last exposure, by summing observed and expected cancers over cumulative exposure categories and computing person-year-weighted averages of cumulative exposure and times since last exposure.

Table 7-3 shows the resulting fit of the U.S. EPA lung cancer model to the Wittenoom lung cancer data categorized by time since last exposure. The RRs rise to a maximum between 10 and 30 years from last exposure and then decline thereafter. However, a very similar pattern is seen with cumulative exposure, which peaks between 10 and 15 years from last exposure, and then declines due to higher mortality among more heavily exposed workers. The U.S. EPA lung cancer model (which does not assume a decrease in RR with time, but does account for any decrease in exposure with increasing time since last exposure) provides an adequate fit to these data ($p=0.13$, α estimated), and there is no apparent tendency for the predicted deaths to fall below observed at the longest times since last exposure. To the contrary, the model-predicted number of lung cancer deaths more than 35 years since last exposure (53.3) is very close to, but slightly larger than, the observed number (51). Likewise, the parameter K was not significantly different from zero ($p=0.16$). Thus, the lung cancer model (Equation 7-2) provides a good description of the Wittenoom lung cancer data categorized by time since last exposure and there is no indication of a drop in the RR up to 45 or more years after exposure has ended that cannot be accounted for by reduced exposures in the longest time categories. It should also be noted

that the values of α (2.1) and K_L (0.0051 f/ml-y) estimated from this bivariate analysis are very similar to those estimated from the univariate analysis summarized in Table 7-1.

Table 7-3. Fit of EPA Lung Cancer Model to Observed Lung Cancer Mortality Among Wittenoom, Australia Miners (Deklerk 2001) Categorized by Years Since Last Exposure

Years Since Last Exposure		Average Exposure Lagged 10 Years (f-y/ml)	Observed Deaths	Expected Deaths	Relative Risk	Predicted Deaths by Model (α=2.1)
Range	Average					
0–1	0.27	1.2	0	0.6	0	1.5
1–5	3.0	1.2	1	1.6	0.6	3.9
5–10	7.5	7.7	8	3.9	2.0	10.3
10–15	12.5	24.8	19	7.0	2.7	19.2
15–20	17.5	24.1	26	11.4	2.3	29.1
20–25	22.5	22.8	42	16.4	2.6	39.8
25–30	27.4	22.0	54	20.1	2.7	47.2
30–35	32.3	21.7	50	20.3	2.5	46.6
35–40	37.1	20.0	31	13.9	2.2	31.4
40–45	43.3	16.7	20	9.6	2.1	21.1
45+	51.2	13.0	0	0.4	0	0.8
Total			251	105.1		250.9
			Goodness of Fit P-value			0.19

Table 7-4 shows the corresponding fit of the U.S. EPA lung cancer model to the South Carolina lung cancer data. This table indicates a marked decrease in RR with increasing time since last exposure. However, there is a concomitant decrease in cumulative exposure. The U.S. EPA lung cancer model provides an adequate fit to these data (p=0.31, α estimated), and the estimates of α (1.3) and K_L (0.20 $(\text{f-y/ml})^{-1}$) are very similar to those obtained from the univariate analysis (Table 7-2). There is no obvious tendency for the model to underestimate risk at the longest times since last exposure, and the value of K estimated for this cohort is not significantly different from zero (p=0.12).

Table 7-4. Fit of EPA Lung Cancer Model to Observed Lung Cancer Mortality Among South Carolina Textile Workers (Schnoor 2001) Categorized by Years Since Last Exposure

Years Since Last Exposure		Average Exposure Lagged 10 Years (f-y/ml)	Observed Deaths	Expected Deaths	Relative Risk	Predicted Deaths by Model (α=1.3)
Range	Average					
0–1	0.06	21.8	15	4.1	3.7	13.4
1–5	3.0	13.1	7	2.2	3.2	7.3
5–10	7.5	16.5	14	3.5	3.9	11.5
10–15	12.5	16.5	8	3.8	2.1	10.4
15–20	17.5	11.5	3	3.6	0.8	7.0
20–25	22.5	9.9	15	5.1	2.9	8.8
25–30	27.5	9.2	13	7.1	1.8	11.7
30–35	32.5	8.5	11	9.5	1.2	15.0
35–40	37.4	7.8	17	10.5	1.6	16.2
40–45	43.5	7.1	19	13.8	1.4	20.8
45+	50.4	31.6	0	0.0	0.0	0.0
Total			122	63.4		122.0
			Goodness of Fit P-value			0.31

Raw lung cancer data were not available from any additional studies, so that the corresponding analysis could not be performed on any other cohort. However, the report by Seidman et al. (1986) on workers at a factory in Patterson, New Jersey that utilized amosite as a raw material contains data in a form that permit a similar analysis using time since onset of exposure rather than time since last exposure. The result of this analysis is shown in Table 7-5, which corresponds to Tables 7-3 and 7-4 except that Table 7-5 presents mortality by time since first exposure rather than time since last exposure.[2] Since exposures in the Seidman study averaged

[2]Table 7-5 was created in the following manner. Table XIV of Seidman et al. (1986) contains expected numbers of deaths from all causes cross-classified by cumulative exposure and time since onset of exposure. Assuming that in each time-since-exposure-onset category the number of deaths from all causes is proportional to the number of person-years, an average cumulative exposure was estimated for each time-since-exposure-onset category. Similarly, using Table V in Seidman et al. (1986), which contains expected numbers of deaths from all causes cross-classified by cumulative exposure and time since onset of exposure, an average duration of exposure was estimated for each time-since-exposure-onset category. The ratio of the estimate of cumulative exposure and duration of exposure provides an estimate of the exposure intensity (f/ml) in each time-since-exposure-onset category. Using this estimate of exposure and the midpoint of the duration of exposure range for each cell, an average cumulative exposure was estimated for each cell in Table X of Siedman et al., in which lung cancer data were cross-classified using the same scheme as was used in Table V for deaths from all causes. The EPA lung cancer model (Equation 7-2) was then fit to the lung cancer mortality data in this table. This bivariate table was then collapsed by summing over cumulative exposure categories to produce Table 7-5, which categorizes the Seidman et al. (1986) lung cancer data by time-since-exposure-onset.

only 1.5 years, time since first exposure approximates time since last exposure. Because Seidman et al. (1986) did not include a lag in their exposure estimates, only data for times since first exposure >10 years are included in our analysis, since (in this range) lagged and unlagged exposures would be very similar.

Table 7-5. Fit of EPA Lung Cancer Model to Observed Lung Cancer Mortality Among New Jersey Factory Workers (Siedman et al. 1986) Categorized by Years Since First Exposure

Years Since First Exposure	Observed Deaths	Expected Deaths	Relative Risk	Predicted Deaths by Model (α=3.4)
10–14	13	8.1	1.6	16.2
15–19	20	8.8	2.3	18.8
20–24	17	9.0	1.9	20.1
25–29	22	8.6	2.5	20.8
30–34	21	6.1	3.5	17.8
35+	16	4.2	3.8	15.3
Total	109	44.7		109.0
	Goodness of Fit P-value			0.55

The RR of lung cancer increases with time since the beginning of exposure in the Seidman cohort. Nevertheless, the fit of the U.S. EPA model to these data with α estimated is very good (p=0.55) and the numbers of cancer deaths predicted by the model agree closely with the observed numbers, even up through 35+ years from the beginning of exposure. Time since last exposure (estimated in each cell as time since first exposure minus average duration of exposure) is not a significant predictor of lung cancer mortality (K is not significantly different from zero, p=0.33). The values of α (3.4) and K_L (0.01 $(\text{f-y/ml})^{-1}$) estimated from this analysis agree closely with those estimated in Appendix A by a different approach (cf. Table A-13 in Appendix A). The analysis in Appendix A was also repeated after eliminating workers who worked longer than 2 years (i.e., workers for whom time since first exposure was not a good approximation to time since last exposure). Results obtained in this analysis are very similar to those shown in Table 7-5.

These analyses of the relationship between lung cancer mortality and time after exposure ends are based on cohorts exposed to relatively pure asbestos fiber types: crocidolite (Wittenoom, Table 7-3), chrysotile (South Carolina factory, Table 7-4) and amosite (Patterson, New Jersey factory, Table 7-5). All three of these were consistent with the assumption inherent in the U.S. EPA lung cancer model (Equation 7-2) that RR of lung cancer mortality remains constant after 10 years past the end of exposure. Thus, the U.S. EPA model appears to adequately describe the time-dependence of lung cancer mortality in asbestos exposed cohorts.

7.2.1.3 Smoking-Asbestos Interaction With Respect to Lung Cancer

The existence of an interaction between smoking and asbestos in causing lung cancer has been known for many years. For example, Hammond et al. (1979), in a study of U.S. insulation workers, found a multiplicative relationship between smoking and asbestos exposure in causing lung cancer. A multiplicative relationship for the interaction between smoking and asbestos is also the relationship inherent in the U.S. EPA lung cancer model (Equations 7-1 and 7-2), by virtue of the fact that increased risk from smoking in reflected in the background risk, which is multiplied by the asbestos-induced RR. More recent work, however, suggests that the interaction between smoking and asbestos exposure may be more complicated.

As described by Liddell (2001), many reviews of the interaction between smoking and asbestos exposure have tended to conclude that the interaction is multiplicative due primarily to (1) the conclusions of Hammond et al. (1979), which was the largest of the early studies and was thus most heavily weighted, and (2) lack of viable alternatives among the options considered. As Liddell (2001) explains, commonly, reviewers examined fits of a simple multiplicative model or a simple additive model and found that (of these two) the multiplicative model tended to provide a better fit, although the fits of either model were sometimes relatively poor. Moreover, only limited sets of mortality data from asbestos exposed cohorts could be used to evaluate these model fits because only limited smoking histories had been collected among such cohorts and, among the data sets studied, the evaluation was typically limited to distinguishing effects among dichotomous groups (i.e., non-smokers and smokers, the latter of which were treated as a single, collective group).

In a more recent analysis of cigarette smoking among the cohort of Quebec miners and millers exposed to chrysotile (which had been previously described in numerous studies, see Appendix A), Liddell and Armstrong (2002) found that the interaction between smoking and asbestos exposure was complex: certainly less than multiplicative, but not quite linear either.

To get some idea of the possible impact of a non-multiplicative asbestos-smoking interaction upon our work to reconcile lung cancer exposure-response coefficients calculated from different environments, consider the generalized model for RR,

$$RR = \delta + \beta_S * S + \beta_A * A + \gamma * A * S \qquad \text{(Eq. 7-3)}$$

where S is a measure of the amount smoked, A is a measure of asbestos exposure, and δ, β_S, β_A and γ are parameters. If $\gamma=0$, the model predicts an additive smoking/asbestos interaction, and if $\gamma=\beta_S * \beta_A / \delta$, the model becomes

$$RR = \delta * [1 + (\beta_S / \delta) * S] * [1 + (\beta_A / \delta) * A] \qquad \text{(Eq. 7-4)}$$

which is a multiplicative smoking/asbestos interaction. Thus, this model generalizes both additive and multiplicative interaction, and has been used by a number of researchers, including Liddell and Armstrong (2002), to study smoking/asbestos interactions.

Note that the generalized model Equation 7-4 can be written in the form

$$RR = (\delta + \beta_S * S) * [1 + A * (\beta_A + \gamma * S)/(\delta + \beta_S * S)] \qquad \text{(Eq. 7-5)}$$

Further, note that Equation 7-5 is of the form: $const_1$ * (1+$const_2$*[asbestos exposure]), which is the same form as the U.S. EPA lung cancer model (Equation 7-2), except that in Equation 7-5 $const_1$ (=$\delta+\beta_{S*}S$) and $const_2$ (=$(\beta_A+\gamma_*S)/(\delta+\beta_{S*}S)$) depend upon the amount smoked, while in the U.S. EPA lung cancer model (Equation 7-2) $const_1$ (=α) likewise depends upon the amount smoked, but the $const_2$ (=K_L) does not. Thus even with this generalized model, the U.S. EPA model would still apply, although the K_L estimated would depend upon the smoking habits of the underlying cohort. That the generalized model Equation 7-3 is at least approximately correct is supported by the fact that the U.S. EPA model (Equation 7-2), which we have noted is comparable to Equation 7-3 except that the K_L value may depend upon smoking, provided a valid fit to data from all of the 20 studies to which it was applied.

This at least suggests that, even if the multiplicative interaction assumed by the U.S. EPA model (Equation 7-2) is not correct, as long as the smoking habits in different cohorts don't differ extremely, the K_L value from different cohorts will be estimates of nearly the same quantity. In particular, the differences in the estimated K_L produced by differences in smoking habits in different cohorts is likely to be a relatively small component of the very large variation in the K_L computed from different studies (see, e.g., Table A-1 in Appendix A). In that case, K_L computed from different environments using the U.S. EPA model (Equation 7-2) would still be comparable and it would be meaningful to search for measures of asbestos exposure ("exposure indices") that better rationalize K_L values (calculated using Equation 7-2) from different studies.[3]

Although the above argument suggests that efforts to reconcile K_L values from different cohorts is still a valid and useful exercise, even if the smoking/asbestos interaction is not multiplicative, as assumed by the U.S. EPA model, further evaluation of the interaction between smoking and asbestos exposure, including evaluation of different exposure-response models, is clearly warranted. However, it must be recognized that the ability to conduct such evaluation will be limited by the small number of asbestos-related epidemiology studies in which smoking data are available, and possibly further limited by the ability to gain access to the raw data from these studies. It should also be recognized that smoking data are not available for most of the studies currently available (see, e.g., Table A-1 in Appendix A), and, for most of those studies, the published data are probably not sufficient to allow fitting of a model that incorporates any smoking/asbestos interaction other than multiplicative.

[3]However, if the interaction is not multiplicative as assumed by the EPA model, it could be problematic to use a K_L value estimated from the model to quantify absolute asbestos risk (e.g., from lifetime exposure) while taking into account smoking habits.

7.2.1.4 Conclusions Concerning the Adequacy of the U.S. EPA Lung Cancer Model

Three principle assumptions inherent to the U.S. EPA lung cancer model were considered in this study to evaluate the overall adequacy of the model for describing the manner in which asbestos exposure induces lung cancer. These are:

- that lung cancer RR is proportional to cumulative exposure (lagged 10 years);
- that risk remains constant following 10 years after the cessation of exposure; and
- that the interaction between smoking and asbestos exposure is multiplicative.

The findings from this evaluation are summarized briefly below. For convenience, timed-dependence is addressed first.

In Section 7.2.1.2, the time response predicted by the lung cancer model (Equation 7-2) was evaluated using the Wittenoom and South Carolina data, along with the data from a New Jersey amosite factory (Seidman et al. 1986). Follow-up in the Wittenoom and South Carolina was sufficient to permit evaluation of the adequacy of the model 40–45 years past the end of exposure, and follow-up in the New Jersey factory permitted the model to be evaluated up through 35+ years past the end of exposure.

The data from all three studies were consistent with the assumption inherent in the lung cancer model that RR of lung cancer mortality remains constant after 10 years past the end of exposure. That this result holds equally for a cohort exposed to chrysotile (South Carolina) as for cohorts exposed to crocidolite (Wittenoom) and amosite (New Jersey factory) is particularly noteworthy, because chrysotile fibers have been reported to be much less persistent than amphibole fibers *in vivo* (see Section 6.2.4). The fact that the lung cancer risk in South Carolina remained elevated 40–45 years following the cessation of exposure, along with the fact that the K_L from the South Carolina cohort is the largest K_L value obtained from our review of 20 studies (see Table A-1 in Appendix A) suggests that carcinogenic potency of asbestos is not strongly related to durability, at least for lung cancer (see Section 6.2).

Based on the results indicated in Section 7.2.1.1, the linear, RR exposure-response model for lung cancer (Equation 7-2) provides an adequate description of the exposure-response relationship from 20 studies. There is little evidence that exposure-response is sub-linear or “threshold-like”. However, in a number of these cases the fitted model predicts a background response that is higher than that in the control population. If the background rate in the control population was actually appropriate in these studies, the exposure-response relationship in these studies would appear in some cases to be supra-linear. These results further reinforce the recommendation of the expert panel (Appendix B) that evaluation of a broader range of exposure-response models (including those that incorporate smoking-asbestos interactions that are other than multiplicative) for lung cancer is appropriate.

Although further evaluation of alternate models is warranted, the specific studies for which α=1.0 does not provide an adequate fit to the data do not appear to be related by mineral type, industry, or size of study cohort and such studies total fewer than half of the studies evaluated. Coupled with the additional evidence that the linear, RR model for lung cancer (Equation 7-2) provides a good description of the time-dependence of disease mortality during and following exposure and that it is not likely to grossly underestimate exposure despite limitation in the manner that smoking is addressed (Section 7.2.1.3), this suggests that use of this model may be adequate for estimating exposure-response factors for the existing studies, at least unless and until a model that provides a superior fit to the data is identified.

Further support for the U.S. EPA lung cancer model is also provided by Stayner et al. (1997). Stayner et al. evaluated the relative fit of a variety of additive, multiplicative, and more complex, empirical models to the same raw data from the South Carolina textile plant that we evaluated and conclusions drawn by these researchers generally parallel and reinforce those reported here.

Stayner et al. (1997) found a highly significant exposure-response relationship for lung cancer and that a linear, RR model (similar to that described by Equation 7-1, except that they initially assumed a lag of 15 years) provided the best overall fit to the data (among the additive and multiplicative models evaluated). Moreover, the fit to the data was not significantly improved by adding additional parameters, nor was there any indication of a significant interaction with any of the covariates evaluated (age, race, sex, or year). These researchers did find an interaction with time such that by applying different slopes for different latencies (15–29 years, 30–39 years, and >40 years), they were able to obtain a significantly better fit. However, Stayner et al. (1997) did not evaluate a RR model with a single slope using a lag of 10 years. Therefore, their analysis cannot be used to evaluate the effect of assuming different slopes for different latencies with respect to the U.S. EPA model, which assumes a lag of 10 years.

Because we found that mortality among the South Carolina cohort is adequately described with α=1.0, the Stayner et al. (1997) study does not directly address questions concerning supra linearity that have been suggested in our findings. Nevertheless, taken as a whole, the evidence evaluated here suggests that the model described in Equation 7-2 may be adequate for evaluating the relationship between asbestos exposure and lung cancer mortality among the existing epidemiology studies. Certainly, no clearly superior model has yet been identified. Therefore, the U.S. EPA lung cancer model was employed in this study for evaluating lung cancer risk while we also recognize that further evaluation of alternate models is warranted. The primary obstacle to more fully evaluating alternate models has been and continues to be lack of access to the raw data for a greater number of cohorts.

7.2.2 Estimating K_L values from the Published Epidemiology Studies

The U.S. EPA model for lung cancer (Equation 7-2) was applied to each of the available epidemiology data sets to obtain study-specific estimates for the lung cancer exposure-response coefficient, K_L. Based on the results presented in Section 7.2.1.4, while there is some evidence that models in addition to the U.S. EPA lung cancer model should be explored, there is little indication that the current model does not provide an adequate description of lung cancer mortality that is sufficient to support general risk assessment. The set of K_L values derived from

available epidemiology studies are presented in Table 7-6, which is a reproduction of Table A-1 in Appendix A.

In Table 7-6, Column 1 lists the fiber types for the various studies, Column 2 lists the exposure settings (industry type), and Column 3 indicates the specific locations studied. Column 4 presents the best estimate of each K_L value derived for studies, as reported in the original 1986 Health Effects Update and Column 5 presents the reference for each respective study. Columns 6, 7, and 8 present, respectively: the best-estimates for the K_L values derived in our evaluation for all of the studies currently available (including studies corresponding to those in the 1986 Health Effects Update); a statistical confidence interval for each K_L value (derived as described in Appendix A); and an uncertainty interval for each K_L value (also derived as described in Appendix A). The reference for the respective study from which the data were derived for each K_L estimate is provided in the last column of the table. To assure comparability across studies, values for all studies (even those that have not been updated since their inclusion in the 1986 Health Effects Update) were re-derived using the modified procedures described in Appendix A.

As explained in Appendix A, the uncertainty intervals for K_L values (and corresponding intervals for K_M values, the exposure-response coefficients for mesothelioma) are intended to reflect, in addition to statistical variation, other forms of uncertainty that are difficult to quantify, such as model uncertainty and uncertainty in exposure estimates. We interpret these informally as providing a range of K_L values that are reasonable, based on the data available for a given study. Accordingly, if uncertainty intervals for two K_L values do not overlap, these two underlying sets of data are considered to be incompatible. Potential reasons for such incompatibility include the possibility that the K_L values are based on an exposure measure that does not correlate well with biological activity of asbestos. One of the goals of this report is to determine an exposure index that correlates better with biological activity, and consequently brings the K_L values into closer agreement. The degree of overlap of the corresponding uncertainty intervals provides an indication of the extent to which a groups of K_L values are in agreement.

The K_L values derived in this study and the corresponding values derived in the original 1986 Health Effects Update generally agree at least to within a factor of 3; a couple vary by a factor of 4; one varies by a factor of 5; and one varies by a factor of about 15. However, in every case the K_L from the 1986 update lies within the uncertainty interval for the K_L derived in the current update.

Perhaps the most interesting of the changes between the 1986 K_L value estimates and the current K_L value estimates involves the friction products plant in Connecticut (McDonald et al. 1984). Although a relatively small, positive exposure-response was estimated from this study in the 1986 Health Effects Update, the best current estimate is that this is essentially a negative study (no excess risk attributable to asbestos). The difference derives primarily from allowing α to vary in the current analysis. The exposure groups in this cohort do not exhibit a monotonically increasing exposure-response relationship and, in fact, the highest response is observed among the group with the lowest overall exposure. As indicated in Appendix A, lack of a monotonically increasing exposure-response relationship is a problem observed in several of the studies evaluated.

Table 7-6. Lung Cancer Exposure-Response Coefficients (K_L) Derived from Various Epidemiological Studies

Fiber Type	Operation	Cohort	EPA (1986) K_L*100	Reference	This Update K_L*100	90% Confidence Interval	Uncertainty Interval[a]	Reference
Chrysotile	Mining and Milling	Quebec mines and mills	0.06	McDonald et al. 1980b	0.029	(0.019, 0.041)	(0.0085, 0.091)	Liddell et al. 1997
			0.17	Nicholson et al. 1979				
		Italian mine and mill	0.081	Piolatto et al. 1990	0.051	(0, 0.57)	(0, 1.1)	Piolatto et al. 1990
	Friction Products	Connecticut plant	0.01	McDonald et al. 1984	0	(0, 0.17)	(0, 0.62)	McDonald et al. 1984
	Cement Manufacture	New Orleans plants			0.25	(0, 0.66)	(0, 1.5)	Hughes et al. 1987
	Textiles	South Carolina plant	2.8	Dement et al. 1983b	2.1	(1.2, 3.4)	(0.81, 5.1)	Dement et al. 1994[b]
			2.5	McDonald et al. 1983a	1	(0.44, 2.5)	(0.22, 4.9)	McDonald 1983a
Crocidolile	Mining and Milling	Wittenoom			0.47	(0.17, 0.87)	(0.084, 1.7)	de Klerk et al. 1994[c]
Amosite	Insulation Manufacture	Patterson, NJ factory	4.3	Seidman 1984	1.1	(0.58, 1.9)	(0.17, 6.6)	Seidman et al. 1986
		Tyler, Texas factory			0.13	(0, 0.6)	(0, 1.8)	Levin et al. 1998
Tremolite	Vermiculite Mines and Mills	Libby, Montana			0.51	(0.11, 2.0)	(0.049, 4.4)	Amandus and Wheeler 1987
					0.39	(0.067, 1.2)	(0.03, 2.8)	McDonald et al. 1986
Mixed	Friction Products	British factory	0.058	Berry and Newhouse 1983	0.058	(0, 0.8)	(0, 1.8)	Berry and Newhouse 1983

Table 7-6. Lung Cancer Exposure-Response Coefficients (K_L) Derived from Various Epidemiological Studies *(continued)*

Fiber Type	Operation	Cohort	EPA (1986) K_L*100	Reference	This Update K_L*100	90% Confidence Interval	Uncertainty Interval[a]	Reference
	Cement Manufacture	Ontario factory	4.8	Finkelstein 1983	0.29	(0, 3.7)	(0, 22)	Finkelstein 1984
		New Orleans plants	0.53	Weill 1979, 1994	0.25	(0, 0.66)	(0, 1.5)	Hughes et al. 1987
		Swedish plant			0.067	(0, 3.6)	(0, 14)	Albin et al. 1990
		Belgium factory			0.0068	(0, 0.21)	(0, 0.84)	Laquet et al. 1980
	Factory workers	US. retirees	0.49	Henderson and Enterline 1979	0.11	(0.041, 0.28)	(0.011, 1.0)	Enterline et al. 1986
	Insulation Application	U.S. insulation workers	0.75	Seilkoff et al. 1979	0.18	(0.065, 0.38)	(0.012, 2.1)	Seilkoff and Seidman 1991
	Textiles	Pennsylvania plant	1.4	McDonald et al. 1983b	1.8	(0.75, 4.5)	(0.2, 16)	McDonald et al. 1983b
		Rochedale plant	1.1	Peto 1980a	0.41	(0.12, 0.87)	(0.046, 2.3)	Peto et al. 1985

[a]Uncertainty Interval formed by combining 90% confidence interval with uncertainty factors in Table A-3.
[b]With supplemental raw data from Terri Schnorr (NIOSH) and Dement
[c]With supplemental unpublished raw data with follow-up through 2001

Among the K_L values derived in the current study, the lowest and highest of the best-estimate values differ by a factor of 300 (excluding the negative study of the Connecticut friction products plant, which would make the spread even larger) and several pairs of uncertainty intervals have no overlap. For example, the K_L uncertainty interval for the chrysotile miners in Quebec lies entirely below the corresponding intervals for chrysotile textile workers (in either of the two studies for South Carolina, which are of highly redundant cohorts in the same plant), for textile workers in the Pennsylvania plant, and for amosite insulation manufacturers (in the Seidman study (1986).

The K_L values and the associated uncertainty intervals are plotted in Figure 7-1. Each exposure environment is plotted along the X-axis of the figure and is labeled with a 4-digit code that indicates fiber type (chrysotile, mixed, crocidolite, or tremolite), industry (mining, friction products, asbestos-cement pipe, textiles, insulation manufacturing, or insulation application); and a 2-digit code indicating the study from which the data were derived. A key is also provided. In Figure 7-1, the chrysotile studies are grouped on the left, amphibole studies are grouped on the right, and mixed studies are in the middle.

For studies conducted at the same facility (generally among highly overlapping cohorts), such as the Dement et al. (1994) and the McDonald et al. (1983a) studies of the same South Carolina textile facility, a single study was selected for presentation in Figure 7-1. Thus, for South Carolina, the Dement et al. (1994) study is presented because we had access to the raw data for this study. It is also a newer study. Similarly, the Amandus and Wheeler (1987) study was selected to represent the Libby Vermiculite site over the other study at this facility (McDonald et al. 1986). The effects of such selection is expected to be small in any case because the K_L values estimated for the individual studies in each pair vary only by a factor of 2.

Comparisons of K_L values across the available studies are instructive. Within chrysotile studies alone (and excluding the negative friction products study), lowest and highest K_L values vary by approximately a factor of 70. Moreover, as previously indicated, the uncertainty intervals for the lowest (non-zero) value (for Quebec miners) and the highest value (textile workers) have no overlap. Uncertainty intervals for the negative friction product study and the other estimates for chrysotile do overlap, primarily due to the wide confidence interval associated with the negative study.

Among the apparent variations, differences in lung cancer potency observed among Quebec miners versus that observed among South Carolina textile workers has been the subject of much discussion and evaluation, which is worthy of review (Appendix D). The inability to reconcile these differences, appears to be among the biggest obstacles to reliably estimating an overall chrysotile dose-response coefficient for lung cancer.

As indicated in Appendix D, the leading hypothesis for the apparent differences in lung cancer risk per unit of exposure observed between chrysotile mining and textile manufacturing is the relative distribution of fiber sizes found in dusts in these industries. Evidence from several studies indicates that textile workers were exposed to dusts containing substantially greater concentrations of long structures than dusts to which miners were exposed. Thus, the effects of fiber size is considered further in Section 7.4.

Figure 7-1:
Plot of Estimated K_L Values and Associated Uncertainty Intervals by Study Environment

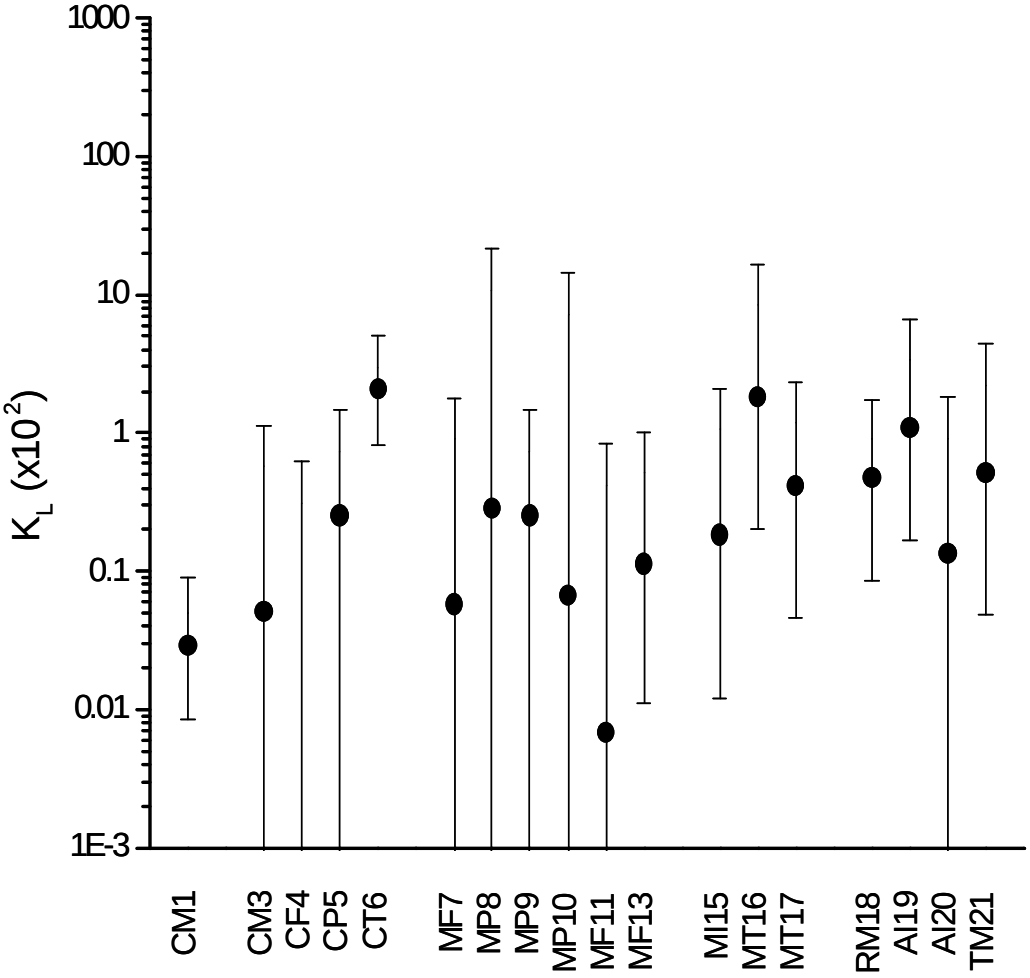

Key for Figures 7-1 through 7-6 Code

Fiber Types (First Digit of Code)	Study Environment (Second Digit of Code)
A = amosite	A = insulation application
C = chrysotile	F = friction products manufacturing
M = mixed fibers	I = insulation manufacturing
R = crocidolite	M = mining
T = tremolite (in vermiculite)	P = ac pipe manufacturing
	T = textile manufacturing
	X = misc. products manufacturing

Study Cohorts
(Last 2 digits)

1 = Quebec miners (Liddell et al. 1997)
2 = Quebec miners (Liddell et al. 1997, raw data)
3 = Italian miners (Piolatto et al. 1990)
4 = Connecticut friction product workers (McDonald et al. 1984)
5 = New Orleans ac pipe manufacturers (Hughes et al. 1987)
6 = South Carolina textile manufacturers (Dement et al. 1994, raw data)
7 = British friction product manufacturers (Berry and Newhouse 1983)
8 = Ontario ac pipe manufacturers (Finkelstein 1984)
9 = New Orleans ac pipe manufacturers (Hughes et al. 1987)
10 = Swedish ac pipe manufacturers (Albin et al. 1990)
11 = Belgium ac pipe manufacturers (Laquet et al. 1980)
13 = Retired factory workers (Enterline et al. 1986)
14 = Factory workers (Liddell et al. 1997)
15 = Insulation appliers (Selikoff and Seidman 1991)
16 = Pennsylvania textile workers (Mcdonald et al. 1983b)
17 = British textile workers (Peto et al. 1985)
18 = Australian crocidolite miners (de Klerk, unpublished, raw data)
19 = New Jersey insulation manufacturers (Seidman et al. 1986)
20 = Texas insulation manufacturers (Levin et al. 1998)
21 = Libby vermiculite miners (Amandus and Wheeler 1987)

Ignoring the negative Connecticut friction products study, the range of K_L values observed across chrysotile studies (70) appears to be substantially narrower than the range observed across all studies (300). However, if the nearly negative study of the Belgium asbestos-cement pipe manufacturers is also removed, the range observed for chrysotile studies is almost identical to the range observed across all studies. This is because the K_L values for Quebec represents the low extreme of both ranges and South Carolina represents the high extreme of both ranges.

Among "pure" amphibole studies, the lowest and highest of the best-estimate K_L values vary by a factor of approximately 9 and the two extremes both derive from within the same industry (amosite insulation). The two studies in question are of amosite insulation manufacturing plants (one in Patterson, New Jersey, and one in Tyler, Texas) that utilized the same equipment (literally) and apparently had similar sources of asbestos (South Africa). Despite the 9-fold difference in K_L values, the uncertainty intervals for these two estimates have substantial overlap. If the arithmetic mean of the values for the two amosite insulation studies is used, K_L values estimated, respectively, for crocidolite mining, amosite insulation manufacture, and mining of vermiculite contaminated with tremolite vary by less than a factor of 2. However, this is possibly fortuitous, given the magnitude of the associated uncertainty intervals (Figure 7-1).

As indicated in Appendix D, for example, it is possible that mining studies tend to exhibit low K_L values relative to studies of asbestos products industries. This is due to the presence of large numbers of cleavage fragments in the dusts that may not contribute to biological activity (because the majority of these may not exhibit the requisite size to be biologically active) but which, nevertheless, are included in estimates of asbestos concentrations in the original epidemiology studies. If the K_L estimates for Libby and Wittenoom could be adjusted for this effect, they might be closer in value to that obtained from the Seidman study.

It is also instructive to compare variation within and between industries. Within industries (especially for a single fiber type), the data are limited. The studies from the two chrysotile mines (Quebec and Italy) show remarkably close agreement, varying by less than a factor of 2. The three studies involving mining of amphibole (Wittenoom and the two studies of Libby) also vary by less than a factor of 2. However, the mean of the amphibole mining group is approximately 10 times the mean of the chrysotile mining group. Moreover, based on inspection of their respective uncertainty intervals, the K_L values for chrysotile mining in Quebec and Crocidolite mining in Wittenoom appear to be incompatible.

Across all asbestos types (including mixed), the asbestos-cement pipe industry shows the greatest variation, including a nearly negative study (best estimate K_L=0.000068) and four more studies with K_L values that range up to 0.0029 producing a variation within this industry of a factor of 40. The friction products industry includes one negative and one positive study. Better agreement is observed among textiles. The two mixed textile plants show K_L values that vary by no more than a factor of 5 from each other and from the K_L for the South Carolina chrysotile textile plant.

7.3 MESOTHELIOMA

The model proposed in the Airborne Health Assessment Update (U.S. EPA 1986) to describe the mortality rate from mesothelioma in relation to asbestos exposure assumes that the mortality rate from asbestos-induced mesothelioma is independent of age at first exposure and increases according to a power of time from onset of exposure, as described in the following relationship:

$$I_M = K_M \cdot f \cdot [(T - 10)^3 - (T - 10 - d)^3] \quad \text{for } T > 10 + d \qquad \text{(Eq. 7-6)}$$

$$= K_M \cdot f \cdot (T - 10)^3 \quad \text{for } 10 + d > T > 10$$

$$= 0 \quad \text{for } 10 > T$$

where:

I_M is the mesothelioma mortality rate at T years from onset of exposure to asbestos for duration d and concentration f;

K_M is the proportionality constant between exposure and mesothelioma response and represents the potency of asbestos;

A more general expression that holds for variable exposure is given by

$$I_M = 3 K_M \int_0^t f(x)(t - 10 - x)^2 dx \qquad \text{(Eq. 7-7)}$$

where f(x) is the concentration of fibers at time x following the beginning of exposure. This expression reduces to Equation 7-6 when exposure is constant (see Appendix A).

7.3.1 The Adequacy of the Current U.S. EPA Model for Mesothelioma

Access to the raw epidemiology data from a few key studies allowed us to evaluate the adequacy of the U.S. EPA model (Equation 7-6) for describing the time-dependence for mesothelioma in asbestos-exposed cohorts. For this analysis, the raw data from a cohort of chrysotile miners in Quebec was graciously provided by Drs. Douglass Liddell and Corbett McDonald (described in Liddell et al. 1997), the raw data for the cohort of crocidolite miners in Whittenoom, Australia was graciously provided by Dr. Nick de Klerk (unpublished) and the raw data for the cohort of chrysotile textile workers (described by Dement et al. 1994) was graciously provided by Ms. Terri Schnoor of NIOSH and Dr. John Dement of Duke University. The Whittenoom cohort was originally described by Armstrong et al. (1988), but the data provided by Dr. de Klerk included additional follow-up through 1999.

To identify potential effects due to varying statistical procedures, different methods for fitting the U.S. EPA mesothelioma model to epidemiological data were evaluated. In this evaluation, three methods were used to fit the U.S. EPA mesothelioma model to data from Wittenoom.

In the first approach the data were categorized in a manner often available in published form, so this method mimics the method generally used when raw data are not available. The observed mesotheliomas and person-years of observation were categorized by time since first exposure, and the mean exposure level and duration of exposure were calculated for each such category. The U.S. EPA model was then applied to such data using the approach for the typical situation (as described in Appendix A) and results for the Wittenoom cohort are presented in Table 7-7. The K_M value estimated for Wittenoom using this approach is 7.15×10^{-8} (90% CI: 6.27×10^{-8}, 8.11×10^{-8}). The fit of this model to data categorized by time since first exposure is good (p=0.65).

For most of the published epidemiology data sets, the average level and duration of exposure for individual time-since-first-exposure categories are not provided and have to be estimated from cruder data representing cohort-wide averages. Thus for most of the epidemiology data sets, the calculation of K_M is based on cruder information than the calculation presented in Table 7-7.

Table 7-7. Fit of EPA Mesothelioma Model to Observed Mesothelioma Mortality Among Wittenoom, Australia Miners (Deklerk 2001) Categorized by Years Since First Exposure

Years Since First Exposure		Average Duration (years)	Average Concentration (f/ml)	Observed Deaths	Predicted Deaths by Model
Range	Average				
0–5	0	0.643	30.2	0	0.0
5–10	0.19	0.91	30.2	0	0.0
10–15	0.69	0.958	30.0	1	0.6
15–20	1.6	0.970	29.7	5	6.6
20–25	3.3	0.953	29.5	20	17.6
25–30	6.2	0.957	29.3	25	30.1
30–40	11.8	1.05	29.0	90	78.1
40–100	21.5	1.13	28.1	23	31.1
Total				164	164.0
			Goodness of Fit P-value		0.65

Estimates of K_M
$K_M = 7.15 \times 10^{-8}$
90% CI: (6.27×10^{-8}, 8.11×10^{-8})

A second approach to fitting the U.S. EPA model to epidemiology data exploits the fact that the mesothelioma model (Equation 7-7) expresses the mesothelioma mortality rate as the product of K_M and an integral involving the exposure pattern, the time of observation, and the 10-year time lag, but not any parameters that require estimation.

The value of this integral was calculated for each year of follow-up of each subject. Person-years of follow-up and mesothelioma deaths were then categorized according to the values of the

integral, and the average value of the integral determined for each category. Results are presented in Table 7-8.

Table 7-8. Fit of EPA Mesothelioma Model to Observed Mesothelioma Mortality Among Wittenoom, Australia Miners (Deklerk 2001) Categorized by Average Value of Integral (Equation 6-12)

Average Value of Integral	Observed Deaths	Predicted Deaths by Model
0	0	0.0
28.4	0	0.0
206.3	1	0.3
732.3	4	1.0
2,038.1	10	2.9
5,153.7	23	6.8
12,385.8	32	13.8
30,639.7	27	25.8
144,801	67	113.3
Total	164	164.0
Goodness of Fit P-value		<0.0001

Estimates of K_M
$K_M=9.00x10^{-8}$
90% CI: ($7.89x10^{-8}$, $10.2x10^{-8}$)

K_M was estimated by maximum likelihood from Table 7-8 assuming that the observed numbers of cancer deaths in the different categories of the integral were independently Poisson distributed with a mean equal to the mean value of the integral for that category times K_M. The value of K_M obtained in this fashion was $K_M=9.00x10^{-8}$ (90% CI: $7.89x10^{-8}$, $10.2x10^{-8}$). This estimate is about 25% larger than obtained with the data categorized by time since first exposure, although confidence intervals obtained from the two procedures overlap. The fit of the model to data categorized by the integral is poor ($p<0.00001$), as the model predicts too few mesotheliomas for small values of the integral and too many mesotheliomas for large values of the integral.

A third method of estimating K_M (termed the "exact method") employs a likelihood that does not involve any categorization of data. With this method, the hazard function, $h(t)=I_M(t)$ and the corresponding survival function (probability of surviving to age t without death from mesothelioma in the absence of competing causes of death), $S(t)=\exp(-\int_0^t h(s)ds)$, are computed for time at the end of follow-up. The contribution to the likelihood of a subject who died of mesothelioma t years after beginning of follow-up is $h(t)*S(t)$, and the contribution of a subject whose follow-up was not terminated by death from mesothelioma is $S(t)$. The complete likelihood is the product of such terms over all members of the cohort. The estimate of K_M

obtained by maximizing the logarithm of this likelihood was 7.95×10^{-8} (90% CI: 7.0×10^{-8}, 9.0×10^{-8}).

We consider the exact method of computing K_M to be the most accurate and results from this method are reported in the summary table for mesothelioma (Table 7-9, which is a reproduction of Table A-2). The Quebec and South Carolina data sets were thus evaluated using the exact method. However, it is noteworthy that the two other methods described above, one of which is often applied to published data, give similar estimates of K_M, at least for this data set.

The Quebec cohort was subdivided into three subcohorts, believed to correspond to differing amounts of amphibole exposure due to tremolite contamination of the ore at different mining locations, and to use of some imported commercial amphibole at one factory location (Liddell et al. 1997). Location I consisted of workers at the mine at Asbestos where the ore reportedly had less tremolite contamination. Locations 3 and 4 consisted of workers at the large central mine and at smaller mines, respectively, near Thetford, where the ore was more heavily contaminated with tremolite. Location 2 consisted of workers at an asbestos products factory at Asbestos, which processed some commercial amphibole fibers in addition to chrysotile. The exact method of calculating K_M produced the following estimates: Location 1 (8 cases): $K_M=1.3 \times 10^{-10}$ (90% CI: 0.3×10^{-10}, 4.9×10^{-10}); Location 2 (5 cases): $K_M=9.2 \times 10^{-10}$, (90% CI: 2.0×10^{-10}, 35×10^{-10}); Locations 3 and 4 (22 cases): $K_M=2.1 \times 10^{-10}$ (95% CI: 0.65×10^{-10}, 6.5×10^{-10}).

The relative magnitudes of these estimates track with the relative amounts of amphibole exposure estimated for these locations (Liddell et al. 1997), which is consistent with the hypothesis that the mesothelioma risk in this cohort is due, at least in large measure, to exposure to amphiboles.

There were only two confirmed mesothelioma deaths in the South Carolina cohort and four additional suspected deaths. These were too few to permit detailed analysis. Based on both confirmed and suspected mesothelioma deaths, the exact method of analysis gave an estimate of $K_M=0.43 \times 10^{-8}$, 90% CI: (0.20×10^{-8}, 0.79×10^{-8}). Using only the two confirmed mesotheliomas, the same analysis yielded $K_M=0.14 \times 10^{-8}$, 90% CI: (0.034×10^{-8}, 0.38×10^{-8}). Very similar estimates were obtained by estimating K_M from data categorized by time since first exposure and fitting a linear model to the categorized value of the integral in the definition of the U.S. EPA model. Thus, for this cohort comparable K_M values are estimated no matter which of the three methods described above are used for fitting the U.S. EPA mesothelioma model to the epidemiology data.

Table 7-9. Mesothelimoa Exposure-Response Coefficients (K_M) Derived from Various Epidemiological Studies

Fiber Type	Operation	Cohort	EPA (1986) K_M*100	Reference	This Update K_M*100	90% Confidence Interval	Uncertainty Interval[a]	Reference
Chrysotile	Mining and Milling	Asbestos, Quebec			0.013	(0.0068, 0.022)	(0.003, 0.049)	Liddell et al. 1997[b]
		Thedford Mines			0.021	(0.014, 0.029)	(0.0065, 0.065)	Liddell et al. 1997[b]
	Friction Products	Connecticut plant			0	(0, 0.12)	(0, 0.65)	McDonald et al. 1984
	Cement Manufacture	New Orleans plant			0.2	–	(0.033, 1.2)	Hughes et al. 1987
	Textiles	South Carolina plant			0.25	(0.034, 0.79)	(0.023, 1.2)	Dement et al. 1994[c]
					0.088	(0.0093, 0.32)	(0.0025, 1.2)	McDonald et al. 1983a
Crocidolile	Mining and Milling	Wittenoom			7.9	(7, 9)	(3.5, 18)	de Klerk et al. 1994[d]
Amosite	Insulation Manufacture	Patterson, NJ factory	3.2	Seidman 1984	3.9	(2.6, 5.7)	(0.74, 20)	Seidman et al. 1986
Mixed	Cement Manufacture	Ontario factory	12	Finkelstein 1983	18	(13, 24)	(2, 160)	Finkelstein 1984
		New Orleans plant			0.3	–	(0.089, 1)	Hughes et al. 1987
	Factory Workers	Asbestos, Quebec			0.092	(0.04, 0.18)	(0.018, 0.39)	Liddell et al. 1997[b]
	Insulation Application	U.S. insulation workers	1.5	Seilkoff et al. 1979	1.3	(1.2, 1.4)	(0.25, 6.5)	Seilkoff and Seidman 1991
	Textiles	Pennsylvania plant			1.1	(0.76, 1.5)	(0.17, 6.6)	McDonald et al. 1983b
		Rochedale plant	1	Peto 1980; Peto et al. 1982	1.3	(0.74, 2.1)	(0.28, 5.6)	Peto et al. 1985

[a]Uncertainty Interval formed by combining 90% confidence interval with uncertainty factors in Table A-3.
[b]With supplemental raw data from Liddell
[c]With supplemental raw data from Terri Schnorr (NIOSH) with Dement
dWith supplemental unpublished raw data with follow-up through 2001

7.3.1.1 Time Dependence

The U.S. EPA mesothelioma model (Equation 7-6 or 7-7) was next evaluated to determine whether it adequately describes the time-dependence of mesothelioma mortality following cessation of exposure in the Wittenoom and Quebec cohorts. The small number of mesotheliomas observed among the South Carolina cohort precluded a meaningful evaluation of this issue for that cohort.

For times since first exposure longer than 10 years past the end of exposure the mesothelioma model (Equation 7-6) can be rewritten as

$$I_M = 3 * KM * f * d * (t - 10)^2 * \{1 - 3 * [d / (t - 10)] + [d / (t - 10)]^2 \} \qquad \text{(Eq. 7-8)}$$

From this expression we see that, when time since first exposure lagged 10 years, (t–10), is large compared to duration of exposure, (d), the model predicts that the mesothelioma mortality rate is approximately proportional to the product of cumulative exposure (the exposure level, f, (f/ml) times the duration of exposure, (d) and the square of time since first exposure lagged 10 years. Thus, the model predicts that the mesothelioma mortality will increase indefinitely with age as the square of time since first exposure lagged 10 years. The availability of raw data from the Wittenoom and Quebec cohorts provides an opportunity to evaluate this assumption.

Table 7-10 shows the fit of the U.S. EPA mesothelioma model to Wittenoom data characterized by time since last exposure, based on the K_M estimated from the exact analysis. There is no indication from this table that the mesothelioma mortality rate declines after the cessation of exposure, or that the model over-predicts the mesothelioma risk at long times after the cessation of exposure. In fact, the model under-predicts the number of deaths at the longest times, as it predicts 76.8 deaths after 30 years from the end of exposure, whereas 96 were observed.

Table 7-11 shows the observed number of mesothelioma deaths in the three separate locations at Quebec, categorized by time since last exposure, and compared with the predicted numbers obtained using the K_M values obtained using the exact fitting method. From all three locations combined the model predicts 10.6 deaths from mesothelioma after more than 30 years following the cessation of exposure, whereas 10 were observed. Although the small numbers of mesotheliomas make it difficult to draw definite conclusions about the adequacy of the model, there is little evidence that the model under or over-predicts the numbers of mesotheliomas at long periods after the end of exposure.

7.3.1.2 Exposure Dependence

The lack of fit of the mesothelioma model (Equations 7-7 and 7-8) to the Wittenoom data categorized by the value of the integral in Equation 7-8 (Table 7-8) suggests that the Wittenoom data may not be consistent with the assumption that the mortality rate is linear in the intensity of exposure (f/ml). Specifically, the mesothelioma model predicts that for fixed time since first exposure and duration of exposure the mesothelioma mortality rate varies linearly with f, the asbestos air concentration. To test this prediction, expected numbers of mesothelioma deaths were calculated for each of four categories of asbestos air concentrations while controlling for

both time since first exposure and duration of exposure.[4] Person-years in the first 10 years following the beginning of exposure were ignored since no mesothelioma deaths occurred in this time interval, as predicted by the model. The relatively few workers who were employed for longer than 5 years were also excluded from this analysis (exposure durations were generally quite short in this cohort, with the average employment duration being <1 year), which means that all follow-up in this analysis occurred after exposure had ended. Results of this analysis are shown in Table 7-12.

Table 7-10. Fit of EPA Mesothelioma Model to Observed Mesothelioma Mortality Among Wittenoom, Australia Miners (Deklerk 2001) Categorized by Years Since Last Exposure

Years Since Last Exposure		Average Value of Integral	Observed Deaths	Predicted Deaths by Model	Observed/ Predicted
Range	Average				
0–1	0.3	35	0	0	0
1–5	3	72	0	0.1	0
5–10	7.5	327	0	0.6	0
10–20	14.9	4025	10	14.4	0.7
20–30	24.7	18058	58	52.9	1.1
30–40	34	39802	79	61.3	1.3
40+	43.6	57952	17	15.5	1.1
30+			96	76.8	1.3
Total			164	144.9	
			Goodness of Fit P-value		0.21

[4]In this analysis the Wittenoom data were categorized by time since first exposure (10–20, 20–30, 30–40, and 40+ years), exposure intensity (0–15, 15–30, 30–60, and 60+ f/ml), and duration of exposure (0–1 and 1+ years). This categorization was facilitated by the facts that in the subcohort being analyzed, exposure had ended prior to the beginning of follow-up, and in the Wittenoom data base exposure intensity was assumed to be constant throughout employment. Within each of the eight [time since first exposure] x [duration of exposure] categories the total number of mesothelioma deaths were allocated to the various exposure intensity sub-categories in proportion to the product of the average exposure intensity times the person-years of observation in each sub-category, thereby producing the expected number of deaths in each sub-category under the assumption that the response was linear in exposure intensity within each [time since first exposure] x [duration of exposure] category, as predicted by the mesothelioma model. These expected deaths and the corresponding numbers of observed deaths were summed across time-since-first-exposure and duration categories to yield observed and expected deaths categorized only by exposure intensity

Table 7-11. Fit of EPA Mesothelioma Model to Observed Mesothelioma Mortality Among Quebec Miners (Liddell 2001) in Each of Three Mining Areas, Categorized by Years Since Last Exposure

Years Since Last Exposure	Average Value of Integral	Person-Years	Observed Deaths	Predicted Deaths by Model	K_M
Location 1					
0–10	94,267.5	77,008	3	3.1	1.34×10^{-10}
10–20	119,190	27,225	2	1.4	
20–30	119,971	22,831	0	1.2	
30–40	181,470	18,321	1	1.4	
40–50	278,118	11,846	2	1.4	
50+	339,160	6,673	0	1.0	
30+			3	3.7	
Total			8	9.3	
Location 2					
0–10	56,377.5	15,065	0	2.5	9.55×10^{-10}
10–20	56,445.7	4,835	2	0.8	
20–30	58,307.7	3,991	0	0.7	
30–40	78,685.8	3,129	2	0.7	
40–50	88,541.2	1,844	0	0.5	
50+	59,590.4	795	1	0.1	
30+			3	1.4	
Total			5	5.4	
Locations 3 and 4					
0–10	194,913	95,299	13	12.7	2.18×10^{-10}
10–20	262,898	23,885	5	4.3	
20–30	179,052	18,777	0	2.3	
30–40	251,766	14,311	0	2.5	
40–50	348,264	8,800	1	2.1	
50+	298,743	4,451	3	0.9	
30+			4	5.5	
Total			22	24.8	

Table 7.12. Comparison of Wittenoom, Australia (DeKlerk 2001) Mesothelioma Deaths to Predicted Deaths Assuming Risk Varies Linearly with Exposure Intensity After Controlling for Years Since First Exposure and Duration of Exposure

Intensity (f/ml)		Mesothelioma Deaths		
Range	Average	Person-Years	Observed	Predicted
0–15	9.7	50,736	32	19.5
15–30	17.0	23,881	51	22.4
30–60	50.3	18,166	27	41.9
>60	100.2	13,353	40	66.3
Total			150	150.0
		Goodness of Fit P-value		<0.0001

Table 7-12 shows that the assumption that the mesothelioma risk varies linearly with exposure intensity leads to a 2-fold under-prediction of risks for exposure intensities below 60 f/ml (83 deaths compared to only 41.8 predicted) and a corresponding over-prediction for exposure intensities above 60 f/ml (only 67 deaths compared to 108.2 predicted). Thus, instead of risk varying linearly with exposure intensity, Table 7-12 indicates that the exposure response is supra-linear, with lower fiber intensities being more potent per f/ml.

7.3.1.3 Discussion of Adequacy of Mesothelioma Model

The mesothelioma model (Equations 7-6 and 7-7) provides adequate fits to each of the three data sets evaluated (Wittenoom, Quebec and South Carolina) when the data are categorized by time since first exposure. The value of K_M estimated from the cohort of crocidolite miners (Wittenoom) was largest and was about 60-fold larger than the K_M estimated from the South Carolina chrysotile textile workers (based only on confirmed mesotheliomas in South Carolina) and more than 100-fold larger than the estimates obtained from the Quebec chrysotile miners who did not work in the factory that utilized crocidolite. This is consistent with numerous indications from the literature that crocidolite is more potent than chrysotile in causing mesothelioma. The relative magnitudes of the K_M for the Quebec data estimated from three locations track with the relative amounts of amphibole exposure estimated for these locations, which is also consistent with the hypothesis that the mesothelioma risk is greater from amphibole exposure than from chrysotile exposure. Despite the very few mesotheliomas in the South Carolina cohort, the K_M estimated from these data is larger than those from Quebec, although the discrepancy is not as large as estimated for lung cancer.

The Wittenoom and Quebec data were evaluated further to see if they were consistent with the prediction of the mesothelioma model that risk continues to increase indefinitely after exposure has ceased. By comparing the observed number of mesothelioma deaths to the number predicted by the mesothelioma model at various times since the cessation of exposure, no evidence was found that mesothelioma risk dropped off below that predicted by the model, at least up to 40 to 50 years after the cessation of exposure. To the contrary, in Wittenoom there was some evidence that the model under-predicted at the longest times since the end of exposure, as past 30 years

from the cessation of exposure there were 96 observed mesothelioma deaths compared to only 76.8 predicted by the model.

Chrysotile is much more soluble than crocidolite and consequently a chrysotile fiber exhibits a much shorter residence time in the body than a comparable-sized crocidolite fiber. Based on *in vitro* studies a chrysotile fiber with a diameter of 1 μm will dissolve in body fluid in approximately 1 year whereas a 1-μm crocidolite fiber will take 60 years to dissolve (see Section 6.2.4). It is noteworthy that despite the short residence time of chrysotile fibers, mesotheliomas deaths have occurred in the Quebec cohort more than 50 years following the cessation of exposure. This suggests that either these mesotheliomas are the result of amphibole contamination of the ore, or else long residence times for inhaled fibers are not necessary for the production of mesotheliomas.

The mesothelioma model predicts that risk is proportional to the intensity of exposure (Equation 7-6) and, at long times past the end of exposure, to cumulative exposure (Equation 7-8). Two analyses of the Wittenoom mesothelioma data suggest that the assumption of a linear exposure-response may not be valid. First, whereas the model is linear in the value of the integral in Equation 7-7, a very poor fit was obtained when the data were categorized according to the value of the integral (Table 7-8). Second, an analysis that categorized the data by intensity of exposure, while controlling for both duration of exposure and time since last exposure, also provided a poor fit (Table 7-12). Both of these analyses exhibit a supra-linear exposure-response in which less intense lower exposures are more potent per f/ml than more intense ones.

In light of these findings, it is interesting that supra-linearity in the exposure-response relationship for lung cancer has also been suggested by fits of data in several studies (see Section 7.2.1.1). Although the effects for lung cancer are difficult to separate from the confounding effects from smoking, common suggestions of supra linearity for both disease endpoints certainly indicate a need to evaluate the nature of the exposure-response models for asbestos in greater detail. This is consistent with the recommendations of the expert panel (Appendix B) that evaluation of a broader range of exposure-response models for mesothelioma is appropriate.

This analysis of the Wittenoom data appear to be one of very few that provide information on the shape of the exposure-response relationship for mesothelioma. It is possible that systematic errors in the exposure data for Wittenoom could have resulted in an apparent supra-linear exposure response. Like most asbestos-exposed cohorts, the estimated exposures for Wittenoom are uncertain. If higher estimated intensities are overestimates, a linear exposure response would appear to be supra-linear, and a linear fit to such data would underestimate the true K_M.

In addition, errors in exposure measurement even if unbiased, can tend to make a linear dose-response appear supra-linear (Crump 2003). Even if the supra-linear exposure response in the Wittenoom data is real, the exposure-response at lower doses is likely to be linear, but with a larger K_M value than was obtained in the fit to the complete data set. If this is the case, our analysis (Table 7-12) suggests that the K_M for the lower exposures is about a factor of two larger than the value estimated from the complete cohort. A factor of 2 is not extremely large compared to the other sources of uncertainty in the analysis. Provisionally, the value of K_M estimated from the complete Wittnoom cohort will be applied in our analysis. In revisions to this

document, it will be important to attempt to evaluate the exposure-response for mesothelioma using data from additional other cohorts.

Given the importance of these two issues: (1) the relative potencies of chrysotile and the amphiboles and (2) the adequacy of U.S. EPA models for predicting the time and exposure dependence of disease, limited analysis of raw data from a small number of additional cohorts is warranted. Recommendations for further research along these lines are discussed in the conclusions to this Chapter (Section 7.6) and parallel the recommendations of the expert panel (Appendix B).

7.3.2 Estimating K_M Values from Published Epidemiology Studies

At the time that the Health Effects Update was published (U.S. EPA 1986), four studies were found to provide suitable quantitative data for estimating a value for K_M and six additional studies provided corroborative support for the mesothelioma model applied. Currently, there are 14 published studies with adequate data for deriving an estimate of K_M (including updates to all four of the quantitative studies evaluated in 1986).

The U.S. EPA mesothelioma model (Equations 7-6 and 7-7) was applied to each of these data sets to obtain study-specific estimates for the mesothelioma dose-response coefficient, K_M. The resulting set of K_M values are presented in Table 7-9. The format for this table is identical to that described in Section 7.2.2 for Table 7-6. As with the K_L values in Table 7-6, the K_M values for all studies presented in Table 7-9 (including those studies that have not been updated since their inclusion in the 1986 Health Effects Update) were re-derived using the modified procedures described in Appendix A. Uncertainty intervals in Table 7-9 for each estimated K_M were derived using the method described in Appendix A.

As Table 7-9 indicates, the K_M values derived in this study and the corresponding values derived in the original 1986 Health Effects Update are in close agreement, none vary by more than a factor of 1.5. Among the K_M values derived in the current study, the lowest and highest of the best-estimate values differ by a factor of approximately 1,400 (excluding the one negative study of Connecticut friction product manufacturers) and many of the pair-wise sets of uncertainty intervals do not overlap. For example, none of the uncertainty intervals for the K_M values derived for any of the environments involving exposure to chrysotile overlap the uncertainty intervals associated with the K_M values derived for either crocidolite mining or asbestos-cement manufacture using mixed fibers at the Ontario plant (Finkelstein 1984). Furthermore, neither of the uncertainty intervals for the K_M values derived for chrysotile mines in Quebec (Asbestos and Thetford) overlap the intervals around K_M values for any of the amphibole environments or any of the mixed environments, except the Quebec factory that is associated with the Asbestos mine (Liddell et al. 1997).

The K_M values and the associated uncertainty bounds derived in the current study are plotted in Figure 7-2. Each exposure environment is plotted along the X-axis of the figure and is labeled with a 4-digit code that indicates fiber type (chrysotile, mixed, crocidolite, or tremolite), industry (mining, friction products, asbestos-cement pipe, textiles, insulation manufacturing, or insulation application); and a 2-digit numeric code indicating the study from which the data were derived.

The key for Figure 7-1 also applies to this figure. In Figure 7-2, the chrysotile studies are grouped on the left, amphibole studies are grouped on the right, and mixed studies are in the middle. As in Figure 7-1, data from the Dement et al. (1994) study are used to represent the South Carolina textile cohort and data from the Amandus and Wheeler (1987) are used to represent the Libby mine cohort in Figure 7-2. Also, the estimated K_M values for the Quebec miners (Liddell raw data) from Asbestos and Thetford Mines, respectively, are averaged in this figure.

Figure 7-2:
Plot of Estimated K_M Values and Associated Uncertainty Intervals by Study Environment

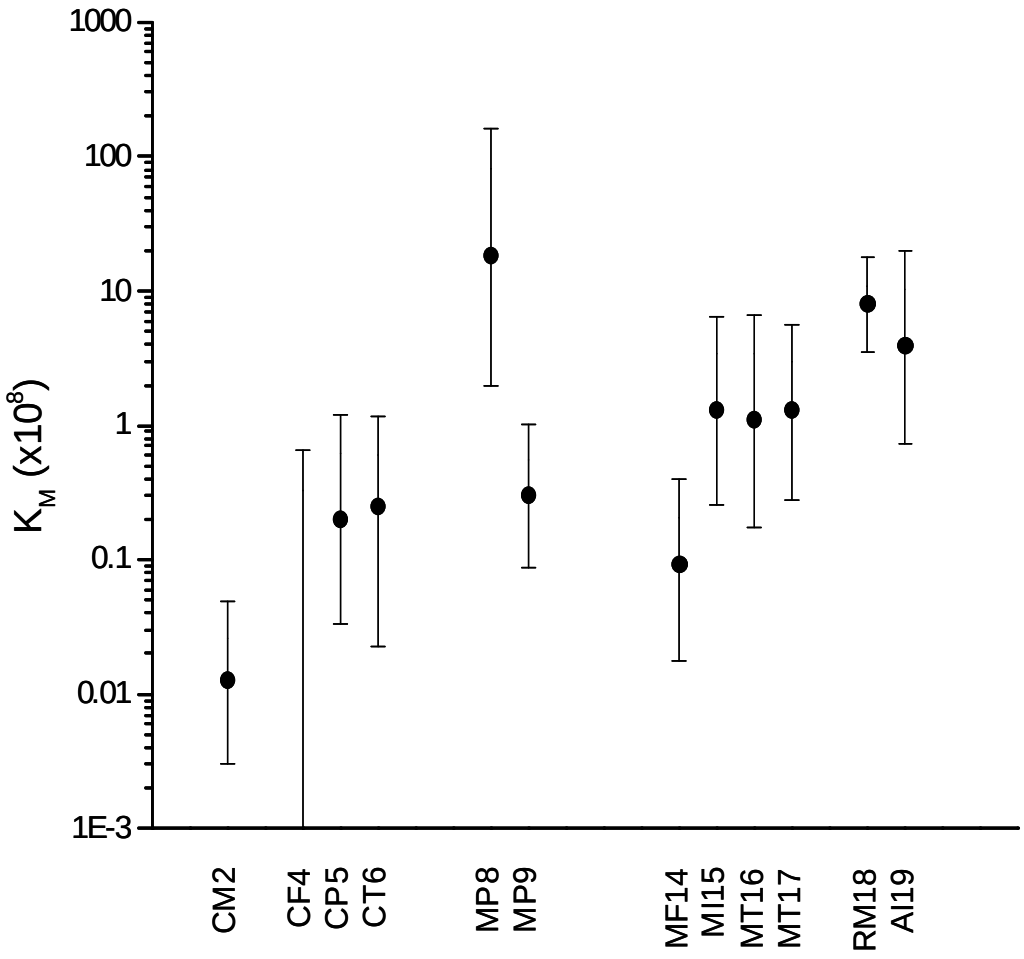

Figure 7-2 indicates that, within chrysotile studies alone, lowest and highest K_M values vary by approximately a factor of 15 (excluding the negative friction products study), which is minimal variation relative to the spread across the values from all of the studies in the table. Also, the corresponding uncertainty intervals have considerable overlap.

The K_M values for the two "pure" amphibole studies (crocidolite mining and amosite manufacturing) agree to within a factor of 2 and, with the exception of the value from the Ontario asbestos-cement plant (MP8 in Figure 7-2 and the ninth study listed in Table 7-9) and the factory plant associated with the Asbestos, Quebec mines (MF14 in Figure 7-2 and the 11th study listed in Table 7-9), the mixed exposure K_M values lie between the high values for the "pure" amphibole exposures and the lower values reported for all of the chrysotile sites. Although the K_M value for the asbestos-cement plant (MP8) appears high, its corresponding uncertainty interval overlaps those of the other "pure" amphibole studies as well as those of a number of the other mixed exposures. The K_M value reported for the factory associated with the Asbestos, Quebec mine (MF14) is the lowest of those reported for mixed exposures, but its uncertainty interval overlaps those for several of the other mixed exposures, as well as all of those involving only chrysotile exposures.

As with K_L values, the asbestos-cement pipe industry shows the greatest variation in K_M values across all asbestos types, with a range of more than a factor of 90. Moreover, the uncertainty intervals for the largest and smallest values in this industry do not overlap. Within the textile industry, the K_M value for the South Carolina chrysotile plant is only an eighth of the values reported for the two textile plants using mixed fibers, although there is considerable overlap in their uncertainty intervals. The potential sources of variation across all of the K_M values are likely attributable to the same sources of variation identified for the K_L values and previously described in detail (Section 7.22).

7.4 EVALUATION OF ASBESTOS EXPOSURE INDICES

As indicated in Chapter 3, for exposure-response coefficients derived from one environment to be applicable in a different environment requires that both of the following two conditions be satisfied:

- that asbestos be measured in both environments in an identical manner; and
- that such measurements reflect (or at least remain proportional to) the characteristics of asbestos exposure that determine biological activity.

When these two conditions are met, it is possible to define an "exposure index" that accurately reflects biological activity, and consequently an exposure-response coefficient based upon such an exposure index derived in one environment can confidently be applied in a different environment. Such an index can be defined as a weighted sum of concentrations of categories of structures of different asbestos types and sizes, where the weights reflect the relative carcinogenic potencies of the different type and size categories. For example, as described in Section 6.4.3, Berman et al. (1995) derived an optimal exposure index from an analysis of rat inhalation studies involving exposures to different types of asbestos and fibrous structures of differing dimensions. The optimum index (defined in Equation 6-11) consists of a weighted sum

of the air concentrations of structures between 5 and 40 μm in length and >40 μm in length (all thinner than 0.4 μm).

There is considerable evidence that the manner in which asbestos is quantified in the available epidemiology studies (i.e., PCM) may not adequately reflect the characteristics that relate to biological activity (Sections 6.4 and 6.5). Therefore, the second of the above two criteria may not be satisfied when exposure-response coefficients (i.e., K_L and K_M values) derived from these studies are used to predict risk in new environments. We therefore investigated the possibility of adjusting the K_L and K_M values so as to apply to a measure of exposure that better reflects biological activity. Such an adjustment requires both (1) data from each studied environment on fiber size and asbestos type needed to adjust the corresponding K_L and K_M and (2) evidence regarding what measure of exposure better reflects biological activity.

7.4.1 Fiber Type and Size Distribution Data Available for Deriving Exposure Indices

Since the range of possible adjustments to the K_L and K_M values is constrained by the data on fiber size and type available from each studied environment, we first consider the characteristics of the data currently available for making such adjustments. The data considered to be pertinent consisted of TEM analyses of samples conducted in the same environment in which an epidemiological study was conducted or from an environment involving a similar operation (e.g., mining, textile manufacture, etc.). Table 7-13 lists available fiber size distributions obtained from a search of the literature and categorized by fiber type and type of operation. The epidemiological studies from which K_L or K_M have been calculated are categorized accordingly.

Assuming that the available TEM size distributions are representative of dust characteristics for the exposure settings (industries) studied, these were paired with corresponding epidemiology studies. The TEM size distributions were then used to convert the exposure measurements used in the epidemiology studies to the new exposure index that potentially better reflects biological activity. Studies were paired as indicated in Table 7-13.

Only a subset of the TEM size distributions listed in Table 7-13 were actually employed in the effort to normalize K_L and K_M values. To minimize variability resulting from differences in TEM analysis methodology employed by different authors, it was decided to employ distributions from common studies conducted by common groups of researchers, to the extent that this could be accomplished without reducing the number of “size-distribution-epidemiological study” pairs available for inclusion in the analysis. Also, studies containing the best documented procedures were favored. Ultimately, with one exception the size distributions selected for use came from only two studies, which were reported in three publications: Dement and Harris (1979), Gibbs and Hwang (1980), and Hwang and Gibbs (1981). In the case of the one exception, size distributions for Libby (tremolite asbestos in vermiculite) were derived from unpublished TEM data recently acquired directly from the site.

Table 7-13. Correlation Between Published Quantitative Epidemiology Studies and Available Tem Fiber Size Distributions

Fiber Type	Exposure Setting	Distribution Reference	Epidemiology Reference
Chrysotile	Textiles	Dement and Harris 1979	Dement et al. 1994, 1983b
		Cherrie et al. 1979	McDonald et al. 1983a,b
			Peto 1980a; Peto et al. 1985
	Friction Products	Dement and Harris 1979	Berry and Newhouse 1983
		Marconi et al. 1984	McDonald et al. 1984
		Winer and Cossett 1979	
		Roberts and Zumwalde 1982	
		Rood and Scott 1989	
	Mining and Milling	Gibbs and Hwang 1980	Liddell et al. 1997
		Winer and Cossett 1979	McDonald et al. 1980b
			Nicholson et al. 1979
			Piolatto et al. 1990
	Asbestos Cement Manufacturing	Dement and Harris 1979	Hughs et al. 1987
		Snyder et al. 1987	
		Winer and Cossett 1979	
Chrysotile and Crocidolite	Asbestos Cement Manufacturing	Hwang and Gibbs 1981	Finkelstein 1984
			Finkelstein 1983
			Hughs et al. 1987
			Weill et al. 1979
			Weill et al. 1994
			Albin et al. 1990
Crocidolite	Mining and Milling	Gibbs and Hwang 1980	Armstrong et al. 1988
		Hwang and Gibbs 1981	de Klerk, unpublished data
Amosite	Insulation Manufacturing	Dement and Harris 1979	Levin et al. 1998
			Seidman et al. 1986
			Seidman 1984
	Insulation Application		Selikoff et al. 1979
	Insulation Clearance	Snyder et al. 1987	
		Cherrie et al. 1979	
Tremolite	Vermiculite Mining	U.S. EPA, unpublished	McDonald et al. 1986
			Amandus and Wheeler 1987

Table 7-14 presents the resulting bivariate fiber size distributions derived from the published TEM data that are paired with representative K_L and K_M values from the corresponding epidemiology studies. This table shows 17 K_L values and 11 K_M values matched with a fiber size distribution from the literature. In this table some length and width categories from some published distributions have been combined, so that, for the most part, only those categories available for all of the epidemiological studies are presented. The column labeled "PCME" ("PCM-equivalent") provides the relative concentrations of asbestos fibers that would have been identified by PCM ($\geq$5 µm in length and $\geq$0.2 µm in width).

The fiber size distributions in Table 7-14 are not all of equal relevance to the respective epidemiological studies to which they were paired. As indicated in Table 7-15, some of the distributions are based on data collected at the same facility, others are based on data collected at a similar facility, still others are based on a combination of data from similar facilities, etc. The uncertainty factors listed in Table 7-15 were developed to quantify the relevance of each fiber size distribution to its paired epidemiological study, where larger factors indicate a less certain relevance. How these factors were used is explained below. It should also be kept in mind that, whereas these fiber distributions were based on air samples collected over a fairly narrow time range, they are used to represent the fiber size distributions throughout the exposure period, which in most of the epidemiological studies covers many years.

As indicated in Tables 7-14 and 7-15, for the two environments for which multiple studies were available (i.e., the South Carolina textile plant and the Libby, Montana vermiculite mine), a single study was selected to represent each environment. For the South Carolina textile plant the Dement et al. (1994) study was selected and for Libby, the Amandus and Wheeler (1987) study was selected.

7.4.2 Modification of Existing K_L and K_M to Conform to a New Exposure Index

The fiber size distribution data in Table 7-14 are used to transform the existing K_L and K_M values (which are defined in terms of PCM measurements) so they conform to a different exposure index based on TEM. To see how this is accomplished, consider a K_L value pertaining to a specific environment, let C_{PCM} be an air concentration from that environment measured by PCM, let C_{new} be the concentration in the same air measured by a new exposure index using TEM (e.g., perhaps defined as a weighted sum of TEM concentrations in various length, width and asbestos type categories), and let K_L* be the adjusted exposure-response coefficient corresponding to the new exposure index. It is clear that for the U.S. EPA lung cancer model (Equation 7-1 or 7-2) to estimate the same risk from the given air concentration using either exposure index, it is necessary that

$$(K_L)\,(C_{PCM}) = (K_L^*)\,(C_{NEW}) \qquad \text{(Eq. 7-9)}$$

Using C_{PCME} (the air concentration of PCM-equivalent fibers - fibers measured by TEM that would be identified by PCM) as a replacement for C_{PCM}, we get

$$K_L^* = K_L\,(C_{PCME} / C_{NEW}) \qquad \text{(Eq. 7-10)}$$

Table 7-14. Representative KL and KM Values Paired with Averaged TEM Fiber Size Distributions From Published Papers

Environment	Study Code	K_L (x100)	K_M (x108)	PCME	Size Distributions																		Size Reference	Adjusted	
					w<0.2 L<5	5<L<10	10<L	w<0.3 L<5	5<L<10	10<L	w<0.4 L<5	5<L<10	10<L	w>0.3 L <5	5<L<10	10<L	w>0.4 L <5	5<L<10	10<L	Total L<5	5<L<10	10<L		K_L (x100)	K_M ($x10^8$)
Quebec mines and mills	CM1	0.029	–	00.14	0.93545	0.00955	0.0023	0.954	0.0113	0.0031	–	0.01322	0.00372	0.0189	0.00915	0.0023	(0.4 Not available in dist)			0.9729	0.02045	0.0054	G&H 1980	0.11	–
Quebec mines	CM2	–	0.0165	0.014	0.93545	0.00955	0.0023	0.954	0.0113	0.0031	–	0.01322	0.00372	0.0189	0.00915	0.0023	(0.4 Not Available in dist)			0.9729	0.02045	0.0054	G&H 1980	–	0.1
Italian mine and mill	CM3	0.051	–	0.014	0.93545	0.00955	0.0023	0.954	0.0113	0.0031	–	0.01322	0.00372	0.0189	0.00915	0.0023	(0.4 Not available in dist)			0.9729	0.02045	0.0054	G&H 1980	0.19	–
Connecticut plant	CF4	0	0	0.07235	0.76359	0.02613	0.01874	0.82804	0.03428	0.02706	0.84938	0.03902	0.03123	0.05473	0.02021	0.03569	0.03339	0.01546	0.03152	0.8877	0.05448	0.06275	D&H 1979	0	0
New Orleans plants	CP5	0.25	0.2	0.05071	0.77469	0.02283	0.01574	0.85992	0.03069	0.02043	0.88663	0.03676	0.02343	0.05080	0.01767	0.02049	0.02408	0.0116	0.01749	0.91072	0.04836	0.04092	D&H 1979	0.54	0.43
South Carolina plant	CT6	1.6	0.17	0.12963	0.65629	0.03024	0.0271	0.74047	0.04333	0.03983	0.7671	0.04959	0.0488	0.07256	0.03921	0.06461	0.04593	0.03294	0.05564	0.81303	0.08253	0.10443	D&H 1979	4.3	0.45
Wittenoom, Australia	RM18	0.47	7.9	0.01167	0.89017	0.02657	0.00503	0.93773	0.03303	0.00617	0.95043	0.0351	0.0063	0.01893	0.00357	0.0005	0.00623	0.0015	0.00037	0.95667	0.0366	0.00667	H&G 1981	0.88	15
Patterson, NJ factory	AI19	1.1	3.9	0.35198	0.17109	0.02872	0.00717	0.30052	0.06018	0.03099	0.37736	0.09111	0.0526	0.31161	0.13463	0.16207	0.23477	0.1037	0.14046	0.61213	0.19481	0.19306	D&H 1979	7	26
Tyler, Texas factory	AI20	0.13	–	0.35198	0.17109	0.02872	0.00717	0.30052	0.06018	0.03099	0.37736	0.09111	0.0526	0.31161	0.13463	0.16207	0.23477	0.1037	0.14046	0.61213	0.19481	0.19306	D&H 1979	0.87	–
Libby, Montana	TM21	0.45	–	4	Not available in distribution							1	1	Not available in distribution									2001 Libby sampling	1.8	–
British factory	MF7	0.058	–	0.07235	0.76359	0.02613	0.01874	0.82804	0.03428	0.02706	0.84938	0.03902	0.03123	0.05473	0.02021	0.03569	0.03339	0.01546	0.03152	0.88277	0.05448	0.06275	D&H 1979	0.13	
Ontario factory	MP8	0.29	18	0.00755	0.93345	0.01125	0.00155	0.95403	0.01378	0.00215	0.9746	0.0163	0.00275	0.02573	0.00298	0.00145	0.00515	0.00045	0.00085	0.97975	0.01675	0.0036	H&G 1981	0.8	49
New Orleans plants	MP9	0.25	0.3	0.00755	0.93345	0.01125	0.00155	0.95403	0.01378	0.00215	0.9746	0.0163	0.00275	0.02573	0.00298	0.00145	0.00515	0.00045	0.00085	0.97975	0.01675	0.0036	H&G 1981	0.7	0.82
Swedish plant	MP10	0.067		0.00755	0.93345	0.01125	0.00155	0.95403	0.01378	0.00215	0.9746	0.0163	0.00275	0.02573	0.00298	0.00145	0.00515	0.00045	0.00085	0.97975	0.01675	0.0036	H&G 1981	0.18	
Belgium factory	MP11	0.01		0.00755	0.93345	0.01125	0.00155	0.95403	0.01378	0.00215	0.9746	0.0163	0.00275	0.02573	0.00298	0.00145	0.00515	0.00045	0.00085	0.97975	0.01675	0.0036	H&G 1981	0.02	
U.S. retirees	MX13	0.11																							
Asbestos, Quebec	MX14		0.092																						
U.S. insulation workers	MI15	0.18	1.3	0.32751	0.1179	0.02183	0	0.27074	0.06114	0.00437	0.34498	0.08734	0.01747	0.37991	0.1441	0.13974	0.30568	0.1179	0.12664	0.65066	0.20524	0.1441	D&H 1979	3.375	24
Pennsylvania plant	MT16	1.8	1.1	0.12963	0.65629	0.03024	0.0271	0.74047	0.04333	0.03983	0.7671	0.04959	0.0488	0.07256	0.03921	0.06461	0.04593	0.03294	0.05564	0.81303	0.08253	0.10443	D&H 1979	4.8	2.9
Rochedale, England plant	MT17	0.41	1.31	0.12963	0.65629	0.03024	0.0271	0.74047	0.04333	0.03983	0.7671	0.04959	0.0488	0.07256	0.03921	0.06461	0.04593	0.03294	0.05564	0.81303	0.08253	0.10443	D&H 1979	1.1	3.5

Table 7-15. Estimated Uncertainty Assigned to Adjustment for Fiber Size

Study Location	Study Code	Estimated Uncertainty Factor	Explanation	KL Reference	KM Reference
Quebec mines and mills	CM1	1	Location common to epidemiology study and size study	Liddell et al. 1997	
Quebec mines	CM2	1	Location common to epidemiology study and size study		Liddell et al. 1997 (raw data Loc. 1,3,4)
Italian mine and mill	CM3	1.75	Same industry, separate locations for epidemiology and size studies	Piolatto et al. 1990	
Connecticut plant	CF4	1.25	Epidemiology location one of several combined for size study	McDonald et al. 1984	McDonald et al. 1984
New Orleans plants	CP5	1.25	Epidemiology location one of several combined for size study	Hughes et al. 1987	Hughes et al. 1987
South Carolina plant	CT6	1.25	Epidemiology location one of several combined for size study	Dement et al. 1994 (raw data)	Dement 2001 (personal communication)
British factory	MF7	1.5	Same industry, separate locations for epidemiology and size studies	Berry and Newhouse 1983	
Ontario factory	MP8	1.5	Epidemiology location probably one of several combined for size study	Finkelstein 1984	Finkelstein 1984
New Orleans plants	MP9	2	Same industry, separate locations, mixed exposures	Hughes et al. 1987	Hughes et al. 1987
Swedish plant	MP10	2	Same industry, separate locations, mixed exposures	Albin et al. 1990	
Belgium factory	MP11	2	Same industry, separate locations, mixed exposures	Laquet et al. 1980	

Table 7-15. Estimated Uncertainty Assigned to Adjustment for Fiber Size *(continued)*

Study Location	Study Code	Estimated Uncertainty Factor	Explanation	KL Reference	KM Reference
U.S. retirees	MX13			Enterline et al. 1986	
Asbestos, Quebec	MX14				Liddell et al. 1997 (raw data)
U.S. insulation workers	MI15	2	Generally similar industries studied for epidemiology and size	Selikoff and Seidman 1991	Selikoff and Seidman 1991
Pennsylvania plant	MT16	2	Same industry, separate locations, mixed exposures	McDonald et al. 1983b	McDonald et al. 1983b
Rochedale, England plant	MT17	2	Same industry, separate locations, mixed exposures	Peto et al. 1985	Peto et al. 1985
Whitenoom, Australia	RM18	1.75	Same industry, separate locations for epidemiology and size studies	DeKlerk, unpublished data	DeKlerk, unpublished data
Patterson, NJ factory	AI19	1.25	Epidemiology location one of several combined for size study	Seidman et al. 1986	Seidman et al. 1986
Tyler, Texas factory	AI20	1.25	Epidemiology location one of several combined for size study	Levin et al. 1998	
Libby, Montana	TM21	1.75	Extrapolated from limited, marginally associated air data	Amandus and Wheeler 1987	

In the actual calculation of K_L*, this equation is applied with the ratio of air concentrations appearing on the right side of this expression replaced by the equivalent ratio of fiber proportions from Table 7-14.

As an example of the calculation of a K_L*, an earlier draft of this report proposed use of an exposure index defined as the weighted sum,

$$0.997\ C_{L>10;W<0.4} + 0.003\ C_{5<L<10;W<0.4} \qquad \text{(Eq. 7-11)}$$

where $C_{L>10;W<0.4}$ is the air concentration of fibers longer than 10 µm and thinner than 0.4 µm, etc. This index is the same as the optimal index derived from animal data (Berman et al. 1995) except the cutoff for the longest length category is 10 µm, rather than 40 µm. To modify, for example, the K_L=0.0029 value from the Quebec mines and mills environment to conform to the exposure index defined by Equation 7-11, we proceed as follows (using the appropriate data from Table 7-14):

$$K_L^* = 0.0029\ [0.014 / (0.003 * 0.013221 + 0.997 * 0.00372)] = 0.0108.$$

K_M* values are derived from K_M values using an identical procedure.

7.4.3 Derivation of an Improved Exposure Index for Asbestos

Based on an evaluation of the broader literature and the results from a series of supplemental studies (Chapter 6), it appears that the asbestos structures that correlate best with biological activity are almost certainly longer and likely thinner than those measured by PCM. As noted above, Berman et al. (1995) found that an exposure index involving only fibers thinner than 0.4 µm, and giving high weight to fibers longer than 40 µm and no weight to fibers shorter than 5 µm, best reconciled data from a collection of studies in rats. Unfortunately, fiber-size distributions available for adjusting epidemiology data (Table 7-14) cover only a fairly limited number of discrete length and width categories. In particular, the largest cut point for fiber length is only 10 µm. This places a severe restriction upon the extent to which the relative potency of fibers of different lengths can be accommodated in an exposure index designed to reflect biological activity.

Although there is evidence that fiber width plays a role in determining potency, the literature suggests that fiber type and length are more important. An earlier draft of this report, which was reviewed by an expert panel (Appendix B), proposed using the exposure index defined by Equation 7-11 for assessing asbestos risk. Panelists agreed that there is a considerably greater lung cancer and mesothelioma risk attributable to fibers longer than 10 µm. However, the panel was uncertain as to an exact cut size for length and the magnitude of the relative potency. They were also uncertain whether the optimal indices for lung cancer and mesothelioma would precisely conform. Some of the panelists recommended determining the specific weighting (i.e., between longer and shorter fibers) that would optimize the fit of the recommended index (Equation 7-11) to the epidemiological studies. That recommendation was followed in this revised document. To address the previously stated concern, the index was optimized separately for lung cancer and for mesothelioma.

In view of the limitations of the fiber distribution data, it was decided, as an interim measure, to adopt a maximum fiber width of 0.4 μm in the proposed exposure index for both lung cancer and mesothelioma. This is the width indicated by the animal data (Berman et al. 1995). Subject to that decision, we then derived separate exposure index indices for lung cancer and mesothelioma, respectively, that are each optimal (as defined below) with respect to fiber type (chrysotile and amphibole) and fiber length (5–10 μm and >10 μm). Based on results of Berman et al. (1995) and lack of compelling evidence elsewhere in the literature (assuming that size effects are adequately addressed, see Chapter 6), it was assumed that all similarly-sized amphibole fibers are equipotent.

To develop separate potency estimates for chrysotile and amphibole fibers (adjusted for fiber size) it was necessary to estimate the relative amounts of chrysotile and amphibole in each environment. Table 7-16 presents our estimates of the fraction of exposure in each study environment contributed by amphibole asbestos, based on information on each environment available in the literature. The source of the information used to develop each estimate as well as a brief description of how the estimate was developed is also provided.

7.4.3.1 Optimizing the Exposure Index for Lung Cancer

A statistical model was fit to the K_L values in Table 7-14 and results from the fitting were used to estimate separate potencies for amphibole and chrysotile, to estimate relative potencies of fibers of different sizes, and to test certain hypotheses. In this model $Ln(K_L)$ (the log transform of a K_L value in Table 7-14) was assumed to be normally distributed with mean equal to

$$Ln\{K_{La}^* * [f_{amph} + rpc * (1 - f_{amph})] * [q * C_{5\text{-}10} + (1 - q) * C_{>10}] / C_{PCME}\} \qquad \text{(Eq. 7-12)}$$

In this expression $C_{5\text{-}10}$, and $C_{>10}$ are the fractions of fibers among those thinner than 0.4 μm that are between 5 and 10 μm in length or longer than 10 μm, respectively (from Table 7-14), C_{PCME} is the fraction of PCME fibers (also from Table 7-14), and f_{amph} is the fraction of amphiboles estimated for each environment (from Table 7-16). In addition there are four parameters that are estimated by fitting the model to the K_L values:

q – the relative potency of fibers thinner than 0.4 μm and between 5 and 10 μm in length, relative to fibers thinner than 0.4 μm and >10 μm in length;

K_{La}^* – the potency (K_L value) of pure amphibole (based upon the exposure index defined by q);

rpc – the relative potency of chrysotile, relative to amphibole

The fourth parameter, σ, is described below.

Note that the part of Equation 7-12 that is inside the curly brackets is like Equation 7-9 solved for K_L but with an additional term to account for the relative amounts of chrysotile and amphibole.

Table 7-16. Estimated Fraction of Amphiboles in Asbestos Dusts

Study Location	Study Code	Fraction of Amphiboles: Best Estimate (%)	Fraction of Amphiboles: Estimated Range (%)	Source of Estimate	KL Reference	KM reference
Quebec mines and mills	CM1	1	0–4	Sebastien et al. 1986, extrapolated from air data	Liddell et al. 1997	
Quebec mines	CM2	1	0–4	Sebastien et al. 1986, extrapolated from air data		Liddell et al. 1997 (aw data Loc. 1,3,4)
Italian mine and mill	CM3	0.3	0.1–0.5		Piolatto et al. 1990	
Connecticut plant	CF4	0.5	0–2	McDonald et al. 1984, extrapolated from plant history	McDonald et al. 1984	McDonald et al. 1984
New Orleans plants	CP5	1	0–2	Hughs et al. 1987, extrapolated from plant history.	Hughes et al. 1987	Hughes et al. 1987
South Carolina plant	CT6	0.5	0–2	Sebastien et al. 1989 (based on), extrapolated from Quebec source material	Dement et al. 1994 (raw data)	Dement 2001 (personal communication)
British factory	MF7	0.5	0–2	Berry and Newhouse 1983, extrapolated from plant history	Berry and Newhouse 1983	
Ontario factory	MP8	30	10–50	Finkelstein 1984, extrapolated from plant history	Finkelstein 1984	Finkelstein 1984
New Orleans plants	MP9	5	2–15	Hughes et al. 1987, extrapolated from plant history	Hughes et al. 1987	Hughes et al. 1987
Swedish plant	MP10	3	0–6	Albin et al. 1990, extrapolated from plant history	Albin et al. 1990	

Table 7-16. Estimated Fraction of Amphiboles in Asbestos Dusts *(continued)*

Study Location	Study Code	Fraction of Amphiboles: Best Estimate (%)	Fraction of Amphiboles: Estimated Range (%)	Source of Estimate	KL Reference	KM reference
Belgium factory	MF11				Laquet et al. 1980	
U.S. retirees	MX13				Enterline et al. 1986	
Asbestos, Quebec	MX14					Liddell et al. 1997 (raw data)
U.S. insulation workers	MI15	50	25–75	Guess estimate for broad industry	Selikoff and Seidman 1991	Selikoff and Seidman 1991
Pennsylvania plant	MT16	8	3–15	McDonald et al. 1983b, extrapolated from plant history	McDonald et al. 1983b	McDonald et al. 1983b
Rochedale, England plant	MT17	5	2.5–15	Peto et al. 1985, extrapolated from plant history	Peto et al. 1985	Peto et al. 1985
Whitenoom, Australia	RM18	97	95–100	General estimate[a]	DeKlerk, unpublished data	DeKlerk, unpublished data
Patterson, NJ factory	AI19	97	95–100	General estimate[a]	Seidman et al. 1986	Seidman et al. 1986
Tyler, Texas factory	AI20	97	95–100	General estimate[a]	Levin et al. 1998	
Libby, Montana	TM21	95	90–100	General estimate[a]	Amandus and Wheeler 1987	

[a]Allows for the possibility of some foreign material. Practical effect for the analysis is nil. Might just as well assume 100%.

With this formalism, the potency, K_{Lc}*, of pure chrysotile is defined by the product, rpc * K_{La}*. Thus rpc=1 corresponds to equal potency of amphibole and chrysotile and rpc=0 corresponds to chrysotile being non-potent for causing lung cancer. Similarly, q=1 corresponds to fibers between 5 and 10 μm in length having the same potency as fibers longer than 10 μm and q=0 corresponds to such fibers being non-potent for causing lung cancer.

The variance of Ln(K_L) was assumed to be composed of two components. The first component, σ_i, was calculated so as to reflect the uncertainty in the K_L values as reflected by both the uncertainty intervals reported in Table 7-6 and the uncertainty in the relevance of the size distributions applied to each environment, as reported in Table 7-15. Specifically, the upper bound of the uncertainty interval for K_L in Table 7-6 was modified by multiplying it by the uncertainty factor in Table 7-15. This modified upper bound was then divided by the best estimate of K_L from Table 7-6, and then divided by 2.0. The log transform of the result was defined as σ_i. A second component, σ, of the standard deviation, assumed to be constant for all studies, was also estimated. This component may be thought of as representing the uncertainty in the K_L estimate resulting from random variation that is not represented in the σ_i. The overall standard deviation of the Ln(K_L) from the study was assumed to be $(\sigma_i^2+\sigma^2)^{½}$.

Using the model described by Equation 7-12, parameters (q, K_{La}*, rpc, and σ) were estimated by maximum likelihood and likelihood tests were used to test the hypotheses that chrysotile was non-potent (rpc=0) or equally potent (rpc=1) with amphibole (Wilks 1963). Results from the analysis are summarized in Table 7-17. Shaded values in the table indicate parameter values that were fixed rather than estimated for each particular model run. By holding certain parameters fixed, we evaluated the fit of a range of exposure indices, defined as indicated. This table also contains results from a similar analysis of mesothelioma dose-response coefficients (K_M), which are discussed in Section 7.4.3.2.

The results of fitting the model defined by Equation 7-12 to the K_L values in Table 7-14 are shown in the columns of Table 7-17 labeled “Equation 7-12". The first column, labeled “optimized values” contains the resulting parameter estimates and log-likelihood with all four parameters estimated. Note that the estimate of q is q=0. Since q represents the potency of fibers between 5 and 10 μm in length, relative to fibers >10 μm in length (considering only fibers thinner than 0.4 μm), the model predicts that fibers between 5 and 10 μm are non-potent in causing lung cancer.

The estimate of rpc for the optimized model run of Equation 7-12 is rpc=0.266, which predicts that chrysotile is about 25% as potent as amphibole in causing lung cancer (after adjusting for fiber size). The fourth and fifth columns of Table 7-17 contain results of fitting the model with rpc fixed at either rpc=0 or rpc=1 (both with q fixed at q=0). These results are used to conduct likelihood ratio tests of the hypotheses that rpc=0 and rpc=1. The resulting test for rpc=0 is highly significant (p=0.007). Thus, with this formulation the hypothesis that chrysotile is non-potent in causing lung cancer can be rejected. The test for rpc=1 is non-significant (p=0.54),indicating that even though the best estimate is that chrysotile is only one-fourth as potent in causing lung cancer as amphibole, the hypothesis that chrysotile and amphibole are equally potent cannot be rejected.

Table 7-17. Results from Fitting Exposure Indices Defined by Equation 7.12 and Pcme to Lung Cancer and Mesothelioma Exposure-response Coefficients Estimated from Different Environments

Variable	Index Defined by Equation 7.11	Equation 7.12			PCME		
		Optimized Values	RPC=1	RPC=0	Optimized Values	RPC=1	RPC=0
Lung Cancer (N=16)							
RPC	0.267	0.266	1	0	0.469	1	0
$100*(K_{LA})$	2.3	2.34	0.953	15.80	0.48	0.29	4.42
s	1.007	1.004	1.092	1.730	1.050	1.070	1.915
Log-likelihood	-17.1022	-17.0833	-17.2659	-20.6989	-17.3451	-17.6271	-21.8543
q	0.003	0	0	0	NA	NA	NA
Hypothesis tests			H_0: RPC=1 p=0.20	H_0: RPC=0 p=0.001		H_0: RPC=1 p=0.54	H_0: RPC=0 p=0.007
$100*(K_{LC})$	0.61	0.61	0.953	0	0.23	0.29	0
Mesothelioma (N=11)							
RPC	0.0013	0.0013	1	0	0.0033	1	0
$10^8*(K_{MA})$	26.78	26.99	2.54	28.8	7.69	0.737	8.87
s	0.6062	0.6038	1.903	0.6099	0.7605	1.805	0.7782
Log-likelihood	-9.33248	-9.31812	-16.7403	-9.35267	-10.4599	-16.16	-10.5931
q	0.003	0	0	0	NA	NA	NA
Hypothesis tests			H_0: RPC=1 p=0.0007	H_0: RPC=0 p=0.61		H_0: RPC=1 p=0.0001	H_0: RPC=0 p=0.79
$10^8*K_{MC})$	0.035	0.035	2.54	0	0.025	0.74	0

Notes: Shaded areas indicate values that were fixed in advance of the analyses.

"NA" means not applicable.

Also shown in Table 7-17 are the results of applying the exposure index proposed in the earlier draft of this report (Equation 7-11). This index assigns a small relative potency of 0.003 to fibers between 5 and 10 μm in length, compared to the fully optimized model, which, as noted above, assigns zero potency to these fibers. Table 7-17 indicates that both the quality of fit (by comparison of likelihoods) and the resulting parameter estimates are virtually identical. Accordingly, unless the ratio of fibers between 5 and 10 μm in length to those longer than 10 μm (among those thinner than 0.4 μm) in an environment is extremely large (e.g., >300-fold), the two indices will provide practically equivalent results.

As previously indicated, the current approach for estimating asbestos-related risk (U.S. EPA 1986) uses (effectively) PCME as the exposure index. To allow comparison with this approach, analyses were also conducted using PCME as the exposure index, rather than the size range of fibers considered heretofore (i.e., Equation 7-12 was simplified to $Ln\{K_{La}^* * [f_{amph} + rpc * (1 - f_{amph})]\}$). Results of this analysis are shown on the right side of Table 7-17. With this exposure index, the best estimate is that chrysotile is about one-half as potent as amphibole, the hypothesis that chrysotile is non-potent can be rejected (p=0.001), and the hypothesis that chrysotile and amphibole are equally potent cannot be rejected (p=0.20).

Based upon a comparison of either the residual variance, σ, or the likelihood, it appears that the exposure index defined by fibers longer than 10 μm and thinner than 0.4 μm (corresponding to q=0 in Table 7-17) provides at most a very marginal improvement in fit over use of PCME as the exposure index for lung cancer when rpc is held at 1. Similarly, adjusting for fiber type but not size (i.e., optimizing rpc to reflect separate potencies for chrysotile and the amphiboles) also provides at best a marginal improvement over the current approach (PCME with rpc=1). However, when the exposure index is adjusted for both fiber size and type, (comparing the optimized values for Equation 7-12 to PCME with rpc=1), a small improvement is apparent. The log-likelihood increases by half a unit and the spread in the estimated K_L values (represented by σ) decreases by about 7%. Moreover, as discussed in the following section, the improvement for mesothelioma is substantial..

In addition to the analyses reported in Table 7-17, other analyses were conducted in which an additional term was added to the linear combination of fiber lengths appearing in Equation 7-12 to represent fibers shorter than 5 μm (still considering only fibers thinner than 0.4 μm). In this analysis, the best estimate of both the potencies of fibers shorter than 5 μm, and between 5 and 10 μm in length, was zero.

Discussion of the results from the analysis of the mesothelioma values (also presented in Table 7-17) is provided in Section 7.4.3.2. Based on this analysis and the rest of the evaluation described in this chapter, a recommended set of lung cancer and mesothelioma exposure-response coefficients is presented in Section 7.5.

7.4.3.2 Optimizing the Exposure Index for Mesothelioma

Concomitant with the analysis reported in Section 7.4.3.1 regarding development and evaluation of an improved exposure index for lung cancer exposure-response coefficients (K_L values) that correlates better with biological activity, a parallel analysis was performed for the mesothelioma exposure-response coefficients (K_M values) presented in Table 7-14. This table presents data from 11 environments in which K_M values are paired with fiber size distribution data. The corresponding uncertainty intervals for these 11 K_M values are provided in Table 7-9. The same relationship defined by Equation 7-9 was used to adjust these K_M values to a different exposure index and the same statistical model (Equation 7-12) was applied both to evaluate different adjustments and to develop an adjustment that was optimal for the available data. The results of this analysis of K_M values are presented in the bottom half of Table 7-17, which also contains the results of the comparable analysis of K_L values.

The results of fitting the model defined by Equation 7-12 to the K_M values in Table 7-14 are shown in the columns of Table 7-17 labeled “Equation 7-12". The first of these columns, labeled “optimized values” contains the resulting parameter estimates and log-likelihood with all four parameters estimated. Just as was the case with the analysis of K_L values, the best estimate of q is q=0. Since q represents the potency of fibers between 5 and 10 μm in length, relative to fibers >10 μm in length (considering only fibers thinner than 0.4 μm), just as was the case for lung cancer, the model predicts that fibers between 5 and 10 μm are non-potent in causing mesothelioma.

For mesothelioma, the best estimate of rpc is rpc=0.0013, which predicts that chrysotile is only 0.13% as potent as amphibole in causing mesothelioma (after adjusting for fiber size). This small estimate for rpc is not significantly different from rpc=0 (p=0.79). Consequently, in this analysis, the data are consistent with the hypothesis that all of the mesotheliomas occurring in cohorts exposed primarily to chrysotile are due to small amounts of amphibole contamination within the chrysotile. Moreover, the hypothesis that chrysotile and amphibole are equally potent in causing mesothelioma (the assumption inherent in the U.S. EPA (1986) asbestos health effect document) is clearly rejected (p=0.0001).

Results using PCME as the exposure index for mesothelioma (the bottom right side of Table 7-17) are similar. The best estimate is that chrysotile is only 0.0033 as potent as amphibole, the hypothesis that chrysotile is non-potent cannot be rejected (p=0.61), and the hypothesis that chrysotile and amphibole are equally potent is definitely rejected (p=0.0007).

Based upon a comparison of either the residual variance, σ, or the likelihood, it appears that the exposure index defined by fibers longer than 10 μm and thinner than 0.4 μm (corresponding to q=0 in Table 7-17) provides an improvement in fit over use of PCME as the exposure index for mesothelioma. Even after adjusting for the effects of fiber type (i.e., comparing the σ values estimated for the optimized values with PCME and Equation 7-12 as the exposure index, respectively), the variation across K_M values appears to decrease by more than 20% when values are adjusted to the index of fibers that are longer than 10 μm and thinner than 0.4 μm. Moreover, comparing σ values between the index in current use (PCME with rpc=1) (U.S. EPA 1986) and the optimized index of longer and thinner fibers (with rpc=0.0013), use of the latter exposure index results in a 67% reduction in variation across K_M values.

As was also the case for the lung cancer analysis, the fit based on the exposure index defined by Equation 7-11, which was proposed in an earlier version of this report (with q, the relative potency of fibers between 5 and 10 μm compared to fibers longer than 10 μm fixed at q=0.003), is virtually identical to the fully optimized fit (which predicts q=0).

In addition to the analyses reported in Table 7-17, another analysis for mesothelioma were conducted in which an additional term was added to the linear combination of fiber lengths appearing in Equation 7-12 to represent fibers shorter than 5 μm (still considering only fibers thinner than 0.4 μm). In this analysis, the best estimate of the potency of fibers shorter than 5 μm was also zero.

Based on results in this section and the corresponding evaluation of lung cancer (Section 6.4.3.1) a recommended set of lung cancer (and mesothelioma) exposure-response coefficients are developed and presented in Section 7.5.

7.5 THE OPTIMAL EXPOSURE INDEX

7.5.1 Definition of the Optimal Index and the Corresponding Exposure-Response Factors

Table 7-17 presents the results of fitting a statistical model to asbestos exposure-response coefficients to estimate the relative potencies for fibers of various sizes and types that define an optimized exposure index for asbestos. Although the coefficients for lung cancer (the K_L values) and mesothelioma (the K_M values) were separately evaluated, the optimal index for each incorporates the same size range of fibers (at least based on the limited range of options evaluated). These are fibers longer than 10 μm and thinner than 0.4 μm.

Results in Table 7-17 also differentiate between the potency of chrysotile and amphibole for both lung cancer and mesothelioma. Amphibole is estimated as being about four times as potent as chrysotile for lung cancer (although the difference is not significant) and about 800 times as potent as chrysotile for mesothelioma (a highly significant difference). Moreover, the data are consistent with the hypothesis that chrysotile has zero potency toward the induction of mesothelioma.

The optimized dose-response coefficients (rounded up) from Table 7-17 for pure fiber types (chrysotile or amphibole) are summarized in Table 7-18. These coefficients apply to exposures quantified in terms of concentrations (in f/ml) of fibers longer than 10 μm and thinner than 0.4 μm.

Table 7-18. Optimized Dose-Response Coefficients for Pure Fiber Types

Fiber Type	K_{L*} x 100	K_{M*} x 10^8
Chrysotile	0.6	0.04
Amphiboles	3	30

7.5.2 Evaluation of the Optimal Exposure Index

The optimal coefficients presented in Table 7-18, result from adjustments for both fiber type and fiber size to the K_L and K_M values obtained directly from the literature (Tables 7-6 and 7-9), which are linked to PCM measurements. To get some idea of the relative effects of adjustments for fiber size (from PCM to fibers longer than 10 μm and thinner than 0.4 μm) and fiber type toward the goal of rationalizing the K_L and K_M values obtained from different environments, the effect of the two adjustments are considered sequentially—first the effect of adjusting for fiber size is considered and next the added effect of adjusting for fiber type is evaluated.

To compare the effects of adjusting K_L and K_M values for fiber size, the K_{L*} and K_{M*} values, which are adjusted to the optimal exposure index (using Equation 7-9) are plotted (along with their associated uncertainty intervals) in Figure 7-3, and 7-4. These figures are in a format identical to that of Figures 7-1 and 7-2 of the untransformed values. The "key" provided for Figure 7-1 is also directly transferable to Figures 7-2, 7-3, and 7-4.

Note that one of the points plotted in Figures 7-1 and 7-2 was omitted from Figures 7-3 and 7-4 (for the Enterline study [1986] of retired factory workers: study MX13) because it was felt that none of the available size distributions were suitably applicable for this study site, so no conversions were possible. Also, the confidence intervals are larger in Figures 7-3 and 7-4 because, as previously indicated, we have attempted throughout our analysis of the epidemiology data to account for major sources of uncertainty. Thus, the confidence intervals depicted in Figure 7-3 and 7-4 are modified from those depicted in Figures 7-1 and 7-2 to account for the uncertainty of making the adjustment for fiber size using paired data from published size distributions. The intervals were adjusted by multiplying the upper bound and dividing the lower bound by a factor thought to represent the relative contribution to uncertainty contributed by the need to match data from separate studies to perform the conversions. The factors employed (along with the rationale for selecting the value of each factor) are provided in Table 7-15.

The visual impressions from a comparison between Figures 7-1 and 7-3 for lung cancer and between Figures 7-2 and 7-4 for mesothelioma are that the changes resulting from adjusting for fiber size are subtle. This visual impression is reinforced by the relative similarity of the fits (based on comparison of σ and log-likelihoods) reported in Table 7-17 for PCME and the optimal exposure index, particularly for lung cancer.

Figures 7-5 and 7-6 show the effects of adjusting exposure-response coefficients for both fiber size and type. To develop Figure 7-5 for lung cancer, a size-adjusted K_L, as plotted in Figure 7-3, was further adjusted to correspond to pure amphibole by dividing it by the factor $[f_{amph} + rpc_* (1 - f_{amph})]$, where f_{amp} is the proportion of amphibole fibers estimated for a given environment (as listed in Table 7-16) and rpc=0.267, the optimal value from Table 7-17. The corresponding adjusted factors corresponding to pure chrysotile can be calculated simply by multiplying the amphibole value by rpc=0.267. Since the study-specific values for pure amphibole all differ from the corresponding value for pure chrysotile by a multiplicative constant, values for both types of asbestos are plotted simultaneously in Figure 7-5 by using a different scale for amphibole and chrysotile. The same method was used to develop Figure 7-6 for mesothelioma exposure-response coefficients, from the size-adjusted K_M values plotted in Figure 7-4, the only difference being that the mesothelioma rpc=0.0013 (Table 7-17) was used for this latter conversion. Comparing Figure 7-5 to 7-1 suggests that the adjustments for size and type resulted in as somewhat better reconciliation of the dose-response coefficients for lung cancer, although the improvement is still somewhat subtle. However, a comparison of Figures 7-6 to 7-2 indicates a much more dramatic improvement in the case of mesothelioma. Comparisons of Figures 7-2, 7-4, and 7-6 indicate this is primarily due to the adjustment for fiber type, although the subsequent adjustment for fiber size provides further, noticeable improvement.

Figure 7-3:
Plot of Estimated (Adjusted) K_{L*} Values and Associated Uncertainty Intervals by Study Environment

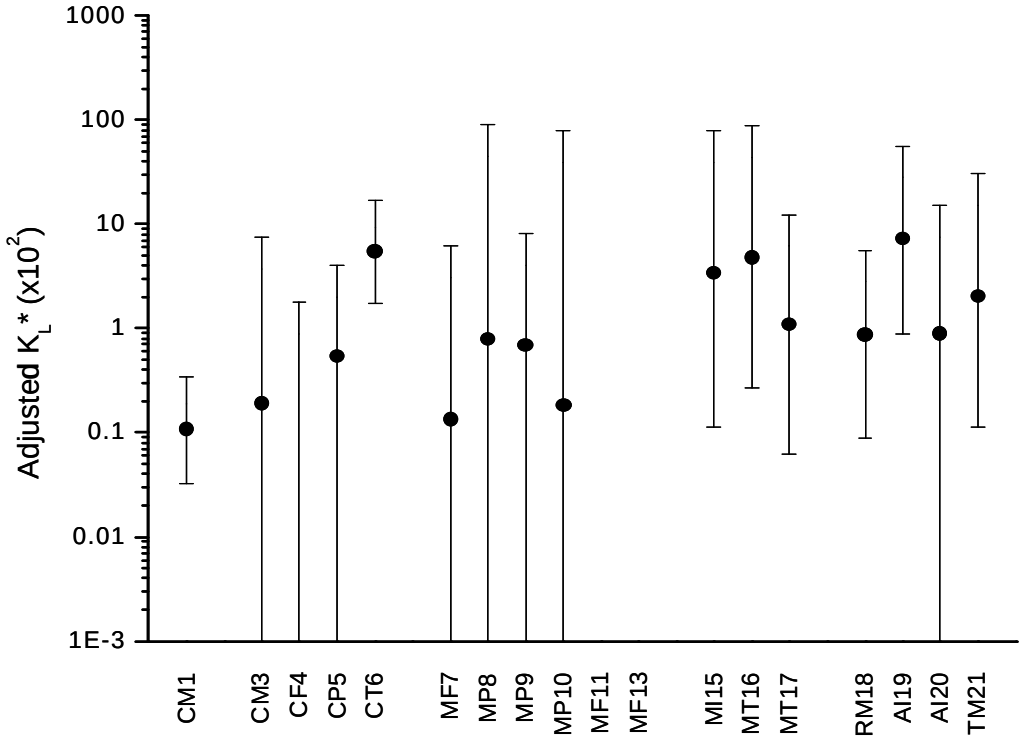

Figure 7-4:
Plot of Estimated (Adjusted) K_M Values and Associated Uncertainty Intervals by Study Environment

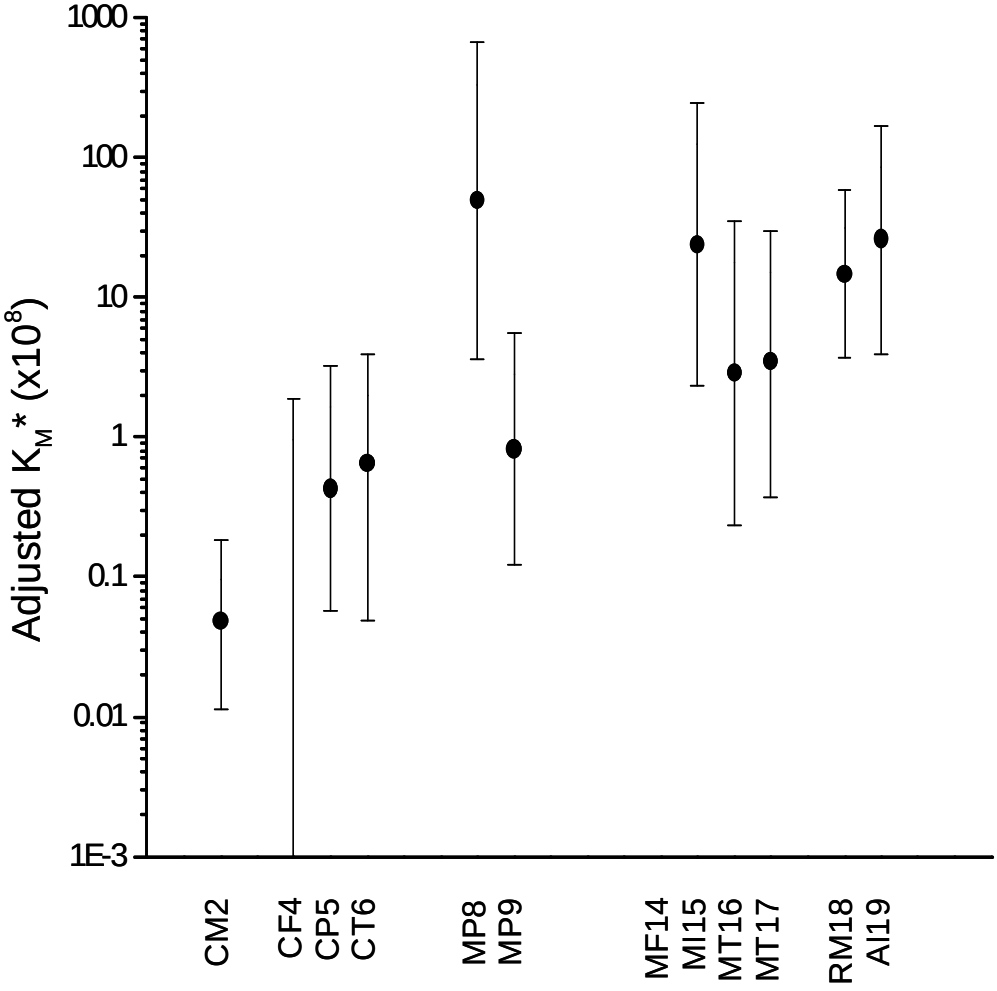

Figure 7-5:
Plot of Estimated K_{LA} and K_{LC} Values and Associated Uncertainty Intervals by Study Environment

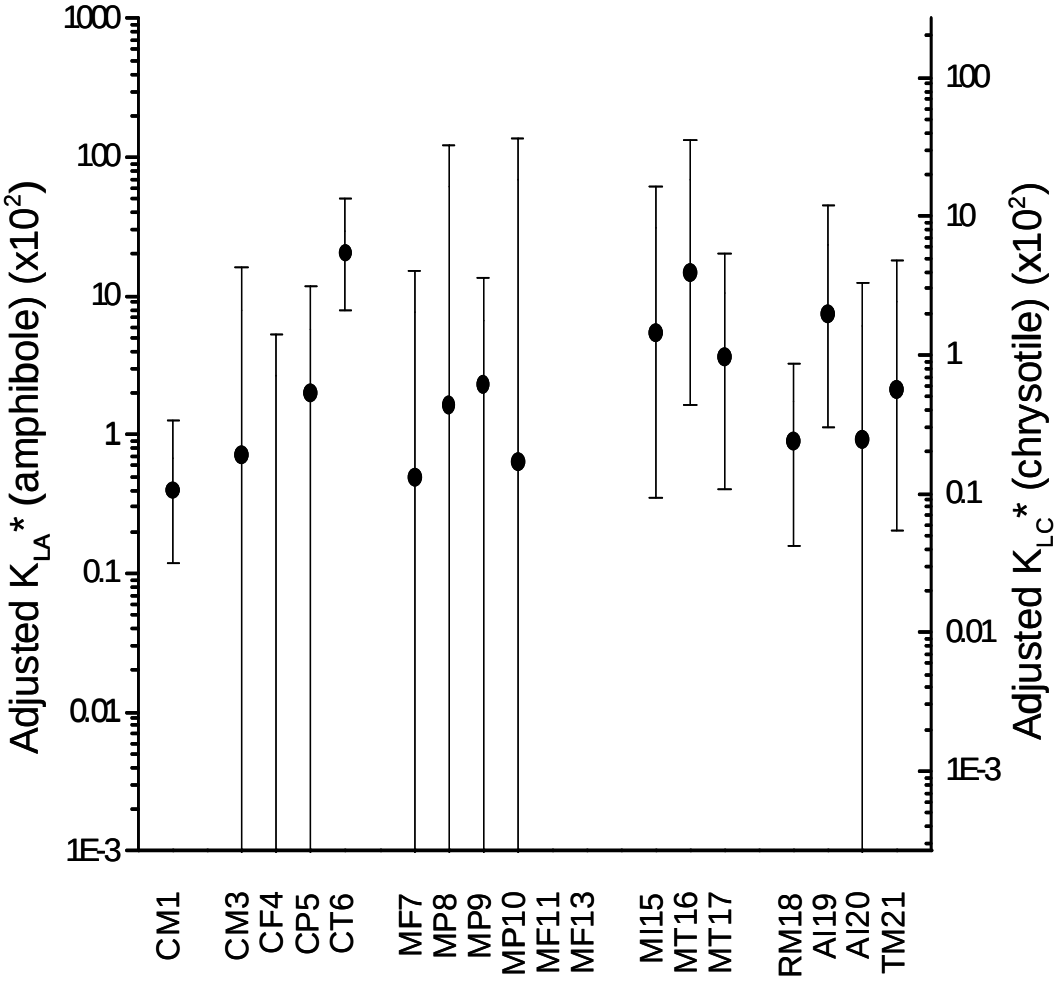

Figure 7-6:
Plot of Estimated K_{MA} and K_{MC} Values and Associated Uncertainty Intervals by Study Environment

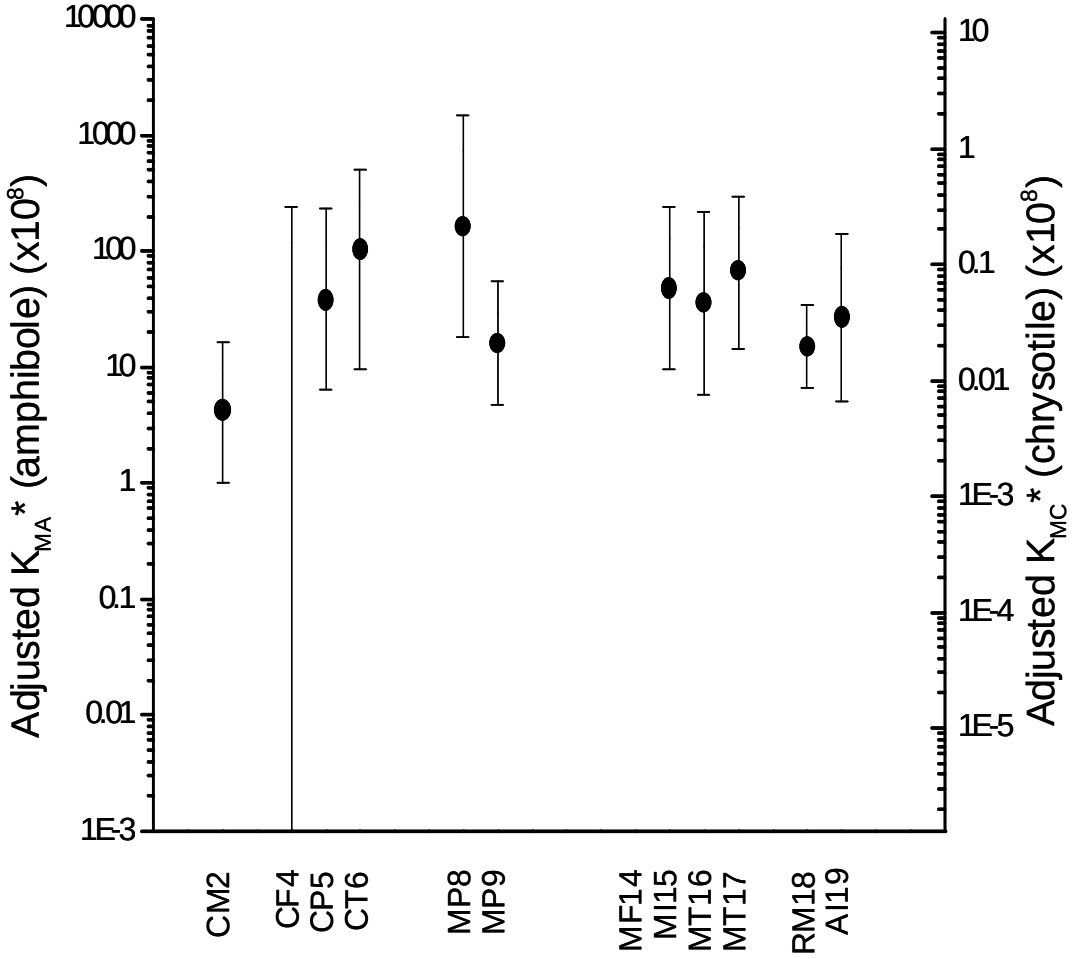

In addition to the graphical comparisons, it is also instructive to consider numerical comparisons. Table 7-19 reproduces values for all of the original (study-specific) K_L and K_M (from Tables 7-6 and 7-9, respectively) along with all the corresponding values for the adjusted K_{L*} and K_{M*}. Study-specific estimates for the all the corresponding K_{LA}, K_{LC}, K_{MA}, and K_{MC} are also presented.

Table 7-20 presents the magnitude of the spread in the range of original and adjusted K_L and K_M values estimated as the quotient of the maximum and minimum values of each range. Note that, of necessity, such an analysis requires that the zero values obtained for the Connecticut friction products plant (CF4) be omitted. Note further that the data sets evaluated in Table 7-20 for the original and adjusted values are identical (i.e., the one study for which no suitable fiber size distribution could be found was excluded).

In Table 7-20, for mesothelioma, the spread in unadjusted values among "pure" fiber types (i.e., chrysotile only or amphibole only) are both substantially smaller than those for mixed data sets (containing both fiber types). This provides further evidence of differences in the potencies of each fiber type toward mesothelioma. It is also apparent that adjusting for fiber size decreases the range within pure fiber types. Moreover, by simultaneously adjusting for both fiber size and type (as illustrated by the column labeled, "K_{mx}"), the range of variability across the entire data set of 10 mesothelioma studies is reduced from almost 1,100 to a factor of 30, which is a clear and substantial improvement.

For lung cancer, the results presented in Table 7-20 are a bit more complicated. While there is a substantial reduction in the spread of unadjusted values among "pure" amphibole environments when mixed environments are excluded, the spread among "pure" chrysotile environments is no different than that observed for the entire data set. This is because, as previously described (Section 7.2.2) the difference between the K_L values observed among chrysotile miners in Quebec and chrysotile textile workers in South Carolina represent the extremes of the entire range of reported K_L values. Adjusting these exposure-response coefficients for size provides some improvement in agreement across these two environments. This reinforces the finding from Appendix D that, if size adjustments incorporating cutoffs for longer fibers could be incorporated into a new exposure index for asbestos, the apparent discrepancy between the exposure-response observed among Quebec miners and South Carolina textile workers (and, thus, among K_L values as a whole) is likely to be further reconciled. The impressions from the figures discussed above and from Table 7-20 confirm the conclusions concerning the quantitative improvement in agreement across exposure-response coefficients highlighted in Sections 7.4.3.1 and 7.4.3.2 and reinforce the conclusion that, especially with regard to mesothelioma, adjusting exposure-response coefficients for fiber size and type leads to substantially improved agreement across studies.

Table 7-19. Study Specific K_l, K_m, K_{l*}, K_{m*}, K_{la}, K_{ma}, K_{lc}, and K_{mc} Values

								Amphiboles		Chrysotile	
Environment	**Study Code**	**K_L Reference**	**K_M Reference**	**K_L (x100)**	**K_M (x10^8)**	**K_L' (x100)**	**K_M' (x10^8)**	**K_{LA} (x100)**	**K_{MA} (x100)**	**K_{LC} (x10^8)**	**K_{MC} (x10^8)**
Quebec mines and mills	CM1	Liddell et al. 1997		0.029		0.108		0.399		0.106	
Quebec mines	CM2		Liddell et al. 1997 (raw data)		0.0165		0.062		5.51		0.00716
Italian mine and mill	CM3	Piolatto et al. 1990		0.051		0.131		0.716		0.190	
Connecticut plant	CF4	McDonald et al. 1984	McDonald et al. 1984	0	0	0	0				
New Orleans plants	CP5	Hughes et al. 1987	Hughes et al. 1987	0.25	0.2	0.864	0.432	1.979	38.3	0.526	0.0498
South Carolina plant	CT6	Dement et al. 1994 (raw data)	Dement 2001 (person. comm.)	2.1	0.25	6.38	0.660	20.7	106	5.50	0.137
Wittenoom, Australia	RM18	DeKlerk, unpublished data	DeKlerk, unpublished data	0.47	7.9	0.87	14.43	0.9	15.08	0.24	0.02
Patterson, NJ factory	AI19	Seidman et al. 1986	Seidman et al. 1986	1.1	3.9	17.36074	26.04111	7.526804	26.9044	2.00213	0.034976
Tyler, Texas factory	AI20	Levin et al. 1998		0.13		0.868037		0.889531		0.236615	
Libby, Montana	TM21	Amandus and Wheeler 1987		0.45		2.44		1.868577		0.497041	
British factory	MF7	Berry and Newhouse 1983		0.058		0.134276		0.498301		0.132548	
Ontario factory	MP8	Finkelstein 1984	Finkelstein 1984	0.29	18	3.246555	48.69833	1.63756	164.2291	0.435591	0.213498

Table 7-19. Study Specific K_l, K_m, K_{l*}, K_{m*}, K_{la}, K_{ma}, K_{lc}, and K_{mc} Values *(continued)*

								Amphiboles		Chrysotile	
Environment	**Study Code**	**KL Reference**	**KM Reference**	**KL (x100)**	**KM ($x10^8$)**	**KL' (x100)**	**KM' ($x10^8$)**	**K_{LA} (x100)**	**K_{MA} (x100)**	**K_{LC} ($x10^8$)**	**K_{MC} ($x10^8$)**
New Orleans plants	MP9	Hughes et al. 1987	Hughes et al. 1987	0.25	0.3	1.082185	0.811639	2.267472	16.07566	0.603147	0.020898
Swedish plant	MP10	Albin et al. 1990		0.067		0.189382		0.638655		0.169882	
Belgium factory	MP11	Laquet et al. 1980		0.0068							
U.S. retirees	MX13	Enterline et al. 1986		0.11							
Asbestos, Quebec	MX14		Liddell et al. 1997 (raw data loc 2)		0.092						
U.S. insulation workers	MI15	Selikoff and Seidman 1991	Selikoff and Seidman 1991	0.18	1.3	7.411067	24.08597	5.331754	48.68671	1.418246	0.063293
Pennsylvania plant	MT16	McDonald et al. 1983b	McDonald et al. 1983b	1.8	1.1	4.781501	2.922028	14.72572	35.9891	3.917041	0.046786
Rochedale, England plant	MT17	Peto et al. 1985	Peto et al. 1985	0.41	1.31	2.39075	3.47987	3.598193	67.9231	0.957119	0.0883

Table 7-20. Comparison of Spread in Range of Original and Adjusted K_l and K_m Values for Specific Fiber Types

Fiber Type	Ranges of Values							
	Number in K_L, K_{L*},K_{LX} Sets	K_L	K_{L*}	K_{LX}	Number in K_M, K_{M*},K_{MX} Sets	K_M	K_{M*}	K_{MX}
All fiber types combined	15	72	67	52	10	1,089	795	30
Chrysotile only (excluding mixed)	4	72	51	52	3	15	11	19
Chrysotile only (also excluiding textiles)	3	8.6	5.0	5.0	2	12	7.0	7.0
Chrysotile and mixed settings	11	72	51	52	8	1,089	794	30
Textiles only	3	5.1	5.1	5.7	3	5.2	5.2	2.9
Amphibole and mixed settings	11	31	55	30	7	60	60	11
Amphiboles only (excluding mixed)	4	8.5	8.5	8.5	2	2.0	1.7	1.7

7.6 GENERAL CONCLUSIONS FROM QUANTITATIVE ANALYSIS OF HUMAN EPIDEMIOLOGY STUDIES

The following conclusions result from our evaluation of the available epidemiology studies.

(1) To study the characteristics of asbestos that relate to risk, it is necessary to combine results (i.e., in a meta analysis) from studies of environments having asbestos dusts of differing characteristics. More robust conclusions regarding risk can be drawn from an analysis of the set of epidemiology studies taken as a whole than results derived from individual studies.

(2) By adjusting for fiber size and fiber type, the existing database of studies can be reconciled adequately to reasonably support risk assessment.

(3) The U.S. EPA models for lung cancer and mesothelioma both appear to track the time-dependence of disease at long times following cessation of exposure, however, the relationship between exposure concentration and response may not be adequately described by the current models for either disease. There is some evidence that these relationships are supra-linear.

(4) Whereas the U.S. EPA model for lung cancer assumes a multiplicative relationship between smoking and asbestos, the current evidence suggests that the relationship is less than multiplicative, but possibly more complex than additive. However, even if the smoking-asbestos interaction is not multiplicative as predicted by the U.S. EPA model, exposure-response coefficients estimated from the model are still likely to relate to risk approximately proportionally and, consequently, may be used to determine an exposure index that reconciles asbestos potencies in different environments. However, adjustments to the coefficients may be required in order to use them to estimate absolute lung cancer risk for differing amounts of smoking. This issue needs to be investigated further in the next draft of this document.

(5) The optimal adjustment found for fiber size and type that best reconciles the published literature assigns equal potency to fibers longer than 10 μm and thinner than 0.4 μm and assigns no potency to fibers of other dimensions. Different exposure-response coefficients for chrysotile and amphibole are assigned both for lung cancer and mesothelioma. For lung cancer the best estimate of the coefficient (potency) for chrysotile is 0.27 times that for amphibole, and for mesothelioma the best estimate of the coefficient (potency) for chrysotile is only 0.0013 times that for amphibole.

(6) Without adjustments, the lung cancer exposure-response coefficients (K_L values) estimated from 15 studies vary by a factor of 72 and these values are mutually inconsistent (based on non-overlap of uncertainty intervals). By simultaneously adjusting these values for fiber size and type, the overall variation in K_L values across these studies is reduced to a factor of 50.

(7) Without adjustments, the mesothelioma exposure-response coefficients (K_M values) estimated from 10 studies vary by a factor of 1,089, and these values are likewise mutually inconsistent. By simultaneously adjusting these values for fiber size and type, the overall variation in K_M values across these studies is reduced to a factor of 30.

(8) The exposure index and exposure-response coefficients embodied in the risk assessment approach developed in this report are more consistent with the literature than the current U.S. EPA approach. In particular, the current approach appears highly likely to seriously underestimate risk from amphiboles, while possibly overstating risk from chrysotile. Furthermore, most the remaining uncertainties regarding the new proposed approach also apply to the current approach. Consequently, we recommend that the proposed approach begin to be applied in assessment of asbestos risk on an interim basis, while further work, as recommended below, is being conducted to further refine the approach.

(9) The residual inconsistency in both the lung cancer and mesothelioma potency values is primarily driven by those calculated from Quebec chrysotile miners and from South Carolina chrysotile textile workers. The difference in the lung cancer potency estimated between these studies has long been the subject of much attention. A detailed evaluation of the studies addressing this issue, the results of our analysis of the overall epidemiology literature, and implications from the broader literature, indicate that the most likely cause of the difference between these studies is the relative distribution of fiber sizes in the two environments. It is therefore likely that the variation between these studies can be further

reduced by developing improved characterizations of the dusts that were present in each of these environments (relying on either archived samples, or newly generated samples using technologies similar to those used originally).

Recommendations for Limited, Further Study

The two major objectives identified above for further study are:

(1) to evaluate a broader range of exposure-response models in fitting the observed relationship between asbestos exposure and lung cancer or mesothelioma, respectively. For lung cancer models, this would also include an attempt to better account for the interaction between asbestos exposure and smoking; and

(2) to develop the supporting data needed to define adjustments for exposure-response coefficients that will allow them to be used with an exposure index that more closely captures the criteria that determine biological activity (see Section 6.5). Among other things, this work should focus on obtaining data that would permit more complete reconciliation of the exposure-response coefficients derived for Quebec miners and South Carolina textile workers.

The first of the above objectives requires access to raw data from a small number of selected, additional epidemiology studies. The best candidate studies include: (for chrysotile) the lung cancer data from Quebec (best) or, potentially, from the New Orleans asbestos-cement pipe plant studied by Hughes et al. For amphiboles, the best candidate studies include: the lung cancer and *newest* mesothelioma data from Libby, or, potentially the lung cancer and mesothelioma data from the Paterson, New Jersey insulation manufacturing plant studied by Seidman et al. (1986). The possibility of obtaining some or all of these data sets needs to be further explored.

The second of the above objectives requires more detailed size characterization data for the environments of interest. Although archived air samples do not appear to be available from any of the study locations of interest (except South Carolina), we believe that suitable data can be developed from appropriate bulk samples. Thus, for example, it would be useful to obtain samples of the raw ore from Libby, Wittenoom, and Quebec and the textile, asbestos-cement pipe, and friction-product grade products from Quebec.

Results from our review of the supporting literature suggest that the optimum cutoff for increased potency occurs at a length that is closer to 20 μm than 10 μm, (the latter of which is the cutoff in the exposure index provided in this study). Data do not currently exist to improve on this latter cutoff. However, provided that study-specific size distribution data could be obtained as indicated above, with the appropriate analyses, it will be possible to develop the size distributions necessary to evaluate a range of considerations including:

(1) delineation of size fractions among individual length categories out to lengths as long as 30 or 40 μm;

(2) determination of the relative presence and importance of cleavage fragments (of non-biologically relevant sizes) in mine ores vs. finished fibers; and

(3) the relative fraction of fibrous material vs. non-fibrous particles in the various exposure dusts of interest.

8.0 DISCUSSION, CONCLUSIONS, AND RECOMMENDATIONS

Although gaps in knowledge remain, a review of the literature addressing the health-related effects of asbestos (and related materials) provides a generally consistent picture of the relationship between asbestos exposure and the induction of disease (lung cancer and mesothelioma). Therefore, the general characteristics of asbestos exposure that drive the induction of cancer can be inferred from the existing studies and can be applied to define appropriate procedures for evaluating asbestos-related risk. Moreover, such procedures provide substantial improvement in the confidence that can be placed in predicting risks in exposure environments of interest compared to risk predictions based on procedures in current use.

Following a general discussions of the findings of this study, specific recommendations for finalizing a protocol for assessing asbestos-related risks using the procedures identified in this document are provided in Section 8.2. Recommendations are described in Section 8.3 for limited, focused, additional studies to:

(1) settle a small number of outstanding issues (concerning whether better models exist than the current U.S. EPA models for tracking the time and concentration dependence of the exposure-response relationships for asbestos-induced lung cancer and mesothelioma);

(2) improve the manner in which smoking is addressed in the modeling of asbestos-induced lung cancer; and

(3) provide the data required to fully optimize the approach recommended in this document (i.e., reconciling the published epidemiology studies by addressing the effects of fiber size and type).

Moreover, these recommendations parallel those of the expert panel convened to peer-review the previous version of this report (Appendix B).

8.1 DISCUSSION AND CONCLUSIONS

8.1.1 Addressing Issues

The issues identified in the introduction (Chapter 2) as part of the focus of this study can now be addressed. These are:

! adequacy of existing models: whether the exposure-response models currently in use by the U.S. EPA for describing the incidence of asbestos-related diseases adequately reflect the time- and exposure-dependence for the development of these diseases;

- relative potency for different mineral types: whether different potencies need to be assigned to the different asbestos mineral types to adequately predict risk for the disease endpoints of interest;

- biodurability: to the extent that different asbestos mineral types are assigned distinct potencies, whether the relative *in vivo* durability of different asbestos mineral types determines their relative potency;

- minerals of concern: whether the set of minerals included in the current definition of asbestos adequately covers the range of minerals that potentially contribute to asbestos-related diseases;

- analytical methods: whether the analytical techniques and methods currently used for determining asbestos concentrations adequately capture the biologically-relevant characteristics of asbestos (particularly with regard to structure sizes), so that they can be used to support risk assessment; and

- extrapolation of risk coefficients: whether reasonable confidence can be placed in the cross-study extrapolation of exposure-response relationships that are required to assess asbestos-related risks in new environments of interest.

The Adequacy of Existing Models. Regarding the first of the above-listed issues, both the U.S. EPA lung cancer model and mesothelioma model appear to adequately reflect the time-development of asbestos-induced lung cancer. For lung cancer, the assumption in the model that risk remains constant with time following the end of exposure was confirmed for cohorts exposed, respectively, to chrysotile, to crocidolite, and to amosite (Section 7.2.1). A similar analysis for mesothelioma suggests that, as that model predicts, risk for mesothelioma continues to increase with the square of time since the end of exposure (Section 7.3.1).

Regarding exposure concentration, we did find some evidence suggesting that, for both lung cancer and mesothelioma, the relationship between exposure concentration and risk may not be linear, but rather supra-linear (Sections 7.2.1.1 and 7.3.1.2). If confirmed, this would contradict the assumed strictly linear relationship in both the current lung cancer and mesothelioma models.

For 15 of the 18 studies that were fit using the lung cancer model (Equation 7-2) in our analysis (Appendix A and Section 7.2.2), the parameter, α, (which indicates differences in background lung cancer incidence between cohorts and controls) was greater than 1.0 and significantly so in six cases. In these cases, if it is assumed instead that the background lung cancer mortality rate applied to the cohort is appropriate, the correct fitting would be with α=1.0, in which case the exposure-response would appear supra-linear. Similarly, an analysis conducted using the raw data from Wittenoom (Section 7.3.1.2) in which exposure is categorized by intensity while controlling for both time since the end of exposure and duration of exposure suggests a supra-linear relationship between exposure concentration and mesothelioma as well.

Due to these observations and additional concerns about the relationship between smoking and asbestos exposure toward the induction of lung cancer (Section 7.2.1.3), evaluation of the fit of a broader range of models to the available lung cancer and mesothelioma data is recommended.

Importantly, because any such evaluation would be greatly enhanced by broadening the number of data sets utilized, it is further recommended that all means be explored for acquiring raw data sets for cohorts from additional epidemiology studies.

At the same time, although there are suggestions from our analysis that models other than the current models might better describe the relationship between exposure and risk for both mesothelioma and lung cancer any limitation associated with use of the current models for lung cancer and mesothelioma would be common to the procedures recommended in this report and the existing U.S. EPA approach for assessing asbestos-related risks. Therefore, given the degree of improvement demonstrated for the proposed approach over the current U.S. EPA approach, there appears to be little reason not to adopt the proposed approach as an interim measure, while further research is conducted to address the remaining outstanding issues highlighted by the expert panel (Appendix B) and highlighted in this report.

Relative Potency for Different Mineral Types. As indicated in Sections 7.4.3.2 and 7.5.2, our analysis indicates a substantial difference in the relative potency of amphiboles and chrysotile toward the induction of mesothelioma, with amphiboles estimated as almost 1,000 times more potent than chrysotile (fiber-for-fiber). Moreover, this difference was shown to be highly statistically significant. When fiber size and type are simultaneous addressed, variation across the 10 published epidemiology studies included in our analysis drops from a factor of more than 1,000 to a factor of 30 (Table 7-19). This, coupled with the growing evidence in the literature supporting this difference in potency among fiber types, provides strong support for defining distinct risk coefficients for chrysotile and the amphiboles to assess the risk of mesothelioma.

The situation with lung cancer is less clear. Although our analysis suggests that the best estimate is that (fiber-for-fiber) amphiboles are about 4 times more potent than chrysotile toward the induction of lung cancer, this difference was not found to be statistically significant (Sections 7.4.3.1 and 7.5.2). This issue also remains unresolved in the wider literature. It is also possible that the confounding effects of smoking, coupled with the lack of adequate data for properly assessing the effects of smoking may be limiting our ability to address this question. Thus, this is one of the issues that would likely benefit from additional research.

At the same time, when a small difference in potencies is incorporated into our meta analysis of the epidemiology studies we evaluated, variation across the data set is reduced by about 30% (Table 7-20). This suggests that incorporating a small difference in lung cancer risk coefficients for chrysotile and the amphiboles is reasonable.

Biodurability. Because the *in vitro* dissolution rate for chrysotile in biological fluids is substantially greater than for crocidolite and, likely, other amphiboles (Section 6.2.4), effects potentially attributable to differences in the relative biodurability of these asbestos types are addressed in several sections of this document. It is possible that such differential biodurability at least partially explains the clear difference in potency between chrysotile and the amphiboles toward mesothelioma (along with the possible, albeit smaller, difference toward lung cancer). However, that no difference was observed in the time-development of either lung cancer or mesothelioma following exposure to chrysotile or amphibole asbestos (respectively) suggests that any relationship that exists between potency and biodurability must be more subtle and complicated than the obvious effect on internal dose. At the same time, there is ample literature

evidence that some kind of relationship in fact exists (Section 6.2.4). While more research into this relationship may prove interesting (and may be useful for assessing effects of less durable fibers), it is unlikely to have a direct impact on procedures for assessing asbestos-related risk.

Minerals of Concern. Regarding the range of fibrous minerals that potentially contribute to lung cancer and mesothelioma, available evidence (Sections 6.2 and 6.4) suggests that:

- ! several minerals and the most biodurable among synthetic fibers (such as erionite or refractory ceramic fibers) in addition to those included strictly within the definition for asbestos have been shown capable of inducing lung cancer and/or mesothelioma (as long as the corresponding fibers fall within the appropriate size range);

- ! fibrous minerals that differ radically in chemical composition or crystal structure (such as erionite, chrysotile, and the amphibole asbestos types) appear to exhibit substantially different potencies (even after adjusting for size); and

- ! fibrous minerals that exhibit closely related chemical compositions and crystal structures (such as the family of amphibole asbestos types) appear to exhibit relatively similar potencies (once effects are adjusted for size). To illustrate this point for mesothelioma, consider that the range of variation in estimated K_M's over 10 studies (which include studies of exposures to tremolite, amosite, and crocidolite in addition to chrysotile) is reduced to a factor of 30 (from almost 1,100), once the effects of size and differences between the amphiboles and chrysotile are accounted for (Table 7-20). Moreover, among the 7 of these studies reflecting exposure exclusively to amphiboles (which still includes exposures to tremolite[1], crocidolite, and amosite), the range of variation is reduced to a factor of 11 (Table 7-20). Regarding lung cancer, the four studies of "pure" amphibole environments (which includes exposures to tremolite, crocidolite, and amosite) vary by only a factor of 8.5 (Table 7-20) and this range is bounded by studies of the same mineral: amosite, which certainly suggests that mineralogical differences do not drive the observed variation (Section 7.2.2).

Given the above-described observations, it is clear that fibrous minerals beyond those included in the definition for asbestos can contribute to lung cancer and mesothelioma. It is also likely that potencies for minerals that exhibit similar chemistry and crystal structure (and which therefore likely exhibit similar physical-chemical properties) also exhibit corresponding potency (for similarly sized fibers). However, the carcinogenicity of fibers exhibiting radically different chemical compositions and crystal structures than those already identified as carcinogenic should be evaluated on a case-by-case basis.

Two additional considerations may be useful for focusing such evaluations. First, the size distribution for fibers composed of the mineral of concern should be shown to include substantial

[1]Formally, the exposures at Libby are to the amphibole mineral richterite. However, this mineral is closely related to tremolite and has sometimes been called "sodium tremolite" because it contains a greater fraction of sodium than the composition range that is commonly termed tremolite.

numbers within the range of structures that potentially contribute to biological activity (e.g., that fall within the size range defined by the improved index recommended in this study, i.e., structures longer than 10 μm and thinner than 0.4 μm, see Section 7.5). Second, such fibers should also be shown to be relatively biodurable (i.e., that they exhibit dissolution rates less than approximately 100 ng/cm^2-hour, Lippmann 1999).

Analytical Methods. Given the need to detect the thinnest fibers and the need for reliable measurements in outdoor settings, the only analytical technique that appears to be capable of providing quantitative data useful for supporting risk assessment is TEM (Sections 4.3 and 7.6). Further, given the specific size range of structures that need to be evaluated and the specific manner in which they need to be counted (to assure both cross-study comparability and compatibility with the recommended dose-response coefficients), analyses should be performed using the specific analytical methods recommended in this document. These are ISO 10312 (modified to focus on interim index structures) for air and the Modified Elutriator method (Berman and Kolk 2000) for soils or bulk materials. However, on a study-specific basis, other methods may be shown to provide comparable results so that they can also be used as part of a properly integrated investigation.

8.1.2 Comparison with Other, Recent Risk Reviews

Although several other reviews have also recently been published that nominally address risk-related issues for asbestos (including questions concerning the identification of an appropriate exposure index and the relative potency of varying fiber types), these studies are either qualitative or involve analysis of data in a manner that does not allow formal evaluation of the nature of specific exposure-response relationships for the various diseases. Therefore, they are not well suited to support development of a protocol for conducting formal assessment of asbestos-related risks. Nevertheless, the general conclusions from these reviews are not inconsistent with our findings.

Hodgson and Darnton (2000). Hodgson and Darnton (2000) conducted a comprehensive quantitative review of potency of asbestos for causing lung cancer and mesothelioma in relation to fiber type. They concluded that amosite and crocidolite were, respectively, on the order of 100 and 500 times more potent for causing mesothelioma than chrysotile. They regarded the evidence for lung cancer to be less clear cut, but concluded nevertheless that amphiboles (amosite and crocidolite) were between 10 and 50 times more potent for causing lung cancer than chrysotile. In reaching this latter conclusion they discounted the high estimate of chrysotile potency obtained from the South Carolina cohort. Hodgson and Darnton concluded that inter-study comparisons for amphibole fibers suggested non-linear exposure-response relationships for lung cancer and mesothelioma, although a linear relationship was possible for pleural mesothelioma and lung tumors, but not for peritoneal mesothelioma.

The Hodgson and Darnton study was based on 17 cohorts, 14 of which were among the 20 included in the present evaluation. This study had different goals from the present evaluation and used different methods of analysis. Hodgson and Darnton did not use the exposure-response information within a study. Instead, lung cancer potency was expressed as a cohort-wide excess mortality divided by the cohort mean exposure. Likewise, mesothelioma potency was expressed as the number of mesothelioma deaths divided by the expected total number of deaths,

normalized to an age of first exposure of 30, and by the mean exposure for the cohort. These measures have the advantage of being generally calculatable from the summarized data available from a study. However, since they are not model-based, it is not clear how they could be used to assess lifetime risk from a specified exposure pattern, which is an important goal of the current project. Use of average cohort exposure could cause biases in the estimates, if, e.g., a large number of subjects were minimally exposed. Also, the recognized differences between studies in factors, in addition to level of exposure, that may affect risk will also affect the reliability of conclusions concerning the dose response shape based on comparisons of results across studies.

Lippmann (1994, 1999). In the most recent of these reviews, Lippmann (1999) reinforces our general findings that it is longer fibers (those longer than a minimum of approximately 5 μm) that contribute to lung cancer and mesothelioma. He further indicates that, based primarily on the limits observed for fibers that can be phagocytized, fibers that contribute most to lung cancer are likely longer than a minimum of 10 μm. In his review, based on a series of comparisons of mean and median dimensions reported for the relevant exposures across a broad range of studies, Lippmann draws several fairly specific conclusions on the ranges of fiber sizes that may contribute to various diseases (i.e., that the minimum length fibers that contribute to asbestosis, lung cancer, and mesothelioma are 2, 5, and 10 μm, respectively). He also suggests that fibers that contribute to mesothelioma may need to be thinner than 0.1 μm while those that contribute to lung cancer may need to be thicker than 0.15 μm. While it is not clear that drawing such specific conclusions can be firmly supported by the kinds of qualitative comparisons across reported mean and median dimensions for exposures in various studies that are described in this paper, the author indicates that further, more formal study of the dose-response relationships that he posits is warranted. It is noted that many of the studies reviewed by Lippmann (1999) are also incorporated in our analysis.

In the earlier review, Lippmann (1994) plots lung tumor incidence as a function of inhaled animal dose for data from a series of broadly varying studies based, respectively, on fibers longer than 5, 10, and 20 μm (no widths considered) and suggests that the quality of the fits are comparable. The author further suggests, based on this evaluation, that PCM seems to provide a reasonable index of exposure. However, no formal goodness-of-fit tests were performed in this analysis and, based on visual inspection, none of the plots would likely show an adequate fit. Moreover, the plot of the tumor response vs. dose as a function of fibers longer than 5 μm appears to be substantially worse than the other two plots; if one removes the single highest point in this plot, it appears that any correlation will largely disappear.

Stayner et al. 1996. In the context of evaluating the “amphibole hypothesis”, Stayner et al. (1996) computed the excess relative risk of lung cancer per fiber/ml/year from 10 studies categorized by the fiber types to which the cohort was exposed. Each of these studies was also included in the present evaluation. Both the lowest and highest excess relative risks came from cohorts exposed exclusively to chrysotile. Based on their evaluation, they concluded that the epidemiologic evidence did not support the hypothesis that chrysotile asbestos is less potent than amphibole for inducing lung cancer. However, based on a review of the percentage of deaths in various cohorts from mesothelioma, they concluded that amphiboles were likely to be more potent than chrysotile in the induction of mesothelioma. They also noted that comparison of the potency of different forms of asbestos are severely limited by uncontrolled differences in fiber sizes. None of these conclusions are inconsistent with our general findings.

8.2 RECOMMENDATIONS FOR ASSESSING ASBESTOS-RELATED RISKS

The optimum values for the risk coefficients for lung cancer and mesothelioma (the adjusted K_L and K_M values) derived in our analysis are provided in Table 7-18. Although these values are optimized (within the constraints of the current analysis) and use of these values reduces the apparent variation across published studies substantially (Section 7.5.2), the need to manage and minimize risk when developing a general approach for assessing risk, is also recognized. Thus, to reduce the chance of under-estimating risks, a conservative set of potency estimates were developed (Table 8-1) by adjusting upward the best-estimate potency coefficients listed in Table 7-18 to provide additional health protectiveness. The manner in which this was accomplished is described in the following paragraphs.

Table 8-1. Conservative Risk Coefficients for Pure Fiber Types

Fiber Type	K_{L*} x 100	K_{M*} x 10^8
Chrysotile	5.5	0.15
Amphiboles	20	100

Reviewing the K_{Lc} and K_{La} dose response coefficients values listed in Table 7-19, it is apparent that the maximum values for lung cancer derive from the Dement et al. (1994) study of the South Carolina textile plant. As indicated in Appendix A, the South Carolina study is a high quality study. Moreover, we were able to obtain the raw data from this study and have analyzed these data in detail. We found, among other things, a well-behaved (i.e., monotonic) exposure-response trend in this study for lung cancer. Therefore, because this study is of high quality and provides the largest values of K_{Lc} and K_{La}, the values from this study were selected for our conservative estimates of the corresponding potency coefficients.

Reviewing the K_{Ma} and K_{Mc} values listed in Table 7-19, it is apparent that the maximum values derive from the Finkelstein study (1984) of the Ontario asbestos-cement factory. As indicated in Appendix A, the data from this study appear problematic. Among other things, the exposure-response relationships observed in this study are not well-behaved (i.e., not monotonic). Moreover, the value for α estimated for this study is the highest of any study we evaluated. Possible reasons for such a large α include large discrepancies between the background incidence of lung cancer between cohort and controls in this study and/or serious errors in exposure estimates. Given the potential problems associated with this study, (which suggests that the potency coefficients estimated from this study may be less reliable than for many of the other available studies), we decided to bypass this study and select the next highest values in Table 7-19 for K_{Ma} and K_{Mc} as the conservative estimates to be recommended in this study. Interestingly, these also turn out to be from the South Carolina textile study. Note that the difference in the estimates from these two studies vary by less than a factor of two in any case.

Based on the above evaluation, conservative estimates for the various potency coefficients recommended in this report are presented in Table 8-1.

Importantly, a measure of the degree of reconciliation among the results of the published epidemiology studies that has been accomplished by the analysis presented in this report is indicated by the ratios of the values presented in Tables 7-18 and 8-1, respectively. The ratios between the corresponding coefficients in Tables 7-18 and 8-1 are no more than 10 for the lung cancer potency coefficients and no more than 4 for the mesothelioma potency coefficients. Moreover, the bounding study for the values presented in Table 8-1 is once again the South Carolina textile study, which further reinforces earlier discussions identifying the particular need to reconcile this study with the other chrysotile studies (particularly the Quebec mining study).

To assess risk, depending on the specific application, either the best-estimate risk coefficients presented in Table 7-18 or the conservative estimates presented in Table 8-1 can be incorporated into procedures described below for assessing asbestos-related risks.

Tables 8-2 and 8-3 present estimates of the additional risk of death from lung cancer, from mesothelioma, and from the two diseases combined that are attributable to lifetime, continuous exposure at an asbestos concentration of 0.0001 f/cm^3.(for fibrous structures longer than 10 μm and thinner than 0.4 μm) as determined using TEM methods recommended herein. Table 8-2 was developed using the best-estimate values for risk coefficients defined in Table 7-18, and Table 8-3 was developed using the conservative estimates defined in Table 8-1. Separate risk estimates are provided for males and females and for smokers and non-smokers. The method used to construct these tables is described in detail in Appendix E.

Separate estimates are presented for smokers and nonsmokers because the lifetime asbestos-induced risk of both lung cancer and mesothelioma differ between smokers and non-smokers. The asbestos-induced risk of lung cancer is higher among smokers because the lung cancer model (Equation 7-2) assumes that the increased mortality rate from lung cancer risk due to asbestos exposure is proportional to background lung cancer mortality, which is higher among smokers. Note that, while this is consistent with a multiplicative effect between smoking and asbestos exposure that has been reported by several researchers (see, for example, Hammond et al. 1979), some of the latest studies of the interaction between smoking and asbestos exposure suggest a more complicated relationship (Section 7.2.1.3). This issue needs to be addressed more fully in future analyses of these data. However, we believe the effects of such considerations on the overall accuracy of asbestos-related risk estimates is likely to be small relative to other sources of error.

Table 8-2. Estimated Additional Deaths from Lung Cancer or Mesothelioma per 100,000 Persons from Constant Lifetime Exposure to 0.0001 TEM f/cc Longer than 10 um and Thinner than 0.4 um – Based on Optimum Risk Coefficients (Table 7-18)

Chrysotile				
	NonSmokers		**Smokers**	
	Males	**Females**	**Males**	**Females**
Lung Cancer	0.185	0.207	1.6	1.5
Mesothelioma	0.0836	0.096	0.0482	0.0702
Combined	0.269	0.303	1.65	1.57
Amphibole				
Lung Cancer	0.2	0.286	2.22	2.47
Mesothelioma	62.7	72.3	36.1	52.7
Combined	62.9	72.5	38.3	55.1

Table 8-3. Estimated Additional Deaths from Lung Cancer or Mesothelioma per 100,000 persons from Constant Lifetime Exposure to 0.0001 TEM f/cc Longer than 10 um and Thinner than 0.4 um - Based on Conservative Risk Coefficients (Table 8-1)

Chrysotile				
	Non-Smokers		**Smokers**	
	Males	**Females**	**Males**	**Females**
Lung Cancer	1.7	1.9	14.7	13.8
Mesothelioma	0.314	0.361	0.181	0.263
Combined	2.02	2.26	14.9	14
Amphibole				
Lung Cancer	3.77	4.41	34.1	33.2
Mesothelioma	209	241	120	175
Combined	213	245	154	209

If there is a desire to generate population averaged risks, this can also be accomplished using the data in Tables 8-2 or 8-3. For such a case, simply choose the appropriate row (for lung cancer, mesothelioma, or combined risk) from either Table 8-2 or 8-3 and substitute the four values given in the row into the following equation to derive a single, population averaged risk:

$$R_{avg} = 0.5*[0.214*(MS + FS) + 0.786*(MNS + FNS) \qquad \text{(Eq. 8-1)}$$

Where:

R_{avg}	is the population averaged risk for the chosen disease endpoint;
MS	is the corresponding risk for male smokers;
FS	is the corresponding risk for female smokers;
MNS	is the corresponding risk for male non-smokers; and
FNS	is the corresponding risk for female non-smokers.

Note that Equation 8-1 is derived based on the assumption that 21.4% of the general population smokes (see Appendix E).

The asbestos-induced risk of mesothelioma is smaller among smokers because the mesothelioma model (Equation 7-6) assumes that risk from constant exposure increases rapidly with age, with the result that the predicted mortality rate is highest among the elderly. Thus, since smokers have a shorter life span than non-smokers, their risk of dying from mesothelioma is also predicted to be smaller.

Risks from lifetime exposures to asbestos levels other than 0.0001 may be estimated from the appropriate entry in Tables 8-2 or 8-3 by multiplying the value in the selected cell from the table by the airborne asbestos concentration of interest and dividing by 0.0001 (i.e., by assuming that the additional risk is proportional to the asbestos exposure level). Airborne asbestos concentrations to be used in this manner *must* be estimates of lifetime average exposure and *must* be expressed as structures longer than 10 μm and thinner than 0.4 μm derived as described below.

Importantly, the risks provided in Tables 8-2 and 8-3 relate to exposure estimates expressed in terms of the interim exposure index (i.e., estimates including *only* asbestos structures longer than 10 μm and thinner than 0.4 μm). Only exposures expressed in terms of the same exposure index can be used to adjust the risk estimates to other levels of exposure (in the manner described above). Use of exposures expressed in terms of any other index of exposure (such as the PCME index in current use) will result in invalid estimates of risk.

The procedure described above for estimating risks using Tables 8-2 or 8-3 should provide good approximations as long as the projected risk is no greater than 1,000 per 100,000. Risks greater than 1,000 per 100,000 (i.e., 1 in 100) that are derived from the tables are likely to be over-estimated. However, for risks associated with short-duration exposures or exposures that differ radically over time, it may be better to use a lifetable analysis or a modified version of Tables 8-2 or 8-3 that reflect the differences in exposure duration and frequency. This is to avoid substantially under- or over-estimating risk (depending on how the table might otherwise be applied).
Tables 8-2 and 8-3 were derived using the approach described in Appendix E by incorporating

the age-, sex-, and smoking-specific death rates reported for the general U.S. population and assuming that exposure is constant and continuous at the level indicated in the table. The underlying models are provided in Chapter 7 for cases in which exposure is not constant throughout life and for which sufficient data exist to characterize the time-dependence of such exposure. If available, there may also be cases in which it is advantageous to employ mortality data from a control population that better matches the exposed population of interest than the U.S. population as a whole.

For the interim, it is recommended that asbestos-related risks from constant low-level exposures be estimated using Tables 8-2 and 8-3. Although it is possible also to use the tables to estimate risk from short-term exposures by applying the corresponding long-term average exposure *(derived from appropriate measurements, as described below),* this method can result in significant errors in some cases. It is anticipated that a flexible and user-friendly software package for evaluating risk will eventually be developed to supplement this document. Such a package will be capable of accurately implementing the calculation method presented in Appendix E to calculate risks from general exposure patterns, rather than from constant exposures only.

Requirements for Asbestos Measurements. One additional advantage of the approach for evaluating asbestos-related risks recommended in this document (in comparison to the current approach) is that the procedure for assessing risks is tied unambiguously to a specific index for measuring and expressing exposure (i.e., the index of all fibrous structures longer than 10 μm and thinner than 0.4 μm, as defined in Section 7.5) and this, in turn, is tied unambiguously to requirements for analyzing asbestos samples.

Estimates of airborne asbestos concentrations that are required to support risk assessment can be derived either by extrapolation from airborne measurements or by modeling release and dispersion of asbestos from sources (soils or other bulk materials). In either case, exposure estimates must be representative of actual (time-dependent) exposure and must provide measurements that include only fibrous structures satisfying the dimensional criteria listed in the last paragraph. Additional considerations that need to be addressed to assure the validity of risk estimates derived using this protocol include:

- the array of samples collected for estimating airborne asbestos concentrations must be representative of the exposure environment;

- the time variation of airborne asbestos concentrations must be properly addressed;

- airborne samples must be collected on membrane filters that are suitable for preparation for analysis by transmission electron microscopy (TEM). Appropriate rocedures for sample collection are described in Chatfield and Berman (1990) or the ISO Method (ISO 10312)[2];

[2]Note that the ISO Method (ISO 10312) is a refinement of the method originally published as the Interim Superfund Method (Chatfield and Berman 1990). It incorporates improved rules for evaluating fiber morphology. Both methods derive from a common development effort headed by Eric Chatfield.

- sample filters must be prepared for analysis using a direct transfer procedure (e.g., ISO 10312). Should indirect preparation be required (due, for example, to problems with overloading of sample filters), a sufficient number of paired samples will need to be collected and analyzed to establish a site-specific correlation between directly and indirectly prepared samples;

- samples must be analyzed by TEM;

- samples must be analyzed using the counting and characterization rules defined in ISO 10312 and the structures used to determine exposure concentrations for use with this protocol need to satisfy the dimensional criteria defined in Section 7.5 (i.e., structures longer than 10 μm and thinner than 0.4 μm). Importantly, ISO Method rules require separate enumeration and characterization of component fibers and bundles that are observed within more complex clusters and matrices. Such components, if they meet the dimensional criteria defined above must be included in the structure count;

- when risks are estimated using the risk tables (Tables 8-2 or 8-3) the risk values selected from the tables must be appropriate for the fiber type (i.e., chrysotile or amphibole) and the disease endpoint (i.e., lung cancer or mesothelioma) relevant to the situation of interest; and

- to use Tables 8-2 or 8-3, the concentration of total asbestos structures longer than 10 μm and thinner than 0.4 μm must be derived, divided by 0.0001, and multiplied by the risk estimate listed in the appropriate cell of the selected table to generate the risk estimate of interest.

Considerations that need to be addressed to assure the validity of risk estimates derived from soil or bulk measurements combined with release and transport modeling include:

- the array of samples collected for estimating source concentrations must be representative of the surface area or volume of source material from which asbestos is expected to be released and contribute to exposure;

- samples must be prepared and analyzed using the Modified Elutriator Method for soils and bulk materials (Berman and Kolk 1997, 2000), which is the only method capable of providing bulk measurements that can be related to risk;

- membrane filter samples prepared using the tumbler and vertical elutriator per the Superfund method must themselves be prepared for TEM analysis using a direct transfer procedure;

- TEM analysis must be conducted using the counting and characterization rules defined in the ISO Method (ISO 10312) in precisely the same manner that is described above for air measurements. Also, the same size categories need to be evaluated (in the same manner described above) to estimate exposures for use with this protocol to assess risk; and

- release and dispersion models that are selected for assessing risks must be appropriate to the exposure scenario and environmental conditions of interest. Such models must also be adapted properly so that they accept input estimates expressed in terms of fiber number concentrations. Procedures suggested for adapting such models are illustrated in a recent publication (Berman 2000).

Note, if new analytical procedures can be designed to focus on long structures, risks can be evaluated more cost-effectively. The alternate approach of spending a large proportion of available resources counting many (potentially non-potent or marginally potent) short structures, while not characterizing longer structures with adequate sensitivity or precision, leaves open the possibility of missing potentially serious hazards because a small population of extremely potent, long fibers were missed in a particular environment. Moreover, any potential contribution to risk by shorter structures will be incorporated to some extent by default, i.e., to the extent that similar proportions of such structures were also present in the environments from which the exposure-response coefficients were derived and such structures are known to have been ubiquitous in these environments (see, for example, Dement and Harris 1979**;** Gibbs and Hwang 1980; Hwang and Gibbs 1981).

8.3 RECOMMENDATIONS FOR FURTHER STUDY

A small number of limited and focused studies (described previously) are recommended in this document because they are likely to provide very cost-effective improvements to the quality of this document and may support substantial improvement to the recommended procedures for assessing asbestos-related risks. The recommended studies are:

(1) a focused study to expand our evaluation of the current U.S. EPA models to include other candidate models that might better track the exposure dependence of asbestos-related disease (Sections 7.2.2 and 7.3.2). Such models should also be used to explore and better represent the relationship between smoking and asbestos exposure (to the extent that data suitable for supporting such an analysis can be acquired); and

(2) a focused study to develop the supporting data needed to define adjustments for potency factors that will allow them to be used with an exposure index that even more closely captures asbestos characteristics that determine biological activity than the currently proposed index (Section 7.5).

Note that, by properly designing the second of the above-listed studies, it may also be possible to further address another outstanding issue that was previously identified: the question of whether exposure-response coefficients derived from mining studies are under-estimated relative to studies involving asbestos products because exposures in the mining studies may contain large numbers of non-asbestos particles contributed by the disturbance of host rock (Appendix D).

9.0 REFERENCES

Aalto M; Heppleston AG. Fibrogenesis by Mineral Fibres: An *In-Vitro* Study of the Roles of the Macrophage and Fibre Length. *British Journal of Experimental Pathology*. 65:91–99. 1984.

Adamson IYR. Early Mesothelial Cell Proliferation After Asbestos Exposure: *In Vivo* and *In Vitro* Studies. *Environmental Health Perspectives*. 105(Suppl 5):1205–1208. September. 1997.

Addison J. Consultant Mineralogist, John Addison Consultancy, Cottingham, East Yorkshire, UK. 2001. (private communication)

Afaq F; Abidi P; Matin R; Rahman Q. Activation of Alveolar Macrophages and Peripheral Red Blood Cells in Rats exposed to Fibers/Particles. *Toxicology Letters*. 99:175–182. 1998.

Albin M; Jakobsson K; Attewell R; Johansson L; Welinder H. Mortality and Cancer Morbidity in Cohorts of Asbestos Cement Workers and Referents. *British Journal of Industrial Medicine*. 79(9):602–610. September. 1990.

Albin M; Pooley FD; Stromberg U; Attewell R; Mitha R; Johansson L; Welinder H. Retention Patterns of Asbestos Fibres in Lung Tissue Among Asbestos Cement Workers. *Occupational and Environmental Medicine*. 51:205–211. 1994.

Albin M; Magnani C; Krstev S; Rapiti E; Shefer I. Asbestos and Cancer: An Overview of Current Trends in Europe. *Environmental Health Perspectives*. 107(2):289–298. May. 1999.

Amandus HE; Wheeler R. The Morbidity and Mortality of Vermiculite Miners and Millers Exposed to Tremolite-Actinolite: Part II. Mortality. *American Journal of Industrial Medicine* 11:15–26. 1987.

Amandus HE; Wheeler R; Jankovic J; Tucker J. The Morbidity and Mortality of Vermiculite Miners and Millers Exposed to Tremolite-Actinolite: Part I. Exposure Estimates. *American Journal of Industrial Medicine*. 11:1–14. 1987.

Armstrong BK; de Klerk NH; Musk AW; Hobbs MST. Mortality in Miners and Millers of Crocidolite in Western Australia. *British Journal of Industrial Medicine*. 45:5–13. 1988.

Asgharian B; Yu CP. Deposition of Inhaled Fibrous Particles in the Human Lung. *Journal of Aerosol Medicine*. 1:37–50. 1988.

Barchowsky A; Lannon BM; Elmore LC; Treadwell MD. Increased Focal Adhesion Kinase- and Urokinase-Type Plasminogen Activator Receptor-Associated Cell Signaling in Endothelial Cells Exposed to Asbestos. *Environmental Health Perspectives*. 105:(Suppl)5:1131–1137. September. 1997.

Barchowsky A; Roussel RR; Krieser RJ; Mossman BT; Treadwell MD. Expression and Activity of Urokinase and its Receptor in Endothelial and Pulmonary Epithelial Cells Exposed to Asbestos. *Toxicology and Applied Pharmacology*. 152(2):388–396. 1998.

Baris YI; Simonato L; Artvinli M; Pooley F; Saracci R; Skidmore J; Wagner C. Epidemiological and Environmental Evidence of the Health Effects of Exposure to Erionite Fibres: A Four-Year Study in the Cappadocian Region of Turkey. *International Journal of Cancer*. 39:10–17. 1987.

Bauman MD; Jetten AM; Bonner JC; Kumar RK; Bennett RA; Brody AR. Secretion of a Platelet-Derived Growth Factor Homologue by Rat Alveolar Macrophages Exposed to Particulates *In Vitro*. *European Journal of Cell Biology*. 51:327–334. 1990.

Beckett ST. The Generation and Evaluation of UICC Asbestos Clouds in Animal Exposure Chambers. *Annals of Occupational Hygiene*. 18:187–198. 1975.

Bellman B; Konig H; Muhle H; Pott F. Chemical Durability of Asbestos and of Man-Made Mineral Fibres *In Vivo*. *Journal of Aerosol Science*. 17(3):341–345. 1986.

Bellman B; Muhle H; Pott F; Konig H; Kloppeel H; Spurny K. Persistence of Man-Made Fibers (MMF) and Asbestos in Rat Lungs. *Annals of Occupational Hygiene*. 31:693–709. 1987.

Berman DW. Asbestos Measurement in Soils and Bulk Materials: Sensitivity, Precision, and Interpretation – You Can Have It All. In *Advances in Environmental Measurement Methods for Asbestos*. ASTM STP 1342. Beard ME; Rook HL (eds.). American Society for Testing and Materials. 2000.

Berman DW. President, Aeolus, Inc., Albany, CA. (unpublished data)

Berman DW Chatfield EJ. Interim Superfund Method for the Determination of Asbestos in Ambient Air. Part 2: Technical Background Document. Office of Solid Waste and Remedial Response. U.S. Environmental Protection Agency, Washington, D.C. EPA/540/2-90/005b. May. 1990.

Berman DW and Crump KS. Methodology for Conducting Risk Assessments at Asbestos Superfund Sites. Part 2: Technical Background Document. Prepared for: Kent Kitchingman, U.S. Environmental Protection Agency, Region 9. Work Assignment No. 59-06-D800 under Contract No. 68-W9-0059. 1999.

Berman DW; Crump KS. Technical Support Document for a Protocol to Assess Asbestos-Related Risk. Final Draft. Prepared for the Volpe Center, U.S. Dept. of Transportation, Cambridge, MA and the U.S. EPA, Region 8, Denver , CO. Prepared under Contract No. DTRS57-01-C-10044. September. 2001.

Berman DW; Kolk AJ. Superfund Method for the Determination of Asbestos in Soils and Bulk Materials. Office of Solid Waste and Emergency Response. U.S. Environmental Protection Agency, Washington, D.C., EPA 540-R-97-028. 1997.

Berman DW; Kolk AJ. Draft: Modified Elutriator Method for the Determination of Asbestos in Soils and Bulk Materials. Aeolus, Inc. 751 Taft St., Albany, CA 94706. 2000. (unpublished)

Berman DW; Crump KS; Chatfield EJ; Davis JMG; Jones AD. The Sizes, Shapes, and Mineralogy of Asbestos Structures that Induce Lung Tumors or Mesothelioma in AF/HAN Rats Following Inhalation. *Risk Analysis*. 15(2):181–195. 1995.

Berman DW; Crump KS; Chatfield EJ; Davis JMG; Jones AD. The Size Distribution of Fibers and Particles in Airborne Dust Generated for Selected Animal Inhalation Studies. (in preparation)

Bernstein DM; Morscheidt C; Grimm H-G; Thevenaz P; Teichert U. Evaluation of Soluble Fibers Using the Inhalation Biopersistence, a Nine-Fiber Comparison. *Inhalation Toxicology*. 8:345–385. 1996.

Berry G; Newhouse ML. Mortality of Workers Manufacturing Friction Materials Using Asbestos. *British Journal of Industrial Medicine*. 40:1–7. 1983.

Bertrand R; Pezerat H. Fibrous Glass: Carcinogenicity and Dimensional Characteristics. In *Biological Effects of Mineral Fibres*. Wagner JC (ed.). IARC Scientific Publications. pp. 901–911. 1980.

Bignon J; Monchaux G; Sebastien P; Hirsch A; Lafuma J. Human and Experimental Data on Translocation of Asbestos Fibers Through the Respiratory System. *Annals of New York Academy of Sciences*. 330:745–750. 1979.

Blake T; Castranova V; Schwegler-Berry D; Baron P; Deye GL; Li C; Jones W. Effect of Fiber Length on Glass Microfiber Cytotoxity. *Journal of Toxicology and Environmental Health.* 54(Part A):243–259. 1998.

Bolton RE; Davis J; Donaldson K; Wright A. Variation in the Carcinogenicity of Mineral Fibres. *Annals of Occupational Hygiene*. 26(1-4):569–582. 1982.

Bolton RE; Davis JMG; Miller B; Donaldson K; Wright A. The Effect of Dose of Asbestos on Mesothelioma Production in the Laboratory Rat. *Proceedings of the VIth International Pneumonoconiosis Conference*. 2:1028–1035. 1984.

Bolton RE; Addison J; Davis JMG; Donaldson K; Jones AD; Miller BG; Wright A. Effects of the Inhalation of Dusts from Calcium Silicate Insulation Materials in Laboratory Rates. *Environmental Research*. 39:26–43. 1986.

Bonneau L; Malard C; Pezerat H. Studies on Surface Properties of Asbestos. *Environmental Research*. 41:268–275. 1986.

Boutin C; Dumortier P; Rey F; Viallat JR; De Vuyst P. Black Spots Concentrate Oncogenic Asbestos Fibers in the Parietal Pleura: Thoracoscopic and Mineralogic Study. *American Journal of Respiratory and Critical Care Medicine*. 153:444–449. 1996.

Brass DM; Hoyle GW; Poovey HG; Liu J-Y; Brody AR. Reduced Tumor Necrosis Factor-Alpha and Transforming Growth Factor-Beta-1 Expression in the Lungs of Inbred Mice That Fail to Develop Fibroproliferative Lesions Consequent to Asbestos Exposure. *American Journal of Pathology*. 154(3)853–862. 1999.

Broaddus VC; Yang L; Scabo LM; Ernst JD; Boylan AM. Crocidolite Asbestos Induces Apoptosis of Pleural Mesothelial Cells: Role of Reactive Oxygen Species and Poly(ADP-ribosyl) Polymerase. *Environmental Health Perspectives*. 105(Suppl 5):1147–1152. September. 1997.

Brody AR; Hill LH; Adkins B; O'Connor RW. Chrysotile Asbestos Inhalation in Rats: Deposition Pattern and Reaction of Alveolar Epithelium and Pulmonary Macrophages. *American Review of Respiratory Diseases*. 123:670–679. 1981.

Brody AR; Liu J-Y; Brass D; Corti M. Analyzing the Genes and Peptide Growth Factors Expressed in Lung Cells *In Vivo* Consequent to Asbestos Exposure. *Environmental Health Perspectives*. 105(Suppl 5):1165–1171. September. 1997.

Brown DM; Fisher C; Donaldson K. Free Radical Activity of Synthetic Vitreous Fibers: Iron Chelation Inhibits hydroxyl Radical Generation by Refractory Ceramic Fiber. *Journal of Toxicology and Environmental Health Part A*. 53(7):545–561. 1998.

Campbell WJ; Huggins CW; Wylie AG. Chemical and Physical Characterization of Amosite, Chrysotile, Crocidolite, and Nonfibrous Tremolite for Oral Ingestion Studies by the National Institute of Environmental Health Sciences. Report of Investigations 8452. National Library of Natural Resources, U.S. Department of the Interior. 1980.

Case BW; Dufresne A. Asbestos, Asbestosis, and Lung Cancer: Observations in Quebec Chrysotile Workers. *Environmental Health Perspectives*. 105(Suppl 5):1113–1120. September. 1997.

Case BW; Dufresne A; McDonald AD; McDonald JC; Sebastien P. Asbestos Fiber Type and Length in Lungs of Chrysotile Textile and Production Workers: Fibers Longer than 18 µm. *Inhalation Toxicology*. 1(Suppl 1):411–418. 2000.

Castranova V; Vallyathan V; Ramsey DM; McLaurin JL; Pack D; Leonard S; Barger MW; Ma JUC; Dalal NS; Teass A. Augmentation of Pulmonary Reactions to Quartz Inhalation by Trace Amounts of Iron-Containing Particles. *Environmental Health Perspectives*. 105(Suppl 5):1319–1324. September. 1997.

Chang L-Y; Overby LH; Broday AR; Crapo JD. Progressive Lung Cell Reactions and Extracellular Matrix Production After a Brief Exposure to Asbestos. *American Journal of Pathology*. 131(1):156–170. 1989.

Chao C-C; Park S-H; Aust AE. Participation of Nitric Oxide and Iron in the Oxidation of DNA in Asbestos-Treated Human Lung Epithelial Cells. *Archives of Biochemistry and Biophysics*. 326(1):152–157. 1996.

CHAP (Chronic Hazard Advisory Panel on Asbestos). Report to the U.S. Consumer Product Safety Commission. July. 1983.

Chatfield EJ. Ambient Air: Determination of Asbestos Fibres, Direct Transfer Transmission Electron Microscopy Procedure. Submitted to the International Standards Organization: ISO/TC 10312. 1995.

Chatfield EJ; Berman DW. Interim Superfund Method for the Determination of Asbestos in Ambient Air. Part 1: Method. Office of Solid Waste and Remedial Response. U.S. Environmental Protection Agency, Washington, D.C. EPA/540/2-90/005a. May. 1990.

Chen YK. Ph.D. Dissertation. Mechanical and Aerospace Engineering, State University of New York at Buffalo. 1992.

Chen YK; Yu CP. Deposition of Charged Fiber in the Human Lung. *Journal of Aerosol Science*. 24(Suppl 1):5459–5460. 1993.

Cherrie JW; Dodgson J; Groat S; Carson M. Comparison of Optical and Electron Microscopy for Evaluating Airborne Asbestos. Institute of Occupational Medicine, Edinburgh, (U.S. Department of Commerce). 1979.

Cherrie JW; Dodgson J; Groat S; Carson M. Comparison of Optical and Electron Microscopy for Evaluating Airborne Asbestos. Institute of Occupational Medicine, Edinburgh, U.S. Department of Commerce. 1987.

Chesson J; Rench JD; Schultz BD; Milne KL. Interpretation of Airborne Asbestos Measurements. *Risk Analysis*. 10(3):437–47. 1990.

Choe N; Tanaka S; Xia; W; Hemenway DR; Roggli VI; Kagan E. Pleural Macrophage Recruitment and Activation in Asbestos-Induced Pleural Injury. *Environmental Health Perspectives*. 105(Suppl 5):1257–1260. September. 1997.

Choe N; Tanaka S; Kagan E. Asbestos Fibers and Interleukin-1 Upregulate the Formation of Reactive Nitrogen Species in Rat Pleural Mesothelial Cells. *American Journal of Respiratory Cell and Molecular Biology*. 19(2):226–236. 1998.

Choe N; Zhang J; Iwagaki A; Tanaka S; Hemenway DR; Kagan E. Asbestos Exposure Upregulates the Adhesion of Pleural Leukocites to Pleural Mesothelial Cells via VCAM-1. *American Journal of Physiology*. 277(2:Part 1):L292–L300. 1999.

Churg A. Deposition and clearance of chrysotile asbestos. *Annals of Occupational Hygiene*. 38(4):625–633. 1994.

Churg A; Wright JL; Stevens B. Exogenous mineral particles in the human bronchial mucosa and lung parenchyma. I. Nonsmokers in the general population. *Experimental Lung Research*. 16:159–175. 1990.

Churg A; Wiggs B; Depaoli L; Kampe B; Stevens B. Lung Asbestos Content in Chrysotile Workers with Mesothelioma. *American Review of Respiratory Disease*. 130:1042–1045. 1984.

Coin PG; Roggli VL; Brody AR. Deposition, Clearance, and Translocation of Chrysotile Asbestos from Peripheral and Central Regions of the Rat Lung. *Environmental Research*. 58:970–116. 1992.

Coin PG; Roggli VL; Brody AR. Persistence of Long, Thin Chrysotile Asbestos Fibers in the Lungs of Rats. *Environmental Health Perspectives*. 102(Suppl 5):197–199. 1994.

Costa DL; Dreher KL. Bioavailable Transition Metals in Particulate Matter Mediate Cardiopulmonary Injury in Healthy and Compromised Animal Models. *Environmental Health Perspectives*. 105(Suppl 5):1053–1060. September. 1997.

Cox D; Lindley D. *Theoretical Statistics*. Chapman and Hall, London. 1974.

Cox D; Oakes DV. *Analysis of Survival Data*. Cox DR; Hinkley DV (eds.). Chapman and Hall, London. 1984.

Crump KS. The Effect of Random Error in Exposure Measurement upon the Shape of the Dose Response. *Nonlinearity in Biology, Toxicology and Medicine*. 2003. (pending publications)

Crump KS. Asbestos Potency Assessment for EPA Hearing. Prepared for Asbestos Information Association/North America. 116 pp. 1986.

Davis JMG; Cowie HA. The Relationship Between Fibrosis and Cancer in Experimental Animals Exposed to Asbestos and Other Fibers. *Environmental Health Perspectives*. 88:305–309. 1990.

Davis JMG; Jones AD. Comparisons of the Pathogenicity of Long and Short Fibres of Chrysotile Asbestos in Rats. *British Journal of Exposure Pathology*. 69(5):171–738. 1988b.

Davis JMG; Beckett ST; Bolton RE; Collings P; Middleton AP. Mass and Number of Fibres in the Pathogenesis of Asbestos-Related Lung Disease in Rats. *British Journal of Cancer*. 37:673–688. 1978.

Davis JMG; Beckett ST; Bolton RE; Donaldson K. A Comparison of the Pathological Effects in Rats of the UICC Reference Samples of Amosite and Chrysotile with Those of Amosite and Chrysotile Collected from the Factory Environment. In *Biological Effects of Mineral Fibres*. Wagner JC (ed.). IARC Scientific Publications. pp. 288–292. 1980.

Davis JMG; Addison J; Bolton RE; Donaldson K; Jones AD; Miller BG. Inhalation Studies on the Effects of Tremolite and Brucite Dust in Rats. *Carcinogenesis*. 6(5):667–674. 1985.

Davis JMG; Addison J; Bolton R; Donaldson K; Jones AD; Smith T. The Pathogenicity of Long Versus Short Fibre Samples of Amosite Asbestos Administered to Rats by Inhalation and Intraperitoneal Injection. *British Journal of Experimental Pathology*. 67:415–430. 1986a.

Davis JMG; Gylseth G; Morgan A. Assessment of Mineral Fibres from Human Lung Tissue. *Thorax*. 41:167–175. 1986b.

Davis JMG; Bolton RE; Brown D; Tully HE. Experimental Lesions in Rats Corresponding to Advanced Human Asbestosis. *Exposure Molecular Pathology*. 44(2):207–221. 1986c.

Davis JMG; Addison J; Bolton RE; Donaldson K; Jones AD. Inhalation and Injection Studies in Rats Using Dust Samples from Chrysotile Asbestos Prepared by a Wet Dispersion Process. *British Journal of Pathology*. 67:113–129. 1986d.

Davis JMG; Jones AD; Smith T. Comparisons of the Pathogenicity of Long and Short Fibres of Chrysotile Asbestos in Rats. Institute for Research and Development of Asbestos, Montreal (ed.). Institute of Occupational Medicine. Report No. TM-87/08. 1987.

Davis JMG; Bolton RE; Douglas AN; Jones AD; Smith T. Effects of Electrostatic Charge on the Pathogenicity of Chrysotile Asbestos. *British Journal of Industrial Medicine*. 45(5):292–309. 1988a.

Davis JMG; Addison J; McIntosh C; Miller BG; Niven K. Variations in the Carcinogenicity of Tremolite Dust Samples of Differing Morphology. *Annals New York Academy of Sciences*. 473–490. 1991.

de Klerk N. Unpublished Raw Data Provided to Dr. Wayne Berman by Dr. Nick de Klerk from Study of Crocidolite Miners in Wittenoom, Australia, originally described in Armstrong et al. (1988) but with followup extended through 1999. 2001.

de Klerk NH; Musk AW; Armstrong BK; Hobbs MST. Diseases in Miners and Millers of Crocidolite from Wittenoom, Western Australia: A Further Followup to December 1986. *Annals of Occupational Hygiene*. 38(Suppl 1):647–655. 1994.

Dement JM. Estimation of Dose and Evaluation of Dose-Response in a Retrospective Cohort Mortality Study of Chrysotile Asbestos Textile Workers. Ph.D. Thesis. The University of North Carolina at Chapel Hill. 1980.

Dement JM; Brown DP. Lung Cancer Mortality Among Asbestos Textile Workers: A Review and Update. *Annals of Occupational Hygiene*. 38(4):525–532. 1994.

Dement JM; Brown DP. Cohort Mortality and Case-Control Studies of White Male Chrysotile Asbestos Textile Workers. *Journal of Clean Technology, Environmental Toxicology, and Occupational Medicine*. 7:1052–1062. 1998.

Dement JM; Harris RL. Estimates of Pulmonary and Gastrointestinal Deposition for Occupational Fiber Exposure. NTIS PB80-149644. U.S. HEW Contract #78-2438. 1979.

Dement JM; Harris RL; Symons MJ; Shy CM. Estimates of Dose-Response for Respiratory Cancer Among Chrysotile Asbestos Textile Workers. *Annals Occupational Hygiene*. 26(1-4):869–887. 1982.

Dement JM; Harris RL; Symons MJ; Shy CM. Exposures and Mortality Among Chrysotile Workers. Part I: Exposure Estimates. *American Journal of Industrial Medicine*. 4:399–419. 1983a.

Dement JM; Harris RL; Symons MJ; Shy CM. Exposures and Mortality Among Chrysotile Workers. Part II: Mortality. *American Journal of Industrial Medicine*. 4:421–433. 1983b.

Dement JM; Brown DP; Okun A. Follow-up Study of Chrysotile Asbestos Textile Workers: Cohort Mortality and Case-Control Analysis. *American Journal of Industrial Medicine*. 26:431–447. 1994.

Doll R; Peto R. Cigarette Smoking and Bronchial Carcinoma: Dose and Time Relationships Among Regular Smokers and Lifelong Non-Smokers. *Journal of Epidemiology and Community Health*. 32:303–313. 1978.

Doll R; Peto J. Asbestos: Effects on Health of Exposure to Asbestos. Health and Safety Commission, London, United Kingdom. 1985.

Dopp E; Schiffmann D. Analysis of Chromosomal Alterations Induced by Asbestos and Ceramic Fibers. *Toxicology Letters*. 96-97:155–162. 1998.

Driscoll KE; Carter JM; Hassenbein DG; Howard B. Cytokines and Particle-Induced Inflammatory Cell Recruitment. *Environmental Health Perspectives*. 105(Suppl 5):1159–1164. September. 1997.

Eastes W; Hadley JG. A Mathematical Model of Fiber Carcinogenicity and Fibrous in Inhalation and Intraperitoneal Experiments in Rats. *Inhalation Toxicology*. 8:323–343. 1994.

Eastes W; Hadley JG. Dissolution of Fibers Inhaled by Rats. *Inhalation Toxicology*. 7:179–196. 1995.

Eastes W; Hadley JG. A Mathematical Model of Fiber Carcinogenicity and Fibrous in Inhalation and Intraperitoneal Experiments in Rats. *Inhalation Toxicology*. 8:323–343. 1996.

Economou P; Samet JM; Lechner JF. Familial and Genetic Factors in the Pathogenesis of Lung Cancer. In: *Epidemiology of Lung Cancer*. Chapter 14. Samet JM (ed.). Marcel Dekker, Inc., New York. 1994.

Enterline PE; Harley J; Henderson V. Asbestos and Cancer -- A Cohort Followed to Death. Graduate School of Public Health, University of Pittsburgh. 1986.

Everitt JI; Gelzleichter TR; Bermudez E; Mangum JB; Wong BA; Janszen DB; Moss OR. Comparison of Pleural Responses of Rats and Hamsters to Subchronic Inhalation of Refractory Ceramic Fibers. *Environmental Health Perspectives*. 105(Suppl 5):1209–1213. September. 1997.

Finkelstein MM. Mortality Among Long-Term Employees of an Ontario Asbestos-Cement Factory. *British Journal of Industrial Medicine*. 40:138–144. 1983.

Finkelstein MM. Mortality Among Employees of an Ontario Asbestos-Cement Factory. *American Review of Respiratory Disease*. 129:754–761. 1984.

Finkelstein MM; Dufresne A. Inferences on the Kinetics of Asbestos Deposition and Clearance Among Chrysotile Miners and Millers. *American Journal of Industrial Medicine*. 35(4):401–412. April 1999.

Finkelstein JN; Johnston C; Barrett T; Oberdorster G. Particulate-Cell Interactions and Pulmonary Cytokine Expression. *Environmental Health Perspectives*. 105(Suppl 5):1179–1182. September. 1997.

Floyd RA. Role of Oxygen Free Radicals in Carcinogenesis and Brain Ischemia. *The FASEB Journal*. 4:2587–2597. June. 1990.

Fubini B. Surface Reactivity in the Pathogenic Response to Particulates. *Environmental Health Perspectives*. 105(Suppl 5):1013–1020. September. 1997.

Gehr P; Geiser M; Stone KC; Crapo JD. Morphometric Analysis of the Gas Exchange Region of the Lung. In *Toxicology of the Lung*, 2nd edition. Gardner DE; Crapo JD; McClellan RO (eds.). Raven Press, New York. 1993.

Ghio AJ; Kadiiska MB; Xiang Q-H; Mason RP. *In Vivo* Evidence of Free Radical Formation After Asbestos Instillation: An ESR Spin Trapping Investigation. *Free Radical Biology and Medicine*. 24(1):11–17. 1998.

Gibbs GW; Hwang CY. Physical Parameters of Airborne Asbestos Fibres in Various Work Environments - Preliminary Findings. *American Industrial Hygiene Association Journal*. 36(6):459–466. 1975.

Gibbs GW; Hwang CY. Dimensions of Airborne Asbestos Fibers. In *Biological Effects of Mineral Fibers*. Wagner JC (ed.). IARC Scientific Publication. pp. 69–78. 1980.

Gilbert O. *Statistical Method for Environmental Pollution Monitoring*. Van Nostrand Reinhold, New York. 1987.

Gold J; Amandusson H; Krozer A; Kasemo B; Ericsson T; Zanetti G; Fubini B. Chemical Characterization and Reactivity of Iron Chelator-Treated Amphibole Asbestos. *Environmental Health Perspectives*. 105(Supple 5):1021–1030. 1997.

Goldstein B; Rendall R; Webster I. A Comparison of the Effects of Exposure of Baboons to Crocidolite and Fibrous-Glass Dusts. *Environmental Research*. 32:334–359. 1983.

Golladay SA; Park S-H; Aust AE. Efflux of Reduced Glutathione after Exposure of Human Lung epithelial Cells to Crocidolite Asbestos. *Environmental Health Perspectives*. 105(Suppl 5):1273–1278. 1997.

Goodglick LA; Kane AB. Cytotoxicity of Long and Short Crocidolite Asbestos Fibers *In Vitro* and Iin Vivo. *Cancer Research*. 50:5153–5163. 1990.

Governa M; Camilucci L; Amati M; Visona I; Valentino M; Botta GC; Campopiano A; Fanizza C. Wollastonite Fibers *In Vitro* Generate Reactive Oxygen Species Able to Lyse Erythrocytes and Activate the Complement Alternate Pathway. *Toxicological Sciences*. 44(1):32–38. 1998.

Gross TJ; Cobb SM; Peterson MW. Asbestos Exposure Increases Paracellular Transport of Fibrin Degradation Products Across Human Airway Epithelium. *American Journal of Physiology*. 266(3):L287–295. March. 1994.

Hammond EC; Selikoff IJ; Seidman H. Asbestos Exposure, Cigarette Smoking and Death Rates. *Annals New York Academy of Sciences*. 330:473–490. 1979.

Harris RL; Timbrell V. The Influence of Fibre Shape in Lung Deposition - Mathematical Estimates. *Inhaled Particles IV*. Walton WH (ed.). Pergamon Press. 1977.

Hart GA; Kathman LM; Hesterberg TW. *In Vitro* Cytotoxicity of Asbestos and Man-Made Vitreous Fibers: Roles of Fiber Length, Diameter and Composition. *Carcinogenesis*. 15(5):971–977. May. 1994.

Health Effects Institute - Asbestos Research (HEI-AR). Asbestos in Public and Commercial Buildings: A Literature Review and Synthesis of Current Knowledge. HEI-AR, 141 Portland St., Suite 7100, Cambridge, MA. 1991.

Health Effects Institute (HEI). Asbestos in Public and Commercial Buildings: A Literature Review and Synthesis of Current Knowledge. 1991.

Hei TK; Wu LJ; Piao CQ. Malignant Transformation of Immortalized Human Bronchial Epithelial Cells by Asbestos Fibers. *Environmental Health Perspectives*. 105(Suppl 5):1085–1088. September. 1997.

Heidenreich WF; Luebeck EG; Moolgavkar SH. Some Properties of the Hazard Function of the Two-Mutation Clonal Expansion Model. *Risk Analysis*. 17:391–399. 1997.

Henderson VL; Enterline PE. Asbestos Exposure: Factors Associated with Excess Cancer and Respiratory Disease Mortality. *Annals New York Academy of Sciences*. 330:117–126. 1979.

Hesterberg TW; Miller WC; McConnell EE; Chevalier J; Hadley JG; Bernstein DM; Thevenaz P; Anderson R. Chronic Inhalation Toxicity of Size-Separated Glass Fibers in Fischer 344 Rats. *Fundamental and Applied Toxicology*. 20:464–476. 1993.

Hesterberg TW; Miiller WC; Thevenaz P; Anderson R. Chronic Inhalation Studies of Man-Made Vitreous Fibres: Characterization of Fibres in the Exposure Aerosol and Lungs. *Annals of Occupational Hygiene*. 39(5):637–653. 1995.

Hesterberg TW; Miiller WC; Musselkman RP; Kamstrup O; Hamilton RD; Thevenaz P. Biopersistence of Man-Made Vitreous Fibers and Crocidolite Asbestos in Rat Lung Following Inhalation. *Fundamentals and Applied Toxicology*. 29:267–279. 1996.

Hesterberg TW; Axten C; McConnell EE; Oberdorster G; Everitt J; Miller WC; Chevalier J; Chase GR; Thevenaz P. Chronic Inhalation Study of Fiber Glass and Amosite Asbestos in Hamsters: Twelve-Month Preliminary Results. *Environmental Health Perspectives*. 105(Suppl 5):1223–1230. September. 1997.

Hesterberg TW; Chase G; Axten C; Miller WC; Musselman RP; Kamstrup O; Hadley J; Morscheidt C; Bernstein DM; Thevenaz P. Biopersistence of Synthetic Vitreous Fibers and Amosite Asbestos in the Rat Lung Following Inhalation. *Toxicology and Applied Pharmacology*. 151:262–275. 1998a.

Hesterberg TW; Hart GA; Chevalier J; Miller WC; Hamilton RD; Bauer J; Thevenaz P. The Importance of Fiber Biopersistence and Lung Dose in Determining the Chronic Inhalation Effects of X607, RCF1, and Chrysolite Asbestos in Rats. *Toxicology and Applied Pharmacology*. 153(1):68–82. 1998b.

Hodgson AA. Fibrous Silicates. Lecture Series No. 4. The Royal Institute of Chemistry, London, United Kingdom. 1965.

Hodgson J; Darnton A. The Quantitative Risk of Mesothelioma and Lung Cancer in Relation to Asbestos Exposure. *Annals of Occupational Hygiene*. 44(8):565–601. 2000.

Holian A; Uthman MO; Goltsova T; Brown SD; Hamilton RF. Asbestos and Silica-Induced Changes in Human Alveolar Macrophage Phenotype. *Environmental Health Perspectives*. 105(Suppl 5):1139–1142. September. 1997.

Hughes JM; Weill H. Asbestos Exposure: Quantitative Assessment of Risk. *American Review of Respiratory Disease*. 133:5–13. 1986.

Hughes JM; Weill H; Hammad YY. Mortality of Workers Employed at Two Asbestos Cement Plants. *British Journal of Industrial Medicine*. 44:161–174. 1987.

Hume LA; Rimstidt. The Biodurability of Chrysotile Asbestos. *American Mineralogist*. 77:1125–1128. 1992.

Hwang CY; Gibbs GW. The Dimensions of Airborne Asbestos Fibres --I. Crocidolite from Kuruman Area, Cape Province, South Africa. *Annals Occupational Hygiene*. 24(1):23–41. 1981.

Ilgren E; Chatfield E. Coalinga Fibre: A Short, Amphibole-Free Chrysotile. Part 3: Lack of Biopersistence. *Indoor Built Environment*. 7:98–100. 1998.

International Agency for Research on Cancer (IARC). Monographs on the Evaluation of Carcinogenic Risks to Man. Volume 14. IARC Scientific Publications. Lyon, France. 1977.

Integrated Risk Information System (IRIS). Toxicological Review of Asbestos. U.S. Environmental Protection Agency. Office of Research and Development, National Center for Environmental Assessment. Washington, D.C. http://www.epa.gov/iris/subst/0371.htm. 1998.

Ishizaki T; Yano E; Evans PH. Cellular Mechanisms of Reactive Oxygen Metabolite Generation from Human Polymorphonuclear Leukocytes Induced by Crocidolite Asbestos. *Environmental Research*. 75(2):135–140. 1997.

International Organization for Standardization (ISO). Ambient Air-Determination of Asbestos Fibres - Direct-Transfer Transmission Electron Microscopy Method. ISO 10312. 1995.

Jagirdar J; Lee TC; Reibman J; Gold LI; Aston C; Begin R; Rom WN. Immunohistochemical Localization of Transforming Growth Factor Beta Isoforms in Asbestos-Related Diseases. *Environmental Health Perspectives*. 105(Suppl 5):1197–1203. September. 1997.

Jaurand MC. Observations on the Carcinogenicity of Asbestos Fibers. *Annals New York Academy of Science*. 643:258–70. 1991.

Jaurand MC. Mechanisms of Fiber-Induced Genotoxicity. *Environmental Health Perspectives*. 105(Suppl 5):1073–1084. September. 1997.

Jesch NK; Dorger M; Enders G; Rieder G; Vogelmeier C; Messmer K; Krombach F. Expression of the Inducible Nitric Oxide Synthase and Formation of Nitric Oxide by Alveolar Macrophages. *Environmental Health Perspectives*. 105(Suppl 5):1297–1300. September. 1997.

Johnson NF. Asbestos-Induced Changes in Rat Lung Parenchyma. *Journal of Toxicology and Environmental Health*. 21:193–203. 1987.

Johnson NF; Jaramillo RJ. P53, Cip 1, and Gadd 153 Expression Following Treatment of A549 Cells with Natural and Man-Made Vitreous Fibers. *Environmental Health Perspectives*. 105(Suppl 5):1143–1145. September. 1997.

Jones AD; McMillan CH; Johnston AM; McIntosh C; Cowie H; Bolton RE; Borzuki G; Vincent JH. Pulmonary Clearance of UICC Amosite Fibres Inhaled by Rats During Chronic Exposure at Low Concentrations. *British Journal of Industrial Medicine*. 45:300–304. 1988.

Kaiglova A; Hurbankova M; Kovacikova Z. Impact of Acute and Subchronic Asbestos Exposure on Some Parameters of Antioxidant Defense System and Lung Tissue Injury. *Industrial Health*. 37(3):348–351. July. 1999.

Kamp DW; Graceffa P; Pryor WA; Weitzman SA. The Role of Free Radicals in Asbestos-Induced Diseases. *Free Radical Biology & Medicine*. 12:293–315. 1992.

Kamp DW; Dunne M; Dykewicz MS; Sbalchiero JS; Weitzman SA; Dunn MM. Asbestos-Induced Injury to Cultured Human Pulmonary Epithelial-Like Cells: Role of Neutrophil Elastase. *Journal of Leukocyte Biology*. 54:73–80. July. 1993.

Kamp DW; Greenberger MJ; Sbalchierro JS; Preusen SE; Weitzman SA. Cigarette Smoke Augments Asbestos-Induced Alveolar Epithelial Cell Injury: Role of Free Radicals. *Free Radical Biology & Medicine*. 25(6):728–739. 1998.

Kane AB; MacDonald JL. Mechanisms of Mesothelial Cell Injury, Proliferation, and Neoplasia Induced by Asbestos Fibers. Chapter 14. *Fiber Toxicology*. pp. 323–347. 1993.

Kauffer E; Vigneron JC; Hesbot A; Lemonnier M. A Study of the Length and Diameter of Fibres, in Lung and in Broncho-Alveolar Lavage Fluid, Following Exposure of Rats to Chrysotile Asbestos. *Annals of Occupational Hygiene*. 31(2):233–240. 1987.

Keane MJ; Miller WE; Ong T; Stephens JW; Wallace WE; Zhong B-Z. A Study of the Effect of Chrysotile Fiber Surface Composition on Genotoxicity *In Vitro*. *Journal of Toxicology and Environmental Health Part A*. 57(8):529–541. August. 1999.

Kimizuka G; Wang N; Hayashi Y. Physical and Microchemical Alterations of Chrysotile and Amosite Asbestos in the Hamster Lung. *Journal of Toxicology and Environmental Health*. 21:251–264. 1987.

Kodama Y; Boreiko CJ; Maness SC; Hesterberg TW. Cytotoxic and Cytogenetic Effects of Asbestos on Human Bronchial Epithelial Cells in Culture. *Carcinogenesis*. 14(4):691–697. 1993.

Kostyuk VA; Potapovich AI. Antiradical and Chelating Effects in Flavonoid Protection Against Silica-Induced Cell Injury. *Archives of Biochemistry and Biophysics*. 355(1):43–48. 1998.

Kravchenko IV; Furalyov VA; Vasylieva LA; Pylev LN. Spontaneous and Asbestos-Induced Transformation of Mesothelial Cells *In Vitro*. *Teratogenesis Carcinogenesis and Mutagenesis*. 18(3):141–151. 1998.

Krombach F; Münzing S; Allmeling AM; Gerlach JT; Behr J; Dörger M. Cell Size of Alveolar Macrophages: An Interspecies Comparison. *Environmental Health Perspectives*. 105(Suppl 5):1261–1263. September. 1997.

Lacquet LM; VanderLinden L; Lepoutre J. Roentgenographic Lung Changes, Asbestosis and Mortality in a Belgian Asbestos-Cement Factory. In *Biological Effects of Mineral Fibres*, Wagner JC (ed.). IARC Sci Publ. pp. 783–793. 1980.

Law BD; Bunn WB; Hesterberg TW. Solubility of Polymeric Organic Fibers and Manmade Vitreous Fibers in Gambles Solution. *Inhalation Toxicology*. 2:321–339. 1990.

Law BD; Bunn WB; Hesterberg TW. Dissolution of Natural Mineral and Man-Made Vitreous Fibers in Karnovsky's and Formalin Fixatives. *Inhalation Toxicology*. 3:309–321. 1991.

Leanderson P; Soderkvist P; Tagesson C; Axelson O. Formation of 8-hydroxydeoxyguanosine by Asbestos and Man-Made Mineral Fibres. *British Journal of Industrial Medicine*. 45:309–311. 1988.

Le Bouffant L. Physics and Chemistry of Asbestos Dust. In *Biological Effects of Mineral Fibres*. Wagner JC (ed.). IARC Scientific Publications. pp. 15–34. 1980.

Le Bouffant L; Daniel H; Heninn JP; Martin JC; Normand C; Tichoux G; Trolard F. Experimental Study on Long-Term Effects of Inhaled MMF on the Lungs of Rats. *Annals of Occupational Hygiene*. 31(4B):765–790. 1987.

Lechner JF; Tesfaigzi J; Gerwin BI. Oncogenes and Tumor-Suppressor Genes in Mesothelioma - A Synopsis. *Environmental Health Perspectives*. 105(Suppl 5):1061–1067. September. 1997.

Lee KP; Barras CE; Griffith RS; Waritz RS; Lapin CA. Comparative Pulmonary Responses to Inhaled Inorganic Fibers with Asbestos and Fiberglass. *Environmental Research*. 24:167–191. 1981.

Leigh J; Wang H; Bonin A; Peters M; Ruan X. Silica-Induced Apoptosis in Alveolar and Granulomatous Cells *In Vivo*. *Environmental Health Perspectives*. 105(Suppl 5):1241–1246. September. 1997.

Leikoff G; Driscoll K. Cellular Approaches in Respiratory Toxicology. In *Toxicology of the Lung*, 2nd edition. Gardner DE; Crapo JD; McClellan RO (eds.). Raven Press, New York. 1993.

Levin JL; McLarty JW; Hurst GA; Smith AN; Frank AL. Tyler Asbestos Workers: Mortality Experience in a Cohort Exposed to Amosite. *Occupational and Environmental Medicine*. 55:155–160. 1998.

Levresse V; Reiner A; Fleury-Feith J; Levy F; Moritz S; Vivo C; Pilatte Y; Jaurand M-C. Analysis of Cell Cycle Disruptions in Cultures of Rat Pleural Mesothelial Cells Exposed to Asbestos Fibers. *American Journal of Respiratory Cell and Molecular Biology*. 17(6):660–671. 1997.

Li XY; Gilmour PS; Donaldson K; MacNee W. *In Vivo* and *In Vitro* Proinflammatory Effects of Particulate Air Pollution (PM10). *Environmental Health Perspectives*. 105(Suppl 5):1279–1284. September. 1997.

Liddell FDK. The Interaction of Asbestos and Smoking in Lung Cancer. *Annals of Occupational Hygiene*. 45:341–56. 2001a.

Liddell FDK. Unpublished raw mesothelioma data provided to Dr. Wayne Berman by Dr. FDK Liddell from multiple studies of the 1891–1920 Birth Cohort of Quebec Chrysotile Miners and Millers most recently described in Liddell et al. 1997. 2001b.

Liddell FDK; Armstrong BG. The Combination of Effects on Lung Cancer of Cigarette Smoking and Exposure in Quebec Chrysotile Miners and Millers. *Annals of Occupational Hygiene*. 46(1):5–13. 2002.

Liddell FDK; McDonald AD; McDonald JC. The 1891–1920 Birth Cohort of Quebec Chrysotile Miners and Millers: Development From 1904 and Mortality to 1992. *Annals of Occupational Hygiene*. 41:13–36. 1997.

Lim Y; Kim S-H; Kim K-A; Oh M-W; Lee K-H. Involvement of Protein Kinase C, Phospholipase C, and Protein Tyrosine Kinase Pathways in Oxygen Radical Generation by Asbestos-Stimulated Alveolar Macrophage *Environmental Health Perspectives*. 105(Suppl 5):1325–1328. September. 1997.

Lippmann M. Deposition and Retention of Inhaled Fibres: Effects on Incidence of Lung Cancer and Mesothelioma. *Occupational and Environmental Medicine*. 51:793–798. 1994.

Lippmann M. Asbestos and Other Mineral and Vitreous Fibers. In *Environmental Toxicants: Human Exposures and Their Health Effects*. Lippman M (ed). Wiley-Interscience; 2nd edition. December. 1999.

Lippmann M; Schlesinger RB. Interspecies Comparisons of Particle Deposition and Mucociliary Clearance in Tracheobronchial Airways. *Journal of Toxicology and Environmental Health*. 3:441[261]–469[289]. 1984.

Luster MI; Simeonova PP. Asbestos Induces Inflammatory Cytokines in the Lung Through Redox Sensitive Transcription Factors. *Toxicology Letters (Shannon)*. 102-103:271–275. 1998.

Lynch JR; Ayer HE; Johnson DJ. The Interrelationships of Selected Asbestos Exposure Indices. *American Industrial Hygiene Association Journal*. 31(5):598–604. 1970.

Marconi A; Menichini E; Paoletti L. A Comparison of Light Microscopy and Transmission Electron Microscopy Results in the Evaluation of the Occupational Exposure to Airborne Chrysotile Fibres. *Annals of Occupational Hygiene*. 28(3):321–331. 1984.

Marsella JM; Liu BL; Vaslet CA; Kane AB. Susceptibility of p53-Deficient Mice to Induction of Mesothelioma by Crocidolite Asbestos Fibers. *Environmental Health Perspectives*. 105(Suppl 5):1069–1072. September. 1997.

Martin LD; Krunkosky TM; Dye JA; Fischer BM; Jiang NF; Rochelle LG; Akley NJ; Dreher KL; Adler KB. The Role of Reactive Oxygen and Nitrogen Species in the Response of Airway Epithelium to Particulates. *Environmental Health Perspectives*. 105(Suppl 5):11301–1308. September. 1997.

Mattson SM. Glass Fiber Dissolution in Simulated Lung Fluid and Measures Needed to Improve Consistency and Correspondence in *In-Vitro* Studies. Presented at the IARC Conf. Biopersistence of Respirable Synthetic Fibres and Minerals. Lyon, France, September 7–9. 1992. *Environmental Health Perspectives*. 1994.

McConnell E; Wagner J; Skidmore J; Moore J. A Comparative Study of the Fibrogenic and Carcinogenic Effects of UICC Canadian Chrysotile B Asbestos and Glass Microfibre (JM 100). Biological Effects of Man-Made Fibres. Proceedings of a WHO/IARC Conference. pp. 234–252. 1982.

McConnell EE; Rutter HA; Ulland BM; Moore JA. Chronic Effects of Dietary Exposure to Amosite Asbestos and Tremolite in F344 Rats. *Environmental Health Perspectives*. 53:27–44. 1983.

McConnell EE; Adkins B. Studies on the Chronic Toxicity (Inhalation) of Wollastonite in Fischer 344 Rats. *Inhalation Toxicology*. 3:323–337. 1991.

McConnell EE; Mast RW; Hesterberg TW; Chevalier J; Kotin P; Bernstein DM; Thevenez P; Glass LR; Anderson R. Chronic Inhalation Toxicity of a Kaolin-Based Refractory Ceramic Fiber in Syrian Golden Hamsters. *Inhalation Toxicity*. 7:503–532. 1995.

McDonald AD; Fry JS; Wooley AJ; McDonald JC. Dust Exposure and Mortality in an American Chrysotile Textile Plant. *British Journal of Industrial Medicine*. 39:361–367. 1983a.

McDonald AD; Fry JS; Woolley AJ; McDonald JC. Dust Exposure and Mortality in an American Factory Using Chrysotile, Amosite, and Crocidolite in Mainly Textile Manufacture. *British Journal of Industrial Medicine.* 40:368–374. 1983b.

McDonald AD; Fry JS; Woolley AJ; McDonald JC. Dust Exposure and Mortality in an American Chrysotile Asbestos Friction Products Plant. *British Journal of Industrial Medicine*. 41:151–157. 1984.

McDonald JC. Mineral Fibre Persistence and Carcinogenicity. *Industrial Health*. 36(4):372–375. October. 1998a.

McDonald JC. Invited Editorial: Unfinished Business - The Asbestos Textiles Mystery. *Annals of Occupational Hygiene*. 42(1):3–5. 1998b.

McDonald JC; Gibbs GW; Liddell FDK. Chrysotile Fibre Concentration and Lung Cancer Mortality: A Preliminary Report. In *Biological Effects of Mineral Fibres*. Wagner JC (ed). IARC Scientific Publications. pp. 811–817. 1980a.

McDonald JC; Liddell FDK; Gibbs GW; Eyssen GE; McDonald AD. Dust Exposure and Mortality in Chrysotile Mining, 1910–1975. *British Journal of Industrial Medicine*. 37:11–24. 1980b.

McDonald JC; McDonald AD; Armstrong B; Sebastien P. Cohort Study of Mortality of Vermiculite Miners Exposed to Tremolite. *British Journal of Industrial Medicine*. 43:436–444. 1986.

McDonald JC; Liddell FDK; Dufresne A; McDonald AD. The 1891–1920 Birth Cohort of Quebec Chrysotile Miners and Millers: Mortality 1976–1988. *British Journal of Industrial Medicine*. 50:1073–1081. 1993.

McGavran PD; Butterick CJ; Brody AR. Tritiated Thymidine Incorporation and the Development of an Interstitial Lesion in the Bronchiolar-Alveolar Regions of the Lungs of Normal and Complement Deficient Mice After Inhalation of Chrysotile Asbestos. *Journal of Environmental Pathology, Toxicology, and Oncology*. 9(5-6):377–391. December. 1989.

McGavran PD; Moore LB; Brody AR. Inhalation of Chrysotile Asbestos Induces Rapid Cellular Proliferation in Small Pulmonary Vessels of Mice and Rats. *American Journal of Pathology*. 136(3):695–705. 1990.

Mercer RR and Crapo JD. Three-Dimensional Analysis of Lung Structure and its Application to Pulmonary Dosimetry Models. In *Toxicology of the Lung*, 2nd edition, Gardner DE; Crapo JD; McClellan RO (eds.). Raven Press, New York. 1993.

Middleton AP; Beckett ST; Davis JMG. Further Observations on the Short-Term Retention and Clearance of Asbestos by Rats, Using UICC Reference Samples. *Annals of Occupational Hygiene*. 22:141–152. 1979.

Miller FJ; Overton JH; Kimbell JS; Russell ML. Regional Respiratory Tract Absorption of Inhaled Reactive Gases. In *Toxicology of the Lung*, 2nd edition, Gardner DE; Crapo JD; McClellan RO (eds.). Raven Press, New York. 1993.

Moolgavkar SH; Dewanji A; Venzon DJ. A Stochastic Two-Stage Model for Cancer Risk Assessment. 1: The Hazard Function and the Probability of Tumor. *Risk Analysis*. 8(3):383–392. 1988.

Moolgavkar SH; Luebeck EG; De Gunst M; Port RE; Schwarz M. Quantitative Analysis of Enzyme-Altered Foci in Rat Hepatocarcinogenesis Experiments. Single Agent Regimen. *Carcinogenesis*. 11(8):1271–1278. 1990.

Moolgavkar SH; Luebeck EG; Krewski D; Zielinski JM. Radon, Cigarette Smoke, and Lung Cancer: A Re-Analysis of the Colorado Plateau Uranium Miners' Data. *Epidemiology*. 4:204–217. 1993.

Morgan A; Holmes A. Concentrations and Dimensions of Coated and Uncoated Asbestos Fibres in the Human Lung. *British Journal of Industrial Medicine*. 37:25–32. 1980.

Morgan A; Talbot RJ; Holmes A. Significance of Fibre Length in the Clearance of Asbestos Fibres from the Lung. *British Journal of Industrial Medicine*. 35:146–153. 1978.

Morgan A; Black A; Evans N; Holmes A; Pritchard JN. Deposition of Sized Glass Fibres in the Respiratory Tract of the Rat. *Annals of Occupational Hygiene*. 23:353–366. 1980.

Morrow PE. Issues: Possible Mechanisms to Explain Dust Overloading of the Lungs. *Fundamental and Applies Toxicology*. 10:369–384. 1988.

Mossman BT. Mechanisms of Asbestos Carcinogenesis and Toxicity: The Amphibole Hypothesis Revisited. *British Journal of Industrial Medicine*. 50:673–676. 1993.

Mossman BT; Churg A. Mechanisms in the Pathogenesis of Asbestosis and Silicosis. *American Journal of Critical Care Medicine*. 157:1666–1680. 1998.

Mossman BT; Marsh JP. Role of Active Oxygen Species in Asbestos-Induced Cytotoxicity, Cell Proliferation, and Carcinogenesis. In *Cellular and Molecular Aspects of Fiber Carcinogenesis*, Cold Spring Harbor Laboratory Press. 0-87969-361-4/91. pp. 159–168. 1991.

Mossman BT; Bignon J; Corn M; Seaton A; Gee JBL. Asbestos: Scientific Developments and Implications for Public Policy. *Science*. 247:294–301. 1990.

Mossman BT; Kamp DW; Sigmund A; Weitzman SA. Mechanisms of Carcinogenesis and Clinical Features of Asbestos-Associated Cancers. *Cancer Investigation*. 14(5):466–480. 1996.

Mossman BT; Faux S; Janssen Y; Jimenex LA; Timblin C; Zanella C; Goldberg J; Walsh E; Barchowsky A; Driscoll K. Cell Signaling Pathways Elicited by Asbestos. *Environmental Health Perspectives*. 105(Suppl 5):1121–1125. September. 1997.

Muhle H; Bellman B; Takenata S; Ziem Y. Inhalation and Injection in Rats to Test the Carcinogenicity of MMMF. *Annals Occupational Hygiene*. 31(4B):755–764. 1987.

Nario RC; Hubbard AK. Localization of Intercellular Adhesion Molecule-1 (ICAM-A) in the Lungs of Silica-Exposed Mice. *Environmental Health Perspectives*. 105(Suppl 5):1183–1190. September. 1997.

Nehls P; Seiler F; Rehn B; Greferath R; Bruch J. Formation and Persistence of 8-Oxoguanine Rat Lung Cells as an Important Determinant for Tumor Formation following Particle Exposure. *Environmental Health Perspectives*. 105(Suppl 5):1231–1240. September. 1997.

Nicholson WJ. Part III. Recent Approaches to the Control of Carcinogenic Exposures. Case Study 1: Asbestos - The TLV Approach. *Annals New York Academy of Science*. 271:152–169. 1976.

Nicholson WJ; Selikoff IJ; Seidman H; Lilis R; Formby P. Long-Term Mortality Experience of Chrysotile Miners and Millers in Thetford Mines, Quebec. *Annals New York Academy of Sciences*. 330:11–21. 1979.

Nikula KJ; Avila KJ; Griffith WC; Mauderly JL. Sites of Particle Retention and Lung Tissue Responses to Chronically Inhaled Diesel Exhaust and Coal Dust in Rats and Cynomolgus Monkeys. *Environmental Health Perspectives*. 105(Suppl 5):1231–1240. September. 1997.

National Institute for Occupational Safety and Health (NIOSH). Method for Determination of Asbestos in Air Using Positive Phase Contrast Microscopy. NIOSH Method 7400. NIOSH, Cincinnati, Ohio, U.S.A. 1985.

National Institute for Occupational Safety and Health (NIOSH). Method for Determination of Asbestos in Air Using Transmission Electron Microscopy. NIOSH Method 7402. NIOSH, Cincinnati, Ohio, U.S.A. 1986.

Oberdorster G. Macrophage-Associated Responses to Chrysotile. *Annals of Occupational Hygiene*. 38(4):601–615. 1994.

Oberdorster G; Morrow PE; Spurny K. Size Dependent Lymphatic Short Term Clearance of Amosite Fibres in the Lung. *Annals of Occupational Hygiene*. 32(Suppl 1):149–156. 1988.

Ollikainen T; Linnainmaa K; Kinnula VL. DNA Single Strand Breaks Induced by Asbestos Fibers in Human Pleural Mesothelial Cells *In Vitro*. *Environmental and Molecular Mutagenesis*. 33(2):153–160. 1999.

Ontario Royal Commission. Report of the Royal Commission on Matters of Health and Safety Arising form the Use of Asbestos in Ontario. Volume 3. 1984.

Osier M; Baggs RB; Oberdörster G. 1997. Intratracheal Instillation vs. Intratracheal Inhalation: Influence of Cytokines on Inflammatory Response. Proceedings of the Sixth International Meeting on the Toxicology of Natural and Man-Made Fibrous and Non-Fibrous Particles. *Environmental Health Perspective*. 105(Suppl 5):1265–1271.

Osornio-Vargas AR; Kalter VG; Badgett A; Hernandez-Rodriguez N; Aguilar-Delfin I; Brody AR. Rapid Communication: Early-Passage Rat Lung Fibroblasts do not Migrate *In Vitro* to Transforming Growth Factor-Beta. *American Journal of Respiratory Cell Molecular Biology*. 8(5):468–471. May. 1993.

Palekar LD; Spooner CM; Coffin DL. Influence of Crystallization Habit of Minerals on *In Vitro* Cytotoxicity. *Annals New York Academy of Sciences*. pp. 673–687. 1979.

Park S-H; Aust AE. Regulation of Nitric Oxide Synthase Induction by Iron and Glutathione in Asbestos-Treated Human Lung Epithelial Cells. *Archives of Biochemistry and Biophysics*. 360(1):47–52. 1998.

Peto J. Lung Cancer Mortality in Relation to Measured Dust Levels in an Asbestos Textile Factory. In *Biological Effects of Mineral Fibres*. Wagner JC (ed.). IARC Scientific Publications. pp. 829–836. 1980a.

Peto J. The Incidence of Pleural Mesothelioma in Chrysotile Asbestos Textile Workers. In *Biological Effects of Mineral Fibres*. Wagner JC (ed.). IARC Scientific Publications. pp. 703–711. 1980b.

Peto J; Doll R; Howard SV; Kinlen LJ; Lewinsohn, HC. A Mortality Study Among Workers in an English Asbestos Factory. *British Journal of Industrial Medicine*. 34:169–173. 1977.

Peto J; Seidman H; Selikoff IJ. Mesothelioma Mortality in Asbestos Workers: Implications for Models of Carcinogenesis and Risk Assessment. *British Journal of Cancer*. 45:124–135. 1982.

Peto J; Doll R; Hermon C; Binns W; Clayton R; Goffe T. Relationship of Mortality to Measures of Environmental Asbestos Pollution in an Asbestos Textile Factory. *Annals of Occupational Hygiene*. 29(3):305–355. 1985.

Pinkerton KE; Brody AR; McLauren DA; Adkins B Jr; O'Connor RW; Pratt PC; Crapo JD. Characterization of the Three Types of Chrysotile Asbestos After Aerosolization. *Environmental Research*. 31:32–35. 1983.

Pinkerton KE; Pratt PC; Brody AR; Crapo JD. Fiber Localization and its Relationship to Lung Reaction in Rats After Chronic Inhalation of Chrysotile Asbestos. *American Journal of Pathology*. 117:484–498. 1984.

Pinkerton KE; Plopper CG; Mercer RR; Rogli VL; Patra AL; Brody AR; Crap JD. Airway Branching Patterns Influence Asbestos Fiber Location and the Extent of Tissue Injury in the Pulmonary Parenchyma. *Laboratory Investigation*. 55(6):688–695. 1986.

Piolatto G; Negri E; LaVecchia C; Pira E; Decarli A; Peto J. An Update of Cancer Mortality Among Chrysotile Asbestos Miners in Balangero, Northern Italy. *British Journal of Industrial Medicine.* 47:810–814. 1990.

Platek SF; Groth DH; Ulrich CE; Stettler LE; Finnell MS; Stoll M. Chronic Inhalation of Short Asbestos Fibers. *Fundamental and Applied Toxicology*. 5:327–340. 1985.

Pooley FD. An Examination of the Fibrous Mineral Content of Asbestos Lung Tissue from the Canadian Chrysotile Mining Industry. *Environmental Research*. 12:281–298. 1976.

Pooley FD. Tissue Burden Studies. In *Short and Thin Mineral Fibres: Identification, Exposure, and Health Effects*. Chatfield EJ (ed). pp. 96–129. 1982.

Pott F. Some Aspects on the Dosimetry of the Carcinogenic Potency of Asbestos and Other Fibrous Dusts. *Staub-Reinhalt*. 38(12):486–490. 1978.

Pott F. Animal Experiments with Mineral Fibers. In *Short and Thin Mineral Fibers: Identification, Exposure, and Health Effects*. Chatfield EJ (ed.). pp. 133–161. 1982.

Pott F; Huth F; Friedrichs KH. Tumorigenic Effect of Fibrous Dust in Experimental Animals. *Environmental Health Perspectives*. 9:313–315. 1974.

Pott F; Huth F; Friedrichs KH. Results of Animal Carcinogenesis Studies After Application of Fibrous Glass and Their Implications Regarding Human Exposure. Occupational Exposure to Fibrous Glass. U.S. HEW Publication No. 76–151. pp. 183–191. 1976.

Pott F; Ziem U; Reiffer RJ; Huth F; Ernst H; Mohr U. Carcinogenicity Studies on Fibres, Metal Compounds, and Some Other Dusts in Rats. *Experimental Pathology*. 32:129–152. 1987.

Raabe O. Deposition and Clearance of Inhaled Particles. In *Occupational Lung Diseases*. Gee JB; et al. (eds.). Raven Press. pp. 1047. 1984.

Quinlan TR; Berube KA; Hacker MP; Taatjes DJ; Timblin CR; Goldberg J; Kimberley P; O'Shaughnessy P; Hemenway D; Torino J; Jimenez LA; Mossman BT. Mechanisms of Asbestos-Induced Nitric Oxide Production by Rat Alveolar Macrophages in Inhalation and *In Vitro* Models. *Free Radical Biology and Medicine*. 24(5):778–788. 1998.

Rahman Q; Mahmood N; Khan SG; Arif JM; Athar M. Mechanism of Asbestos-Mediated DNA Damage: Role of Heme and Heme Proteins. *Environmental Health Perspectives*. 105(Suppl 5):1109–1112. September. 1997.

Roberts DR; Zumwalde RD. Industrial Hygiene Summary Report of Asbestos Exposure Assessment for Brake Mechanics. NIOSH Reports No. IWS-32-4A, Industrial Hygiene Section, NTIS# PB 87-105433. 1982.

Robledo R; Mossman B. Cellular and Molecular Mechanisms of Asbestos-Induced Fibrosis. *Journal of Cellular Physiology*. 180:158–166. 1999.

Roggli VL; Brody AR. Changes in Numbers and Dimensions of Chrysotile Asbestos Fibers in Lungs of Rats Following Short-Term Exposure. *Experimental Lung Research*. 7:133–147. 1984.

Roggli VL; George MH; Brody AR. Clearance and Dimensional Changes of Crocidolite Asbestos Fibers Isolated from Lungs of Rats Following Short-Term Exposure. *Environmental Research*. 42:94–105. 1987.

Rood AP; Scott RM. Size Distributions of Chrysotile Asbestos in a Friction Products Factory As Determined by Transmission Electron Microscopy. *Annals of Occupational Hygiene*. 33(4):583–590. 1989.

Rubino GF; Piolatto GW; Newhouse ML; Scansetti G; Aresini GA; Murray R. Mortality of Chrysotile Asbestos Workers at the Balangero Mine, Northern Italy. *British Journal of Industrial Medicine*. 36:187–194. 1979.

St. George JA; Harkema JR; Hyde DM; Plopper CG. Cell Populations and Structure/Function Relationship of Cells in the Airways. In *Toxicology of the Lung*, 2nd edition. Gardner DE; Crapo JD; McClellan RO (eds.). Raven Press, New York. 1993.

Sanden A; Jarvholm B; Larsson S; Thiringer G. The Risk of Lung Cancer and Mesothelioma After Cessation of Asbestos Exposure: A Prospective Cohort Study of Shipyard Workers. *European Respiratory Journal*. 5:281–285. 1992.

Schnoor T. Unpublished Raw Data Provided to Dr. Wayne Berman by Ms. Terri Schnoor of NIOSH from Study of South Carolina Textile Workers (Dement et al. 1994). 2001.

Sebastien P; Plourde M; Robb R; Ross M. Ambient Air Asbestos Survey in Quebec Mining Towns - Part 1, Methodological Study. Environmental Protection Service, Quebec Region, 3/AP/RQ/1E. pp. 1–41. 1984.

Sebastien P; Plourde M; Robb R; Ross M; Nadon B; Wypruk T. Ambient Air Asbestos Survey in Quebec Mining Towns. Part II: Main Study. Environmental Protection Service, Environment Canada. EPS 5/AP/RQ/2E. July. 1986.

Sebastien P; McDonald JC; McDonald AD; Case B; Harley R. Respiratory Cancer in Chrysotile Textile and Mining Industries: Exposure Inferences from Lung Analysis. *British Journal of Industrial Medicine*. 46:180–187. 1989.

Seidman H. Short-Term Asbestos Work Exposure and Long-Term Observation -- July 1984 Update. Department of Epidemiology, American Cancer Society. 1984.

Seidman H; Selikoff IJ; Hammond EC. Short-Term Asbestos Work Exposure and Long-Term Observation. *Annals New York Academy of Sciences*. 330:61–89. 1979.

Seidman H; Selikoff IJ; Gelb SK. Mortality Experience of Amosite Asbestos Factory Workers: Dose-Response Relationships 5 to 40 Years After Onset of Short-Term Work Exposure. *American Journal of Industrial Medicine*. 10(5/6):479–514. 1986.

Selikoff IJ; Seidman H. Asbestos-Associated Deaths among Insulation Workers in the United States and Canada, 1967–1987. *Annals of the New York Academy of Sciences*. 643:1–14. 1991.

Selikoff IJ; Hammond EC; Seidman H. Mortality Experience of Insulation Workers in the United States and Canada 1943–1976. *Annals New York Academy of Sciences*. 330:91–116. 1979.

Smith DM; Oritiz LW; Archuleta RF; Johnson NF. Long-Term Health Effects in Hamsters and Rats Exposed Chronically to Man-Made Vitreous Fibres. *Annals of Occupational Hygiene*. 34(4B):731–754. 1987.

Snyder J; Virta R; Segreti J. Evaluation of the Phase Contrast Microscopy Method for the Detection of Fibrous and Other Elongated Mineral Particulates by Comparison with a STEM Technique. *American Industrial Hygiene Association Journal*. 48(5):471–477. 1987.

Stanton M; Wrench C. Mechanisms of Mesothelioma Induction with Asbestos and Fibrous Glass. *Journal of the National Cancer Institute*. 48:797–821. 1972.

Stanton M; Layard M; Tegeris A; Miller E; May M; Kent E. Carcinogenicity of Fibrous Glass: Pleural Response in the Rat in Relation to Fiber Dimension. *Journal of the National Cancer Institute*. 58(3):587–597. 1977.

Stanton M; Layard M; Tegeris A; Miller E; May M; Morgan E. Relation of Particle Dimension to Carcinogenicity in Amphibole Asbestos and Other Fibrous Minerals. *Journal of the National Cancer Institute*. 67(5):965–975. 1981.

Stayner L; Smith R; Bailer J; Gilbert S; Steenland K; Dement J; Brown D; Lemen R. Exposure-Response Analysis of Risk of Respiratory Disease Associated with Occupational Exposure to Chrysotile Asbestos. *Occupational and Environmental Medicine*. 54:646–652. 1997.

Stayner LT; Dankovic DA; Lemen RA. Occupational Exposure to Chrysotile Asbestos and Cancer Risk: A Review of the Amphibole Hypothesis. *American Journal of Public Health*. 86(2):176–186. February. 1996.

Stober W; McClellen RO; Morrow PE. Approaches to Modeling Disposition of Inhaled Particles and Fibers in the Lung. In *Toxicology of the Lung*, 2nd edition. Gardner DE; Crapo JD; McClellan RO (eds.). Raven Press, New York. 1993.

Strom KA; Yu CP. Mathematical Modeling of Silicon-Carbide Whisker Deposition in the Lung-Comparison Between Rats and Humans. *Aerosol Science and Technology*. 24(3):193–209. 1994.

Sussman RG; Cohen BS; Lippmann M. Asbestos Fiber Deposition in a Human Tracheobronchial Cast. I. Experimental. *Inhalation Toxicology*. 3:145–160. 1991a.

Sussman RG; Cohen BS; Lippmann M. Asbestos Fiber Deposition in a Human Tracheobronchial Cast. II. Empirical Model. *Inhalation Toxicology*. 3:161–179. 1991b.

Takeuchi T; Nakajima M; Morimoto K. A Human Cell System for Detecting Asbestos Cytogenotoxicity *In Vitro*. *Mutation Research*. 438(1):63–70. 1999.

Tanaka S; Choe N; Hemenway DR; Zhu S; Matalon S; Kagan E. Asbestos Inhalation Induces Reactive Nitrogen Species and Nitrotyrosine Formation in the Lungs and Pleura of the Rat. *Journal of Clinical Investigation*. 102(2):445–454. 1998.

Timblin CR; Guthrie GD; Janssen YWM; Walsh ES; Vacek P; Mossman BT. Patterns of C-Fos and C-Jun Proto-Oncogene Expression, Apoptosis, and Proliferation in Rat Pleural Mesothelial Cells Exposed to Erionite or Asbestos Fibers. *Toxicology and Applied Pharmacology*. 151(1):88–97. 1998a.

Timblin CR; Janssen YMW; Goldberg JL; Mossman BT. GRP78, HSP72/73, and CJUN Stress Protein Levels in Lung Epithelial Cells Exposed to Asbestos, Cadmium or H2O2. *Free Radical Biology & Medicine*. 24(4):632–642. 1998b.

Timbrell V. Deposition and Retention of Fibres in the Human Lung. *Annals of Occupational Hygiene*. 26(1-4):347–369. 1982.

Timbrell V; Hyett AW; Skidmore JW. A Simple Dispenser for Generating Dust Clouds From Standard Reference Samples of Asbestos. *Annals of Occupational Hygiene*. 11:273–281. 1968.

Unfried K; Kociok N; Roller M; Pott F; Dehnen W. P53 mutations in tumours induced by intraperitoneal injection of crocidolite asbestos and benzo[a]pyrene in rats. Experimental Toxicololgoy and Pathology. 49:181–187. 1997.

U.S. EPA (U.S. Environmental Protection Agency). Airborne Asbestos Health Assessment Update. Report 600/8-84-003F, U.S. Environmental Protection Agency. 1986.

U.S. Environmental Protection Agency (EPA). Asbestos Hazard Emergency Response Act: Asbestos-Containing Materials in Schools. Final Rule and Notice (Appendix A: AHERA Method). Federal Register, 40 CFR 763, Vol. 52, No. 2, pp. 41826–41903. October. 1987.

Venzon D; Moolgavkar S. A Method for Computing Profile-likelihood-based Confidence Intervals. *Applied Statistics*. 37:87–94. 1988.

Vincent JH. On the Practical Significance of Electrostatic Lung Deposition of Isometric and Fibrous Aerosols. *Journal Aerosol Science*. 16(6):511–519. 1985.

Vincent JH; Johnston AM; Jones AD; Bolton RE; Addison J. Kinetics of Deposition and Clearance of Inhaled Mineral Dusts During Chronic Exposure. *British Journal of Industrial Medicine*. 42:707–715. 1985.

Wagner JC. Opening Discussion -- Environmental and Occupational Exposure to Natural Mineral Fibres. In *Biological Effects of Mineral Fibres*. Wagner JC (ed.). IARC Scientific Publications. pp. 995–998. 1980.

Wagner JC; Berry G; Skidmore JW; Timbrell V. The Effects of the Inhalation of Asbestos in Rats. *British Journal of Cancer*. 29:252–269. 1974.

Wagner JC; Berry G; Skidmore JW. Studies of the Carcinogenic Effects of Fiber Glass of Different Diameters Following Intrapleural Innoculation in Experimental Animals. NIOSH 76-151. pp.193–197. 1976.

Wagner JC; Berry G; Hill R; Munday D; Skidmore J. Animal Experiments with MMM(V)F - Effects of Inhalation and Intrapleural Inoculation in Rats. In *Biological Effects of Man-Made Fibres -- Proceedings of a WHO/IARC Conference*, Copenhagen. pp. 209–233. 1982.

Wagner JC; Skidmore JW; Hill RJ; Griffith DM. Erionite Exposure and Mesotheliomas in Rats. *British Journal of Cancer*. 51:727–730. 1985.

Wagner JC; Griffiths DM; Munday DE. Experimental Studies with Palygorskite Dusts. *British Journal of Industrial Medicine*. 44(11):749–763. 1987.

Walker AM. Declining Relative Risks for Lung Cancer After Cessation of Asbestos Exposure. *Journal of Occupational Medicine*. 26(2):422–426. 1984.

Walton WH. The Nature, Hazards, and Assessment of Occupational Exposure to Airborne Asbestos Dust: A Review. *Annals of Occupational Hygiene*. 25:117–247. 1982.

Warheit DB; Snajdr SI; Hartsky MA; Frame SR. Lung Proliferative and Clearance Responses to Inhaled para-Aramid RFP in Exposed Hamsters and Rats: Comparisons with Chrysotiles Asbestos Fibers. *Environmental Health Perspectives*. 105(Suppl 5):1219–1222. September. 1997.

Weill H. 1994. Cancer Mortality in Chrysotile Mining and Milling: Exposure-Response. Asbestos-Cement. *Annals of Occupational Hygiene*. 38(4):412. 1994.

Weill H; Hughes J; Waggenspack C. Influence of Dose and Fibre Type on Respiratory Malignancy Risk in Asbestos Cement Manufacturing. *American Review of Respiratory Disease*. 120:345–354. 1979.

Wilks SS. Mathematical Statistics. 2nd edition. Wiley Publication, New York. 1963.

Winer AA; Cossette M. The Effect of Aspect Ration on Fiber Counts: A Preliminary Study. *Annals New York Academy of Sciences*. 330:661–672. 1979.

Weitzman SA; Graceffa P. Communication: Asbestos Catalyzes Hydroxyl and Superoxide Radical Generation from Hydrogen Peroxide. *Archives of Biochemistry and Biophysics*. 228(1):373–376. 1984.

World Health Organization (WHO). Reference Methods for Measuring Airborne Man-Made Mineral Fibers (MMMF). 1985.

Wright GW; Kuschner M. The Influence of Varying Lengths of Glass and Asbestos Fibres on Tissue Response in Guinea Pigs. In *Inhaled Particles: Part 2*. Walton WH; McGovern B (eds.). Pergamon Press Oxford. pp. 455–474. 1975.

Wylie AG; Virta RL; Segretti JM. Characterization of Mineral Population by Index Particle: Implications for the Stanton Hypothesis. *Environmental Research*. 43:427–439. 1987.

Wylie AG; Bailey KF; Kelse JW; Lee RJ. The Importance of Width in Asbestos Fiber Carcinogenicity and its Implications for Public Policy. *American Industrial Hygiene Association Journal*. 54:239–252. 1993.

Wylie AG; Skinner HCW; Marsh J; Snyder H; Garzione C; Hodkinson D; Winters R; Mossman BT. Mineralogical Features Associated with Cytotoxic and Proliferative Effects of Fibrous Talc and Asbestos on Rodent Tracheal Epithelial and Pleural Mesothelial Cells. *Toxicology and Applied Pharmacology*. 147:143–150. 1997.

Yamaguchi R; Hirano T; Ootsuyama Y; Asami S; Tsurudome Y; Fukada S; Yamato H; Tsuda T; Tanaka I; Kasai H. Increased 8-Hydroxyguanine in DNA and Its Repair Activity in Hamster and Rat Lung After Intratracheal Instillation of Crocidolite Asbestos. *Japanese Journal of Cancer Research*. 90(5):505–509. 1999.

Yamate G; Agarwal SC; Gibbons RD. Methodology for the Measurement of Airborne Asbestos by Electron Microscopy. U.S. EPA Report No. 68-02-3266. U.S. Environmental Protection Agency, Washington, D.C., U.S.A. 1984.

Yeh H-C; Harkema JR. Gross Morphometry of Airways. In *Toxicology of the Lung*, 2nd edition. Gardner DE; Crapo JD; McClellan RO (eds.). Raven Press, New York. 1993.

Yu CP; Asgharian B. A Kinetic Model of Alveolar Clearance of Amosite Asbestos Fibers from the Rat Lung at High Lung Burdens. *Journal of Aerosol Science*. 21:21–27. 1990b.

Yu CP; Yoon KJ. Investigator's Report: Retention Modeling of Diesel Exhaust Particles in Rats and Humans. 1991.

Yu CP; Asgharian B; Abraham JL. Mathematical Modeling of Alveolar Clearance of Chrysotile Asbestos Fibers from the Rat Lungs. *Journal of Aerosol Science*. 21:587–594. 1990a.

Yu CP; Asgharian B; Pinkerton KE. Intrapulmonary Deposition and Retention Modeling of Chrysotile Asbestos Fibers in Rats. *Journal of Aerosol Science*. 22(6):757–761. 1991.

Yu CP; Zhang L; Oberdoster G; Mast RW; Glass LR; Utell MJ. Deposition Modeling of Refractory Ceramic Fibers in the Rat Lung. *Journal of Aerosol Science*. 25(2):407–417. 1994.

Yu CP; Zhang L; Oberdoster G; Mast RW; Maxim D; Utell MJ. Deposition of Refractory Ceramic Fibers (RCF) in the Human Respiratory Tract and Comparison with Rodent Studies. *Aerosol Science and Technology*. 23(3):291–300. 1995a.

Yu CP; Zhang L; Oberdoster G; Mast RW; Glass LR; Utell MJ. Clearance of Refractory Ceramic Fibers (RCF) from the Rat Lung - Development of a Model. *Environmental Research*. 65(2):243–253. 1995b.

Zalma R; Bonneau L; Guignard J; Pezerat H; Jaurand M-C. Formation of Oxy Radicals by Oxygen Reduction Arising from the Surface Activity of Asbestos. *Canadian Journal of Chemistry*. 65:2338–2341. 1987.

Zanella CL; Timblin CR; Cummins A; Jung M; Goldberg J; Raabe R; Tritton TR; Mossman BT. Asbestos-Induced Phosphorylation of Epidermal Growth Factor Receptor is Linked to c-fos and apoptosis. *American Journal of Physiology*. 277(4:Part 1):L684–L693. 1999.

Zhang Y; Lee TC; Guillemin B; Yu M-C; Rom WN. Enhanced IL-1Beta and Tumor Necrosis Factor-Alpha Release and Messenger RNA Expression in Macrophages from Idiopathic Pulmonary Fibrosis or After Asbestos Exposure. *Journal of Immunology*. 150(9):4188–4196. May. 1993.

Zhu S; Manuel M; Tanaka S; Choe N; Kagan E; Matalon S. Contribution of Reactive Oxygen and Nitrogen Species to Particulate-Induced Lung Injury. *Environmental Health Perspectives*. 106(5):1157–1163. 1998.

Zoitus BK; De Meringl A; Rouyer E; Thelohan S; Bauer J; Law B; Boymel PM; Olson JR; Christensen VR; Guldberg M; Koenig AR; Perander M. *In Vitro* Measurement of Fiber Dissolution Rate Relevant to Biopersistence at Neutral pH: An Interlaboratory Round Robin. *Inhalation Toxicology*. 9:525–540. 1997.